The Development of Chitosan Microspheres for Use as Agrochemical Delivery or Agropollutant Adsorption Systems

A thesis submitted to the National University of Ireland in fulfillment of the requirements for the degree of

Doctor of Philosophy

By

Ciarán Joseph O'Carroll B.Sc. (Hons)

NUI MAYNOOTH

Ollscoil na hÉireann Má Nuad

Department of Chemistry,
Faculty of Science and Engineering,
National University of Ireland Maynooth,
Maynooth,
Co. Kildare,
Ireland.

October 2011

Research Supervisors: Dr. Denise Rooney and Prof. Carmel Breslin

Head of Department: Professor John P. Lowry

Declaration

This is to certify that the material presented within this thesis has not been submitted previously for a Degree to this or any other University. All material presented, except where acknowledged and cited, is the original work of the author.

Ciarán Joseph O'Carroll

_____

October 2011

National University of Ireland, Maynooth.

Acknowledgements

I would like to thank my supervisors Dr. Denise Rooney and Prof Carmel Breslin for their guidance and dedicated support over the course of my work in Maynooth.

Grateful thanks also to Prof John Lowry, Head of Department.

To the rest of the staff in the department I extend my sincerest gratitude. In particular the technical staff, Ria, Barbara, Ollie, Anne, Ken, Noel and the Executive Administrator, Niamh, who were always on hand with assistance and advice.

My sincere gratitude goes to my friends and colleagues in the Department of Chemistry. In particular, Conor McCarthy, Niall McGuinness, Louise Gallagher, Alanna Smith, Catherine Fox, Lynn Garry, Niamh Dolan, Carol Buggy, Declan Gavin, Dr. Niall Finnerty, Dr. Valeria Annibaldi, Dr. Sinead McDermott and Dr. Adelaide Dura.

I would also like to thank my parents, uncles, aunts, cousins for their support. A massive thank you to the McGee family, without whose help I would not have made it as far as a BSc, never mind a PhD.

I would like to thank the Department of Agriculture, Fisheries and Food for their financial support.

Last but not least I thank my wonderful friends, Tom, Cat, Louise, Karl, Steph and Manus for their support, patience and encouragement.

Dedication

To my parents and Uncle David and Auntie Noreen.

"A man must shape himself to a new mark directly the old one goes to ground"

- *Sir Ernest Shackleton*

Abstract

The aim of this thesis was the development of a hydrogel bead agrochemical delivery system for the nitrification inhibitor, dicyandiamide (DCD) and the development of a hydrogel bead adsorption system for the herbicide, paraquat.

The hydrogel bead was based on the biopolymer chitosan which was protonated in order for it to be soluble in water. The aqueous chitosan solution was then used to form hydrogel beads, either by precipitation with NaOH solution or by crosslinking. The resulting chitosan hydrogel beads were loaded with DCD and their release properties investigated using UV/vis spectroscopy. It was found that chitosan hydrogel beads formed by precipitation or ionic crosslinking only exhibited uncontrolled DCD release while chitosan hydrogel beads covalently crosslinked exhibited controlled DCD release. The factors influencing the rate of DCD release from the beads such as, pH, release medium temperature and crosslinking agent, were investigated.

N-acylated chitosan hydrogel beads were synthesised and then characterised using a range of techniques including scanning electron microscopy, Fourier-transform infrared spectroscopy, elemental analysis and differential scanning calorimetry. The *N*-acylated chitosan hydrogel beads were loaded with DCD and their release properties investigated using UV/vis spectroscopy. It was found that these beads exhibited controlled DCD release. The factors influencing the rate of DCD release from the beads such as, pH, release medium temperature and degree of substitution, were investigated.

Chitosan hydrogel beads crosslinked with *p*-sulfonatocalix[4]arene sodium salt were synthesised. These beads were formed in order to investigate their potential use as a pollution remediation technology, as *p*-sulfonatocalix[4]arene sodium salt is known to form a stable inclusion complex with a herbicide called paraquat. The hydrogel beads were characterised using scanning electron microscopy and energy dispersive X-ray analysis. Adsorption experiments were performed using UV/vis spectroscopy and it was found that they were capable of removing paraquat from aqueous solution.

Table of Contents

Chapter 1: Introduction and Literature Review

1.1 Introduction

Since the industrial revolution the lifestyles of humans has become heavily dependent on hydrocarbon inputs from a finite reservoir of fossil fuels. The most widely utilized hydrocarbon is oil, now the major source of transportation fuels, contributes to heating energy, and provides a vast array of molecular structures for polymers, plastics, paints, chemicals and other consumables. Despite the world's reliance on oil and other hydrocarbons to drive economies, petro-based fuels and the chemicals they produce are unsustainable[1]. It has to be assumed that oil production passed its maximum in the previous decade and is currently slowly decreasing. The global oil reserves were estimated at the end of 2001 to last for 40 years[2]. In addition, environmental concerns due to emissions of pollutants from the combustion of hydrocarbons as well as the emissions from agriculture have also become major global problems. Example of these pollutants include nitrate, sulfate and particulate matter, but also greenhouse gases (GHG) such as carbon dioxide (CO_2) and methane (CH_4)[3].

The decline in oil reserves and the continuing world population boom means that resources will have to be used much more efficiently than today using the same or even a lower quantity of resources. The United Nations Conference on Environment and Development, held in Rio de Janeiro in 1992, provided the fundamental principles for achieving sustainable development[2]. Sustainable chemistry is understood as the contribution of chemistry to the implementation of the Rio Declaration and Agenda 21, including its on-going advancements, such as the 2010 United Nations Climate Change Conference held in Cancún, Mexico, from 29 November to 10 December 2010[4].

The sustainable chemistry concept links eco-efficiency, economic growth and quality of life in terms of a cost/benefit analysis. The role of chemists is to minimize this risk and reduce the impact on the environment to a level sustainable by the environment,

assuring a good quality of life[5]. Chemicals from renewable resources have attracted an increasing amount of attention over the last two decades predominantly due to two major reasons: firstly environmental concerns, and secondly the realization that our petroleum resources are finite[6]. The study and utilization of natural polymers is an ancient science. However, the availability of petroleum at a lower cost and the biochemical inertness of petroleum-based products have proven disastrous for the renewable chemical market. It is only after a lapse of almost 50 years that the significance of eco-friendly materials has been realized once again. Sustainable chemicals such as renewable natural polymers and benign chemicals that enhance the efficiency of production processes are now considered to be materials of great futuristic potential[7]. In particular chemistry is looking at more effective and benign chemical processes based on renewable resources such as biopolymers and chemical products that enhance the efficiency of synthesis and products[2]. The study of the mechanisms of reactions is also important to avoid the formation of toxic side products and to optimize the yield of desired products[8]. Research to facilitate a reduction in the use of organic solvents in order to minimize production of atmospheric volatile organic compounds is being driven by an increase in the development of renewable chemical feedstocks. Hence, new chemical synthesis are being developed that allow water and supercritical gases, in particular CO_2 to be used as a solvent[9].

1.2 Biopolymers

Polymers are compounds with a high molecular weight consisting of up to millions of repeated linked units that are relatively light and simple. They are built up from simple 'monomers' or single parts[10]. Carbohydrates are polymers of sugars and a monosaccharide is the simplest type of carbohydrate consisting of a single saccharide unit[11]. Polysaccharides are carbohydrates that contain many monosaccharide units joined by glycoside bonds. Most polysaccharides have hundreds or thousands of simple sugar units linked together to form long polymer chains. They are a class of biopolymer, or naturally occurring polymers[10]. Biopolymers are polymers produced

by living organisms that have unique structures, multidimensional properties, highly sophisticated functions and wide ranging applications in biomedical and industrial areas[12, 13]. To exploit the unique properties and to realize full potential of these versatile polymers research and development work on biopolymers has reached a status of intense activity in many parts of the world[14].

Cellulose (Figure 1.1), a polymer of D-glucose, is the world's most abundant organic material. It is a straight chain polymer composed of D-glucose units linked by equatorial β-1,4-glyocosidic bonds which are rigid and very stable, giving cellulose desirable properties for a structural material in organisms[10].
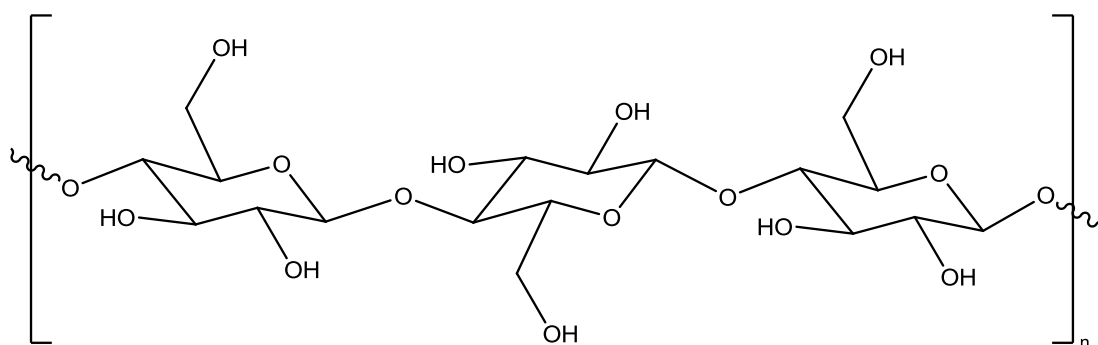
Figure 1.1 Cellulose

Cellulose is abundant in tress and other plants as a structural material to support the weight of the plant. Wood and straw consist of 50% of the polysaccharide. Cellulose is biodegradable but is insoluble in water and most organic solvents which limit its potential applications[14]. However, functionalised cellulose derivatives have been studied and utilised for a long time. Cellulose nitrate has long been one of the world's most popular explosives. The properties of cellulose derivatives are determined primarily by the type of functional group. They can be modified by adjusting the degree of functionalization and the degree of polymerization of the polymer backbone[15].

Starch (Figure. 1.2) is a polymeric carbohydrate consisting of anhydroglucose units linked together primarily through α-D-(1→4) glucosidic bonds[16]. The anhydroglucose unit consists of two types of molecules; amylose (normally 20–30%) and amylopectin (normally 70–80%). In amylase these are α-D-(1→4) glucosidic bonds whereas, in amylopectin about one residue in every twenty or fifty is also α-D-(1→6) glucosidic bonds forming a branch point[17]. Starch granules are synthesised by many plant tissues and act as an energy store. Different plants produce variations in starch granule parameters such as shape, size and composition. In addition, starch may be chemically, enzymatically or physically modified to induce novel characteristics[18]. Starch has proven popular in sustainable chemistry as it's versatile, cheap and has many uses as a thickener, water binder, emulsion stabilizer and a gelling agent[17].
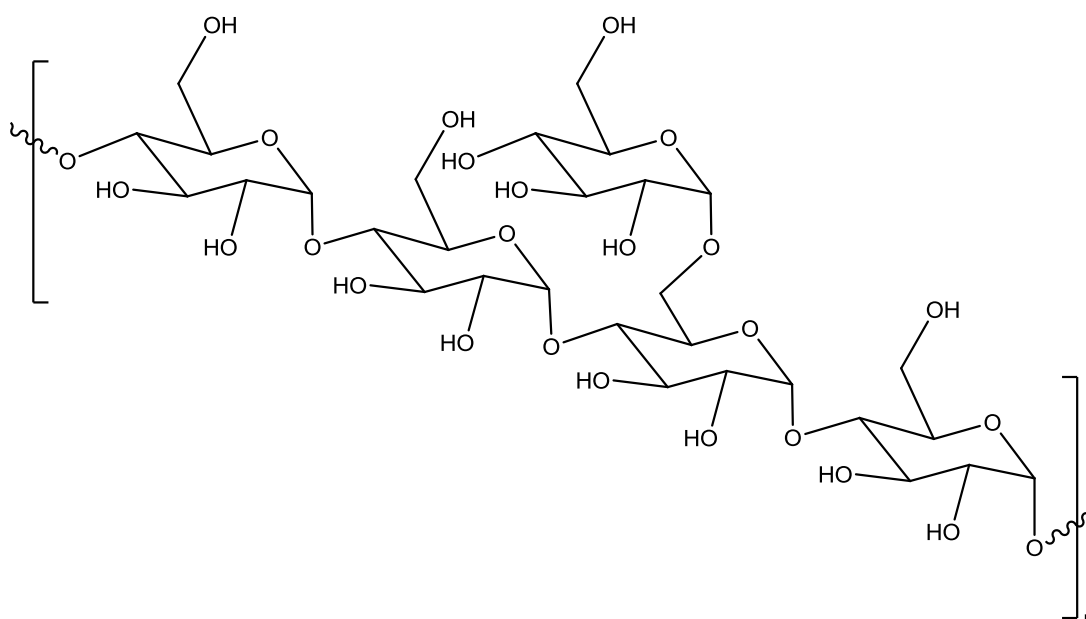
Figure 1.2 Starch

Dextran is a water-soluble polysaccharide produced by bacteria from sucrose which consists mainly of α-1,6 linked D-glucopyranose residues with a low percentage of α-1,2, α-1,3 and α-1,4 linked side chains[19]. The degree of branching depends on the source of dextrans and may vary from 0.5 to 60%. Furthermore, the source of dextran determines the molecular weight distribution of the polymers. By increasing the

branching of the macromolecules this decreases the water solubility of dextrans[20]. Dextran is non-toxic and is therefore useful in medical applications as a blood plasma substitute[19].

Alginate (Figure. 1.3) is a biopolymer that is distributed widely in cell walls of brown algae[21]. It is considered to be biocompatible, non-toxic, non-immunogenic and biodegradable[22]. Its structure contains two uronic acids, (1-4)-linked β-D-mannuronic acid (M) and (1–4) linked α-L-guluronic acid (G), and is composed of homopolymeric blocks M–M or G–G, and blocks with an alternating sequence of M–G blocks. Sodium alginate salt has a unique property of cross-linking in the presence of multivalent cations, such as calcium ions in aqueous media which complex to form insoluble calcium alginate. Depending on the degree of cross-linking, alginate will significantly reduce its swelling in the presence of the solvent, generally resulting in a reduction of the permeability of different solutes. As a consequence, the release of embodied drugs in alginate matrices will be delayed, allowing these systems to be used in drug controlled release[23].
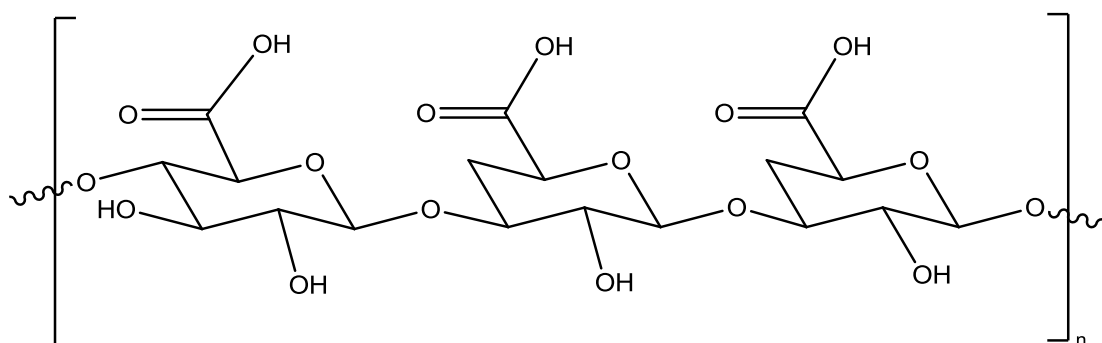
Figure 1.3 Alginate

Chitin is the second most abundant natural biopolymer in the world and is held together by glycosidic bonds and is a polymer of *N*-acetylglucosamine. *N*-acetylglucosamine is an amino sugar that is common in living organisms. Chitin forms in the exoskeletons of insects such as butterflies and spiders[24, 25]. In crustaceans, chitin forms a matrix that binds calcium carbonate crystals into the exoskeleton[26]. The glycosidic bonds in chitin give it a structural rigidity, strength and

stability that exceed even that of cellulose[10]. Owing to the semi-crystalline structure of chitin with extensive hydrogen bonding, the cohesive energy density and hence the solubility parameter are very high and so it is insoluble in all the usual solvents including deionised water[7]. However chitosan is produced by the de-acetylation of chitin and is readily soluble in dilute acid solutions below pH 6. At a low pH, chitosan becomes protonated and positively charged which makes it a water-soluble cationic polyelectrolyte. On the other hand, as the pH increases above 6, the glucosamine units of chitosan become deprotonated and the polymer loses its charge and becomes insoluble. The ability to dissolve chitosan in dilute acid aqueous solutions and its properties such as biodegradability, low toxicity and good biocompatibility is a property that has led to a great deal of interest for its used in agricultural, medical and pharmaceutical applications[27].
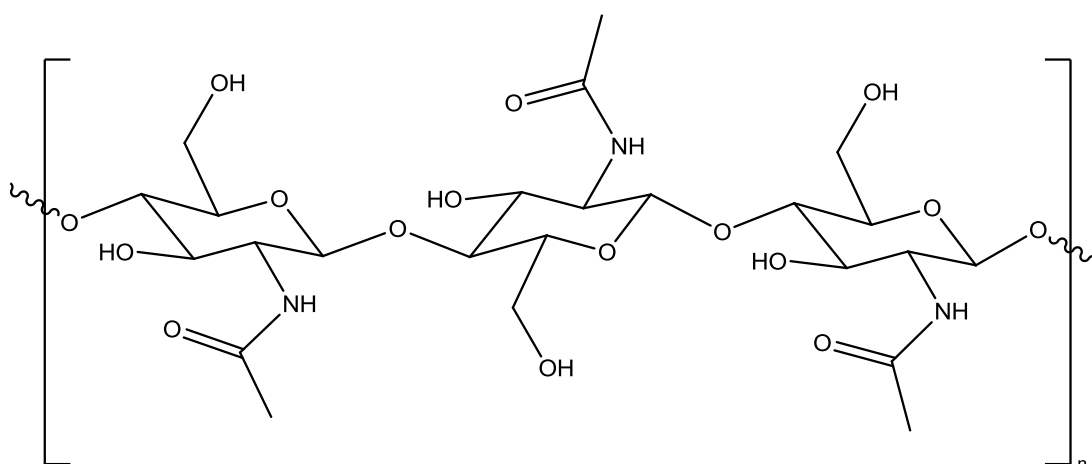
Figure 1.4 Chitin

1.3 Applications of Chitosan

Potential Carrier for Drugs:

Due to its gelling properties chitosan has a great potential for coating pharmaceutical products. It has been shown that it not only improves the dissolution of poorly soluble drugs but also exerts a significant effect on fat metabolism in the body[28]. It has been used as a vehicle for directly compressed tablets, as a disintegrate, as a granulating

agent, in ground mixtures, as a drug carrier for sustained release preparations, as well as a co-grinding diluent for the enhancement of dissolution rate and bioavailability of water insoluble drugs. Chitosan has been shown to possess notable mucoadhesive properties due the positive charge on the chitosan polymer glucosamine unit in acid aqueous solutions which gives rise to strong electrostatic interactions with negatively charged acid residues on the mucosal surface[29].

Seed protection:

Coatings based on chitosan have been used as an antifungal agent for enhancing the germination and quality of artichoke seeds. It has been observed seeds coated with a chitosan gel have reduced fungi levels and increased plant growth[30]. In addition, combining the chitosan coating with the fungicide tetramethylthiuaramdisulfide (TMTD) led to a further increase in plant growth levels[30].

Bandages:

Chitosans properties have been shown to include haemostasis, antimicrobial activity and stimulation of healing. A compressed chitosan acetate dressing has been developed that has been shown to stem blood flow, especially from severely bleeding wounds[31]. The polycationic nature of chitosan is such that the substance possesses natural antimicrobial properties, therefore the chitosan acetate bandage simultaneously has two highly desirable properties in a wound dressing: haemostasis and microbicidal activity[31].

Controlled Delivery of Agrochemicals:

Chitosan has been used as a controlled delivery system for steroid plant hormones called bassinosteroids[32]. These plant hormones are used to promote the crops ability to stimulate cell enlargement and increase vegetable growth. Chitosan microspheres encapsulate brassinosteroids and release the hormones over a 10 hour period at a constant rate[32]. It has been noted that controlled release polymers have great potential to reduce pollution and other side effects accompanying the use of conventional agrochemicals[33].

Adsorbents:

Chitosan can be used as an adsorbent to remove heavy metals due to the presence of amino and hydroxyl groups, which can serve as the active sites[34].   In addition, chitosan and their derivatives have a high affinity for adsorption towards reactive and disperse dyes due to amine groups of chitosan that can be cationized, after which they adsorb anionic dyes strongly by electrostatic attraction in the acidic media[35].

1.3.1 Chitosan Hydrogels

Hydrogels are three-dimensional polymer networks composed of water-soluble polymers which are crosslinked to form a water-insoluble hydrogel. They are able to swell and retain a significant portion of water when placed in an aqueous solution[36]. A superabsorbent hydrogel is defined as a gel which swells over 95% of its composition[37]. Superabsorbent hydrogels have high biocompatibility due to their large degree of water retention and their physiochemical similarity with the native extracellular matrix both compositionally and mechanically.   In addition, they can also be biodegradable[38]. Hydrogels made from biopolysaccharides have played an important role in biotechnology processes including their use in recovery and delivery systems and as support materials[36]. The entrapment of chemicals and biological materials in natural carrier polymers is of interest for a variety of scientific and industrial applications. Natural polymers used as carrier materials in entrapment technology, such as alginate, chitin, and chitosan, have the advantages of being nontoxic, biocompatible, and biodegradable[39]. Hydrogels are often divided into three classes depending on the nature of their network, namely entangled networks, covalently crosslinked networks and networks formed by physical interactions. However for chitosan hydrogels there is no strict borders between classes and there is a continuum of various gels ranging from entangled gels to covalently crosslinked gels. Therefore, it has been suggested to split chitosan hydrogel beads into two classifications; chemical and physical hydrogels[27]. Chemical crosslinked hydrogels are formed by irreversible covalent links[36]. Physical hydrogels are formed by various reversible links. These can be ionic interactions as in ionically crosslinked hydrogel

beads, polyelectrolyte complexes or secondary interactions as in entangled hydrogels.[27]

In crosslinked hydrogels polymeric chains are interconnected by crosslinking agents, leading to the formation of a 3D network. Crosslinkers are molecules of molecular weight much smaller than that of polymers formed between two consecutive crosslinks[40]. The properties of crosslinked hydrogels depend mainly on the crosslinking density, which is the ratio of moles of crosslinking agent to the moles of polymer repeating units[41]. Moreover, a critical number of crosslinks per chain is required to allow the formation of a network, such as that of a hydrogel. Depending on the nature of the crosslinker, the main interactions forming the network are covalent or ionic bonds[42].

Hydrogels based on covalently crosslinked chitosan can be divided into three types with respect to their structure: covalently crosslinked chitosan D-glucosamine units, hybrid polymer networks (HPN) and semi- or full-interpenetrating polymer networks (IPN). In hydrogels formed by HPN, the crosslinking reaction occurs between a structural unit of a chitosan chain and a structural unit of a polymeric chain of another type. Semi- or full- IPNs contain a non-reacting polymer added to the chitosan solution before crosslinking. This leads to the formation of a crosslinked chitosan network in which the non-reacting polymer is entrapped (semi-IPN). It is also possible to further crosslink this additional polymer in order to have two entangled crosslinked networks forming a full-IPN, whose microstructure and properties can be quite different from its corresponding semi-IPN[43].

1.3.2 Formation and Synthesis of Chitosan Hydrogels

Chitosan is a polycationic polymer and therefore reactions with anions which can lead to the formation of a network through ionic bridges between polymeric chains. To form ionically crosslinked chitosan hydrogel beads a charged ionic crosslinker is

required and chitosan should be dispersed in a solvent, commonly water. Ionic crosslinking requires multivalent counter – ions to form bridges between polymeric chains[27]. As chitosan is a polycation, anions or anionic molecules are required. Among anionic molecules, a phosphate-bearing group such as tripolyphosphate is commonly used (Figure 1.5)[44].
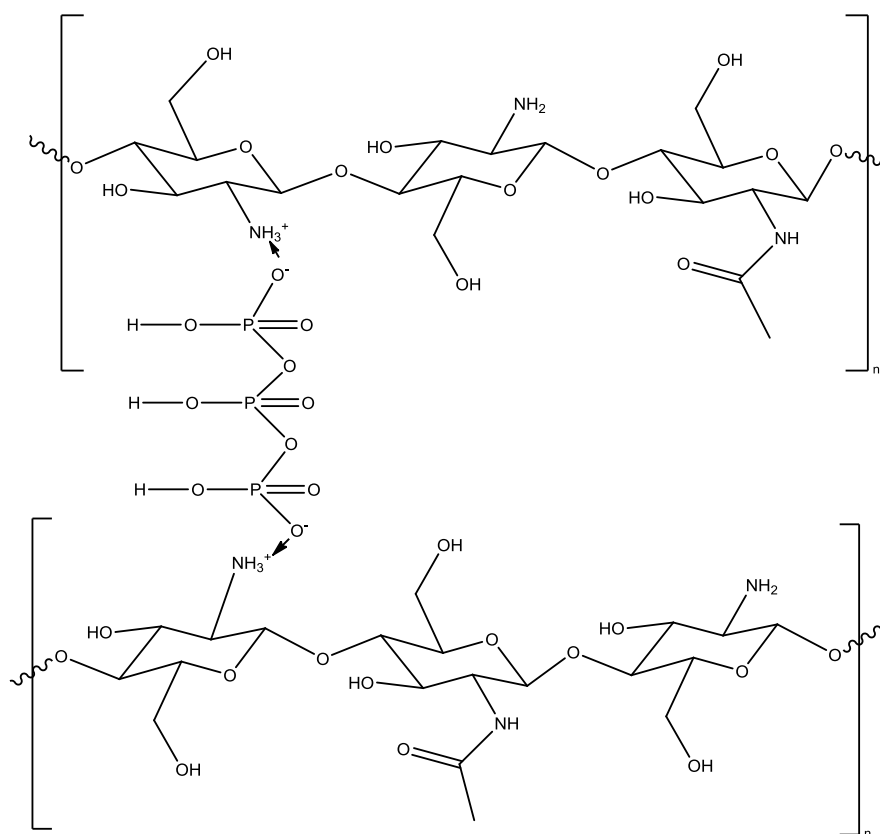
Figure. 1.5 Tripolyphosphate Crosslinked Chitosan

Ionic crosslinking of chitosan is a simple and mild procedure with no auxiliary molecules such as catalysts required[27]. Indeed, ionic crosslinking can be ensured by dissolving the crosslinker and adding it to the chitosan solution[45]. This method allows the formations of a homogeneous hydrogel by a random crosslinking reaction[46]. To modulate hydrogel properties, for applications such as drug release, chitosan has been crosslinked by adding the chitosan solution into the crosslinker solution through a syringe[47]. This system forms a gel bead with a highly crosslinked surface that decreases and finally inhibits the diffusion of crosslinker towards the core of the

network[47]. Following crosslinking, these networks can be further modified by coating with further polymers such as alginate[48] or by covalent crosslinking.

1.3.3 Covalent Crosslinking of Chitosan Hydrogels

Covalent cross-linking is the most straightforward method to produce permanent hydrogel networks using covalent bonding between polymer chains[49]. To date, the most common covalent crosslinkers used with chitosan are dialdehydes such as glyoxal (Figure 1.6) and glutaraldehyde (Figure 1.7)[50]. Their reaction with chitosan is well-documented; the aldehyde groups form covalent imine bonds with the amino groups of chitosan (Figure 1.8) via a Schiff reaction[51].
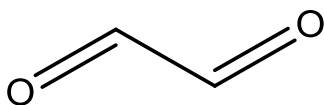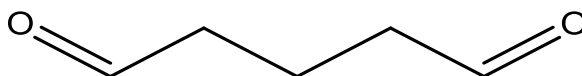
Figure 1.6 Glyoxal   **Figure 1.7 Glutaraldehyde**

Dialdehydes can react with the glucosamine unit of chitosan in a direct reaction in aqueous media and under mild conditions which is advantageous with respect to biocompatibility[52]. The use of genipin is an interesting alternative to dialdehydes. It is a naturally occurring material, which is commonly used in herbal medicine and as a food dye and is particularly effective for cross-linking polymers containing amino groups[49, 53]. Covalent crosslinking of chitosan leads to the formation of permanent network allowing the free diffusion of water and enhancing the mechanical properties of the gel[54]. Covalent crosslinking, and therefore the crosslinking density, is influenced by various parameters, but mainly dominated by the concentration of covalent crosslinker used in the crosslinking solution[55].
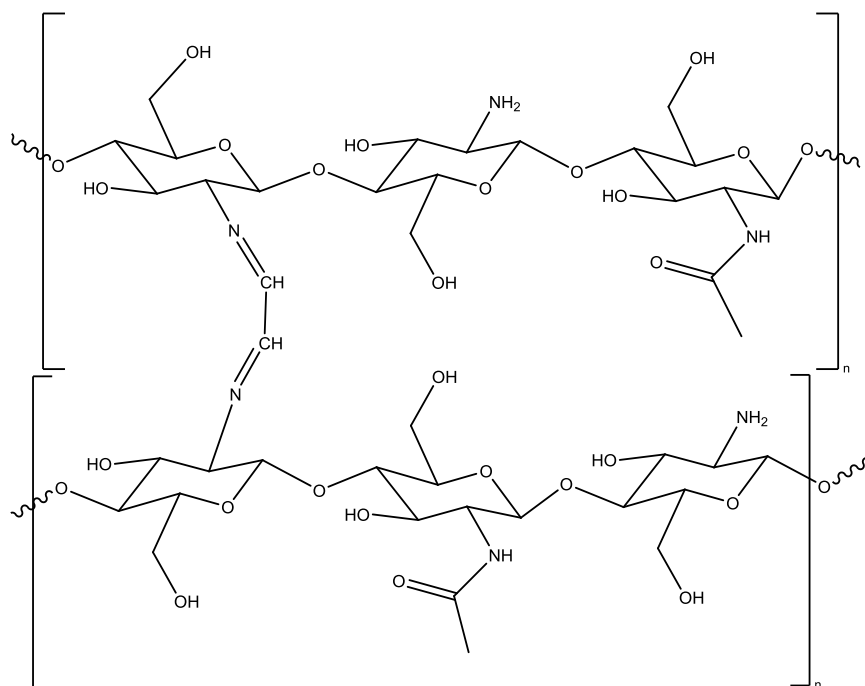
Figure 1.8 Glyoxal Crosslinked Chitosan

1.3.4 Chitosan Hydrogels as a Controlled Delivery System

Drug delivery is a very active research area, especially for employing chitosan as a carrier for various active agents. Chitosan hydrogels are capable of being 'loaded' with a chemical either by encapsulation or absorption. Hydrogels confine a chemical in their polymer network and gradually release it by exchanging the interior gel water with an aqueous solution in a milieu[56]. Whether ionically or covalently crosslinked, hydrogels containing chitosan are considered porous[27]. Due to these pores, 'loaded' crosslinked chitosan hydrogels can be used as delivery systems for agrochemicals, anti-cancer drugs, proteins, antibiotics or vaccines[32, 49] from which the active ingredient are released from the hydrogels by diffusion or polymer chain relaxation[57]. In addition it is possible to introduce chemical modifications to chitosan due to the presence of hydroxyl and amine functional groups to affect the properties of hydrogel beads[58]. *N*-alkyl groups of varying chain lengths have been used to modify the hydrophobicity of these chitosan membranes; the longer the alkyl chain, the more

hydrophobic the chitosan membrane becomes which affects the drug release rate[49]. The release rate of a drug has been shown to be influenced by various factors including the pore size of the gel network, hydrophobicity of the polymer network, the affinity of the macromolecule for chitosan, and the speed at which the hydrogel degrades[49, 59, 60].

1.3.4.1 Chitosan Hydrogels as a Medical Delivery System

Chitosan is currently receiving a great deal of attention as a medical and pharmaceutical delivery system[27]. Chitosan-based systems are used for the delivery of proteins/peptides, growth factors, anti-inflammatory drugs, antibiotics, in gene therapy and bio-imaging applications[49]. This is due to its appealing intrinsic properties. Chitosan is known for its biocompatibility allowing for its use in medical applications such as topical ocular application[61], implantation[62] or injection[63]. Moreover, chitosan is metabolised by certain human enzymes such as lysozyme and is considered biodegradable[64]. In addition it has been reported that chitosan acts as a penetration enhancer by opening tight epithelial junctions. Due to its positive charges at physiological pH, chitosan is also bioadhesive which increases retention at the site of application[65]. The chitosan microspheres exhibit varying drug release characteristics depending on the properties of the encapsulated drugs. The release mechanism and release time of a drug from chitosan microspheres is also dependent on molecular weight of chitosan, concentration of chitosan, drug content and density of crosslinking[29].

1.3.4.2 Chitosan Hydrogels for the Controlled Release of Agrochemicals

The development of chitosan hydrogels to act as a controlled release technology has emerged in recent years for solving problems associated with the application of

conventional agrochemicals[33]. The aim of controlled release formulations is to protect the supply of agrochemical, to maintain the concentration of the agrochemical within the optimum limits over a specific period of time and to allow the automatic release of the agrochemical to the target at a controlled rate[33]. The anti-fungal activity of chitosan and its ability to promote metabolic changes in plants has a favourable influence on the development of crops, inducing increased germination and greater yields[66].

1.3.5 Functionalization of Chitosan

The chemical modification of chitosan is of interest as modifications can maintain the original physicochemical and biochemical properties of the bio-polymer but have the potential to bring new or improved functionality[58]. Several chemical modifications of chitosan such as oligomerization[67], alkylation[68], acylation[69], sulfation[70] and enzymatic modifications[71] along with many other assorted modifications have been carried out in previous research. Of particular interest to this research is that it has been demonstrated that chitosan amino groups are capable of undergoing *N*-acylation with a fatty acid anhydride (Scheme 1.1). This introduces hydrophobicity into the chitosan polymer thereby reducing the hydration of the matrix and potentially allowing for greater controlled drug release[69]. The synthesis of *N*-acylated chitosan under homogenous conditions was pioneered by Shigehiro Hirano and his research group[72]. Hirano and co-workers showed that depending on the structure of the chitosan fibre and the concentration of the carboxylic anhydride in the reaction vessel, chitosan can form a thermally nonreversible gel network[73]. Studies have shown that due to the different reactivates of chitosans amino and hydroxyl sites, the functional group at which *N*-acylation occurs can be controlled[74]. This greatly benefits molecular design for functionalization of chitosan. Choi *et al*. investigated the effect of *N*-acylation of chitosan on its structure and the properties of chitosan fibres. They confirmed by X-ray diffraction that the chemical structure of chitosan fibres was altered by the introduction of *N*-acyl groups[75]. Also, the chemical structural transition occurs by the treated hydrated chitosan fibres becoming randomly stabilised by intramolecular

hydrogen bonding and hydrogen bridging involving water molecules[75]. As a result the chitosan polymer main chain was re-organised into sheet structures via new intermolecular interactions and the substituted hydro-carbon chain resulted in the destruction and new formation of hydrogen bonding[75]. Meanwhile, the hydrophobic interactions enhanced the stability of the fibres and participated in a self-assembly network organisation in accordance with the length of the hydrocarbon chain and the degree of substitution[75].
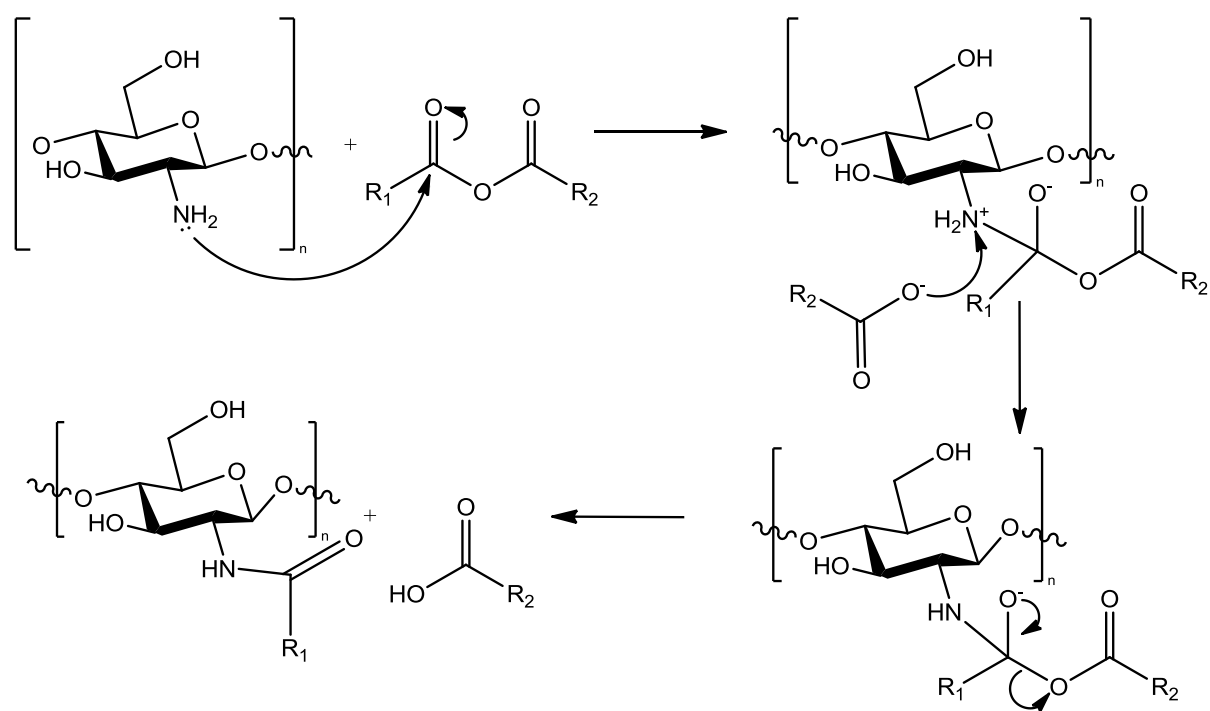
Scheme 1.1 *N*-acylation of chitosan with an acid anhydride

Acylation of chitosan can also take place at the hydroxy site. The *O*-acylation of chitosan has two main benefits; hydrophobic groups contribute organosolubility and the ester linkage is hydrolyzed by an enzyme like lipase[58]. This allows the chitosan to be designed as a biodegradable coating material[58]. The challenge however lies in the higher reactivity of amine group than hydroxyl group. Tong *et al.* managed to achieve selective *O,O'*-acylation by using methanesulfonic acid as an amino site protecting group and then modifying the hydroxyl groups with long hydrophobic alkyl chains (Figure. 1.9)[76]. However selective *O,O'*-acylation is not known to cause a

reorganisation of the chitosan polymer structure in the same way as selective *N-*acylation.
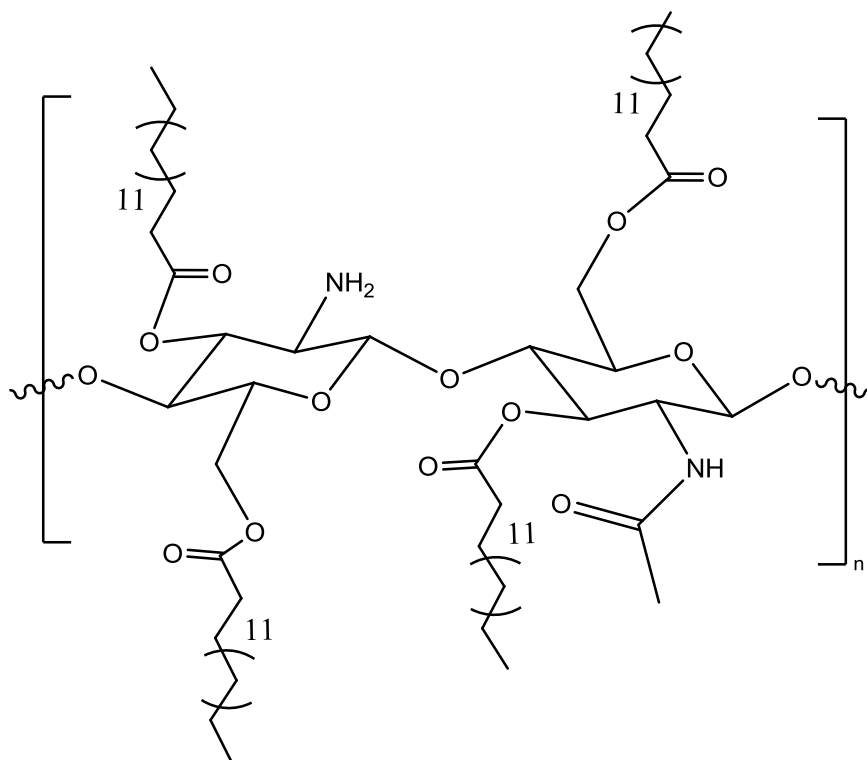
Figure 1.9 *O,O''*-dipalmitoyl chitosan

1.4 Nitrification Inhibitors

Nitrification is an aerobic microbial process by which specialized bacteria oxidize ammonium to nitrite and then to nitrate[77]. Nitrification is a very important part of the nitrogen (N) cycle as for most plants nitrate is the preferred chemical form of nitrogen uptake from soil or water. Nitrification is commonly accomplished by a two stage biological process[78]. The first stage is the oxidation of ammonium (NH_4^+) to nitrite (NO_2^-), a function carried out by bacteria in the genus *Nitrosomonas*. The nitrite formed is rapidly oxidized to nitrate (NO_3^-) by bacteria in the genus *Nitrobacter*[79]. However, NO_3^- is very mobile in the soil[80] and if not absorbed by the crop can be lost by leaching through water movement leading to groundwater contamination or

surface water pollution, which can damage the ecosystem and endanger our drinking water supplies[81]. In studies to combat nitrate leaching nitrification inhibitors have been shown to decrease leaching from urea and ammonium-based fertilisers and from urine patches in grazed pastures[82]. Nitrification inhibitors offer potential for decreased losses through denitrification and delayed leaching through the microbial transformation of ammonium-N (NH_4^+-N) to NO_3^--N, resulting in both greater efficiency of N-use and less pollution[83]. The nitrification inhibitors dicyandiamide (Figure 1.10) and 3,4-dimethyl pyrazole (Figure 1.11) have been known to successfully reduce N_2O emissions from mineral fertilisers[84]. Dicyandiamide (DCD), or cyanoguanidine, is a nitrification inhibitor that is of high importance in agriculture whose ability to limit nitrate leaching has been studied for more than 80 years[85]. DCD is an amine derived from guanidine and is a colourless solid that is soluble in water, acetone, and alcohol. In studies conducted in New Zealand, Di and Cameron showed that N_2O emissions from dairy pasture soils applied with eight applications of 25 kg ha^{-1} throughout the year were reduced by 65-73% when treated with 7.5 – 15 kg ha^{-1} DCD[86]. In Templeton soil, total N_2O emissions were reduced from 37.4 kg N_2O-N ha^{-1} without DCD to 14.6–16.3 kg N_2O-N ha^{-1} when DCD was applied either immediately or 10 days after the urine application[86]. In a separate study, Di and Cameron also showed that the application of DCD at 10 kg ha^{-1} in autumn and late winter decreased NO_3–N leaching from 134 kg N ha^{-1} $year^{-1}$ to 43 kg N ha^{-1} $year^{-1}$ (equivalent to a 68% reduction) from dairy cow urine applied in the autumn at a rate of 1000 kg N ha^{-1} [87].
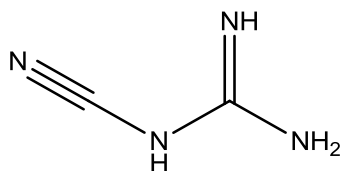
Figure 1.10 Dicyandiamide   Figure 1.11 3,4-dimethylpyrazole
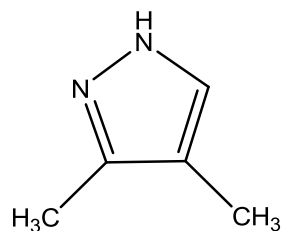
DCD is an amine derived from guanidine and is a colourless solid that is soluble in water, acetone, and alcohol. DCD can also be applied in combination with organic and inorganic nitrogen fertilizers like urea, dung and ammonia compounds. Its nitrification inhibiting potential depends on soil pH, soil structure, humidity, temperature, time, method of fertilization and the rate of inorganic and microbial degradation[85].The persistence of DCD in soil varies with DCD concentration and environmental conditions, in particular temperature and moisture, and the activities of soil microbes that can metabolise DCD as a source of nitrogen. DCD can be leached rapidly during high rainfall, and is generally considered to be active for approximately 4 weeks under field conditions[88]. Currently there are increased economic and environmental requirements to improve nitrogen efficiency on farms. Further studies examining the use of DCD to combat nitrate leaching from urine, fertilizer and manure nitrogen sources are being conducted by Teagasc at Johnstown Castle in collaboration with Lincoln New Zealand, AFBI Northern Ireland and Teagasc Moorepark. This research has shown that DCD significantly reduces NO_3 loads leached (kg ha^{-1}) from urine patches by around 40% or 138 nitrogen/ha and maximum drainage NO_3 concentrations were decreased by 50% on free draining soils[89]. In this thesis a delivery system for DCD based on chitosan hydrogels that can protect the inhibitor as well as allow for controlled release was investigated. Controlled release would be considered to be achieved by developing a delivery system capable of a prolonged delivery time that would maintain an effective concentration of DCD in the release media. As the release time of a small and water soluble water molecule from a porous chitosan gel was likely to be fast, achieving a release time of days would be considered an accomplishment. The amount of DCD released from each chitosan bead was likely to be very small considering soil is often treated with 7.5 – 15 kg ha^{-1}. However, the development a delivery system that can be easily and cost-effectively made in bulk could allow for effective concentrations of DCD to be maintained in the release media.

1.5 Adsorption of Pollutants by Chitosan

Over the years, an increase in some specific pollutants such as industrial chemicals and wastes, have contaminated water supplies and caused deterioration in the quality of drinking water. Waste streams from metal cleaning and plating facilities, mining, corrosion and electronic device manufactures may contain considerable amount of toxic and heavy metals pollutants [90]. Studies have shown that chitosan can be used as a sorbent in adsorption columns or in membrane processes as the biopolymer have a high affinity for metal ions due to the amine ($-NH_2$) and hydroxyl ($-OH$) groups it possesses as these groups function as coordination sites for heavy metal ions[91]. Zhao *et al*. prepared chitosan porous beads for the adsorption and removal of copper(II) ions and reported that the Cu^{2+} loaded porous chitosan beads were stable in water and the heavy metal ion was effectively removed by the chitosan beads[91]. Chen *et al*. investigated the adsorption of three metals of Cu(II), Zn(II), and Pb(II) ions by chitosan crosslinked with epichlorohydrin and found that the chitosan adsorbed all three metal ions by second order kinetics with an adsorption capacity order of Cu^{2+} $>Pb^{2+} >Zn^{2+}$ [92]. Ngah and Fatinathan investigated the adsorption of Pb(II) and Cu(II) ions onto chitosan-tripolyphosphate beads and found that adsorption obeyed the pseudo-second order kinetic model.. It was reported that the chitosan beads were an effective adsorbent for the removal of Pb(II) and Cu(II) ions[93].

1.5.1 Paraquat

Paraquat, (1,1-dimethyl-4,4-bipyridylium dichloride) (Figure 1.12), also known as methyl-viologen, is a pesticide that is extremely hazardous for human health[94]. However, it is one of the most largely used pesticides and is utilized over 130 countries worldwide[95]. It is a quaternary nitrogen herbicide that is widely used in broadleaf weed control. It is a quick acting, non-selective compound that destroys green plant tissue on contact and by translocation within the plant[96].
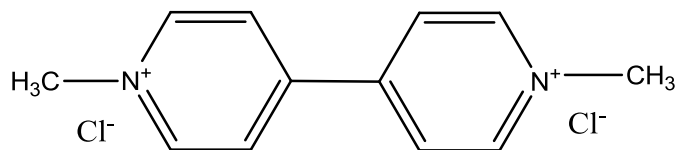
Figure 1.12 Paraquat

Paraquat toxicity in humans occurs almost exclusively through ingestion, of which the major danger is to the lungs[97]. The lungs are mainly affected by direct aspiration, either as the substance is swallowed or by regurgitation from the stomach during vomiting[97]. Recently, the Environmental Protection Agency (EPA) of the United States included paraquat as a possible human carcinogen[98], establishing the drink water equivalent level as 0.2 mg L^{-1} and permitting the commercialization only in a restricted category. A major problem caused by the abusive and uncontrolled use of paraquat is related to its high persistence in the environment where, though only slightly absorbed by soils, it is a potential contaminant of waters due to its high solubility (about 620 g L^{-1} at 25 °C)[99] and therefore its removal from water is imperative.

1.5.2 Removal of Parquat from Water

There are two principal treatment processes for the removal of paraquat from water and wastewater. They are destructive processes such as destructive oxidation[100] and recuperative processes such as adsorption into porous solids[101]. The latter is particularly attractive as its application is relatively easy and requires rather rudimentary apparatus. In addition, its performance is remarkable both for high and low concentrations of paraquat[102]. Literature reports show many studies on paraquat adsorption onto activated carbons which is the most common adsorbent used for its removal from wastewater [103]. However, the cost of this material is the main limitation for its intensive use[104]. As substitution materials, clays have been the subject of numerous research studies and the results obtained to date are often comparable with

those obtained with activated carbons [105]. In recent years, a new class of biosorbents have been investigated as a removal mechanism resulting from their availability, low cost and biodegradability[106]. Accumulation of pollutants on biosorbents and specifically lignocellulosic materials have been investigated thoroughly in recent years[107]. They bind to heavy metals and other waste materials through interactions with the hydroxyl and carboxyl groups that are particularly abundant in polysaccharides (cellulose and hemicelluloses) allowing for the removal of harmful materials from wastewater. Furthermore, the functionalization of the polysaccharides by grafting of organic molecules bearing active groups has been carried out successfully[108]. Interestingly, the use of the resulting hybrid materials as adsorbents leads to significant increases of adsorption capacity of paraquat (sometimes greater than that of activated carbons) compared to raw materials[108, 109]. In addition, polysaccharides have been shown to protect the mucosa against the damaging influence of topical gastric irritants, like paraquat[94]. Preparations of a safer formulation of paraquat which include alginate showed a dose-related reduction in paraquat absorption *in vitro* in isolated rat ileum. Alginates are attractive for this purpose due to their ability to form a gel at low pH, protect the mucosa against topical damage and their extensive use in drug delivery[94].

1.5.3 Calixarenes

Calixarenes are highly versatile synthetic molecules capable of recognising charged and uncharged organic molecules[110]. The tri-dimensional topology of these organic macrocycles is revealed in a hydrophobic cavity and two rims of different size and polarity[110]. Sulfonated calixarenes (*p*-sulfonatocalix[4]arenes) (Figure 1.13) are a class of water soluble calixarenes[111]. They posses three-dimensional, flexible, π-rich cavities that can selectively bind numerous guest molecules such as metal ions, neutral molecules, organic cations, and pharmaceutical molecules in aqueous solution[112-114]. Sulfonated calixarenes are safe with no toxicity *in vivo*[115]. Significantly, studies by Guo *et al.* have showed that sulfonated calixarenes are an

effective detoxification remedy to paraquat poisoning due to the fact that sulfonated calixarenes and paraquat form a stable inclusion complex[116].
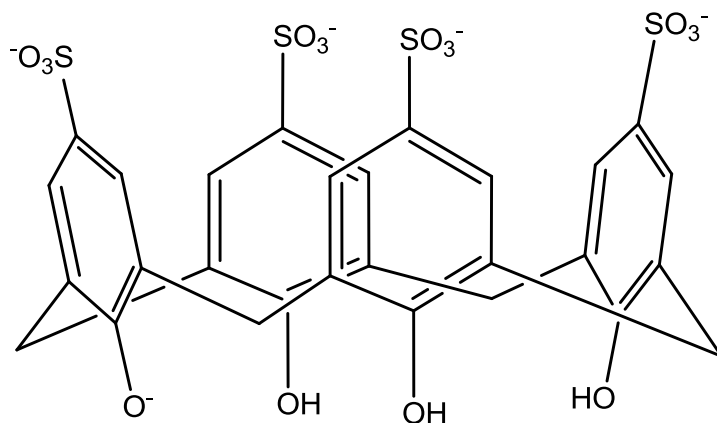
Figure 1.13 Structure of *p*-sulfonatocalix[4]arenes

Chitosan is a polycation that is known to react with negatively charged components, either ions or molecules which leads to the formation of a network structure through ionic bridges between polymer chains[41]. It is also well known for its ability to effectively remove heavy metal pollutants from wastewater by adsorption[92]. Yanagi *et al.* synthesised chitosan beads that were modified with *p*-sulfonatocalix[n]arenes with the aim of adsorbing the organic pollutant di-*n*-butyl phthalate (DBP), a suspected endocrine disruptor, from phosphate buffer. The results indicated that the amount of DBP adsorbed by chitosan beads modified with p-sulfonatocalix[*n*]arenes was approximately five times higher in comparison to the unmodified chitosan beads[117]. Therefore an investigation was performed in this thesis to determine whether chitosan hydrogel beads could be formed by crosslinking with *p*-sulfonatocalix[4]arenes and a study was conducted to determine whether or not this would facilitate the effective adsorption and removal of paraquat from aqueous solutions.

1.6 References

[1]   J. S. McLaren, *Trends in Biotechnology* **2005**, *23*, 339-342.

[2]   J. Metzger and M. Eissen, *Comptes Rendus Chimie* **2004**, *7*, 569-571.

[3]   C. Song, *Catalysis Today* **2006**, *115*, 2-3.

[4]   UN, *COP16/CMP6, Mexico 2010: United Nations Climate Change Conference Official Website*.

[5]   G. Centi and S. Perathoner, *Catalysis Today* **2004**, *77*, 287-297.

[6]   L. Yu, K. Dean and L. Li, *Progress in Polymer Science* **2006**, *31*, 576–602.

[7]   C. Pillai, W. Paul and C. Sharma, *Progress in Polymer Science* **2009**, *34*, 641-678.

[8]   E. Bayer and D. Lenoir, *Chemosphere* **2001**, *43*, 1-135.

[9]   J. O. Metzger, *Chemosphere* **2001**, *43*, 83-87.

[10]   L. G. Wade, *Organic Chemistry*, 4th ed. Addison Wesley Longman, **1999**, p. 1262.

[11]   K. Denniston, R. Caret and J. Topping, *General, Organic and Biochemistry*, 6th ed. McGraw-Hill Science, **2007**, p. 928.

[12]   J. G. Tirrell and D. A. Tirrell, *Current Opinion in Solid State and Materials Science* **1996**, *1*, 407-411.

[13]   D. Chow, M. L. Nunale, D. W. Lim, A. J. Simnick and A. Chilkoti, *Materials Science and Engineering* **2008**, *62*, 125-155

[14]   K. Peter, C. Vollhardt and N. Schore, *Organic Chemistry: Structure and Function*, 5th ed. W. H. Freeman, **1999**, p. 1254.

[15]   T. Heinze and T. Liebert, *Progress in Polymer Science* **2001**, *26*, 1689-1762.

[16]   H. Liu, F. Xie, L. Yu, L. Chen and L. Li, *Progress in Polymer Science* **2009**, *34*, 1348-1368.

[17]   A. Jasim, Al-Karawi, A. Hussein and Al-Daraji, *Carbohydrate Polymers* **2010**, *79*, 769-774.

[18]   R. Tester, J. Karkalas and X. Qi, *Journal of Cereal Science* **2004**, *39*, 151-165.

[19]   R. J. H. Stenekes, H. Talsma and W. E. Hennink, *Biomaterials* **2001**, *22*, 1891.

[20]   R. Mehvar, *Journal of Controlled Release* **2000**, *69*, 2.

[21]   R. Rowe, P. Sheskey and M. Quinn, *Handbook of Pharmaceutical Excipients*, 6th ed. Pharmaceutical Press, **2009**, p. 917.

[22]   J. Yang, Y. Xie and W. He, *Carbohydrate Polymers* **2010**, *84*, 33-39.

[23]   Q. Wang, X. Hu, Y. Du and J. Kennedy, *Carbohydrate Polymers* **2010**, *82*, 842-847.

[24]   A. L. Ingram, O. Deparis, J. Boulenguez, G. Kennaway, S. Berthier and A. R. Parker, *Arthropod Structure & Development* **2011**, *40*, 21-25.

[25]   G. E. Schröder-Turk, S. Wickham, H. Averdunk, F. Brink, J. D. F. Gerald, L. Poladian, M. C. J. Large and S. T. Hyde, *Journal of Structural Biology* **2011**, *174*, 290-295.

[26]   G. Falini, S. Fermani. and A. Ripamonti, *Journal of Inorganic Biochemistry* **2002**, *91*, 475-480.

[27]   J. Berger, M. Reist, J. M. Mayer, O. Felt, N. A. Peppas and R. Gurny, *European Journal of Pharmaceutics and Biopharmaceutics* **2004**, *57*, 19-34.

[28]   W. Xia, P. Liu, J. Zhang and J. Chen, *Food Hydrocolloids* **2011**, *25*, 170-179.

[29]   V. R. Sinha, A. K. Singla, S. Wadhawan, R. Kaushik, R. Kumria, K. Bansal and S. Dhawan, *International Journal of Pharmaceutics* **2004**, *274*, 1-33.

[30]   K. Ziani, B. Ursúa and J. I. Maté, *Crop Protection* **2010**, *29*, 853-859.

[31]   M. Burkatovskaya, G. P. Tegos, E. Swietlik, T. N. Demidova, A. P. Castano and M. R. Hamblin, *Biomaterials* **2006**, *27*, 4157-4164.

[32]   J. P. Quiñones, Y. C. García, H. Curiel and C. P. Covas, *Carbohydrate Polymers* **2010**, *80*, 915-921.

[33]   A. Akelah, *Materials Science and Engineering* **1996**, *4*, 83-98.

[34]   F. Wu, R. Tseng and R. Juang, *Journal of Environmental Management* **2010**, *91*, 798-806.

[35]   V. K. Konaganti, R. Kota, S. Patil and G. Madras, *Chemical Engineering Journal* **2010**, *158*, 393-401.

[36]   K. Deligkaris, T. S. Tadele, W. Olthuis and A. v. d. Berg, *Sensors and Actuators B: Chemical* **2010**, *147*, 765-774.

[37]   I. C. Alupei, M. Popa, M. Hamcerencu and M. Abadie, *European Polymer Journal* **2002**, *38*, 2313-2320.

[38]   I. Al Sarra, S. Neau and M. Howard, *Biomaterials* **2004**, *25*, 2645-2655.

[39]   N. A. Peppas, *Fundamentals* **1986**, *1*, 1–25.

[40]   S. Chen, M. Liu, S. Jin and B. Wang, *International Journal of Pharmaceutics* **2008**, *349*, 180–187.

[41]   J. Berger, M. Reist, J. M. Mayer, O. Felt, N. A. Peppas and R. Gurny, *European Journal of Pharmaceutics and Biopharmaceutics* **2004**, *57*, 20-21.

[42]   M. Z. Wang, Y. Fang and D. D. Hu, *Reactive and Functional Polymers* **2001**, *48*, 215–221.

[43]   F. L. Mi, S. S. Shyu, T. B. Wong, S. F. Jang, S. T. Lee and K. T. Lu, *Journal of Applied Polymer Science* **1999**, *74*, 1093–1107.

[44]   J. Y. Lee, S. H. Nam, S. Y. Im, Y. J. Park, Y. M. Lee, Y. J. Seol, C. P. Chung and S. J. Lee, *Journal of Controlled Release* **2002**, *78*, 187–197.

[45]   K. I. Draget, K. M. Varum, E. Moen, H. Gynnild and O. Smidsrod, *Biomaterials* **1992**, *13*, 635–638.

[46]   F. L. Mi, C. T. Chen, Y. C. Tseng, C. Y. Kuan and S. S. Shyu, *Journal of Controlled Release* **1997**, *44*, 19-32.

[47]   X. Z. Shu, K. J. Zhu and W. Song, *International Journal of Pharmaceutics* **2001**, *212*, 19-28.

[48]   M. Dash, F. Chiellin, R. M. Ottenbrite and E. Chiellini, *Progress in Polymer Science* **2011**, *36*, 981–1014.

[49]   M. N. Khalid, L. Ho, J. L. Agnely, J. L. Grossiord and G. Couarraze, *STP Pharma Sciences* **1999**, *9*, 359-364.

[50]   O. A. C. Monteiro and C. Airoldi, *International Journal of Biological Macromolecules* **1999**, *26*, 119-128.

[51]   G. X. Cheng, J. Liu, R.Z. Zhao, K. D. Yao, P. C. Sun, A. J. Men, W. H. Wang and L. Wei, *Journal of Applied Polymer Science* **1998**, *67*, 983–988.

[52]   F. L. Mi, H. W. Sung and S. S. Shyu, *Journal of Polymer Science* **2008**, *38*, 2804–2814.

[53]   K. Kurita, Y. Koyama and T. Taniguchi, *Journal of Applied Polymer Science* **1986**, *31*, 1169–1176.

[54]   W. Arguelles-Monal, F. M. Goycoolea, C. Peniche and I. Higuera-Ciapra, *Polymer Gels Network* **1998**, *6*, 429–440.

[55]   D. Tada, T. Tanabe, A. Tachibana and K. Yamauchi, *Journal of Bioscience and Bioengineering* **2005**, *100*, 551-555.

[56]   D. Thacharodi and K. P. Rao, *Journal of Chemical Technology & Biotechnology* **1993**, *58*, 177–181.

[57]   V. K. Mourya and N. N. Inamdar, *Reactive and Functional Polymers* **2008**, *68*, 1013-1051.

[58]   M. L. Lorenzo-Lamosa, C. Remunan-Lopez, J. L. Vila-Jato and M. J. Alonso, *Journal of Controlled Release* **1998**, *52*, 109–118.

[59] M. George and T. E. Abraham, *Journal of Controlled Release* **2006**, *114*, 1–14.

[60] O. Felt, P. Furrer, J. M. Mayer, B. Plazonnet, P. Buri and R. Gurny, *International Journal of Pharmaceutics* **1999**, *180*, 185–193.

[61] S. Patashnik, L. Rabinovich and G. Golomb, *Journal of Drug Targeting* **1997**, *4*, 371–380.

[62] J. S. Song, C. H. Such, Y. B. Park, S. H. Lee, N. C. Yoo, J. D. Lee, K. H. Kim and S. K. Lee, *European Journal of Nuclear Medicine* **2001**, *28*, 489–497.

[63] R. A. A. Muzzarelli, *Cellular and Molecular Life Sciences* **1997**, *53*, 131–140.

[64] P. He, S. S. Davis and L. Illum, *International Journal of Pharmaceutics* **1998**, *166*, 75-88.

[65] B. Fristensky, L. Hadwiger and R. Riggleman, *Chitin, Chitosan and Related Enzymes*, 1st ed. Academic Press, **1984**, p. 423.

[66] M. Thanou, A. F. Kotze, T. Scharringhausen, H. L. Lueben, A. G. d. Boer, J. C. Verhoef and H. E. Junginger, *Journal of Controlled Release* **2000**, *64*, 15-25.

[67] M. Li, S. Su, M. Xin and Y. Liao, *Journal of Colloid and Interface Science* **2007**, *311*, 285-288.

[68] C. L. Tien, M. Lacroix, P. Ispas-Szabo and M. A. Mateescu, *Journal of Controlled Release* **2003**, *93*, 1-13.

[69] R. Whistler and M. Kosik, *Biochemistry and Biophysics* **1971**, *143*, 106-110.

[70] G. Kumar, P. J. Smith and G. F. Payne, *Bioresource Technology* **2004**, *91*, 157-162.

[71] S. Hirano, R. Yamaguchi, N. Fukui and M. Iwata, *Carbohydrate Research* **1990**, *201*, 145–149.

[72] L. Félix, J. Hernández, W. M. Argüelles-Monal and F. M. Goycoolea, *Biomacromolecules* **2005**, *6*, 2408–2415.

[73]   Y. Wu, T. Seo, T. Sasaki, S. Irie and K. Sakurai, *Carbohydrate Polymers* **2006**, *63*, 492-499.

[74]   C. Y. Choi, S. B. Kim, P. K. Pak, D. I. Yoo and Y. S. Chung, *Carbohydrate Polymers* **2007**, *68*, 122-127.

[75]   Y. Tong, S. Wang, J. Xu, B. Chua and C. He, *Carbohydrate Polymers* **2005**, *60*, 229-233.

[76]   L. Juliette, M. Hyman and D. Arp, *Applied and Environmental Microbiology* **1993**, *59*, 3718-3727.

[77]   C. Liu, H. Honda, A. Ohshima, M. Shinkai and T. Kobayashi, *Journal of Bioscience and Bioengineering* **2000**, *89*, 420-425.

[78]   C. Grunditz and G. Dalhammar, *Water Research* **2001**, *35*, 443-440.

[79]   S. Wu, L. Wu, Q. Shi, Z. Wang, X. Chen and Y. Li, *Journal of Environmental Sciences* **2007**, *19*, 841-847.

[80]   A. Zhu, J. Zhang, B. Zhao, Z. Cheng and L. Li, *Environment International* **2005**, *31*, 904-912.

[81]   M. O'Callaghan, E. M. Gerard, P. E. Carter, R. Lardner, U. Sarathchandra, G. Burch, A. Ghani and N. Bell, *Soil Biology and Biochemistry* **2010**, *42*, 1425-1436.

[82]   W. R. Cookson and I. S. Cornforth, *Soil Biology and Biochemistry* **2001**, *34*, 1461-1465.

[83]   X. M. B. Macadam, A. d. Prado, P. Merino, J. M. Estavillo, M. Pinto and C. González-Murua, *Journal of Plant Physiology* **2003**, *160*, 1517-1523.

[84]   C. Schwarzer and K. Haselwandter, *Journal of Chromatography A* **1996**, *732*, 390-393.

[85]   H. J. Di and K. C. Cameron, *Biology and Fertility of Soils* **2006**, *42*, 472–480.

[86]   H. J. Di and K. C. Cameron, *Agriculture, Ecosystems and Environment* **2005**, *109*, 202–212.

[87]   M. Hauser and K. Haselwandter, *Soil Biology and Biochemistry* **1990**, *22*, 113-114.

[88]   S. J. Dennis in *Reducing Nitrate Losses from Grazed Grassland in Ireland Using a Nitrification Inhibitor (DCD)*, *Vol. PhD* Lincoln University, **2011**.

[89]   W. S. W. Ngah and S. Fatinathan, *Chemical Engineering Journal* **2008**, *143*, 62–72.

[90]   F. Zhao, B. Yu, Z. Yue, T. Wang, X. Wen, Z. Liu and C. Zhao, *Journal of Hazardous Materials* **2007**, *147*, 67-73.

[91]   A. Chen, S. Liu, C. Chen and C. Chen, *Journal of Hazardous Materials* **2008**, *154*, 184–191.

[92]   W. S. W. Ngah and S. Fatinathan, *Journal of Environmental Management* **2010**, *91*, 958–969.

[93]   J. R. Heylings, M. J. Farnworth, C. M. Swain, M. J. Clapp and B. M. Elliott, *Toxicology* **2007**, *241*, 1-10.

[94]   D. D. Souza and S. A. S. Machado, *Analytica Chimica Acta* **2005**, *546*, 85-91.

[95]   M. A. E. Mhammedi, M. Bakasse and A. Chtani, *Journal of Hazardous Chemicals* **2007**, *145*, 1-7.

[96]   P. Shivhare and V. K. Gupta, *Analyst* **1991**, *116*, 391-393.

[97]   *EPA 822-R-06-013*, United States Office of Water, **2006**.

[98]   E. Halfon, S. Galassi, R. Bruggemann and A. Provini, *Chemosphere* **1996**, *33*, 1543-1562.

[99]   R. Andreozzi, A. Insola, V. Caprio and M. G. D'Amore, *Journal of Environmental Technology* **1993**, *14*, 695-700.

[100]   E. Gonzalez-Pradas, M. Villafranca-Sanchez, A. Gallego-Campo, D. Urena-Amate and M. Socias-Viciana, *J. Chem. Tech. Biotechnol* **1997**, *69*, 173–178.

[101]   A. E. Ofomaja, *Chemical Engineering Journal* **2008**, *143*, 85–95.

[102] N. K. Hamadi, S. Swaminathan and X. D. Chen, *Journal of Hazardous Materials* **2004**, *112*, 133–141.

[103] M. Akhtar, S. M. Hasany, M. I. Bhanger and S. Iqbal, *Chemosphere* **2007**, *66*, 1829–1838.

[104] W. T. Tsai, C. W. Lai and K. J. Hsien, *Journal of Colloid and Interface Science* **2003**, *263*, 29-34.

[105] C. P. Nanseu-Njiki, G. K. Dedzo and E. Ngameni, *Journal of Hazardous Materials* **2010**, *179*, 63-71.

[106] M. C. Basso, E. G. Cerrella and A. L. Cukierman, *Industrial & Engineering Chemistry Research* **2002**, *41*, 3580–3585.

[107] S. Hsu and T. Pan, *Bioresource Technology* **2007**, *98*, 3617-3621.

[108] R. Gong, M. Feng, J. Zhao, W. Cai and L. Liu, *Bioresource Technology* **2009**, *100*, 975-978.

[109] I. García-Sosa and F. Ramírez, *Journal Mexican Chemistry Society* **2010**, *54*, 143-152.

[110] G. Wang, X. Ren, M. Zhao, X. Qiu and A. Qi, *Journal of Agriculture and Food* **2011**, *59*, 4294–4299.

[111] C. Bonal, Y. Israeli, J. P. Morel and N. Morel-Desrosiers, *Journal of the Chemistry Society: Perkins Trans* **2001**, *2*, 1075–1078.

[112] Y. Liu, D. Guo, H. Zhang, Y. Ma and E. Yang, *Journal of Physical Chemistry B* **2006**, *110*, 3428–3434.

[113] D. S. Guo, K. Wang and Y. Liu, *Journal of Inclusion Phenomena and Macrocyclic Chemistry* **2008**, *62*, 1–21.

[114] A. Coleman, S. Jebors, S. Cecillon, P. Perret, D. Garin and D. Marti-Battle, *New Journal of Chemistry* **2008**, *32*, 780–782.

[115] D. Guo, L. Wang and Y. Liu, *Journal of Orangic Chemistry* **2007**, *72*, 7775–7778.

[116]   A. Yanagi, H. Otsuka and A. Takahara, *Polymer Journal* **2005**, *37*, 939-945.

Chapter 2: Experimental

2.1 Introduction

The present research is concerned with the preparation of chitosan beads; their characterisation and dicyandiamide (DCD) release properties. Chitosan is soluble in acidic aqueous solution, which allows it to form hydrogel beads. These beads can then be crosslinked with an ionic or covalent crosslinker and loaded with the nitrification inhibitor, DCD. The release of DCD into aqueous solution was monitored using UV/vis spectroscopy. The release mechanism of DCD from these beads could then be interpreted by the fitting of release data to appropriate models. An investigation was also carried out as to whether the chitosan hydrogel beads could be post-functionalised by *N*-acylation in their hydrogel state. The *N*-acylated chitosan beads were characterised using Fourier transform infrared spectroscopy, differential scanning calorimetry and scanning electron microscopy. The present research is also concerned with the synthesis of chitosan hydrogel beads crosslinked with *p*-sulfonatocalix[4]arene to facilitate the removal of paraquat from an aqueous solution. The ability of the hydrogel beads to remove paraquat from aqueous solution was investigated by UV/vis spectroscopy.

In this chapter, the various materials and methods used throughout this work are described in detail. A brief description of the theoretical background for each of the different experimental techniques is also provided.

2.2 Chemicals and Synthesis

2.2.1 Chemicals

Unless otherwise stated, all chemicals and solvents used in this work were purchased from Sigma-Aldrich. The chitosan purchased was 85% deacetylated, sodium

hydroxide pellets were semiconductor grade (99%), sodium tripolyphosphate (85%), dicyandiamide (99%), trisodium citrate was purchased whose quality level was described as premium by Sigma-Aldrich, sodium molybdate (99.5%) and sodium alginate was purchased with a viscosity of 15-20 cP, 1 % in H_2O. The covalent crosslinkers investigated were glyoxal solution 40 wt. % in H_2O and glutaraldehyde grade 1, 25% in H_2O, while the purity of genipin powder was ≥ 98%. Two carboxylic anhydrides were purchased, hexanoic anhydride (97%) and the acetic anhydride (99.5%). In addition, two acyl chlorides were purchased; octanoyl chloride (99%) and palmitoyl chloride (98%). Triethylamine (≥99%), *p-tert*-butylphenol, *para*formaldehyde (95%), phenol (99%) and aluminium chloride (≥99%) were purchased from Sigma Aldrich. All other chemicals and solvents were of analytical reagent grade and used as received. The chitosan gelling, crosslinking and release solutions were prepared in Millipore water.

2.2.2 Preparation of Hydrogel Bead Delivery Systems

2.2.2.1 Preparation of Chitosan Hydrogel Beads

Chitosan hydrogel beads were synthesised by three methods in this research, precipitation, ionic gelation and by a combination of both.

2.2.2.1 (i) Precipitation

Using a chitosan hydrogel synthesis method adapted from Zhao *et al.*[1]; 2 g of chitosan flakes were added to 100 mL of 1% (v/v) acetic acid Millipore water in a beaker to obtain a chitosan solution and the mixture was stirred overnight. The chitosan solution was then dropped through a tube of inner diameter 0.5 mm into 300 mL of 60 mM DCD and 0.75 M NaOH solution and left to precipitate out for 24 h. After removing the beads from the sodium hydroxide solution they were washed in a 60 mM DCD

Millipore water solution for 24 h until reaching neutrality. The beads were stored in 60 mM DCD Millipore water solution.

2.2.2.1 (ii) Ionic Gelation

Using a chitosan hydrogel synthesis method adapted from Guo *et al.*[2]; 2 g of chitosan flakes were added to 100 mL of 1% (v/v) acetic acid Millipore water in a beaker to obtain chitosan solution and the mixture stirred overnight. Then the chitosan solution was dropped through a syringe needle into 300 mL of 60 mM DCD and 110 mM sodium tripolyphosphate (TPP) solution and was allowed to crosslink for 24 h. After removing the beads from the gelling solution they were washed in a 60 mM DCD Millipore water solution for a further 24 h until reaching neutrality. The beads were stored in 60 mM DCD Millipore water solution.

2.2.2.1 (iii) Precipitation and Ionic Gelation

2 g of chitosan flakes were added to 100 mL of 1% (v/v) acetic acid Millipore water in a beaker to obtain chitosan solution and the mixture was stirred overnight. Then the chitosan solution was dropped through a syringe needle into 300 mL of 60 mM DCD, 0.75M NaOH and 110 mM of a known ionic crosslinker and was allowed to crosslink for 24 h. After removing the beads from the gelling solution they were washed in a 60 mM DCD Millipore water solution for a further 24 h until reaching neutrality. The beads were stored in 60 mM DCD Millipore water solution.

2.2.2.2 Preparation of Dual-Crosslinked and Multilayer Beads

Recently, polyelectrolyte complexes composed of chitosan-alginate reinforced with polyphosphate have been developed[3]. These beads are described as multilayer[3] or dual crosslinked[4] beads. They are considered 'reinforced beads'[3] and are synthesized in a

'coagulation' and 'post-coagulation' fluid. In this research multilayer beads were synthesised using the method devised by Anal and Stevens[3] while dual crosslinked beads were synthesised according to the method employed by Xu *et al*[4].

2.2.2.2 (i) Multilayer Beads

2 g of chitosan flakes were added to 100 mL of 1% (v/v) acetic acid Millipore water in a beaker to obtain chitosan solution and the mixture stirred overnight. The chitosan solution was then dropped through a syringe needle into 300 mL of 0.8% (w/v) sodium alginate, 60 mM DCD and 8% w/v sodium tripolyphosphate solution and the beads were allowed to gel for 24 h. The resulting beads were washed in Millipore water for 24 h and mechanically stirred in a 100 mL aqueous post-coagulation solution which contained 0.08% (w/v) sodium alginate and 2% (w/v) $CaCl_2$ for 10 min. The presence of calcium ions allowed for the gelation of alginate and facilitated its crosslinking with chitosan[5]. After removal from the post-coagulation fluid they were washed in 60 mM DCD Millipore water solution for a further 24 h until reaching neutrality. The beads were stored in 60 mM DCD Millipore water solution.

2.2.2.2 (ii) Dual-Crosslinked Beads

2 g of chitosan flakes were added to 100 mL of 1% (v/v) acetic acid Millipore water in a beaker to obtain chitosan solution and the mixture stirred overnight. The chitosan solution was then dropped through a syringe needle into a 300 mL aqueous solution of 8% (w/v) sodium alginate, 3% (w/v) TTP, 60 mM DCD and 0.75 M NaOH and allowed to gel for 24 h. The hydrogel beads were then washed in Millipore water for 24 h and then put into a 100 mL aqueous 2% (w/v) calcium chloride solution under mechanical stirring at 25 rpm for 15 min and then placed in a 50 mL solution of 2% (w/v) sodium sulfate solution for 15 min. The hydrogel beads were then washed in 60 mM DCD Millipore water solution for a further 24 h until reaching neutrality. The beads were stored in 60 mM DCD Millipore water solution.

2.2.2.3 Covalent Crosslinking

In order to covalently crosslink the chitosan hydrogel beads synthesised in Section 2.2.2.1 the beads were transferred from Millipore water storage to an aqueous solution containing either a known molar concentration of genipin, glyoxal or glutaraldehyde. They were stirred at a rate of 25 rpm for 24 h, then removed from the crosslinking solution and washed with 60 mM DCD Millipore water solution for a further 24 h until reaching neutrality and were stored in a fresh 60 mM Millipore water solution. Unless otherwise stated, the covalently crosslinked beads were first gelled in a 0.75 M NaOH and 110 mM TPP solution.

2.2.2.4. Dehydration of Chitosan Hydrogel Beads

In order to remove the Millipore water from the interior of the bead they were placed in an oven set to 37 ± 1 °C for a minimum of 24 h by which time the water had left the bead and it was no longer considered a 'hydrogel'. The dehydrated chitosan beads are referred to as chitosan 'xerogel' beads.

2.2.2.5 Evaluation of DCD Loading Capacity of Chitosan Hydrogel or Xerogel Beads

DCD loaded chitosan hydrogel or xerogel beads were suspended in a 0.1 M HCL solution for 14 days by which time the bead had disintegrated. The DCD loading capacity was evaluated by measuring the ultraviolet absorption of the supernatant at 214 nm, the λ max of DCD, and comparing it with the equivalent reading from blank chitosan beads. Each experiment was performed in triplicate.

2.2.3 Preparation of *N*-Acylated Chitosan Hydrogel Beads

The *N*-acylation of chitosan hydrogel beads with acid anhydrides and acyl chlorides was investigated in this research. The *N*-acylation of chitosan hydrogel beads in their solid state with long aliphatic carbon chains is based upon synthetic conditions used to modify chitosan fibres developed by Hirano *et al*[6] The *N*-acylation of the chitosan hydrogel beads was carried out either with an acidic anhydride (Section 2.2.3.1) or an acyl chloride (Section 2.2.3.2).

2.2.3.1 *N*-Acylation of Chitosan Hydrogels with an Acidic Anhydride

To prepare the chitosan beads 2 g of chitosan flakes were added to 100 mL of 1% (v/v) acetic acid Millipore water in a beaker to obtain a chitosan solution and the mixture was stirred overnight. The chitosan solution was then dropped through a tube of inner diameter 0.5 mm into a 0.75 M NaOH 300 mL aqueous solution and left to precipitate out for 24 h. After removing the beads from the sodium hydroxide solution they were washed in a Millipore water solution for 24 h until reaching neutrality. The chitosan hydrogel beads were then suspended in 100 mL of methanol in round bottom flask and a pre-determined volume of an acid anhydride was added. The mixture was refluxed for 24 h. Then the treated chitosan hydrogel beads were washed several times with methanol, acetone, and finally Millipore water before being stored in Millipore water solution.

2.2.3.2 *N*-Acylation of Chitosan Hydrogel Beads with an Acyl Chloride

To prepare the chitosan beads 2 g of chitosan flakes were added to 100 mL of 1% (v/v) acetic acid Millipore water in a beaker to obtain a chitosan solution and the

mixture was stirred overnight. The chitosan solution was then dropped through a tube of inner diameter 0.5 mm into a 0.75 M NaOH 300 mL aqueous solution and left to precipitate out for 24 h. After removing the beads from the sodium hydroxide solution they were washed in a Millipore water solution for 24 h until reaching neutrality. Chitosan hydrogel beads were suspended in mixture of 100 mL of acetone and 5 mL triethylamine and mechanically stirred at 25 rpm for 4 h. Then a pre-determined volume of an acyl chloride was added. The mixture was refluxed for 24 h. Then the treated chitosan hydrogel beads were washed several times with acetone, methanol, dichloromethane and finally Millipore water.

2.2.3.3 DCD Loading

The *N*-acylated chitosan hydrogel beads formed in Sections 2.2.3.1 and 2.2.3.2 were loaded in 60 mM DCD Millipore water solution. The hydrogel beads were mechanically stirred at a rate of 25 rpm in the solution for a minimum of 24 h before the beads were used as a delivery system or were dried.

2.2.4 Synthesis of a Paraquat Adsorption System

The hydrogel beads investigated for the adsorption and removal of paraquat from aqueous solution were formed by polyion complexation between cationized chitosan and an ionic calixarene as based upon the synthesis conditions used by Yanagi *et al*[7]. Chitosan is a hydrophilic polymer which allows the hydrophobic cavities of calixarenes to function effectively as molecular receptors. Therefore, *p*-sulonatocalix[4]arenes (C4S) were synthesised and crosslinked with chitosan to form C4S-chitosan hydrogel beads to act as a paraquat adsorption system. The compound was synthesised in four steps in agreement with Doyle[8] using the methods outlined by Gutsche[9-11] and Shinaki[12].

2.2.4.1 Synthesis of *p*-Sulonatocalix[4]arene (C4S)

***Step   1*:   Synthesis   of   5,11,17,23,29,35,41,47-octa-tert-butyl-49,50,51,52,53,54,55,56-octahydroxycalixarene (Compound 1).**
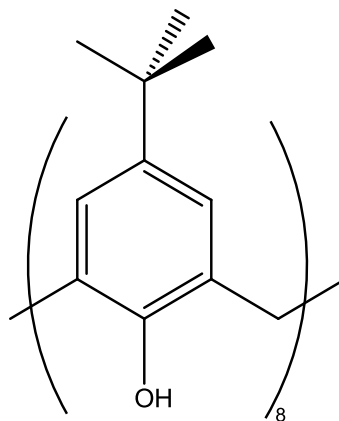
A slurry of *p-tert*-butylphenol (56.0 g, 0.36 mol), *para*formaldehyde (18.0 g, 0.60 mol) and 10 M KOH (0.8 mL, 8 mmol) in xylene (250 mL) was refluxed with stirring for 4 h in a 1000 mL flask equipped with a Dean Stark water collector. The reaction mixture was then cooled, and the precipitate was isolated by filtration. The solid product was washed in succession with 150 mL portions of toluene, ether, acetone and water and then dried in an oven at 50 °C overnight.

Yield: 47.6 g, 81%

^{1}H NMR (CDCl$_3$): (δ ppm)

9.62 (s, 8H, Ar-OH), 7.18 (s, 16H, Ar-H), 4.37 (br d, 8H, CH$_2$, J = 12.9 Hz), 3.50 (br d, 8H, CH$_2$, J= 12.9 Hz), 1.25 (s, 72H, C(CH$_3$)$_3$).

***Step 2*: Synthesis of 5,11,17,23-tera-tert,butyl-25,26,27,28-tetahyroxy-calix[4]arene (Compound 2).**
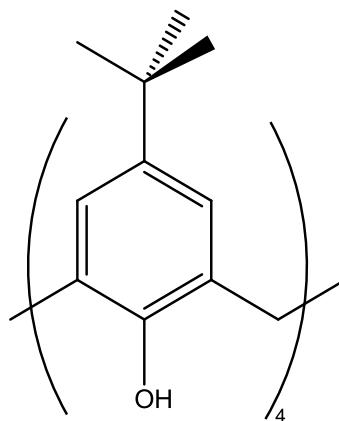
A slurry of Compound 1 (22.0 g, 16.0 mmol) and 10 M NaOH (0.5 mL, 5 mmol) in diphenyl ether (200 mL) was refluxed for 1.5 h in a 1000 mL flask equipped with a Dean Stark water collector. The reaction mixture was cooled and treated with ethyl acetate (200 mL). The precipitate was isolated by filtration and washed in succession with 100 mL portions of toluene, ether, acetone and water, and dried in an oven at 50 °C overnight.

Yield: 14.9 g, 68%

^{1}H NMR (CDCl$_3$): (δ ppm)

10.34 (s, 4H, Ar-OH), 7.05 (s, 8H, Ar-H), 4.25, (br d, 4H, CH$_2$, *J* =12.6 Hz), 3.49 (br d, 4H, CH$_2$, *J* = 12.6 Hz), 1.12 (s, 36H, C(CH$_3$)$_3$).

Step 3: **Synthesis of 25,26,27,28-tetrahydroxycalix[4]arene (Compound 3).**
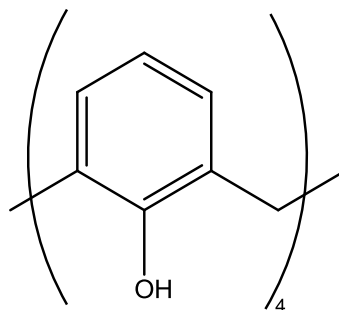
A slurry of Compound 2 (5.0 g, 7.5 mmol), phenol (3.4 g, 36.0 mmol) and $AlCl_3$ (5.3g, 39.5 mmol) in toluene (50 mL) was stirred at room temperature for 4 h in an inert atmosphere. The mixture was poured into 0.2 M HCl (100 mL), the organic layer was separated and the toluene was evaporated under reduced pressure. Upon addition of methanol a precipitate formed, which was recovered by filtration. The final product was recrystallised from methanol/chloroform.

Yield: 2.3g, 70%

^{1}H NMR (CDCl₃): (δ ppm)

10.20 (s, 4H, Ar-OH), 7.05 (d, 8H, Ar-H, *J* = 7.7 Hz), 6.73 (t, 4H, Ar-H, *J* = 7.7 Hz), 4.25 (s, 4H, CH₂), 3.55 (s, 4H, CH₂).

Step 4: Synthesis of *p*-sulfonatocalix[4]arene (C4S)
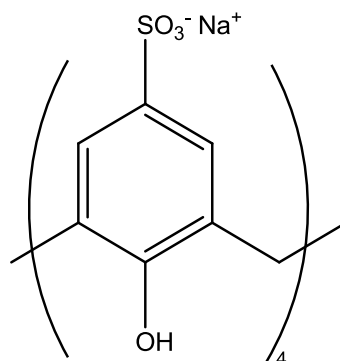
Compound 3 (1.0 g, 2.4 mmol) was mixed with concentrated H_2SO_4 (10 mL) and the solution was heated at 60 °C for 4 h. An aliquot was withdrawn from the reaction mixture and poured into water to determine the progress of the reaction. The reaction was completed when no water-insoluble material was detected in the aliquot. After cooling, the precipitate was filtered off through a sintered glass filter. The precipitate was dissolved in water and the aqueous solution was neutralised by $CaCO_3$. Precipitated $CaCO_4$ was filtered off and washed with hot water. The combined filtrate and washings were evaporated to dryness under reduced pressure. The residue was dissolved in hot water (15 mL) and the solution was adjusted to pH 8 by addition of Na_2CO_3. After filtration, methanol was added to the filtrate to afford a white precipitate. The product was recovered by filtration and tested for carbonate impurities using infrared spectroscopy. To remove these impurities the product was dissolved in boiling distilled water and any insoluble material removed by filtration. The product was then precipitated from solution by the addition of methanol, recovered by filtration and tested for impurities using infrared spectroscopy. This process was repeated until the carbonate signal in the infrared spectrum was no longer observed.

Yield: 1.3 g, 55%

v_{max} / cm^{-1} (KBr):

(OH) 3447, (SO$_3^-$) 1179 and 1048.

.

¹H NMR (CDCl₃): (δ ppm)

7.47 (s, 8H, Ar-H), 3.92 (s, 8H, CH₂) This was in agreement with literature[8].

¹³C NMR (D₂O): (δ ppm)

155.7, 133.5, 130.4, 125.9, 31.8.

2.2.4.2 Synthesis of C4S-Chitosan Hydrogel Beads

Using a chitosan hydrogel synthesis method adapted from Guo *et al.*[2]; 2 g of chitosan flakes were added to 100 mL 1% (v/v) acetic acid in a beaker to obtain chitosan solution and the mixture was stirred overnight. The chitosan solution was then dropped through a syringe needle into a 50 mL, 18 mM, 12 mM or 6 mM C4S solution and the resulting hydrogel beads were allowed to gel for 24 h. After removing the beads from the gelling solution they were washed with Millipore water for a further 24 h until reaching neutrality. The hydrogel beads were stored in Millipore water for further use.

2.3 Experimental Techniques

The analysis and characterisation of synthesised chitosan hydrogel beads were carried out by Fourier transform infrared spectroscopy, differential scanning calorimetry, elemental analysis, scanning electron microscopy and energy-dispersive X-ray analysis. The DCD release and paraquat adsorption studies were performed using a UV/vis spectrometer.

2.3.1 Scanning Electron Microscopy and Energy-Dispersive X-ray Analysis

Scanning Electron Microscopy (SEM) is a type of electron microscope that is used to view solid materials on a macro to submicron range. Images are formed by scanning a sample with a high energy beam of electrons that interact with atoms of the sample. This interaction emits X-rays, backscattered electrons, and secondary electrons which are collected by the detector and converted into an image. The sample must be free from H_2O as the electrons expelled from the electron gun would vaporise the sample which would have an impact on the micrograph obtained. The SEM itself consists of an electron-optical column mounted on a vacuum chamber. The electron gun is placed on the top of the column and is typically a tungsten thermionic cathode. The electron beam is forced down the column and focused on the sample using magnetic lenses and scan coils. The brightness and contrast of the image generated is directly dependent of the surface topography. To improve the images obtained samples are often sputter coated with a thin layer of a noble metal, e.g. Au, which increases the number of secondary electrons emitted.

EDX allows the localised micro-elemental analysis of the top of a few micrometers of a sample. An EDX spectrum is obtained from the X-ray signals generated when the high-energy electron beam hits the sample surface. Since the orbital energies of each element are characteristic, the X-rays generated by the sample are linked to its chemical composition. Thus, an EDX spectrum consists of a series of peaks at specific energies corresponding to the electronic transitions of the different elements present in the sample. Although EDX allows for the identification of the elements present in the sample, it is generally not suitable as a quantitative measurement.

SEM was carried out on a Hitachi S-3200-N with a tungsten filament electron source, maximum magnification of 300,000 and a resolution of 3.5 nm. This microscope was equipped with an Oxford Instrument INCAx-act EDX system with a silicon drift detector.

2.3.2 UV/vis Spectroscopy

UV/vis spectroscopy measures the amount of ulta-violet and visible light transmitted or absorbed by a sample placed in a spectrometer[13]. The absorption of UV/vis energy gives rise to the electronic transition of occupied energy levels to unoccupied energy levels. Common UV spectrometers operate in the range 190 to 400 nm corresponding to photon energies of about 70 to 140 kcal/mol. Spectrometers that also extend into the visible region, from 400 nm to 800 nm, are called UV/visible spectrometers. The wavelengths of UV light absorbed by a molecule are determined by the electronic differences between orbitals in the molecule[13]. To measure the UV-visible spectrum of a compound the sample is dissolved in solvent that does not absorb above 190 nm. The sample is placed in a quartz cell, and a sample of the solvent is placed in a reference cell. An ultraviolet spectrometer operates by comparing the amount of light transmitted through the sample with the amount of light transmitted through the reference beam. Passing the reference beam through the reference cell compensates for any absorption of light by the solvent. The wavelength of maximum absorbance is called the λ_{max}. At this fixed wavelength, the absorbance changes in accordance with concentration. This relationship is known as the Beer-Lambert Law, which states that absorbance is proportional to concentration at a fixed wavelength, as shown in Equation 2.1, where A is absorbance, ε is the molar extinction coefficient in mol^{-1} cm^2, c is the concentration in mol cm^{-3} and l is the patch length in cm[13].

$$A = \varepsilon c l \qquad \qquad (Equation\ 2.1)$$

During this research, a Perkin Elmer 35 spectrometer was used. The spectrometer comprised of a Deuterium and Tungsten lamp with a combined wavelength range of 190-800 nm. Samples were placed in quartz cuvette, with a path length of 1 cm and volume of approximately 3 mL. All samples were colourless, thus the absorption measurements were confined to the UV region of 190 – 400 nm. The data was recorded using Perkin Elmer UV Winlab software version 6 and analysis was carried out using Microsoft Excel 2007 for Windows.

2.3.3 Infra-Red Spectroscopy

Infra-red (IR) spectroscopy measures the vibrational excitation of atoms around the bonds that connect them. At energies slightly lower than those of visible radiation, light causes vibrational excitation of the bonds in a molecule. This part of the electromagnetic spectrum is called the infra-red region[13]. Infrared photons do not have enough energy to cause electronic transitions, but they can cause groups of atoms to vibrate with respect to the bonds that connect them. Like electronic transitions, these vibrational transitions correspond to distinct energies, and molecules absorb infrared radiation only at certain wavelengths and frequencies. The position of the infrared band is specified by its wavelength (λ), measured in microns (μm) or its reciprocal value called wavenumber (ν). The frequency of the vibrations between two atoms is governed by Hooke's law as the frequency of the stretching vibration depends on two quantities: the masses of the atoms and the stiffness of the bond. Heavier atoms vibrate slower that lighter ones and stronger bonds are generally stiffer, requiring more energy to stretch or compress them.

The vibrational bands of many functional groups occur at characteristic wavenumbers which helps aid interpretation of a spectrum and the entire IR spectrum may be used as a unique fingerprint of a compound[13].

In this research infrared spectra (cm^{-1}) were recorded as KBr discs using a Perkin Elmer system 2000 FT-IR spectrometer.

2.3.4 Differential Scanning Calorimetry

Differential scanning calorimetry (DSC) directly measures heat changes that occur in polymers during a controlled increase or decrease in temperature, making it possible to study their thermal properties. The technique takes advantage of the energy changes involved in the various phase transitions of certain polymer molecules[14]. One of the criteria of this technique is that the sample and reference material remain at the same

temperature during heating. This can be achieved by setting the machine to heat both the sample and reference material at a specific rate. This allows the heat flux or difference in energy input between the sample and reference to be measured[15]. Thus several properties of the material can be ascertained; melting points, enthalpies of melting, crystallisation temperatures, glass transition temperatures and degradation temperatures which aids in the characterization of the polymer.

In this research DSC studies were performed on a Perkin Elmer Pyris 6 in a nitrogen atmosphere, and analysis performed using Pyris software version 7.

2.3.5 High Performance Liquid Chromatography

High performance liquid chromatography (HPLC) is liquid chromatography in which a mixture is sent through a column containing packing materials whilst under pressure[16]. The column can be made up in a variety of ways, but the always involves one phase that remains in place, a stationary phase, and another that flows past it, the mobile phase. The components of the mixture are held back by the stationary phase or moved forward by the mobile phase depending on the structure of each compound and the composition of the two phases allowing the operator to identify, quantify and purify the individual components of the mixture[17].

In this research HPLC studies were performed on a Perkin Elmer 200 Series Pump and Autosampler, UV/vis detector and analysis performed using TotalChrom Workstation version 6.2.1. Reverse phase HPLC was used and the mobile phase was methanol.

2.3.6 Elemental Analysis

The major elements of an organic substance namely, carbon, hydrogen, and nitrogen, are commonly determined using CHN elemental analysis[18]. In this technique the substance under study is combusted under an oxygen stream in a furnace at high

temperatures. The end products of the combustion are mostly the oxides of the concerned elements in the form of gases. These are then separated by mass spectroscopy and carried to the detector using inert gases like helium or argon. The detector then determines the presence of the elements carbon, hydrogen and nitrogen in a given substance and gives the result as percentage amount of these atoms against the total weight.

In this research CHN elemental analysis was performed using a Flash EA 1112 Series Elemental Analyser with Eager 300 Operating Software.

2.4 Analysis of DCD Release and Swelling Properties of Chitosan Hydrogel and Xerogel Beads

The DCD release behaviour of the beads was analyzed by calculating the amount of DCD released at different intervals of time from 10 beads in 500 mL of release media (Millipore water unless otherwise stated) at a temperature of 20 ± 1 °C. The amount of DCD released at each time interval was determined by recording the absorbance at λ max = 214 nm using a UV/vis spectrometer (Figure 2.1). The concentration of the release solution was then calculated using a DCD calibration curve (Figure 2.2). It can be said with certainty that UV/vis spectrometry can detect molar concentrations of DCD in solution in the order of one hundredth of a millimole. Therefore when a concentration of a DCD solution is stated in this research that is in the order of one hundredth of a millimole there is a potential experimental error of ± 0.005 mM due to the sensitivity of UV/vis spectrometry. If there is any variation from these conditions it is outlined in the appropriate section.
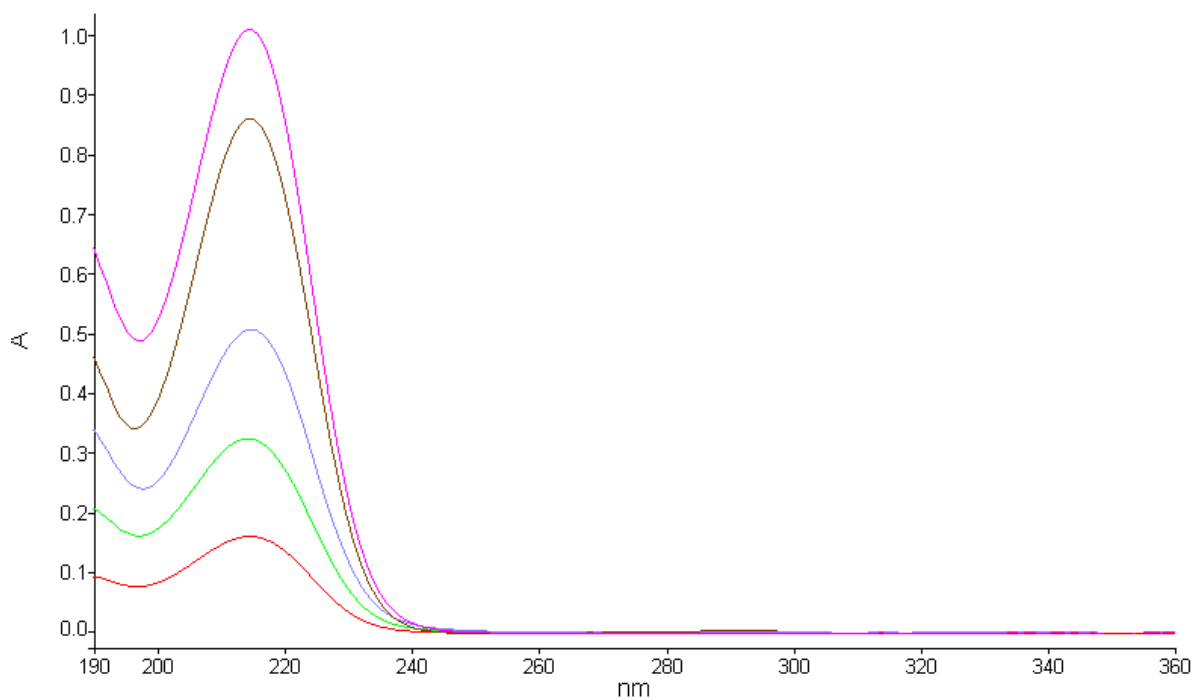
Figure 2.1 UV/vis spectra obtained from samples taken from a DCD solution of concentration (———) 0.06 mM (———) 0.05 mM, (———) 0.03 mM, (———) 0.02 mM and (———) 0.01 mM.

y = 16.839x - 0.0072
R² = 0.9998
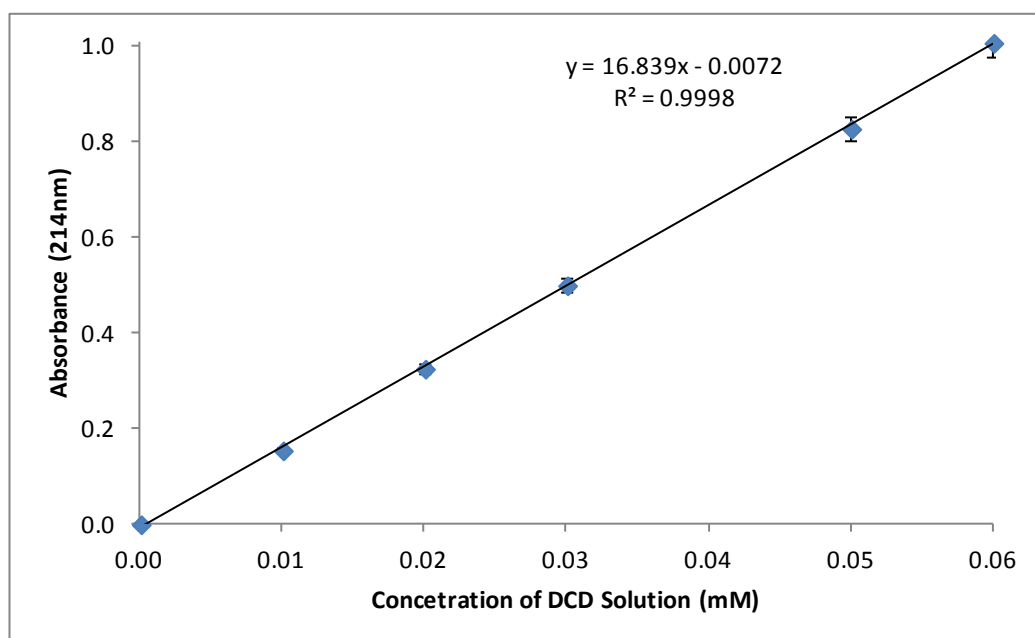
Figure 2.2 UV/vis Spectroscopy DCD Calibration Curve at λ = 214 nm. The experiment was repeated in triplicate.

To confirm that DCD was released from the beads and that it was not degraded in the chitosan polymer matrix, a HPLC spectrum of a stock DCD solution (Figure 2.3) was compared with spectrum obtained from a sample into which DCD loaded chitosan xerogel beads were placed (Figure 2.4). The resulting spectra were identical which confirmed that DCD was released from the chitosan beads.
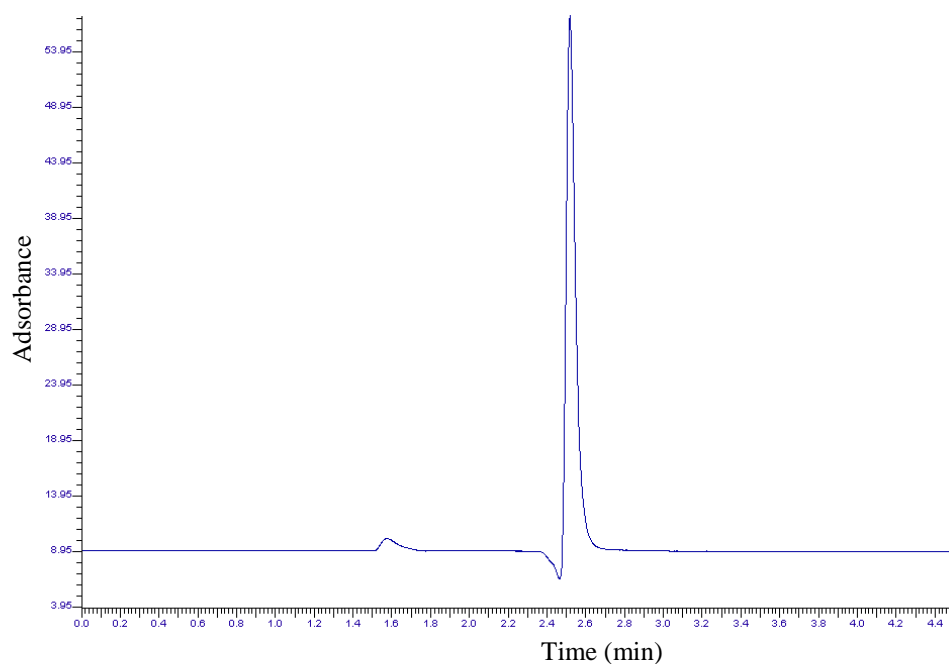
Figure 2.3 HPLC Absorption Spectrum of a DCD Solution at 214 nm
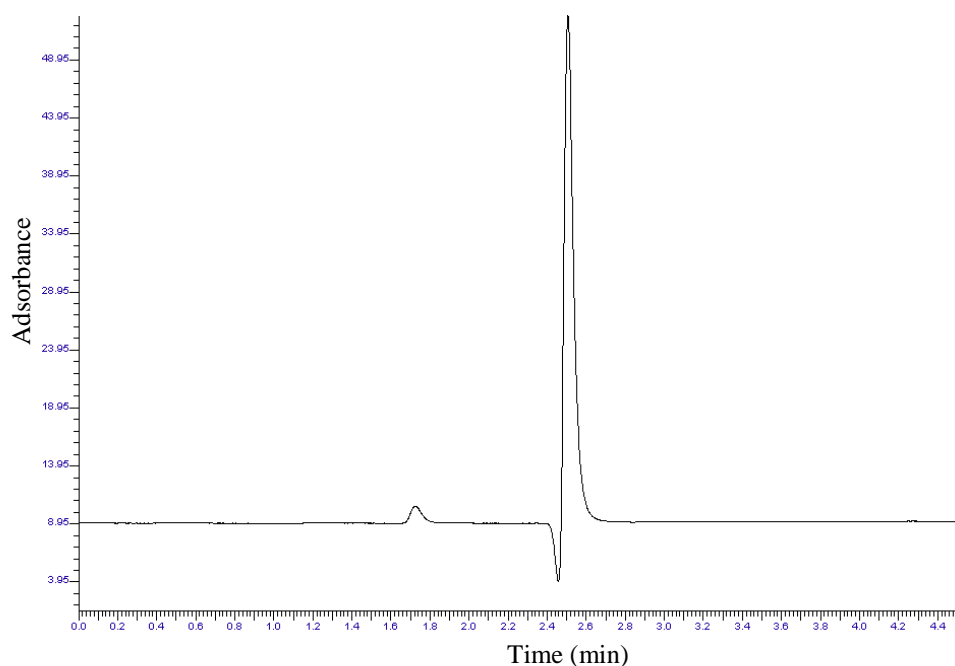
Figure 2.4 HPLC Absorption Spectrum of DCD release from chitosan hydrogel beads at 214 nm

2.4.1 Determination of the Swelling Ratio (%)

The swelling ratio (%) of chitosan xerogel beads was calculated using the following equation:

$$S_w\% = \frac{W_s - W_d}{W_d} \times 100 \qquad (Equation\ 2.2)$$

Where W_s and W_d is the swollen and dry weight of the composite xerogels at time t, respectively[19]. Swelling studies were conducted by placing 15 beads in 30 mL Millipore water at a temperature of 20 ± 1 °C unless otherwise stated. To calculate their weight at a given time the beads were filtered using gravity filtration and extraneous water was removed using filter paper. The beads were then weighed using a four figure balance.

2.4.2 Kinetic Modelling of DCD Release from Chitosan Hydrogel and Xerogel Beads

In order to design a new controlled release system which is based on release from chitosan hydrogel or xerogel beads, the fitting of release data to mathematical expressions which allow the release properties to be treated and analysed using statistical and mathematical methods is highly desirable. Determining the kinetic order and characterising the release mechanism facilitates the interpretation of release results and aids the optimization and predictability of the release system[20]. In the ideal case, the required composition (type and amount of chemical to be loaded, polymer and additives) and geometry (size and shape) of a new controlled delivery system designed to achieve a certain release profile can be predicted theoretically. This would would minimize the number of necessary experiments and the development of new controlled delivery system products would be significantly facilitated [21].

The term 'order' is used in release mathematical models for parameters that do not have much in common with the order parameters known from reaction kinetics. In reaction kinetics the order describes the degree of correlation between the rate of formation of one component and the concentration of another component or multiple components. In a release system there will not be a chemical reaction but a physiochemical change in phase or change of compartment. If a release profile can be described by an order, there is a correlation between the release rate and the amount of DCD loaded in the release system not yet released at any point of the release period. The amount of DCD released at time, t, is denoted M_t and the total amount of DCD in the formulation is denoted M_∞, therefore the fraction of DCD, $Y(t)$, released at time t, is defined as

$$Y(t) = \frac{M(t)}{M_\infty} \qquad\qquad (Equation\ 2.3)$$

thus the definition of the kinetic order is,

$$\frac{dY(t)}{dt} = k\big(1 - Y(t)\big)^n \qquad\qquad (Equation\ 2.4)$$

where n is the kinetic order and k is the rate constant.

Four parameters are needed to characterise a release profile.

(1) n, the kinetic order, is the correlation between release rate $\frac{dY(t)}{dt}$ and the unreleased fraction of drug $(1-Y(t))$. The value of n, will reflect the release mechanism of the system. Mathematically, n is a shape parameter, independent of scaling and is dimensionless.

(2) t_0, the lag time, is the time it takes the initial processes to establish the transport routes and reach a *pseudo* steady state in the release system. For example the permeation of the outer layer of the bead by water is an important lag time process.

(3) k ,the rate constant, is the intrinsic release rate. For $n \geq 0$ it is approximately the maximum release rate of the system which will be the situation when $t > 0$. The unit for k is reciprocal to the time unit.

(4) M_∞, is the total amount of DCD encapsulated by the system.

The mechanism of a release system can be related to a kinetic order;

(1) $n = 0$. Zero order systems are characterised by a constant release rate,

$$\frac{dY(t)}{dt} = k \qquad\qquad (Equation\ 2.5)$$

Erodible systems with a constant surface area and membrane controlled diffusion systems with a constant concentration gradient over the membrane will give zero-order release profiles [18] and are expressed by the following equation:

$$Y = k_0 t \qquad\qquad (Equation\ 2.6)$$

Where, Y is the fraction of DCD released at time t and k_0 is the kinetic rate constant. To study the release kinetics, data obtained from release studies were plotted as the fraction of the total amount of DCD encapsulated in the bead released *versus* time[22].

(2) $n = 1$. In first order systems the release rate at any given time is proportional to the amount of DCD remaining inside the release system. A first-order profile is expected in a membrane controlled diffusion system if the gradient is reduced due to decreasing concentration on the donor side in combination with sink conditions in the release medium.

The release of an encapsulated chemical which follows first order release kinetics can be expressed by the equation:

$$\frac{dQ}{dt} = -k_1 q \qquad\qquad (Equation\ 2.7)$$

where k_1 is the first-order rate constant expressed in units of time[-1].

Equation 2.7 can be expressed as:

$$\ln(100 - Q_t) = \ln Q_0 - k_1 t \qquad\qquad (Equation\ 2.8)$$

Where Q_0 is the initial percentage of DCD in the bead (100%), Q_t is the percentage of DCD that was released at time t and k_1 is the first-order rate constant. The data obtained are plotted as function of the natural logarithm of the cumulative percentage of DCD remaining in the bead against time [22].

Diffusion, swelling and erosion are the most important rate-controlling mechanisms of commercially available release products. As diffusion can be described using Fick's second law there are various equations that can be applied to interpret the release mechanism of release systems. Assuming one-dimensional transport in thin films results in rather simple mathematical expressions, but this approach is only valid for flat planar devices[23]. In the case of the chitosan xerogel delivery system developed in this research, three-dimensional, spherical geometries are more relevant, but mathematically more difficult to treat. In addition it is necessary to decide whether to assume constant or non-constant diffusivities. The mathematical treatment of constant diffusivity problems is much simpler, but only valid in the case of polymers that do not significantly swell upon contact with water. For chitosan xerogels, the DCD diffusion coefficients are dependent on the water content of the system[24]. Here the assumption of constant diffusivities can lead to less realistic mathematical modelling and if polymer dissolution occurs during release this will complicate the solution of Fick's second law of diffusion, leading to boundary moving conditions. In addition to the physiochemical properties of the polymer the characteristics of the encapsulated chemical have to be considered. For example, dissolution has to be taken into account

in case of poorly water-soluble drugs or chemicals. It is desirable to derive explicit analytical solutions where we can obtain direct relationships between the dependent and independent variables but this is only possible in the case of rather simple forms of the diffusion equations, e.g., assuming constant diffusivities. In general, physically more realistic models are mathematically more complex and it is often difficult to find exact solutions of the respective set of equations. In contrast to analytical solutions, only approximate solutions are derived in this research.

In 1961 Higuchi published the most famous and most often used mathematical equation to describe the rate constant of drugs from matrix systems[25]. Initially valid for only planar systems, it was later modified and extended to consider different geometries and matrix characterizations including porous structures[26, 27]. The Higuchi square root law is not related to any order and has a physically realistic meaning that helps us understand the release mechanism[20]. Understanding the mechanism of chemical release offers a convenient way to categorize release systems into one of three categories; (1) diffusion controlled (2) swelling-controlled and (3) chemically controlled. Despite the complexity of the involved mass transport processes of chemical release from a polymer into a perfect sink, Higuchi derived a very simple equation to help describe the release mechanism and potentially facilitate optimization of the release system[23]:

$$\frac{M_t}{A} = \sqrt{D(2C_o - C_s)C_s t} \qquad (Equation\ 2.9)$$

for $C_o > C_s$,

where M_t is the cumulative absolute amount of drug released at time t, A is the surface area of the controlled release device exposed to the release medium, D is the drug diffusivity in the polymer carrier, and C_o and C_s are the initial drug concentration, and the solubility of the drug in the polymer, respectively. Equation 2.9 can also be written in the more general form:

$$\frac{M_t}{M_\infty} = k\sqrt{t} \qquad\qquad (Equation\ 2.10)$$

Where M_t and M_∞ are, respectively, the amount of drug released at time t, and infinite time respectively; and k is a constant reflecting formulation characteristics[28]. According to Equation 2.10, the fraction of drug released is proportional to the square root of time. Alternatively, the DCD release rate constant is proportional to the reciprocal of the square root of time[29]. To study the release kinetics the data obtained from the DCD release studies the data were plotted as the fraction of DCD released at time t *versus* square root of time. If the release data exhibits a good regression line fit for the Higuchi equation this implies release is based on Fickian diffusion[30]. An important advantage of these equations is their simplicity, however when applying them to controlled delivery systems the assumptions of the Higuchi derivation should always be kept in mind. The basic assumption for the derivation of Equation 2.10 is that the initial concentration of drug in the system, C_0 is higher that drug solubility, C_s. Other assumptions are that mathematical analysis is based on one-dimensional diffusion. Thus, edge effects must be negligible. The suspended drug or chemical to be released is in a state such that the particles are much smaller in diameter than the thickness of the system and when the diffusivity of the drug is constant perfect sink conditions are maintained.

Under these particular conditions Higuchi derived the very simple relationship between the rate constant of the drug and the square root of time. It is evident that these assumptions are not entirely valid for controlled delivery systems based on chitosan hydrogel or xerogel beads. The superposition of various different effects, such as swelling, transition of the macromolecules from the glassy to rubbery state, polymer dissolution, concentration-dependent water and diffusion might result in an apparent square root of time kinetics. However, due to the simplicity of the classical Higuchi equation it is often used to analyse experimental release data to get an approximation of the underlying release mechanism.

A more comprehensive, but still simple semi-empirical equation to describe drug release from polymeric system is the Korsmeyer-Peppas model[31]:

$$\frac{M_t}{M_\infty} = kt^n \hspace{3cm} (Equation\ 2.11)$$

Equation 2.11 converted to its linear form:

$$\log\frac{M_t}{M_\infty} = \log k + n \log t \hspace{2cm} (Equation\ 2.12)$$

Where M_t and M_∞ are, respectively, the amount of drug released at time t and the total amount of drug inside the bead, k is a kinetic constant and the exponent n is the shape-dependent parameter[32].

This equation addresses the rate of release of a solute from a matrix, usually a polymer, where the loading of the solute exceeds it solubility, C_s, in the matrix, into a surrounding fluid. Korsmeyer-Peppas model can be seen as a generalization of two steps; first is the physical visualization of dividing the matrix into an inner region where undissolved particles exist and an outer region where the entire drug is dissolved but there is a gradient of concentration that governs the rate constant of solute to the surrounding fluid. The model further envisions this boundary to move inward as the undissolved drug is completely converted to dissolved drug and eventually released from the matrix to the surrounding fluid[33]. Due to the approximate character of Equation 2.11 its use is traditionally confined to the description of the first 60% of the drug release curve.

To determine the exponent n, data obtained from DCD release studies were plotted as the log cumulative (%) released *versus* log time.

Only in two cases, $n = 0.50$ (diffusion controlled drug release) and $n = 1.0$ (release caused by relaxation of the polymeric chain (Case-II transport)), does Equation 2.11 relate to a single release mechanism. When the exponent n takes a value of 1.0, the drug release rate is independent of time. This case corresponds to zero-order release kinetics. Other values for n between 0.5 and 1.0 are an indicator for anomalous

transport kinetics, i.e., a combined mechanism of pure diffusion and Case II transport[34]. The two extreme values for the exponent n, 0.5 and 1.0 are only valid for slab geometry. For spheres and cylinders different values had been derived[34], as listed in Table 2.1.

Table 2.1 Exponent n of the Korsemeyer-Peppas equation and drug release mechanism from polymeric controlled delivery systems for different geometries

Thin Film	Cylinder	Sphere	Release Mechanism
0.5	0.45	0.43	Fickian Diffusion
$0.5 < n < 1.0$	$0.45 < n < 0.89$	$0.43 < n < 0.85$	Anomalous Transport
1.0	0.89	0.85	Case – II Transport

In the case of chitosan xerogel controlled delivery it has to be pointed out that the application of the Korsmeyer-Peppas model can only give limited insight into the exact release mechanism of the chemical. Even if values of exponent n are found that would indicate a diffusion-controlled release mechanism, this is not automatically valid for chitosan xerogels. The derivation of the Higuchi equation and the short time approximation of Fick's second law for slab geometry assume constant diffusivities and constant dimensions of the xerogel during drug release. However chitosan xerogels are known to swell and the diffusion coefficients of water and the encapsulated chemical are pore size and concentration dependent [24]. An apparent square root of time release kinetics can thus be the result of the superposition of various effects, and is not necessarily based on simple diffusion-control over the entrapped molecule. As in the case of the Higuchi equation the information obtained should be viewed with caution. However, the Korsmeyer-Peppas model is more comprehensive than the Higuchi equation.

A further model was developed by Peppas and Sahlin[35]:

$$\frac{M_t}{M_\infty} = k_1 t^n + k_2 t^{2n} \qquad\qquad (Equation\ 2.13)$$

Where k_1 and k_2 and n are constants. The first term on the right hand side represents the Fickian contribution, F, whereas the second term represents the Case-II relaxational contribution, R. The ratio of both contributions can be calculated as follows:

$$\frac{R}{F} = \frac{k_2 t^n}{k_1} \qquad\qquad (Equation\ 2.14)$$

For the spherical geometry of our chitosan xerogel beads an n value of 0.43 is appropriate. The k_1 rate constant is derived by calculating the slope of a plot of the fraction of DCD released from the bead versus time ($s^{0.43}$) while the k_2 rate constant is derived by calculating the slope of a plot of the fraction of DCD released from the bead versus time ($s^{0.86}$). Using this equation the Fickian contribution to the overall release process can be calculated relative to the contribution of case-II relaxation.

2.5 Analysis of Paraquat Adsorption by C4S-Chitosan Hydrogel Beads

The adsorption studies were carried out by placing 0.3 g C4S-chitosan hydrogel beads in a 50 mL aqueous paraquat solution of known concentration held at 25 ± 1°C. The mixture was mechanically stirred at 25 rpm for a predetermined time at which point the concentration of remaining paraquat in solution was determined by sampling the solution at $\lambda = 282$ nm and recording a UV/vis spectrum of the sample (Figure 2.3). The sample was returned to the solution after the absorbance reason was taken. The λ_{max} value ($\lambda = 257$ nm) was not used to determine the calibration curve as higher concentrations of paraquat could be interpreted by setting the calibration curve at $\lambda = 282$ nm (Figure 2.5).
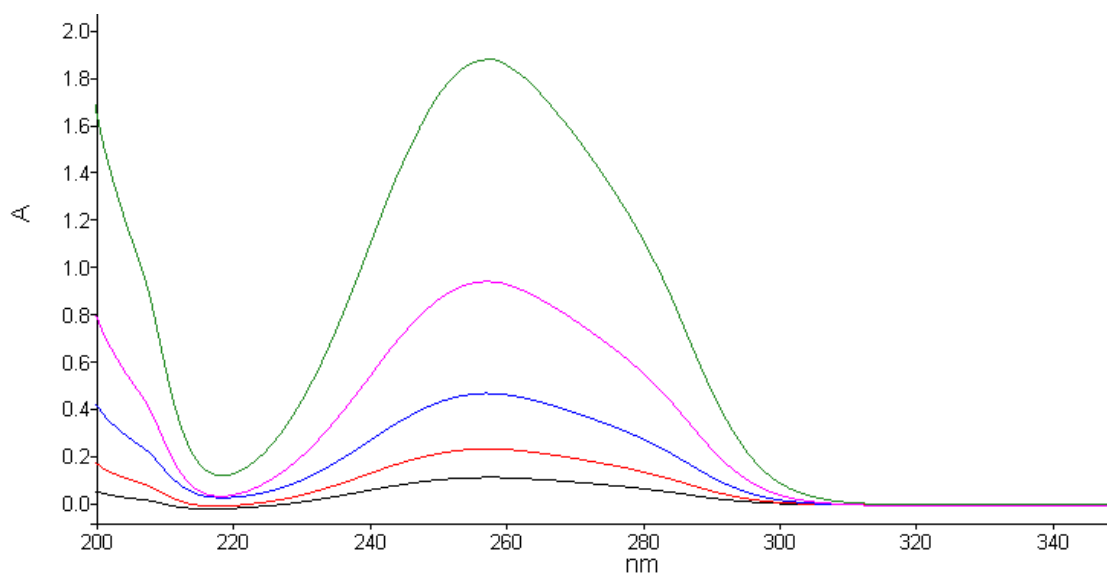
Figure 2.5 UV/vis spectra obtained from paraquat solutions of (——) **30.00 mg/L** (——) **15.00 mg/L** (——) **7.50 mg/L** (——) **3.75 mg/L** **and** (——) **1.87 mg/L.**
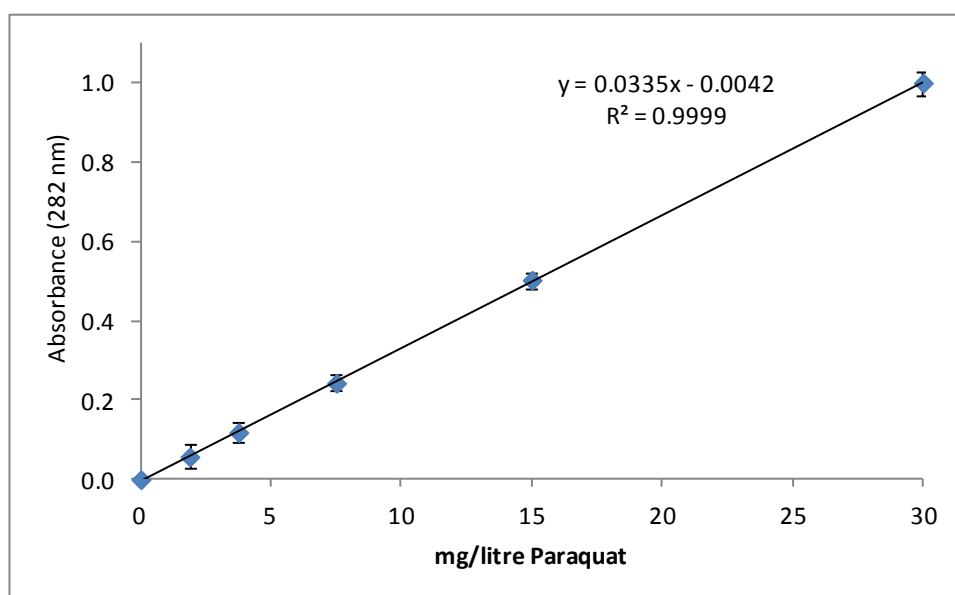
Figure 2.6 UV/vis Spectroscopy Paraquat Calibration Curve at $\lambda = 282$ **nm. The experiment was repeated in triplicate.**

The amount of paraquat adsorbed by C4S-chitosan hydrogel beads was determined by using the following equation[36]:

$$q_t = \frac{C_i - C_t}{W} \times V \qquad\qquad (Equation\ 2.15)$$

Where q_t (mg/g) is the amount of paraquat adsorbed at time t, C_i(mg/L) is the initial concentration of paraquat, C_t (mg/L) is the concentration of paraquat at a given time, V is the experimental volume solution (L) and W is the dry weight of the hydrogel beads (g). As the adsorption studies were conducted using wet hydrogel beads and their dry mass is used to calculate W, it was necessary to calculate their dry weight to determine the q_t value. This was achieved by setting aside 0.3 g of wet C4S-chitosan hydrogel beads of each prepared formulation, placing them in an oven set to $37 \pm 1\ °C$ for 7 days and then weighing the dehydrated beads on a four figure balance.

2.5.1 Adsorption Isotherms

Adsorption Studies are critical in optimising the use of adsorbents as they describe how adsorbates interact with adsorbents. The correlation of equilibrium data, either by theoretical or empirical equations, is essential for the practical design and operation of adsorption systems[37].

In 1918 Irving Langmuir proposed a theory to describe the adsorption of gas molecules onto metal surfaces[38]. The Langmuir adsorption isotherm has found successful applications in many other real sorption processes of monolayer adsorption[39]. Langmuir's model of adsorption depends on the assumption that intermolecular forces decrease rapidly with distance and consequently predicts the existence of monolayer coverage of the adsorbate at the outer surface of the absorbent. Moreover, the Langmuir equation is based on the assumption of a structurally homogenous adsorbent where all sorption sites are identical and

energetically equivalent. Theoretically, the adsorbent has a finite capacity for the adsorbate. Therefore, a saturation value is reached beyond which no further sorption can take place[38].

The non-linear form of the Langmuir isotherm is expressed as:

$$q_e = \frac{K_L C_e}{1 + a_L C_e} \quad (as\ C_e \rightarrow \infty) \qquad (Equation\ 2.16)$$

And the linear form:

$$\frac{C_e}{q_e} = \frac{1}{K_L} + \frac{a_L}{K_L} C_e \qquad (Equation\ 2.17)$$

Where q_e is solid phase sorbate concentration at equilibrium (mg/g), C_e is aqueous phase sorbate concentration at equilibrium (mg/L), a_L and K_L are Langmuir adsorption constants and a_L is related to adsorption energy[40]. Therefore, plots of C_e/q_e versus C_e give a straight line of slope a_L/K_L and intercept $1/K_L$, where K_L/a_L gives the theoretical monolayer saturation capacity, Q_0[37].

Isotherms that are found to have high correlation coefficients with Equation 2.17 indicate that sorption follows the Langmuir model.

The Freundlich equation is an empirical equation employed to describe heterogeneous systems, in which it is characterised by the heterogeneity factor $1/n$[41]. Hence, the empirical equation can be written as:

$$q_e = K_F C_e^{\frac{1}{n}} \qquad (Equation\ 2.18)$$

Where q_e is solid phase sorbate concentration in equilibrium (mg/g), C_e is liquid phase sorbate concentration in equilibrium (mg/L) and $1/n$ is the heterogeneity factor. A linear form of the Freunlich expression can be obtained by taking logarithms of Equation 2.18.

$$\log q_e = \log K_F + \frac{1}{n}\log C_e \qquad (Equation\ 2.19)$$

Therefore, a plot of $\log q_e$ versus $\log C_e$ enables the constant K_F and exponent $1/n$ to be determined. The isotherm is another form of the Langmuir approach for adsorption on an 'amorphous' surface. The amount of adsorbed material is the summation of adsorption on all sites. The Freundlich isotherm describes the reversible adsorption and is not restricted to the formation of the monolayer[37].

2.5.2 Investigation of Adsorption Kinetics

In order to investigate the kinetic process of adsorption the *pseudo*-first order and *pseudo*-second order models were used to study the experimental data obtained. The *pseudo*-first order model of Lagergren can be expressed as:

$$\ln(q_e - q_t) = \ln q_e - k_1 t \qquad (Equation\ 2.20)$$

Where q_e and q_t are the amount of paraquat absorbed onto the absorbent at equilibrium and at time t, respectively, and k_1 is the rate constant of first order adsorption (s^{-1}).

A straight line plot of $\ln(q_e - q_t)$ against t are used to determine the rate constant k_1.

The *pseudo*-second order model can be expressed as:

$$\frac{t}{q_t} = \frac{1}{k_2 q^2_e} + \frac{t}{q_e} \qquad (Equation\ 2.21)$$

Where k_2 is the rate constant of second order adsorption (g mg^{-1} s^{-1}). The straight-line plot of $\frac{t}{q_t}$ against t will give a slope of $\frac{1}{q_e}$ and an intercept of $\frac{1}{k_2 q^2_e}$. The *pseudo*-second order assumes that chemisorption is the rate controlling mechanism.

The adsorbate can be transferred from the solution phase to the surface of the adsorbent in several steps. The steps may include film or external diffusion, pore diffusion, surface diffusion and adsorption on the pore surface. The overall adsorption can occur through one or more steps. The intraparticle diffusion model has been widely applied for the analysis of adsorption kinetics to determine how many stages are involved in the adsorption process[42].

The intraparticle diffusion model is given by the equation:

$$q_t = k_{int}t^{\frac{1}{2}} \qquad (Equation\ 2.22)$$

Where q_t is the amount of paraquat absorbed at time t, and k_{int} is the intraparticle diffusion constant. A straight-line plot of q_t against $t^{1/2}$ can be used to determine the intraparticle diffusion rate k_{int}[43].

2.6 References

[1]   F. Zhao, B. Yu, Z. Yue, T. Wang, X. Wen, Z. Liu and C. Zhao, *Journal of Hazardous Materials* **2007**, *147*, 67-73.

[2]   T. Y. Guo, Y. Q. Xia, G. J. Hao, M. D. Song and B. H. Zhang, *Biomaterials* **2004**, *25*, 5905–5912.

[3]   A. K. Anal and W. F. Stevens, *International Journal of Pharmaceutics* **2005**, *290*, 45-54.

[4]   Y. Xu, C. Zhan, L. Fan, L. Wang and H. Zheng, *International Journal of Pharmaceutics* **2007**, *336*, 329-337.

[5]   F. Mi, H. Sung and S. Shyu, *Carbohydrate Polymers* **2002**, *48*, 61-72.

[6]   S. Hirano, R. Yamaguchi, N. Fukui and M. Iwata, *Carbohydrate Research* **1990**, *201*, 145–149.

[7]   A. Yanagi, H. Otsuka and A. Takahara, *Polymer Journal* **2005**, *37*, 939-945.

[8]   R. Doyle, A Polypyrrole/Sulfonated Calixarene Modified Electrode for the Electrochemical Detection of Dopamine, PhD Thesis, National University of Ireland, 2011.

[9]   C. D. Gutsche, B. Dhawan, K. H. No and R. Muthukrishnan, *Journal American Chemical Society* **1981**, *103*, 3782-3792.

[10]   C. D. Gutsche, D. E. Johnston and D. R. J. Stewart, *Journal of Organic Chemistry* **1999**, *64*, 3747–3750.

[11]   C. D. Gutsche and L. G. Lin, *Tetrahedron* **1986**, *42*, 1633-1640.

[12]   S. Shinaki, K. Araki, J. Shibata and O. J. Manabe, *Perkin Trasactions 1* **1987**, 2297-2299.

[13]   L. G. Wade, *Organic Chemistry*, 4th ed. Addison Wesley Longman, **1999**, p. 1262.

[14]   N. J. Coleman and D. Q. M. Craig, *International Journal of Pharmaceutics* **1996**, *135*, 13-29.

[15]   G. V. Assche, A. V. Hemelrijck, H. Rahier and B. V. Mele, *Thermochimica Acta* **1997**, *304*, 317-334.

[16]   D. Perrin and W. L. F. Armarego, *Purification of Laboratory Chemicals*, Pergamon Press, **1988**, p. 373.

[17]   S. Ege, *Organic Chemistry*, 1st ed. Heath, **1984**, p. 903.

[18]   V. P. Fadeeva, V. D. Tikhova and O. N. Nikulicheva, *Journal of Analytical Chemistry* **2007**, *63*, 1197–1210.

[19]   Q. Wang, X. Xie, X. Zhang, J. Zhang and A. Wanga, *International Journal of Biological Macromolecules* **2010**, *46*, 356–362.

[20]   K. Jørgensen and F. N. Christensenb, *International Journal of Pharmaceutics* **1996**, *143*, 223-232

[21]   J. Siepmann and N. A. Peppas, *Advanced Drug Delivery Reviews* **2001**, *48*, 139–157.

[22]   S. Dash, P. A. Murthy, L. Nath and P. Chowdhury, *Acta Poloniae Pharmaceutica* **2010**, *67*, 217-223.

[23]   J. Siepmann and N. A. Peppas, *International Journal of Pharmaceutics* **2011**, *418*, 6-12.

[24]   B. Falk, S. Garramone and S. Shivkumar, *Materials Letters* **2004**, *58*, 3261–3265.

[25]   T. Higuchi, *Journal of Pharmaceutical Science* **1961**, *50*, 874-875.

[26]   T. Higuchi, *Journal of Pharmaceutical Science* **1963**, *52*, 1145-1149.

[27]   S. J. Desai, A. P. Simonelli and W. I. Higuchi, *Journal of Pharmaceutical Science* **1965**, *54*, 1459-1464.

[28]   G. V. E. Rinaki, P. Macheras, *International Journal of Pharmaceutics* **2003**, *225*, 305-313.

[29]   J. Siepmann and N. A. Peppas, *Advanced Drug Delivery Reviews* **2001**, *48*, 139-157.

[30]   M. H. Shoaib, J. Tazeen, H. A. Merchant and R. I. Yousuf, *Pakistan Journal of Pharmaceutical Science* **2006**, *19*, 119-124.

[31]   P. Costa and J. M. S. Lobo, *European Journal of Pharmaceutical Sciences* **2001**, *13*, 123-133.

[32]   B.T. Liua and J.P. Hsub, *Chemical Engineering Science* **2006**, *61*, 1748-1752.

[33]   D. R. Paul, *International Journal of Pharmaceutics* **2011**, *418*, 13-17.

[34]   P. L. Ritger and N. A. Peppas, *Journal of Controlled Release* **1987**, *5*, 23-42.

[35]   N. A. Peppas and J. J. Sahlin, *International Journal of Pharmaceutics* **1989**, *57*, 169-172.

[36]   N. Li and R. Bai, *Separation and Purification Technology* **2005**, *42*, 237–247.

[37]   Z. G. Hu, J. Zhang, W. L. Chan and Y. S. Szeto, *Polymer* **2006**, *47*, 5838-5842.

[38]   I. Langmuir, *Journal of the American Chemistry Society* **1918**, *40*, 1361–1403.

[39]   Y. C. Wong, Y. S. Szeto, W. H. Cheung and G. McKay, *Process Biochemistry* **2004**, *39*, 695-704.

[40]   S. Chatterjee, D. S. Lee, M. W. Lee and S. H. Woo, *Journal of Hazardous Materials* **2009**, *166*, 508-513.

[41]   H. Freundlich, *Kapillarchemie, Academishe Bibliotek, Leipzig* **1909**.

[42]   F. Wu, R. Tseng and R. Juang, *Chemical Engineering Journal* **2009**, *153*, 1-8.

[43]   W. Ngah and S. Fatinathan, *Chemical Engineering Journal* **2008**, *143*, 62-72.

Chapter 3: Screening of Chitosan Xerogel Beads for Controlled Release of DCD

3.1. Introduction

Chitosan hydrogels are composed of three dimensional polymer networks that can absorb large quantities of water. Consequently, they are soft, pliable, wet materials, with a wide range of biomedical applications[1]. The design of controlled release systems from hydrogels has been well documented[2, 3]. The hydrophilic and hydrophobic balance of a hydrogel can be altered to provide tuneable contributions that present different diffusion characteristics, which in turn influences the release of a drug contained within the gel matrix[1]. Hydrogel beads that are environment and stimuli sensitive have been developed that exhibit oscillatory swelling and respond to changes in pH, temperature, ionic strength or drug concentration[4, 5].

The drug release behaviour and swelling characteristics of hydrogels are the result of cross-links, permanent entanglements, ionic interactions or microcrystalline regions incorporating various chains within the elastic nature of the polymer network[1]. The overall rate of drug release has been shown to be controlled by the rate of water influx. However, as the degree of crosslinking inside the hydrogel bead increases, the network mesh size is reduced. As a result, the rate of drug release from these gels decreases upon the formation of interpolymer complexes[1]. To increase the degree of crosslinking chitosan hydrogels are bound via their protonated amino group to ionic crosslinkers, or undergo a Schiff base reaction with a covalent crosslinker to form a network using covalent bonding between the polymer chains[6].

To reduce the network mesh size further the chitosan hydrogels can be dehydrated to form xerogel beads[7]. Xerogel beads are free of solvent and thus are smaller than the original hydrogel bead. Chitosan xerogel beads have been investigated as a controlled drug release delivery system[2] and as a method of adsorbing metals onto chitosan from aqueous solution[8]. Like hydrogels, they can be ionically or covalently crosslinked, allow the free diffusion of water and are pH swelling sensitive[9].

This chapter investigates the physical characteristics of chitosan hydrogel and xerogel beads, crosslinked both ionically and covalently. Their ability to act as a controlled delivery system for the nitrification dicyandiamide (DCD) is also discussed.

3.2 Results and Discussion

A number of low molecular weight ions and anionic polymers have been used to prepare ionically crosslinked chitosan hydrogel beads in a fast, simple procedure and under mild conditions. It has been reported that the properties of these chitosan hydrogels are largely influenced by the electrostatic interactions between anions and the chitosan polymer and that the stability of complexes formed is dependent on environmental pH[9]. A number of ionic crosslinkers were investigated in this present study.

Sodium Tripolyphosphate (TPP) (Figure 3.1) is a polyanion that interacts with chitosan by electrostatic forces. The formation of salt linkages between amino groups of chitosan and phosphate groups of TPP form a bead that is insoluble in water and capable of encapsulating drugs[10]. Despite a relatively slow formation time, chitosan hydrogel beads crosslinked with TPP are reported to have better mechanical strength than chitosan crosslinked with other polyions such as citrate or sulfate[11].

Trisodium citrate (Figure 3.2) is an important organic salt in biotechnology, pharmaceutics, and agriculture[12]. Its polyanion, citrate, is a multivalent low molecular weight ion in aqueous solution. It is known that contact between chitosan and citrate in aqueous solution immediately induces ionic crosslinking between the NH_3^+ group on chitosan and the COO^- group on citrate. This crosslinking can results in the formation of hydrogel beads. The crosslinking reaction takes place like similar to that of TPP, starting at the surface of the bead and diffusing inwards and is generally complete within 30 minutes[9].

Using sodium molybdate (Figure 3.3) as a crosslinking agent has resulted in the formation of chitosan hydrogel beads with a substantially different structure compared to those produced during alkaline coagulation. For example, Dambies *et al*.

crosslinked chitosan with molybdate and concluded that the hydrogel beads formed had a double layer structure with a very compact 100 μm thick external layer and an internal structure of small pores[13].

Chitosan ionically crosslinked with sodium alginate (Figure 3.4) has been extensively studied as a controlled delivery system for drugs delivered by oral dosage[14, 15]. This is due to sodium alginates adhesive properties that allow it to bind with the mucosal membrane[16]. Sodium alginate reduces the solubility of chitosan hydrogel beads in acidic media making it more stable at low pH. The use of sodium alginate is however limited by its relatively high pore size and instability in higher pH media[17].
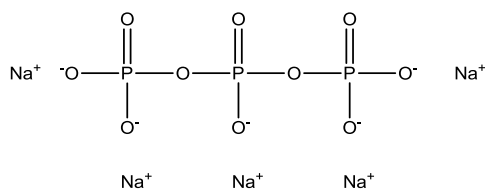
Figure 3.1 Sodium TPP
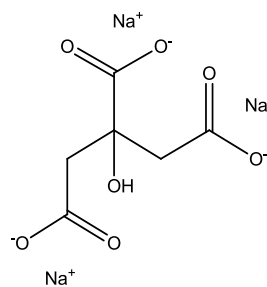
Figure 3.2 Trisodium Citrate
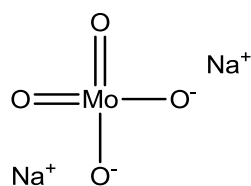
Figure 3.3 Sodium Molybdate
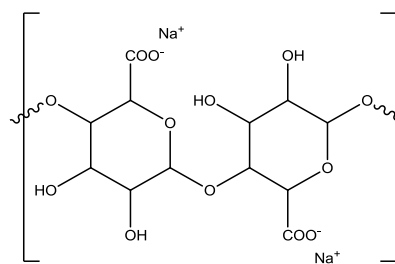
Figure 3.4 Sodium Alginate

3.2.1 Characterization and DCD Release Properties of Ionically Crosslinked Chitosan Hydrogel and Xerogel Beads

Chitosan xerogel beads were prepared either by precipitation (as stated in Section 2.2.2.1 (i)) or by ionic gelation combined with precipitation (as stated in Section 2.2.2.1 (iii)). In brief, 2 g of chitosan flakes were added to 100 mL of 1% (v/v) acetic acid Millipore water in a beaker to obtain a chitosan solution and the mixture was stirred overnight. If the beads were prepared by the precipitation method then the chitosan solution was dropped through a tube of inner diameter 0.5 mm into 300 mL of 60 mM DCD and 0.75 M NaOH aqueous solution and left to precipitate out for 24 h. If the beads were prepared by the ionic gelation combined with precipitation method then the chitosan solution was dropped through a tube of inner diameter 0.5 mm into 300 mL 60 mM DCD, 0.75M NaOH and 110 mM of a known ionic crosslinker aqueous solution and also allowed to crosslink for 24 h. Both sets of beads were then removed from the gelling solution and washed in a 60 mM DCD Millipore water solution for 24 h until reaching neutrality. Both sets of hydrogel beads were then stored in 60 mM DCD Millipore water solution until required. To form xerogel beads the hydrogel beads were placed in an oven at a temperature of 37 ± 1 °C for 24 h by which point they were dehydrated and ready for use.

3.2.1.1 Surface Morphology

The effects of ionic crosslinking on the surface morphology of chitosan xerogel beads were examined by SEM and are shown in Figure 3.5 (a-h). The SEM micrographs illustrate the spherical shape of the beads and dependence of the xerogel morphology on the ionic crosslinker used in the gelling solution. The surface morphology of the chitosan xerogels gelled in only sodium hydroxide solution is a smooth surface with few imperfections. In contrast, the xerogels crosslinked with sodium TPP (Figure 3.5 (c) and (d)) have a rough surface with indents visible on the surface of the bead. Figure 3.5 (e) and (f) show xerogels crosslinked with trisodium citrate; the beads exhibit a surface that is smoother than that of chitosan beads crosslinked with TPP.

The bead shape is also the least spherical of the xerogels with Figure 3.5 (e). The surface morphology of xerogels crosslinked with sodium molybdate is shown in Figure 3.5 (g) and (h). It should be noted from Figure 3.5 (h) that the xerogel beads surface exhibits lacerations which could have implications for these beads when utilized as a delivery system as water may find it easier to permeate the surface of the bead.
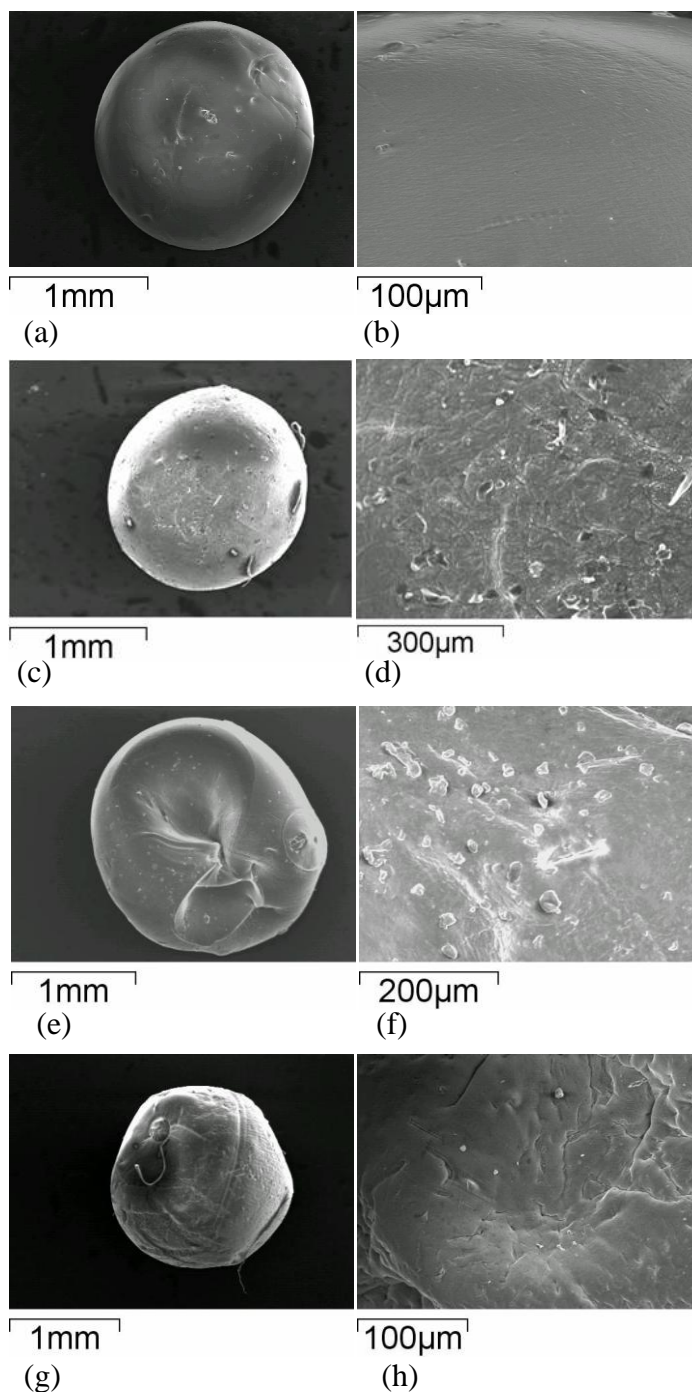
Figure 3.5 SEM micrographs of xerogel beads crosslinked with different ionic crosslinkers. The gelling solution contained 0.75 M NaOH, 60 mM DCD and 110 mM of a stated ionic crosslinker. The beads were kept in the gelling solution for 24 h and were subsequently washed in 60 mM DCD Millipore water solution and then dried in a 37 ± 1 ^{o}C oven for 24 h. The beads in micrographs (a) and (b) were gelled in NaOH solution with no ionic crosslinker. The ionic crosslinkers used to form the beads in micrographs (c) – (h) were [(c) sodium TPP (d) sodium TPP (e) trisodium citrate (f) trisodium citrate (g) sodium molybdate and (h) sodium molybdate.

It is noteworthy that the surface morphology of the chitosan xerogel beads crosslinked with TPP (Figure (a) and (b)) were significantly less porous than that of the beads exhibited by Ko *et al.*, even though the chitosan beads were crosslinked in a 366 mM TPP solution compared to 110 mM TPP here[18]. This is surprising as generally a higher crosslinker concentration in the gelling solution leads to less porous beads[19]. However, a substantially longer gelling time was used in the study presented here and sodium hydroxide was also used in the gelling solution. Likewise, SEM micrographs obtained for trisodium citrate beads by Lin *et al.* displayed a far more porous surface than the SEM obtained in this study for chitosan beads crosslinked in sodium citrate[20]. But once again the gelling solution in this study contains sodium hydroxide and Lin *et al.* used a substantially reduced gelation time of just 30 minutes compared to the 24 hour gelation time used for every bead in this research. Sodium hydroxide was used in the gelling solution in this research as it aided in the formation of a uniform, reproducible and spherical chitosan hydrogel bead, especially when combined with TPP.

3.2.1.2 Influence of Ionic Crosslinker on the DCD Release Properties

The literature indicates that the effective and most generally used way of controlling the drug release rate from a chitosan hydrogel bead is to gel the bead in the presence of an ionic crosslinker[21-23]. However, no one ionic crosslinker has been shown to be the most effective at controlling drug release, instead there have been a variety of different ionic crosslinkers employed by authors. Alsarra *et al.*[24] reported that crosslinking hydrogel beads with TPP was a quick and effective method for producing spherical beads. Chen *et al.*[9] reduced the equilibrium release time of their chitosan xerogels by using sodium citrate as an ionic crosslinker and Dambies *et al.*[13] prepared chitosan hydrogel beads using molybdate as the gelling agent, which resulted in a bead with a significantly reduced pore size. To compare the ionic crosslinkers and determine which is the most effective at creating a controlled DCD release delivery system, a study was carried out. The results are presented in Table 3.1.

Table 3.1 Influence of ionic crosslinker on the release of DCD from xerogel beads. The gelling solution contained the ionic crosslinker, 60 mM DCD and 0.75 M NaOH. The beads were subsequently washed in 60 mM DCD Millipore water solution and dried in an oven at a constant temperature of 37 ± 1 ^{o}C for 24 h.

Ionic crosslinker	Concentration of crosslinker in gelling solution (mM)	Time to reach DCD release equilibrium (min)	Bead size (mm)	Concentration of release solution at release equilibrium (mM)
none	0	40	1.53 ± 0.11	0.06
TPP ions	110	40	1.64 ± 0.13	0.06
Citrate ions	110	35	1.77 ± 0.12	0.04
Molybdate ions	110	30	1.67 ± 0.10	0.03
Alginate ions	1% (w/v)	45	1.82 ± 0.13	0.06

The results show that there was no significant difference between the ionic crosslinkers and that release was rapid and uncontrolled regardless of which ionic crosslinker was used. However, the amount of DCD released at equilibrium by chitosan beads crosslinked with a molybdate or citrate ion was diminished when compared with DCD release from a hydroxide, TPP or alginate ion crosslinked bead. In this research release equilibrium is considered the point in time at which no further DCD release is detected from the chitosan beads by UV/vis spectroscopy. The smaller amount of DCD released at equilibrium by chitosan beads crosslinked with a molybdate or citrate ion may be due to a poor crosslinking density inside the citrate and molybdate ion crosslinked xerogel beads. This resulted in poor DCD encapsulation or perhaps not all of the DCD was released from the beads. As shown in Section 3.2.1.1, using TPP as a crosslinking ion resulted in a simple way to make spherical and uniform xerogel beads. As a result sodium TPP was used as the primary ionic crosslinking agent in this research.

3.2.2 Chitosan Xerogel Beads Crosslinked with Tripolyphosphate

3.2.2.1 Swelling Properties

Investigating the swelling properties of the xerogels was important as it affects the diffusion and release of an encapsulated molecule when the beads are applied as a delivery system[25]. Swelling is primarily influenced by ionic interactions between chitosan chains, which are set by the concentration of the crosslinker used in the gelling solution[19]. The swelling ratio (%) was calculated using Equation 2.2. The effect of TPP concentration in the gelling mixture on swelling ratio (%) of the chitosan xerogel beads in Millipore water was investigated and the results are shown in Figure 3.6.
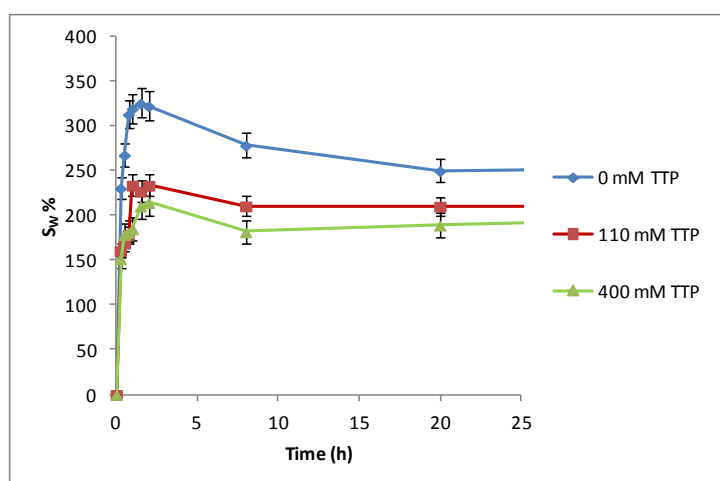
Figure 3.6 A comparison of the swelling ratio (%) of chitosan xerogel beads crosslinked in 0 mM, 110 mM and 400 mM TPP. After crosslinking the beads were washed in Millipore water and dried in an oven for 24 h at 37 ± 1 °C. The weight of the swollen beads was measured after the surface solution was removed by dotting the beads on filter paper. The study was conducted at 20 ± 1 °C and repeated in triplicate.

The results in Figure 3.6 indicated that there was a rapid uptake of water by each of the chitosan xerogels during the initial 60 min at which point in time the swelling ratios (%) observed were 321%, 238% and 215% for chitosan xerogel beads crosslinked in 0 mM TPP, 110 mM TPP and 400 mM TPP solutions, respectively. After 20 h there was a decrease in the swelling ratio (%) observed to 251%, 218 % and 183% for chitosan xerogel beads crosslinked in 0 mM TPP, 110 mM TPP and 400

mM TPP solutions, respectively. A decrease in the swelling ratio (%) suggested the beads were degrading. As the error bars of the swelling ratios (%) of beads crosslinked in 110 mM TPP and 400 mM TPP solutions overlapped it was apparent that there was not a significant difference in their values. The ionically crosslinked xerogel beads exhibited a lower swelling ratio (%) than the beads gelled in sodium hydroxide solution only. These results suggested that crosslinking the beads with TPP resulted in an increase in the crosslinking density, which reduced the swelling ratio (%). This conclusion was in agreement with a study published by Ko *et al*. which reported that an increase in the TPP crosslinking density of chitosan beads resulted in the beads having less swelling ability[18]. The high percentage of swelling seen in the chitosan xerogel beads in Figure 3.6 is not uncommon as Liu *et al*. developed beads using 2% (w/v) chitosan that swelled up to 200%[25]. By increasing the percentage of chitosan in the formulation they were able to decrease the swelling ratio (%); however to do so in this study would impair the spherical shape of the hydrogel beads, as exhibited in Section 3.2.2.3. Wu *et al*. calculated the initial swelling ratio (%) of disulfide crosslinked chitosan beads as being over 550%[26]. It was concluded from the results in Figure 3.6 that crosslinking the chitosan xerogel beads with sodium TPP increased the crosslinking density of the polymer matrix and as a result reduced the swelling capacity of the beads.

3.2.2.2 Influence of the TPP Concentration in the Gelling Solution

As shown previously (Section 3.2.2.1), when the concentration of TPP in the gelling solution increased there was a decrease in the swelling ratio (%) of the chitosan xerogel beads. This meant that crosslinking density of the polymer matrix had increased, which is known to influence the release properties of chitosan beads[19]. An investigation was carried out to see if increasing the TPP concentration in the gelling solution would decrease the DCD release time of the xerogel beads. The results of the study are displayed in Figure 3.7.
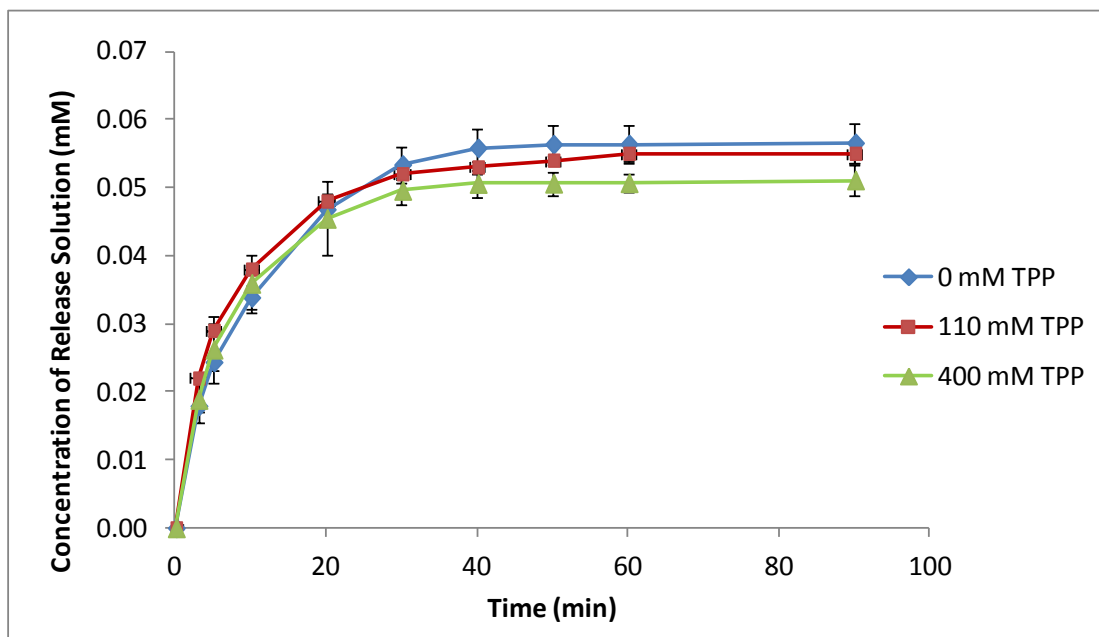
Figure 3.7 Release profile of DCD from xerogel beads crosslinked in different concentrations of TPP. The gelling solution contained the stated concentration of ionic crosslinker, 60 mM DCD and 0.75 M NaOH. The beads were subsequently washed in 60 mM DCD Millipore water solution and dried in an oven at a constant temperature of 37 ± 1 °C for 24 h.

An examination of the data shows that increasing the concentration of TPP in the gelling solution failed to control the release of the DCD from the chitosan xerogel beads. It is also evident from Figure 3.7 that as the concentration of TPP in the gelling solution increased, the amount of DCD released was slightly reduced. This may have been due to an increase in the polymer network density of the beads due to additional ionic crosslinking which led to less DCD being encapsulated. The DCD release data from chitosan xerogel beads crosslinked with increasing concentrations of sodium TPP were fitted to zero-order model (Equation 2.6) and first-order (Equation 2.8) as shown in Figure 3.8 (a-b) to calculate the rate constants (Table 3.2). The advantage of fitting observed data to such expressions is that release properties can be treated and analysed by statistical and mathematical methods[27].

(a)   (b)
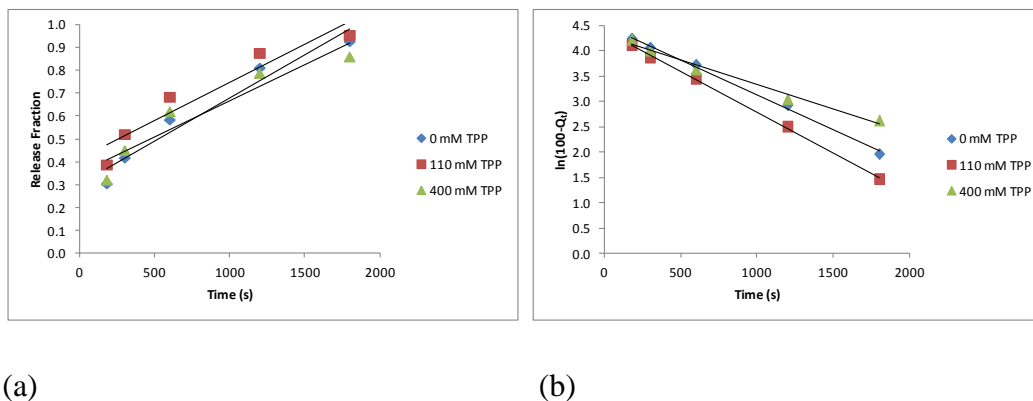
Figure 3.8 Release data from xerogel beads crosslinked in different concentrations of TPP fitted to the (a) Zero-order, (b) First-order models. The gelling solution contained the stated concentration of ionic crosslinker, 60 mM DCD and 0.75 M NaOH. The beads were subsequently washed in 60 mM DCD Millipore water solution and dried in an oven at a constant temperature of 37 ± 1 °C for 24 h.

Table 3.2 Results from the fitting of xerogel beads crosslinked in different concentrations of TPP fitted to the (a) Zero-order and (b) first-order model. The gelling solution contained the stated concentration of ionic crosslinker, 60 mM DCD and 0.75 M NaOH. The beads were subsequently washed in 60 mM DCD Millipore water solution and dried in an oven at a constant temperature of 37 ± 1 °C for 24 h.

Formulation	Zero-Order Model		First-Order Model	
	k_0 (s^{-1})	R^2	k_1 (s^{-1})	R^2
0 mM TPP	3.76×10^{-4}	0.9501	1.38×10^{-3}	0.9965
110 mM TPP	3.35×10^{-4}	0.8997	1.06×10^{-3}	0.9986
400 mM TPP	3.16×10^{-4}	0.8975	9.71×10^{-4}	0.9836

The results in Table 3.2 show that increasing the concentration of sodium TPP in the gelling solution did not affect the rate constant of DCD release from the xerogel beads to any substantial degree. This result complements research published by Shu and Zhu who determined that an increase in TPP cross linkage of chitosan beads resulted in only a slight decrease of the equilibrium release time of their model release drug

riboflavin[2]. The regression line fit was best for first-order release for each of the release profiles. A good first-order fit is consistent with a membrane controlled diffusion system where the gradient is reduced by decreasing concentration on the donor side in combination with sink conditions in the dissolution medium[27]. The similar DCD release characteristics and rate constants of chitosan beads synthesised in a gelling solution of 0.75 M NaOH and 0 mM, 110 mM or 400 mM TPP can indicate that the sodium hydroxide is more influential in the gelling mixture than the TPP. As the beads hit the gelling solution the NaOH neutralises the glucosamine unit of chitosan which hinders ionic crosslinking by TPP. The ionic crosslinker did retain some influence on the physical properties of beads as shown in Section 3.2.1.1. However, NaOH was the most influential component of the gelling solution in each formulation.

3.2.2.3 Influence of Chitosan Concentration

A study was carried out to determine whether or not altering the weight per volume percentage of chitosan in the xerogel bead formulation would affect the release rate or total amount of DCD released from the xerogel beads. Ko *et al.*[18] performed release studies using Felodipine (Figure 3.9), prescribed for hypertension, as a model drug.
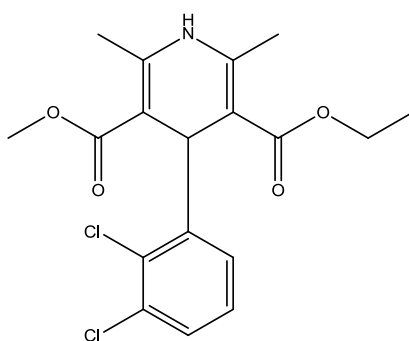
Figure 3.9 Felodipine

Ko *et al.* found that increasing the percentage weight per volume of chitosan in the gelling solution extended the time to reach release equilibrium. This was due to an increase in viscosity of the chitosan solution which slowed the release rate of drug crystals[18].

However, as the results show in Table 3.3, altering the chitosan concentration dropped into the gelling solution resulted in no net change in the release time. A minimal effect was also observed on the concentration of the release solution at equilibrium. This may be due to the fact that Felodipine is a larger molecule than DCD which would make its release easier to control, and DCD is very water soluble mean it would release faster. Thus it was concluded that increasing the chitosan concentration from 1% (w/v) to 2% (w/v) was not enough of an increase to improve the release properties of the chitosan xerogel beads to any tangible degree.

Table 3.3 Influence of chitosan percentage (w/v) in aqueous acetic acid solution on release of DCD from xerogel beads. The gelling solution contained 110 mM TPP and 0.75 M NaOH. The beads were subsequently washed in 60 mM DCD Millipore water solution and dried in an oven at a constant temperature of 37 ± 1 °C for 24 h.

Percentage %(w/v) of chitosan in aqueous acetic acid solution	Time to reach release equilibrium (min)	Concentration of release solution at equilibrium (mM)
2	40	0.06
1	40	0.05

Increasing the concentration of chitosan in the xerogel beads to 3% (w/v) caused the chitosan to form highly viscous solutions which did not form reproducible spherical beads as shown in Figure 3.10. The xerogel beads were closer to a tear-shape rather than the spherical morphology shown previously (Figure 3.5 (a)). Therefore, the weight per volume percentage of chitosan solution used in the gelling solution was maintained at 2% for all future studies.

(a)   (b)
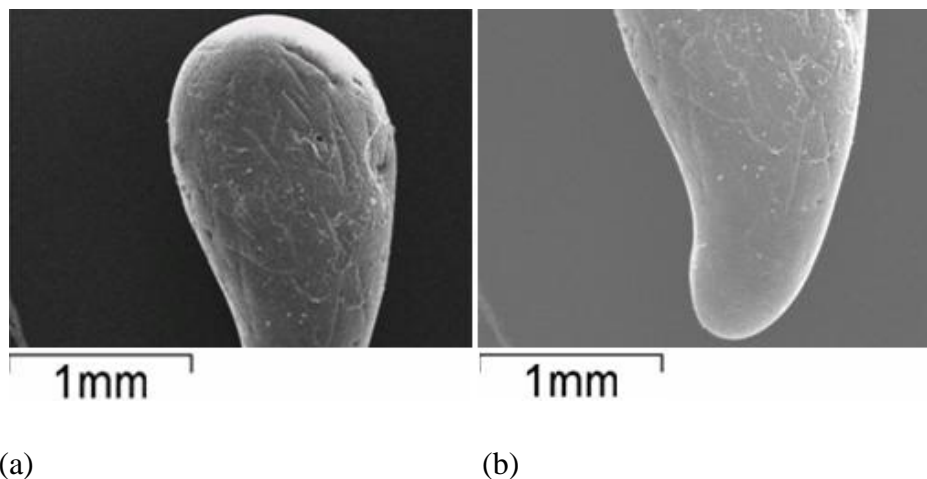
Figure 3.10 SEM micrographs of a xerogel bead synthesised with 3% (w/v) chitosan in acetic acid solution. The gelling solution contained 110 mM sodium TPP and 0.75 M NaOH. The beads were washed in Millipore water and dried in an oven at a constant temperature of 37 ± 1 °C for 24 h.

3.2.2.4 Influence of the DCD Concentration in the Loading Solution

A study was performed to determine whether or not the amount of DCD released by the chitosan xerogel beads could be pre-determined by gelation of the beads in solutions containing different concentrations of DCD. The results presented in Table 3.4 show that the DCD loading concentration did not have an effect on the time for the release to reach equilibrium. It was concluded that changing the DCD concentration in gelling mixture did not help achieve a controlled release system.

Table 3.4 Influence of DCD loading concentration on DCD release from xerogel beads. The gelling solution contained 110 mM sodium TPP and 0.75 M NaOH. The beads were subsequently washed in DCD Millipore water solution and dried in an oven at a constant temperature of 37 ± 1 °C for 24 h.

DCD concentration in gelling mixture (M)	Time to reach release equilibrium (min)	Concentration of DCD in release solution at equilibrium (mM)
1.20	40	0.96
0.80	40	0.71
0.60	40	0.60
0.06	40	0.06

The results in Table 3.4 did show however that the concentration of DCD in the gelling solution has a linear relationship with the amount of DCD released from the xerogel beads at equilibrium release time. A straight line graph of DCD concentration in gelling mixture vs. concentration of DCD in the release solution at equilibrium gives $R^2 = 0.9762$ (Figure 3.11). This relatively positive correlation was beneficial as the hydrogel beads can be tailored to release a pre-determined amount of the DCD. This same conclusion was shared by a number of reports that showed that the amount of drug released from a chitosan microsphere increases with the amount of drug encapsulated[28, 29]. However, the highest amount of DCD released from chitosan xerogel beads was on average 4 mg. For a DCD application of 7.5 kg ha^{-1} an estimated 1.8 million beads would be required. Chitosan xerogel beads used in field trials would have to be capable of encapsulating greater amounts of DCD.   It was important that the time to reach release equilibrium remained the same for each loading concentration as this meant a value could be selected that would allow release experiments to be performed easily. The concentration of DCD in the loading solution was maintained at 60 mM for the rest of the studies as this low concentration facilitated the use of UV/vis spectroscopy to study DCD release.
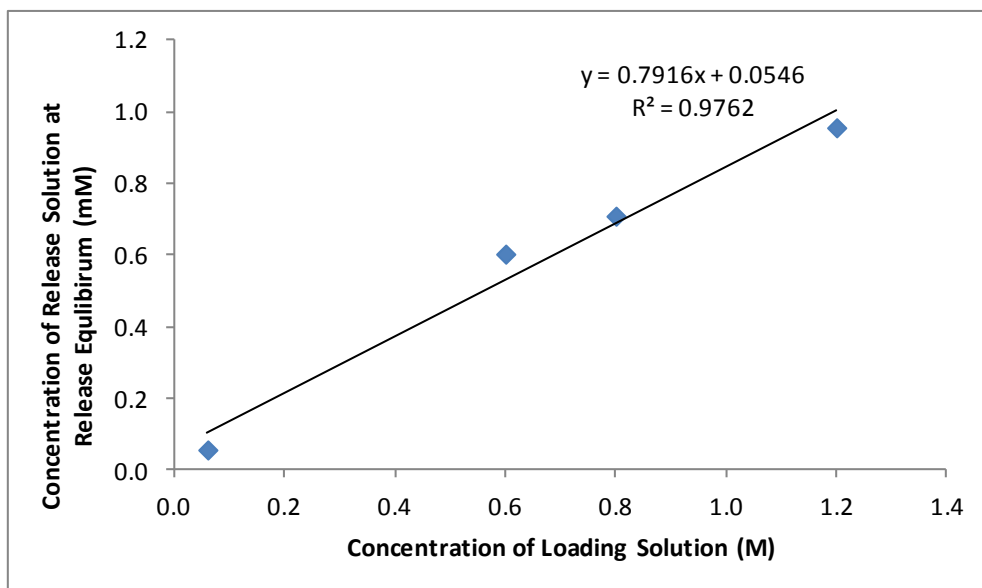
Figure 3.11 The relationship between concentration of DCD in the loading solution and the concentration of the release solution at release equilibrium. The gelling solution contained 110 mM sodium TPP and 0.75 M NaOH. The beads were subsequently washed in Millipore water and incubated in an oven at 37 ±1 °C for 7 days.

3.2.3 Multilayer/Dual Crosslinked Chitosan Xerogel Beads

Recently, polyelectrolyte complexes composed of chitosan-alginate polysaccharides reinforced with polyphosphate anions have been developed that show improved drug release properties compared with beads crosslinked with a single ionic crosslinker[30]. These xerogel beads are described either as multilayer[30] or dual crosslinked[31]. The central principal is that by crosslinking with more than one ionic crosslinker, the release properties of xerogel beads improve. Dual crosslinked beads were synthesised by Xu *et al*. which were found to improve the stability of beads under gastrointestinal tract conditions and released bovine serum albumin in a controlled manner[31]. Anal and Stevens synthesised multilayer beads for the controlled release of the antibiotic ampicillin. They synthesised xerogel beads with various combinations of chitosan and sodium alginate crosslinked with calcium chloride to make the xerogel beads properties more suitable for drug release[30].

3.2.3.1 Surface Morphology

In this study, dual and multilayer crosslinked xerogel beads were synthesised as described in Section 2.2.2.2. The results of a study comparing the surface morphology of dual-crosslinked, multilayer and TPP ion crosslinked xerogels using an SEM are presented in Figure 3.12. The SEM micrographs of dual crosslinked and multilayer xerogels exhibit a substantially different surface morphology compared to chitosan-TPP xerogels. In contrast to the surface of dual and multilayer crosslinked beads the surfaces of the chitosan-TPP beads were smooth and uniform. The surface of the multilayer beads is uneven and appears cracked and brittle, while the surface of the dual crosslinked bead is covered with rough troughs which are unevenly distributed on the surface of the bead. However, unlike chitosan-TPP xerogels, no cracks or indentations are visible on the immediate surface of the dual crosslinked beads which suggests it may be a more water resistant bead. Anal and Stevens[30] did not display any SEM micrographs of their multilayer beads, however Xu *et al*.[31] did show SEM micrographs of their dual crosslinked beads. Those beads exhibited a similar surface morphology to the beads synthesized in this research. Xu *et al*. described the morphology of their dual-crosslinked bead as being 'wrinkled' as a result of the interaction between the alginate and chitosan and suggested that the blend system had formed a random fibrillar network[31].
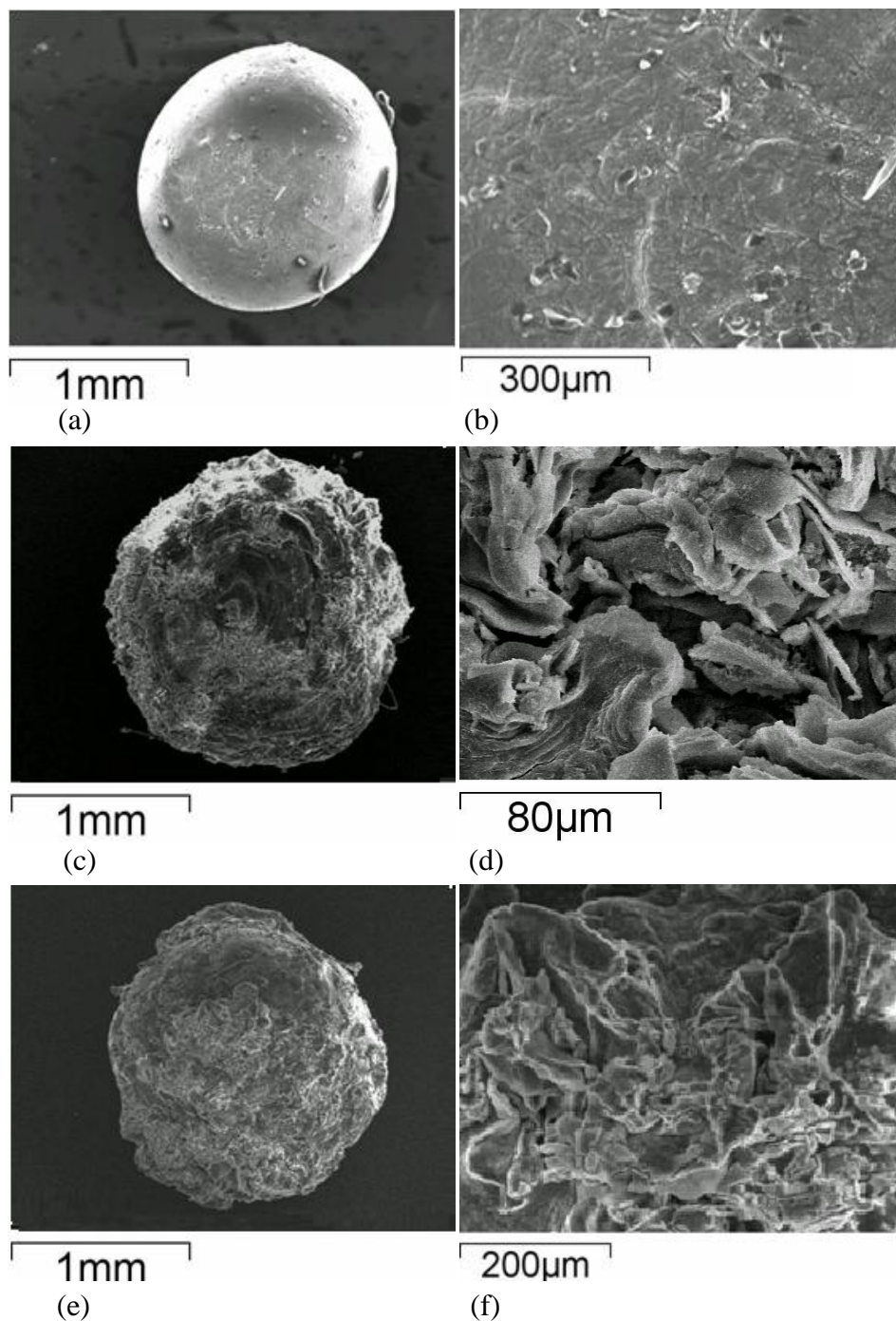
Figure 3.12 SEM micrographs of chitosan-TPP xerogel and dual crosslinked xerogel beads. The gelling solution of (a) and (b) contained 110 mM sodium TPP, 60 mM DCD and 0.75 M NaOH. (c) and (d) are SEM micrographs of multilayer beads and (e) and (f) are SEM micrographs of dual crosslinked beads. All the xerogel beads were subsequently thoroughly washed in 60 mM Millipore water solution and dried in a $37 \pm 1^{\circ}$C oven for 24 h.

3.2.3.2 Swelling Properties

The swelling characteristics of dual crosslinked and multilayer beads are examined in Figure 3.13.
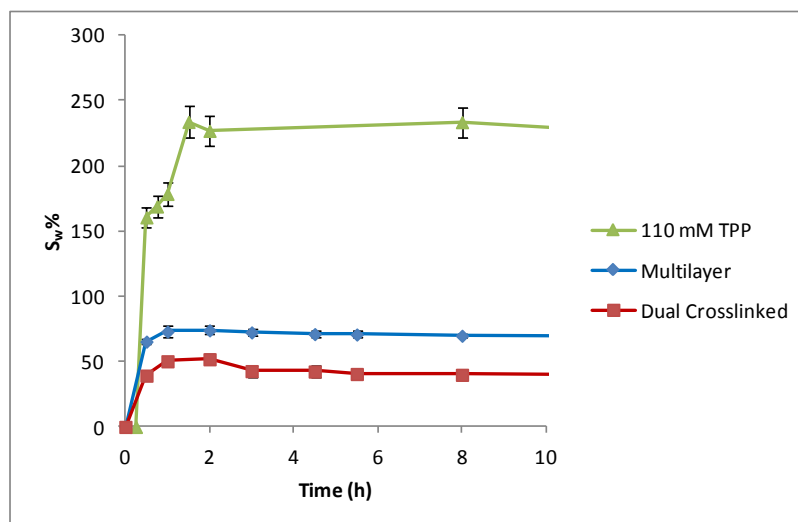
Figure 3.13 Influence of multiple ionic crosslinkers on swelling ratio (%) of chitosan beads in Millipore water. After crosslinking the beads were washed in Millipore water and dried in an oven for 24 h at 37 ± 1 °C. The weight of the swollen beads was measured after surface solution was removed by filter paper. The study was conducted at 20 ± 1 °C and repeated in triplicate.

The swelling ratio (%) values exhibited in Figure 3.13 indicate that dual crosslinked and multilayer beads initially exhibit swelling characteristics similar to chitosan xerogel beads crosslinked with TPP. There was a rapid uptake of water within the first hour followed by a period over approximately 8 h during which there was essentially no change in mass. The primary difference was the swelling ratio (%) which was substantially lower after 2 h for dual crosslinked (51%) and multilayer xerogel beads (74%) than chitosan-110 mM TPP xerogel beads (234%). In contrast, the multilayer beads synthesized by Anal and Stevens[30] had a swelling index of 135%, however their swelling study was conducted in a solution at pH 1.2 and 37 ± 1 °C. This was in order to simulate stomach conditions, and would be expected to show an increase in the swelling ratio (%) compared to a study performed in Millipore water at 20 ± 1 °C. On the other hand, the swelling ratios (%) calculated by Xu *et al*. were closer to the

values obtained in this study for dual crosslinked chitosan beads as the maximum swelling ratio (%) they calculated was approximately 40%, compared with 51 % obtained in this study[31]. Swelling ratio (%) values and crosslinking density are closely related, a reduction in the swelling ratio suggested the stability of the polymer network of dual and multilayer beads was greater than that of chitosan beads crosslinked with TTP ions only[19].

3.2.3.3 DCD Release Properties

The results in Table 3.5 show the results of DCD release experiments from dual-layer and multi-layer xerogel beads.

Table 3.5 Influence of multiple ionic crosslinkers on the release of DCD from xerogel beads. The gelling solution contained multiple ionic crosslinkers including sodium alginate (SA), TPP and 0.75 M NaOH. The beads were washed in 60 mM DCD Millipore water solution before and after each gelling solution and dried in an oven at a temperature of 37 $\pm 1^{o}$C for 24 h.

Formulation	Gelling Solution	Post-gelling solution	Second gelling solution	Mean Size (mm)	Time to reach release equilibrium (min)	Concentration of release solution at equilibrium (mM)
Multilayer Bead	8% (w/v) TPP, 0.8% (w/v) SA	0.08%(w/v) SA, 2% (w/v) CaCl$_2$	-	2.20 $\pm$ 0.10	60	0.06
Dual crosslinked Bead	2% (w/v) SA, 3% (w/v) TPP	2% (w/v) CaCl$_2$	2% (w/v) Na$_2$SO$_4$	1.96 $\pm$ 0.08	75	0.05

The results in Table 3.5 reveal that the dual-layer xerogel beads exhibit a longer release time (75 min) than the multilayer beads (60 min) and the TPP crosslinked xerogel bead examined in Section 3.2.1.2. The dual crosslinked beads released

slightly less DCD at release equilibrium time than the multilayer beads. This may have been due to the dual crosslinked beads having a greater polymer network density, as this influences the porosity of the hydrogel beads which can influence their DCD loading capacity[1]. A greater polymer network density would also account for the dual crosslinked xerogel beads exhibiting a longer time for the DCD release to reach equilibrium. The larger size of the multilayer beads can be explained by having been crosslinked in two separate solutions of sodium alginate. In this research, beads gelled with sodium alginate have consistently proven to produce spherical beads larger in diameter than other ionic crosslinkers. By monitoring the change in the transparency of the dual crosslinked beads (by careful visual observation) an interesting trend was seen taking place. During the initial gelling, crosslinking began from the outer shell and advance inwards, as expected. Consequently, crosslinking was also initiated at the core of the beads and moved outwards towards the outer shell. Crosslinking from the core of the bead outwards has only been observed in the dual crosslinked beads discussed here. The release kinetics were examined in Figure 3.14 and the results are shown in Table 3.6.

(a)   (b)
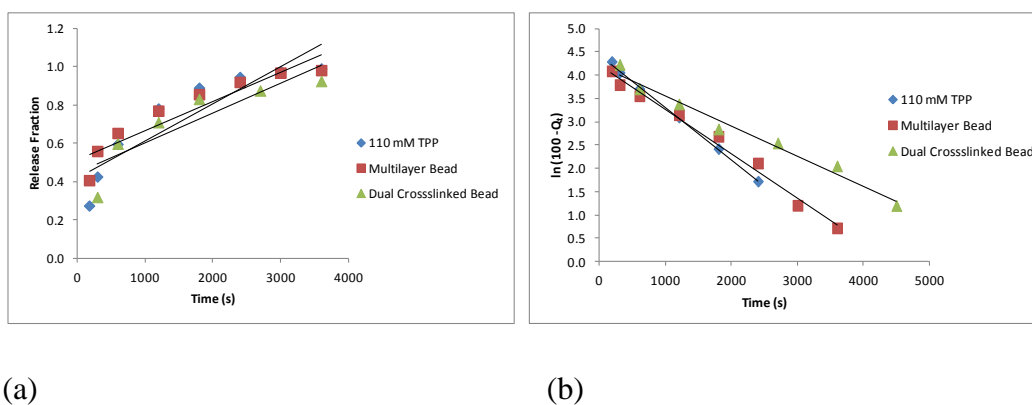
Figure 3.14 Release data for TPP, multilayer and dual crosslinked chitosan xerogel beads fitted to the (a) Zero-order and (b) First-order models. The beads were washed with 60 mM Millipore water solution and incubated in an oven at 37 ±1 °C for 24 h.

Table 3.6 Results from fitting of release data to the (a) Zero order and (b) First-order models. The beads were washed in 60 mM Millipore water solution before and after each gelling solution and dried in an oven at a constant temperature of 37 ± 1 °C for 24 h.

Formulation	Zero-Order Model		First-Order Model	
	k_0 (s^{-1})	R^2	k_1 (s^{-1})	R^2
110 mM TPP	3.18×10^{-4}	0.8997	1.45×10^{-3}	0.9986
Multilayer Bead	1.52×10^{-4}	0.8734	1.54×10^{-4}	0.9809
Dual Crosslinked Bead	1.27×10^{-4}	0.7686	1.08×10^{-4}	0.9768

The results from the fitting of the release data to the models are displayed in Table 3.6. They showed that the release of DCD from multilayer and dual crosslinked xerogels are best described by the first-order model. Dual crosslinked beads exhibited the smallest first-order rate constant (1.08×10^{-4} s^{-1}) which corresponded to DCD from these beads exhibiting a longer time to reach DCD release equilibrium compared to the multilayer or TPP ion crosslinked xerogel beads (Table 3.6). These results suggest that using multiple ionic cross linkers was a more effective method of controlling DCD release than just using a single ionic crosslinker. However, even the dual-layer xerogels still exhibited a relatively short time to reach DCD release equilibrium. Therefore, the beads were crosslinked with a covalent crosslinker in an attempt to extend the release time as discussed in the next section.

3.2.4 Covalently Crosslinked Chitosan Hydrogel and Xerogel Beads

3.2.4.1 Introduction to Covalent Crosslinkers

Chemical crosslinking of chitosan with covalent crosslinkers is considered the simplest and most straightforward way of creating permanent hydrogel networks (Figure 3.15)[1]. These hydrogels are covalently bonded together either by using small cross-linker molecules or secondary polymerizations, and their properties are mainly influenced by their crosslinking densities[32]. Studies have shown that crosslinking chitosan with dialdehydes has led to an improvement in the mechanical properties of chitosan fibre[33]. The most common covalent crosslinkers used are glyoxal and glutaraldehyde. Both glyoxal (Figure 3.16) and glutaraldehyde (Figure 3.17) are dialdehydes and react with chitosan via the same mechanism[34].
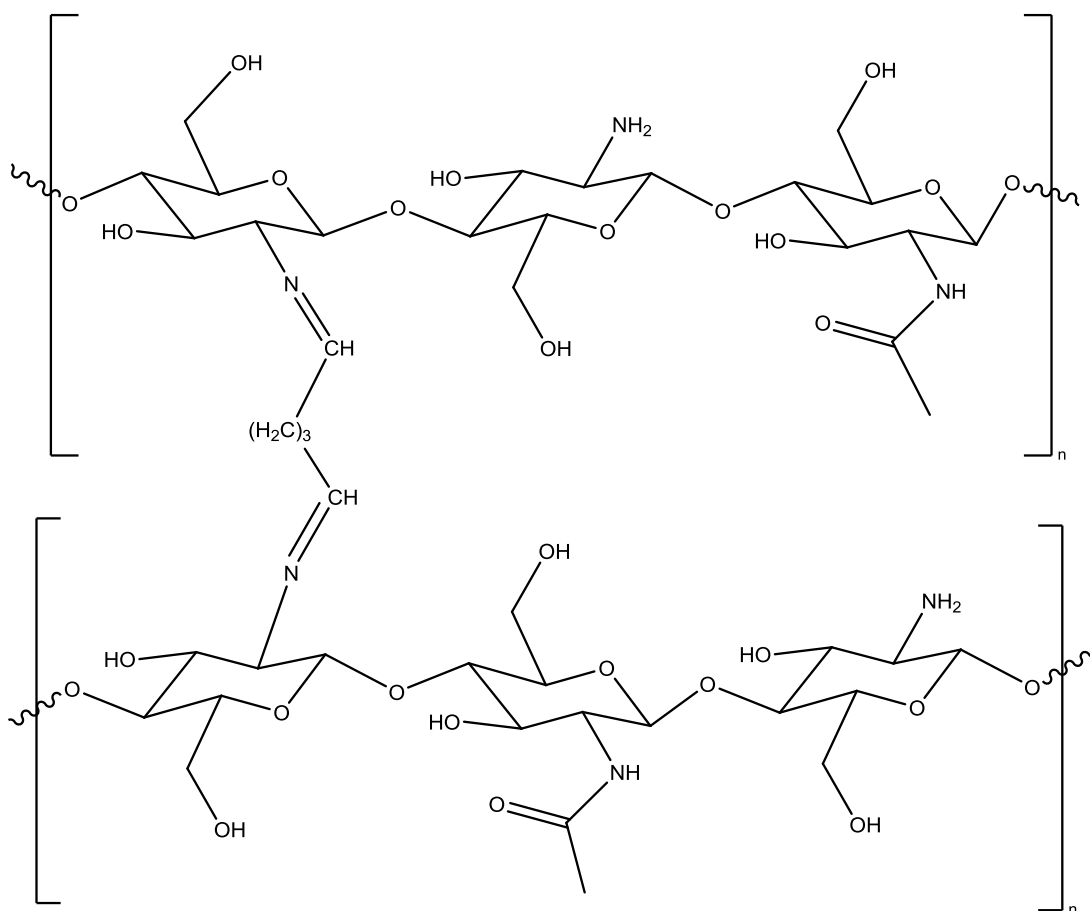
Figure 3.15 Chitosan crosslinked with glutaraldehyde

The aldehyde groups form covalent imine bonds with the amino groups of chitosan via a Schiff base reaction[35]. The reaction can be performed in aqueous media and under mild conditions.
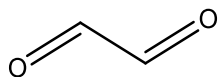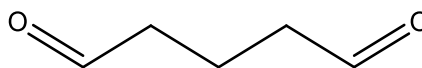
Figure 3.16 Glyoxal   **Figure 3.17 Glutaraldehyde**

A natural crosslinker called genipin has also attracted attention as a covalent crosslinker[36]. Traditionally used as a dyeing agent and as a treatment for diabetes, genipin has been shown to react with chitosan to form covalent bonds under basic aqueous conditions. The reaction occurs when two separate reactions lead to the formation of crosslinks between genipin and chitosan (Scheme 3.1). Crosslinking bridges can also be formed from polymerized genipin macromers or oligomers [37]. Research from other authors has shown that release profiles and the release mechaism of drugs from covalently crosslinked xerogels are influenced by multiple factors including the pH and temperature of the release medium and the polymer network density[34, 38, 39]. In addition, by carrying out the appropriate analysis of the drug release data, it has been demonstrated that the drug transport mechanism and drug release kinetics involved in the release of drugs from covalently crosslinked xerogel beads can be determined [40].
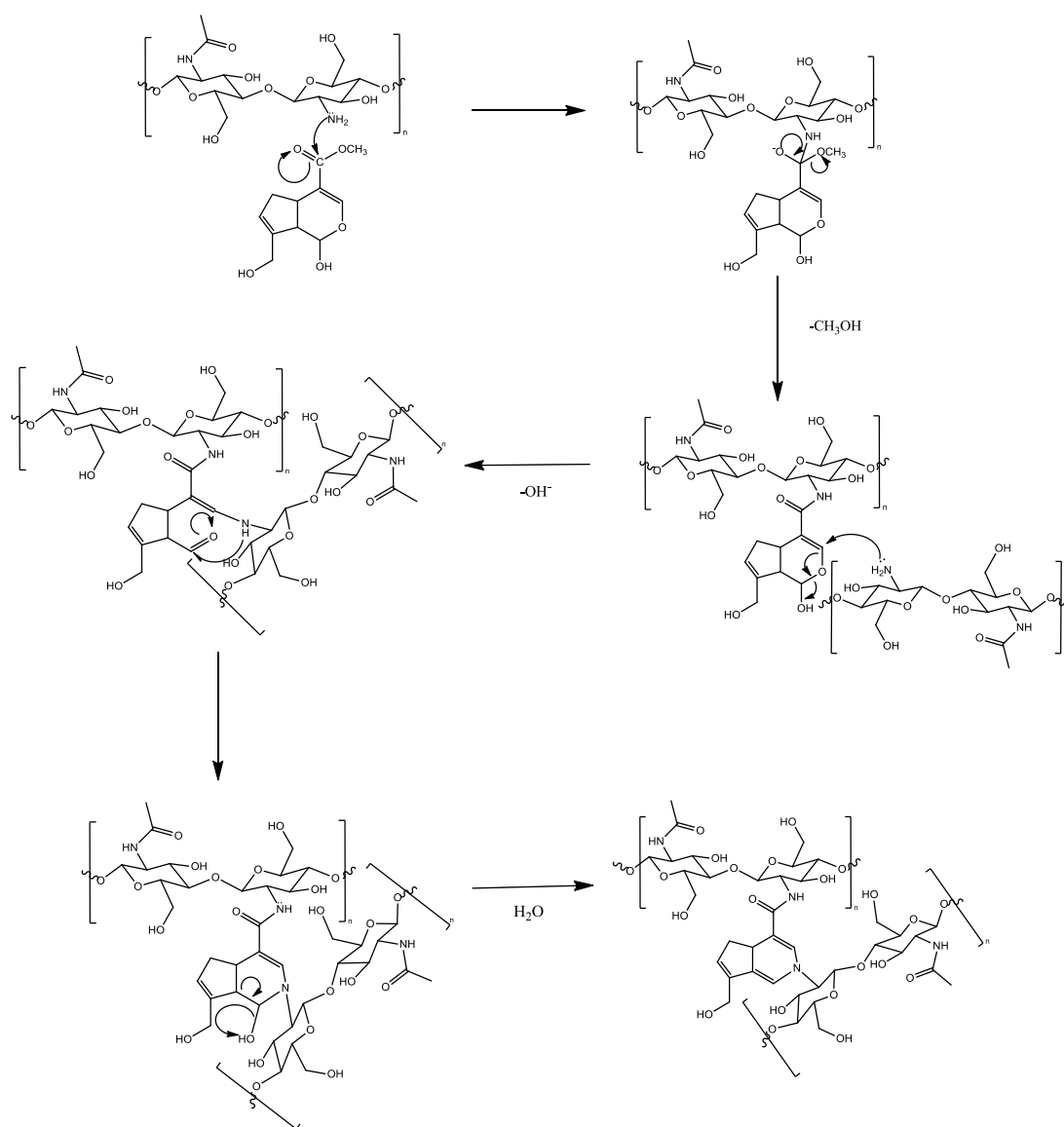
Scheme 3.1 A proposed mechanism for the crosslinking of chitosan by genipin

3.2.4.2 Surface Morphology

Chitosan xerogel beads with covalently bonded cross linkages were prepared as stated in Section 2.2.2.3. In brief, hydrogel beads prepared by a precipitation and ionic gelation were transferred from Millipore water storage to an aqueous solution containing either a known molar concentration of genipin, glyoxal or glutaraldehyde. They were stirred at a rate of 25 rpm for 24 h, then removed from the crosslinking solution and washed with 60 mM DCD Millipore water solution for a further 24 h until reaching neutrality and were stored in a fresh 60 mM Millipore water solution. To form covalently crosslinked xerogel beads the hydrogel beads were removed from storage and placed in an oven set to 37 ± 1 °C for a minimum of 24 h by which time the bead was dehydrated and were considered 'xerogels'. The shape and surface of the xerogels were examined using SEM and the micrographs are displayed in Figure 3.18.

Comparing the surface morphology of the beads crosslinked in TPP and hydroxide ions only in Figure 3.18 (a) to the surface morphology of the TPP and covalently crosslinked beads it is apparent that the covalent crosslinking has a substantive effect on the surface morphology of the xerogel beads. The surface morphology of the beads was no longer smooth, however the shape of the covalently crosslinked beads remained spherical. The surface of the glyoxal crosslinked bead is uneven and shows indentations on the surface; however these appear to be shallow. The xerogels crosslinked in glutaraldehyde solution exhibit a different surface morphology to that of glyoxal crosslinked xerogels. The glutaraldehyde solution crosslinked xerogels are smooth and display no signs of indentations or depressions to the surface of the bead. When the xerogels crosslinked with genipin were examined using SEM they unfortunately showed instant signs of damage caused by the high energy beam of electrons. In the micrograph shown in Figure 3.18 (g) the damage is highlighted by a red circle. Examination of the undamaged surface reveals a surface morphology comparable with that of xerogels crosslinked with glyoxal, but with large deep cracks that appear likely to affect DCD release from the bead.
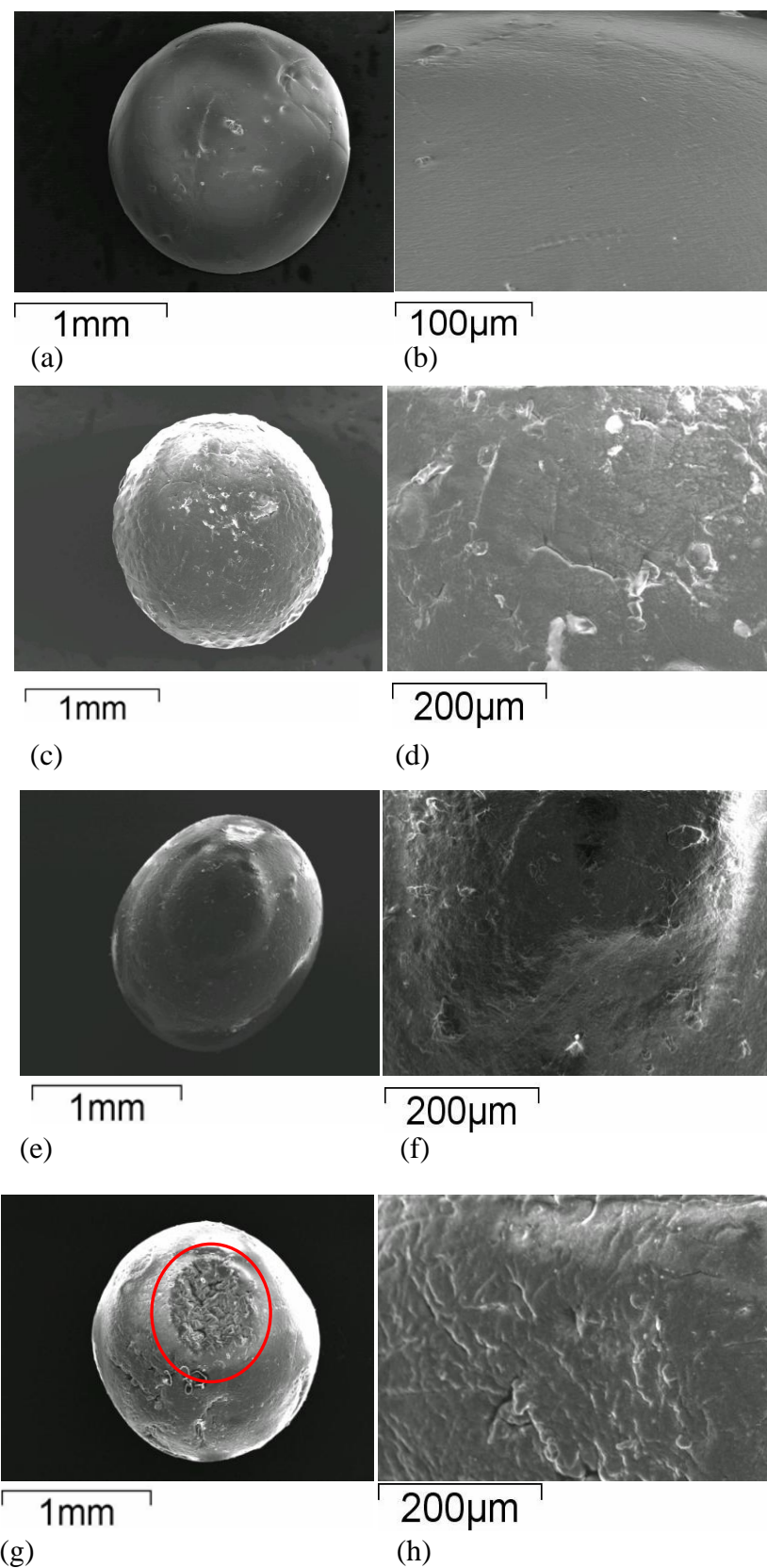
Figure 3.18 SEM micrographs of covalently crosslinked chitosan xerogel beads. Xerogels (a) and (b) were crosslinked in 110 mM TPP only. Xerogels (c) and (d) were crosslinked in 300 mM glyoxal solution. Xerogels (e) and (f) were crosslinked in 300 mM glutaraldehyde and xerogels (g) and (h) were crosslinked in 110 mM genipin solution. All the beads were washed in Millipore water and dried in an oven for 24 h at 37 ± 1 °C.

95

Xerogels crosslinked with genipin were observed to be blue in colour rather than the transparent yellow of glyoxal and glutaraldehyde xerogel beads. Muzzarelli and co-workers also obtained a blue colouration when they crosslinked chitosan with genipin. They state that the blue colouration is associated with the oxygen radical induced polymerization of genipin when it is exposed to air as well as when it reacts with amino groups[36]. The blue coloration of genipin when reacted with amino groups makes it simultaneously useful in colorimetry and fluorimetry[36].

3.2.4.3 DCD Release Properties of Covalently Crosslinked Chitosan Hydrogel Beads

Chitosan hydrogel beads were covalent crosslinked in order to investigate whether the resulting increased polymer network density could control DCD release without the need for the beads to be dehydrated to form a xerogel. However, a comparison of the influence of different covalent crosslinkers on DCD equilibrium release time of hydrogel beads showed no difference between release times (Table 3.7). In fact, crosslinking with a covalent crosslinker did not show an improved release time even when compared with a hydrogel ionically crosslinked with sodium TPP (Table 3.1) and there was no difference in the concentration of DCD in the release solution at equilibrium release time. The conclusion was that despite covalent crosslinking of the hydrogel the pores continued to be too large and release rate of DCD from hydrogel was still uncontrolled.

Table 3.7 Influence of covalent crosslinker on the release of DCD from hydrogel beads. The gelling solution contained the 110 mM Sodium TPP, 60 mM DCD and 0.75 M NaOH. The beads were then covalently crosslinked and washed in 60 mM DCD Millipore water solution.

Covalent crosslinker	Concentration of Covalent Crosslinking Solution (mM)	Concentration of TPP Crosslinker in Gelling Solution (mM)	Time to reach release equilibrium (min)	Concentration of release solution at equilibrium (mM)
None	0	110	40	0.06
Glyoxal	110	110	40	0.06
Glutaraldehyde	110	110	40	0.06
Genipin	110	110	40	0.06

3.2.4.4 DCD Release Properties of Covalently Crosslinked Chitosan Xerogel Beads

The covalently crosslinked hydrogel beads were dehydrated to form xerogels in order to reduce the polymer network mesh size further[7]. The drying of covalently crosslinked hydrogels to form xerogels is well established. Gupta and Jabrail and Mi *et al*. both dried their covalently crosslinked hydrogel beads in order to form beads capable of controlled release[34, 41]. The results from the release studies involving hydrogel beads covalently crosslinked and then dehydrated to form xerogel are shown in Table 3.8.

Table 3.8 Influence of covalent crosslinker on the release of DCD from xerogel beads. The gelling solution contained 110 mM sodium TPP, 60 mM DCD and 0.75 M NaOH. The beads were then covalently crosslinked and washed in 60 mM Millipore DCD solution and dried in an oven at a temperature of 37 ±1°C for 24 h.

Covalent crosslinker	Concentration of covalent crosslinking solution (mM)	Bead Size (mm)	Time to reach release equilibrium (h)	Concentration of release solution at equilibrium (mM)
Glyoxal	110	1.71 ± 0.09	4	0.05
Glyoxal	300	1.64 ± 0.06	6	0.03
Glyoxal	520	1.63 ± 0.04	8	0.03
Glutaraldehyde	300	1.73 ± 0.05	6	0.04
Genipin	110	1.51 ± 0.08	2	0.04

Due to the addition of the drying step to the formation of covalently crosslinked beads each set of beads investigated showed an increase in the time to reach release equilibrium compared with their hydrogel counterparts (Table. 3.7). Genipin crosslinked beads had the shortest equilibrium release time; this was in part due to the fact that beads containing genipin as a crosslinking agent could not be investigated past a concentration of 110 mM genipin in the crosslinking solution. This was due to the substantial cost of genipin which meant that beads crosslinked with the natural chemical were unsustainable as a cost effective release system. However chitosan xerogels crosslinked in 110 mM glyoxal solution showed an advantage over chitosan xerogels crosslinked in 110 mM genipin solution. Chitosan xerogels crosslinked in 110 mM glyoxal solution released a greater concentration of DCD into the release solution at equilibrium and exhibited a longer time to reach release equilibrium than xerogels crosslinked in 110 mM genipin solution. Chitosan xerogel beads crosslinked in 300 mM glutaraldehyde solution had a similar release time (6 h) but released a higher concentration of DCD (0.04 mM) at equilibrium when compared to xerogel beads crosslinked in the same concentration of glyoxal. These results concur with

literature, Gupta and Jabrail[34] compared the release of centchroman from glyoxal and glutaraldehyde crosslinked beads and found that while both significantly improved the control of drug release compared with non-covalently crosslinked xerogels, both exhibited similar release properties. It did not appear that one crosslinker had better properties than the other, although they did attribute the smaller amount of centchroman released by glyoxal crosslinked beads to them smaller than glutaraldehyde crosslinked beads[34]. In our study only glyoxal could be investigated at crosslinking solutions above 300 mM because xerogel beads crosslinked in concentrations greater than 300 mM glutaraldehyde were brittle and broke apart easily. However, xerogel beads crosslinked with glyoxal above 300 mM remained intact. Chitosan xerogel beads crosslinked with 520 mM glyoxal had the longest DCD release time but released the smallest amount of DCD at release equilibrium. The concentration of DCD released decreased as the glyoxal crosslinking concentration increased. This indicated that increasing the polymer crosslinking density reduced the amount of total DCD release as it became trapped in the polymer matrix. The release data from chitosan xerogel beads crosslinked in 110 mM genipin or 110 mM glyoxal solution were fitted to the zero-order and first-order models and exhibited in Figure 3.19 and the resulting rate constants displayed in Table 3.9.

(a)   (b)
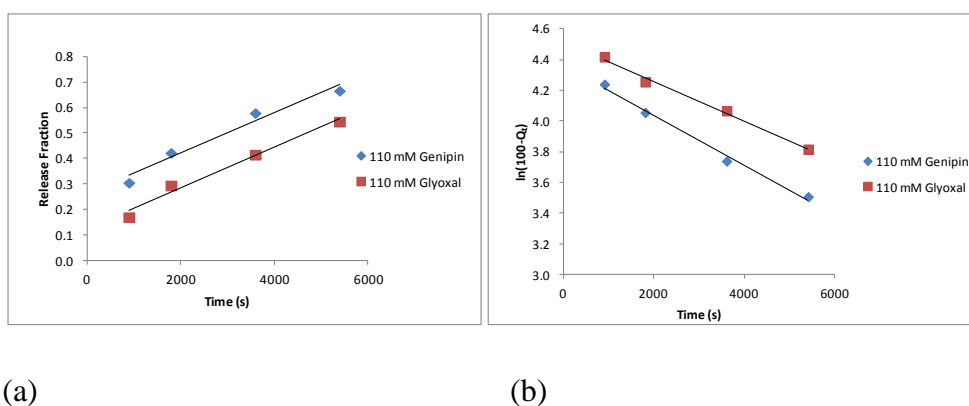
Figure 3.19 Release data from xerogel covalently crosslinked in either 110 mM glyoxal or genipin solution fitted to (a) zero-order and (b) first-order model. The gelling solution contained 0.75 M NaOH, 110 mM TPP and 60 mM DCD; the beads were washed with 60 mM DCD Millipore water and dried in an oven at 37 ±1 °C for 24 h.

Table 3.9 Results of fitted data for DCD release from xerogel covalently crosslinked in either 110 mM glyoxal or genipin solution to the (a) zero-order, (b) first-order models. The gelling solution contained 0.75 M NaOH, 110 mM TPP and 60 mM DCD. The gelling solution contained 0.75 M NaOH, 110 mM TPP and 60 mM DCD; the beads were washed with 60 mM DCD Millipore water and dried in an oven at 37 ±1 °C for 24 h.

Covalent Crosslinker	Zero-Order Model		First-Order Model	
	k_0 (s^{-1})	R^2	k_1 (s^{-1})	R^2
Genipin	7.91×10^{-5}	0.9655	1.62×10^{-4}	0.9914
Glyoxal	4.03×10^{-5}	0.9150	1.01×10^{-4}	0.9680

The results obtained are exhibited in Table 3.9. It is apparent that the first-order model has the best regression line fit for both glyoxal and genipin solution crosslinked xerogel beads. The first-order rate constant of genipin (1.62×10^{-4} s^{-1}) is greater than that of glyoxal (1.01×10^{-4} s^{-1}) which coincided with genipin having a shorter DCD release time as shown in Table 3.8. It was concluded that glyoxal was a more effective crosslinker than genipin as it resulted in a smaller rate constant released more DCD into the release solution (Table 3.8). At this point it was of interest to compare the rate constants of the two dialdehyde crosslinkers glyoxal and glutaraldehyde. The DCD release data from chitosan xerogel beads crosslinked in 300 mM glyoxal or 300 mM glutaraldehyde was fitted to the zero-order and first-order models and are exhibited in Figure 3.20. The results are shown in Table 3.10.
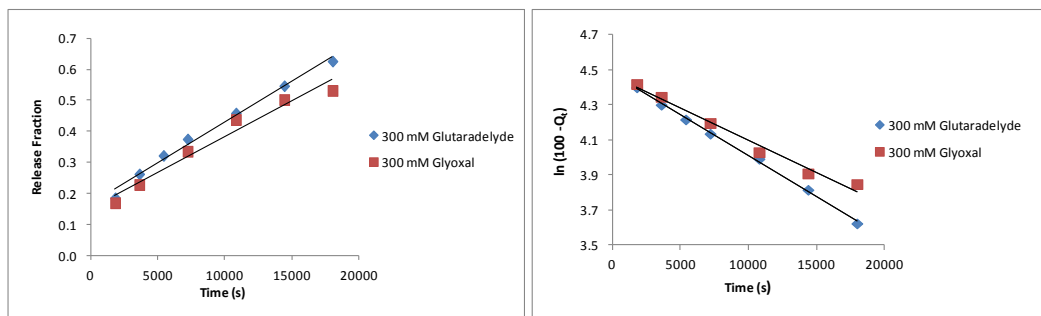
(a)   (b)

Figure 3.20 Release data from xerogel beads covalently crosslinked in either 300 mM glyoxal or glutaraldehyde solution fitted to the (a) zero-order and (b) first-order models. The gelling solution contained 0.75 M NaOH, 110 mM TPP and 60 mM DCD; the beads were then covalently crosslinked and washed with 60 mM DCD Millipore water solution and dried in an oven at 37 ±1 °C for 24 h.

Table 3.10 Results of fitted data for DCD release from xerogel beads covalently crosslinked in either 300 mM glyoxal or glutaraldehyde solution fitted to the zero-order and first-order models. The gelling solution contained 0.75 M NaOH, 110 mM TPP and 60 mM DCD; the beads were then covalently crosslinked and washed with 60 mM DCD Millipore water solution and dried in an oven at 37 ±1 °C for 24 h.

Covalent Crosslinker	Zero-Order Model		First-Order Model	
	k_0 (s^{-1})	R^2	k_1 (s^{-1})	R^2
Glutaraldehyde	2.63×10^{-5}	0.9891	4.44×10^{-5}	0.9981
Glyoxal	2.68×10^{-5}	0.9904	4.12×10^{-5}	0.9978

By examining the data in Table 3.10 it was apparent that the best regression line fit for both covalent crosslinkers was the first-order model. However, the zero-order model also had good fit for DCD release from both glutaraldehyde and glyoxal crosslinked xerogel beads. Obitte *et al.* suggested that the operation of more than one release mechanism is possible if there is more than one opening on the surface of the release system as this may allow multiple release mechanisms to take place simultaneously[42]. DCD release from glyoxal crosslinked xerogel beads exhibited a slightly lower first-order rate constant (4.12×10^{-5} s^{-1}) than DCD release from glutaraldehyde crosslinked xerogel beads (4.44×10^{-5} s^{-1}) but this was not a substantial difference and suggested the release rate was almost identical. It was concluded that glyoxal and glutaraldehyde solution crosslinked chitosan xerogel share many of the same release properties and at the same covalent crosslinker concentration neither was obviously superior to the other. As stated previously, chitosan xerogel beads could not be crosslinked with glutaraldehyde in a solution above 300 mM as the beads lost their structural integrity and broke apart, glyoxal however could crosslink chitosan xerogel at concentrations above 300 mM and was easier to handle. For these reasons it was selected as the primary covalent crosslinker to perform further DCD release studies.

3.3 Conclusions

An examination of the DCD release profiles of chitosan xerogels crosslinked with 110 mM TPP, trisodium citrate, sodium molybdate and sodium alginate revealed that DCD release equilibrium occurred at best within 45 min. The crosslinking of chitosan xerogels with an ionic crosslinker did not increase the release time of DCD from the beads when compared with a xerogel gelled in aqueous hydroxide ion solution only. The surface of the xerogel beads was examined by SEM and it was found that the ionic crosslinker used played a significant role in determining the morphology. The most reproducible spherical beads were obtained by crosslinking the chitosan beads with TPP in a NaOH gelling solution. It was also shown that increasing the concentration of sodium TPP in the gelling solution decreased the swelling ratio of the chitosan xerogel beads which indicated an increase in the crosslinking density of

the xerogels. Therefore TPP was used as the ionic crosslinker in future release experiments.

The highest amount of DCD released from chitosan xerogel beads was by beads ionically crosslinked with 110 mM TPP and loaded in 1.2 M DCD solution. Each of these beads released on average 4 mg of DCD. For a DCD application of 7.5 kg ha^{-1} an estimated 1.8 million beads would be required. Despite the relative ease of making chitosan xerogel beads this high number is unsustainable. The preparation of larger beads capable of encapsulating a greater amount of DCD would be practical for field trials.

No discernable difference was found in the release profiles of 1% and 2% (w/v) chitosan solutions. However, increasing the concentration above 2% (w/v) resulted in the distortion of the spherical shape of the xerogel beads. The formulation of dual-crosslinked xerogel beads resulted in an extension of the equilibrium release time to 75 minutes and a decrease in the swelling ratio (%) when compared with xerogels crosslinked with TTP only. The surface morphology of the of dual-crosslinked and multilayer xerogel beads was examined by SEM and found to be uneven and not nearly as smooth as that of chitosan xerogels crosslinked with TTP.

Despite the increase in the DCD release time by synthesising dual crosslinked beads it was clear that ionic crosslinkers failed to control DCD release from chitosan xerogel beads. Covalent crosslinkers however offer a straightforward method to form covalent bonds between polymer chains potentially giving the beads improved mechanical properties that could result in a controlled release from the chitosan xerogel beads[5].

An investigation was carried out to determine whether using a covalent crosslinker in addition to TPP would result in controlled DCD release from the beads. Chitosan xerogel beads crosslinked in genipin, glutaraldehyde or glyoxal solution were screened to determine which, if any, could aid in the development of controlled release system for DCD. Chitosan xerogel beads crosslinked with glutaraldehyde were found to have the smoothest surface morphology while Chitosan xerogel beads crosslinked genipin exhibited significant pores on their surface. In their hydrogel form the covalently crosslinked beads did not act as a controlled release system. However,

when dehydrated to form xerogel beads the time to reach release equilibrium increased significantly.

The release data from NaOH precipitated; ionically crosslinked and covalently crosslinked chitosan xerogel beads were fitted to the first-order and zero-order model. In each case the data best fit the first-order model. A first-order profile is expected in a membrane-controlled diffusion system if the gradient is reduced due to decreasing concentration of the donor side in combination with sink conditions in the dissolution medium.

Glyoxal was selected as the covalent crosslinker to study in greater detail as it allowed for the controlled release of DCD from the xerogel beads. Furthermore, it was not excessively expensive, release from beads crosslinked with glyoxal exhibited the smallest first-order rate constant, and it was able to crosslink hydrogel beads at higher concentrations than glutaraldehyde.

3.4 References

[1]   M. Dash, F. Chiellini, R. M. Ottenbrite and E. Chiellini, *Progress in Polymer Science* **2011**, *36*, 981-1014.

[2]   X. Z. Shu and K. J. Zhu, *International Journal of Pharmaceutics* **2000**, *201*, 51-58.

[3]   H. Sokker, A. Ghaffar, Y. Gad and A. Aly, *Carbohydrate Polymers* **2009**, *75*, 222-229.

[4]   M. Kumar, *Reactive & Functional Polymers* **2000**, *46*, 1-27.

[5]   N. Bhattarai, J. Gunn and M. Zhang, *Advanced Drug Delivery Reviews* **2010**, *62*, 83-99.

[6]   J. H. Park, G. Saravanakumar, K. Kim and I. C. Kwon, *Advanced Drug Delivery Reviews* **2010**, *62*, 28–41.

[7]   M. Khalida, F. Agnelya, N. Yagoubi, J. Grossiorda and G. Couarrazea, *European Journal of Pharmaceutical Sciences* **2002**, *15*, 425–432.

[8]   M. R. Gandhi, G. N. Kousalya, N. Viswanathan and S. Meenakshi, *Carbohydrate Polymers* **2011**, *83*, 1082-1087.

[9]   S. Chen, M. Liu, S. Jin and B. Wang, *International Journal of Pharmaceutics* **2008**, *349*, 180-187

[10]   P. P. Win, Y. Shinya, K.-J. Hong and T. Kajiuchi, *Carbohydrate Polymers* **2003**, *52*, 305-310.

[11]   X. Z. Shu and K. J. Zhu, *International Journal of Pharmaceutics* **2002**, *233*, 217-225.

[12]   A. Salabat, L. Shamshiri and F. Sahrakar, *Journal of Molecular Liquids* **2005**, *118*, 67-70.

[13]   L. Dambies, T. Vincent, A. Domard and E. Guibal, *Biomacromolecules* **2001**, *2*, 1198-1205.

[14]   P. F. Builders, O. O. Kunle, L. C. Okpaku, M. I. Builders, A. A. Attama and M. U. Adikwu, *European Journal of Pharmaceutics and Biopharmaceutics* **2008**, *70*, 777-783

[15]   Q. Ain, S. Sharma, G. K. Khuller and S. K. Garg, *Journal of Antimicrobial Chemotherapy* **2003**, *51*, 931–938.

[16]   S. Miyazaki, A. Nakayam, M. Oda, M. Takada and D. Attwood, *International Journal of Pharmaceutics* **1995**, *118*, 257-263.

[17]   M. George and T. E. Abraham, *Journal of Controlled Release* **2006**, *114*, 1-14

[18]   J. A. Ko, H. J. Park, S. J. Hwang, J. B. Park and J. S. Lee, *International Journal of Pharmaceutics* **2002**, *249*, 165-174.

[19]   J. Berger, M. Reist, J. M. Mayer, O. Felt, N. A. Peppas and R. Gurny, *European Journal of Pharmaceutics and Biopharmaceutics* **2004**, *57*, 19-34

[20]   W. Lin, D. Yu and M. Yang, *Colloids and Surfaces B: Biointerfaces* **2005**, *44*, 143–151.

[21]   X. Z. Shu, K. J. Zhu and W. Song, *International Journal of Pharmaceutics* **2001**, *212*, 19-28.

[22]   S. Chen, M. Liu, S. Jin and B. Wang, *International Journal of Pharmaceutics* **2008**, *349*, 180.

[23]   P. M. d. l. Torre, S. Torrado and S. Torrado, *Biomaterials* **2003**, *24*, 1459-1468.

[24]   I. A. Alsarra, S. H. Neau and M. A. Howard, *Biomaterials* **2004**, *25*, 2645-2655.

[25]   X. Liu, W. Xu, Q. Liu, W. Yu, Y. Fu, X. Xiong, X. Ma and Q. Yuan, *Carbohydrate Polymers* **2004**, *56*, 459-464.

[26]   Z. M. Wu, X. G. Zhang, C. Zheng, C. X. Li, S. M. Zhang, R. N. Dong and D. M. Yu, *European Journal of Pharmaceutical Sciences* **2009**, *37*, 198–206.

[27]   K. Jørgensen and F. N. Christensenb, *International Journal of Pharmaceutics* **1996**, *143*, 223-232

[28]   M. Bayomi, S. al-Suwayeh, A. el-Helw and A. Mesnad, *Pharmaceutica Acta Helvetiae* **1998**, *73*, 187–192.

[29]   Q. Wang, X. Xie, X. Zhang, J. Zhang and A. Wanga, *International Journal of Biological Macromolecules* **2010**, *46*, 356–362.

[30]   A. K. Anal and W. F. Stevens, *International Journal of Pharmaceutics* **2005**, *290*, 45-54.

[31]   Y. Xu, C. Zhan, L. Fan, L. Wang and H. Zheng, *International Journal of Pharmaceutics* **2007**, *336*, 329-337.

[32]   N. Bhattarai, J. Gunn and M. Zhang, *Advanced Drug Delivery Reviews* **2010**, *62*, 83-99.

[33]   Q. Yang, F. Dou, B. Liang and Q. Shen, *Carbohydrate Polymers* **2005**, *61*, 393–398.

[34]   K. C. Gupta and F. H. Jabrail, *Carbohydrate Research* **2006**, *341*, 744-756.

[35]   O. A. C. Monteiro and C. Airoldi, *International Journal of Biological Macromolecules* **1999**, *26*, 119-128.

[36]   R. A. A. Muzzarelli, *Carbohydrate Polymers* **2009**, *77*, 1-9.

[37]   F. Mi, S. Shyu and C. Peng, *Journal of Polymer Science* **2005**, *43*, 1985-2000.

[38]   L. Serra, J. Domenechc and N. A. Peppas, *Biomaterials* **2006**, *27*, 5440–5451.

[39]   B. Adnajevic, J. Jovanovic and B. Drakulic, *Thermochimica Acta* **2007**, *466*, 38-48.

[40]   H. Peng, H. Xiong, J. L, M. Xie, Y. Liu, C. Bai and L. Chen, *Food Chemistry* **2010**, *121*, 23–28.

[41]   F. Mi, C. Kuan, S. Shyu, S. Lee and S. Chang, *Carbohydrate Polymers* **2000**, *41*, 389-396.

[42]   N. Obitte, A. Chukwu and Onyishi, *International Journal of Applied Research in Natural Products* **2010**, *3*, 1-17.

Chapter 4: Glyoxal Crosslinked Chitosan Xerogel Beads for DCD Release

4.1 Introduction

Glyoxal is an aldehyde capable of enhancing the mechanical properties of chitosan fibre and the release properties of chitosan microspheres[1, 2]. The mechanism for glyoxal crosslinking of chitosan has been attributed to the occurrence of acetalization and Schiff base reaction taking place among the glyoxal and the hydroxyls and amino groups of chitosan[1]. In the previous chapter glyoxal was shown to be an effective covalent crosslinker. Therefore further studies were conducted to investigate the physical properties and release characteristics of chitosan xerogel beads crosslinked with glyoxal (Figure 4.1).
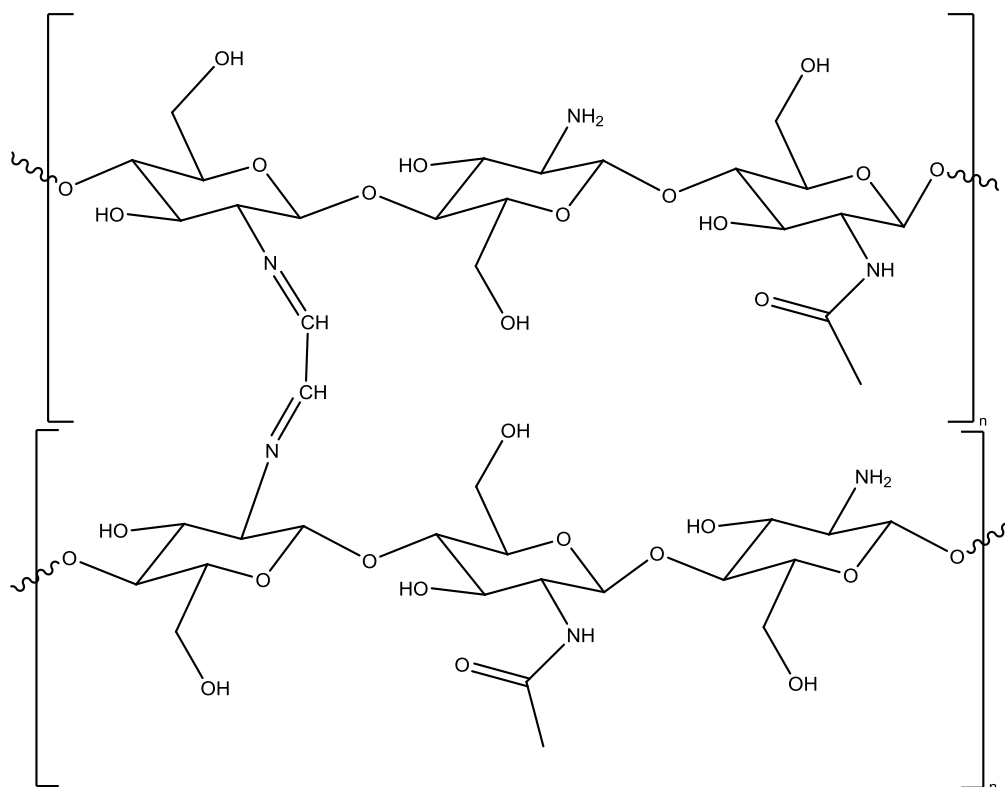
Figure 4.1 Chitosan crosslinked with glyoxal.

4.2 Results and Discussion

In the present chapter chitosan xerogels crosslinked in glyoxal solution were prepared as stated in Section 2.2.2.3. Their physical properties were investigated and the release kinetics analysed at different glyoxal crosslinking solution concentrations.

4.2.1 Surface Morphology

Upon comparing the surface morphology of xerogel beads crosslinked in 110 mM TPP to those gelled in 110 mM TPP and covalently crosslinked in 300 mM glyoxal solution it was apparent that the addition of the covalent crosslinking agent had caused the surface to become uneven and a greater amount of indentations were visible on the surface. However, an examination of the micrographs showed there were no signs of deep pores on the surface of the xerogel or any signs of structural weakness caused by the crosslinking reaction. Furthermore, the surface morphology of the covalent crosslinked xerogels appeared to be uniform which suggested that the crosslinking reaction had influenced the surface morphology of the whole bead. Gupta and Jabrail synthesised chitosan xerogel beads crosslinked with glyoxal and examined their morphology using SEM. They found that crosslinking the chitosan beads in glyoxal solution caused the surface of the beads to become smooth in morphology but the beads were not spherical[2]. This could be due to the fact Gupta and Jabrail were crosslinking the xerogel beads in 12% (w/v) glyoxal, a substantially higher amount than the concentration used to crosslink the beads shown in Figure 4.2.

1mm

1mm

(a)   (b)
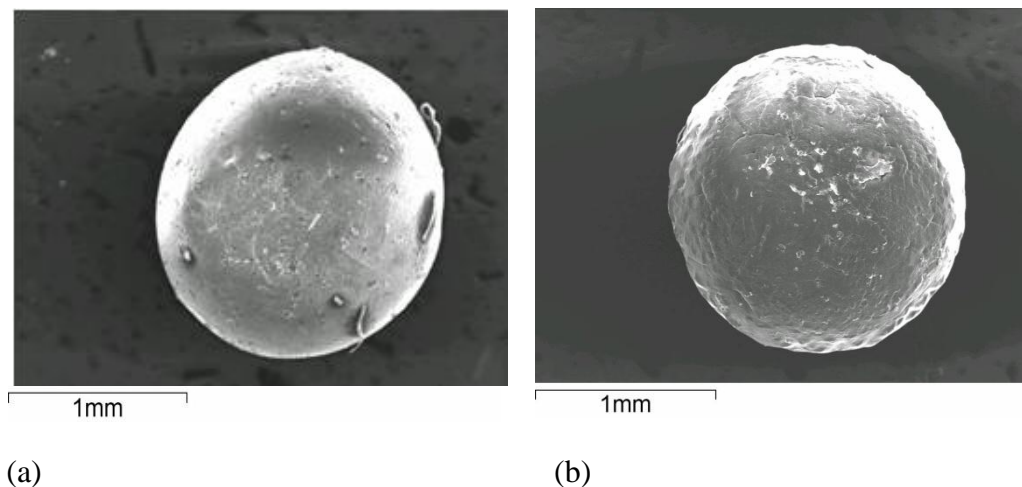
Figure 4.2 SEM micrographs of chitosan xerogels crosslinked with TPP only and SEM of xerogels crosslinked with TPP and in glyoxal solution. The gelling solution of both bead (a) and (b) contained 110 mM TPP, 60 mM DCD and 0.75 M NaOH. After gelling bead (b) was crosslinked in 300 mM glyoxal solution. Both beads were then dried in an oven at a temperature of $37 \pm 1^{o}C$ for 24 h..

4.2.2 Swelling Properties

4.2.2.1 Influence of the Concentration of the Crosslinking Solution

A study was undertaken to investigate the influence of the concentration of glyoxal in the covalent crosslinking solution on the swelling ratio percentage of chitosan xerogel beads. The results are presented in Figure 4.3. The swelling properties of the beads were quantified by using the swelling ratio percentage equation (Equation 2.2).
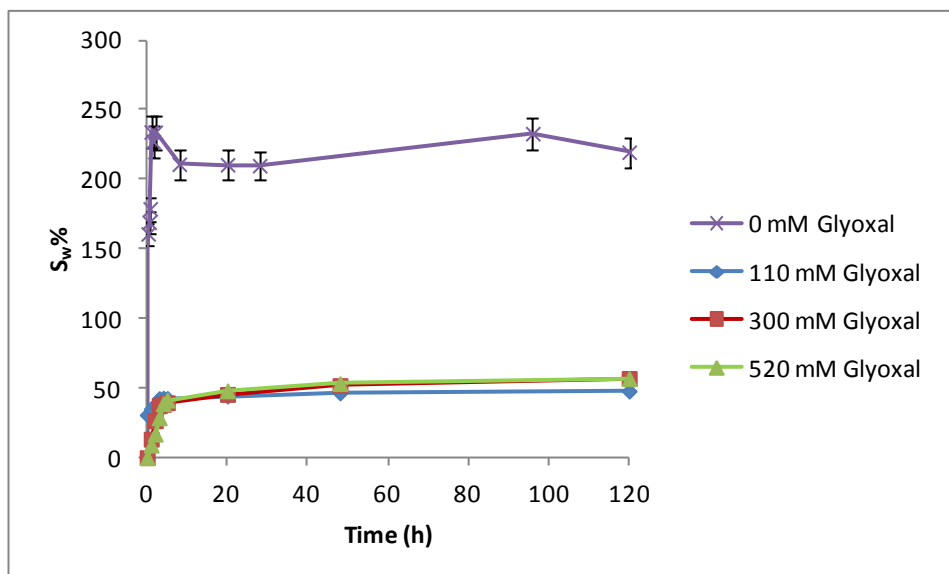
Figure 4.3 Influence of covalent crosslinker concentration on bead swelling ratio (%); The gelling solution contained 110 mM sodium TPP and 0.75 M NaOH. The beads were subsequently washed in Millipore water and dried in an oven at a temperature of $37 \pm 1^{o}C$ for 7 days. The weight of the swollen beads was measured after surface solution was removed by filter paper. The experiment was repeated in triplicate.

The results in Figure 4.3 indicate that covalently crosslinking the xerogel beads had caused the swelling ratio to fall significantly compared with xerogels crosslinked with TPP only. Like the xerogels crosslinked in 110 mM TPP solution only, there was a rapid increase in the swelling ratio of covalently crosslinked chitosan xerogel beads during the first hour. However, the swelling ratio was much smaller than for beads crosslinked with TPP only as these beads had swollen to 233% after one hour. This was compared to 9%, 13% and 15% for beads crosslinked in 110 mM, 300 mM and 520 mM glyoxal solution, respectively. The swelling ratios for beads crosslinked in 110 mM, 300mM and 520 mM glyoxal solutions did not differ significantly, as after 120 h the ratio percentages were 50%, 59% and 57%, respectively. This suggested that the polymer network mesh density of the xerogel beads at all three crosslinking concentrations was similar.

The results given above correspond with research performed by Yang *et al*. who investigated the influence of glyoxal crosslinking percentage on the swelling degree of chitosan xerogels[1]. Yang *et al*. found that crosslinking the xerogels with glyoxal

significantly reduced the degree of swelling of chitosan and they obtained swelling degree percentages ranging from approximately 60-75%, depending on the concentration of glyoxal used in the covalent crosslinking solution [1].

4.2.2.2 Influence of the Release Medium pH

The swelling ratio of glyoxal crosslinked chitosan xerogel beads in acidic and basic solutions was studied and the results presented in Figure 4.4. The pH values of 5.0 and 9.0 were investigated as this would give an insight into swelling behaviour both above and below the pK_a value of chitosan ($pK_a = 6.3$)[3]. The results showed that for all three pH values examined an initial rapid uptake of water was observed. After 7 h the swelling ratios (%) of the xerogels in pH 6.8 and pH 9 solution were 41% and 48%, respectively. and those xerogel beads began to reach a swelling ratio (%) plateau. The swelling ratio (%) of xerogels in pH 5.0 solution after 7.0 h was higher at 66% and did not reach its maximum value until 144 h, at which point in time the swelling ratio had increased significantly to 211%. The higher swelling ratio (%) of xerogels in acidic solution was due to the protonation of the glucosamine units of chitosan in the acidic medium which caused chain repulsion between the polymer units and the cleavage of the imine bond between the chitosan and the dialdehyde crosslinker by hydrolysis which allowed water to diffuse inside the bead. The chitosan glucosamine units in the pH 6.8 and pH 9.0 media were not protonated so limited swelling was taking place due to diffusion of water inside the beads through the pores of the polymer network. It has been well established by authors that an acidic swelling medium causes an increase in the swelling ratio percentage of chitosan xerogel beads like the one observed in this study. Shu and Zhu found that chitosan beads could swell up to 1.8 times more in acidic compared with basic mediums [4]. Risbud *et al*. also did a study on the effects of different pH media and found that a lower pH value caused a substantial increase in swelling ratio and summarised that the acidic medium had a 'pronounced effect' on the swelling profiles of the chitosan beads which coincides with the results that are presented here[5].
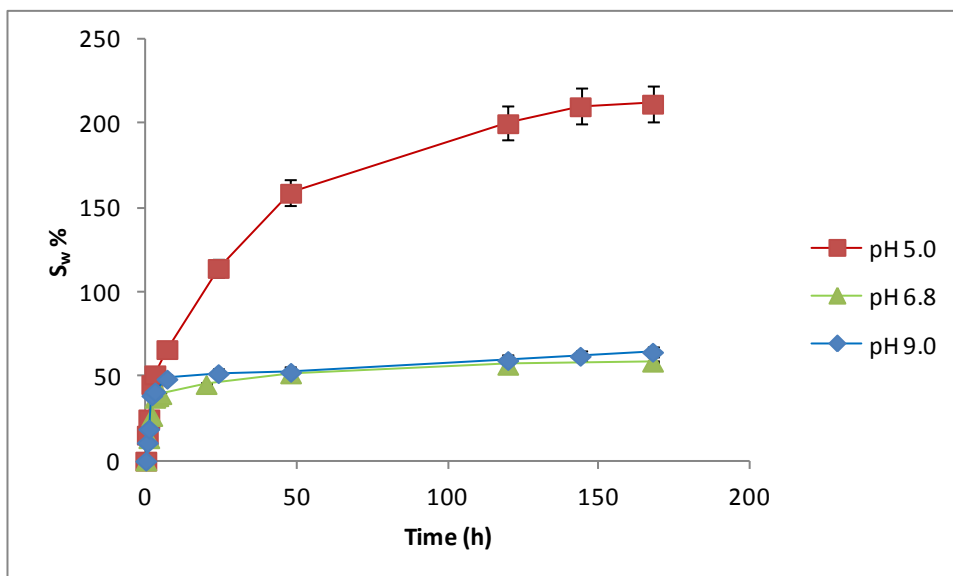
Figure 4.4 Influence of the pH of the swelling solution on swelling ratio percentage of glyoxal crosslinked chitosan xerogel beads; 15 xerogel beads were immersed in Millipore at a temperature of 20 ± 1 ^{o}C. The gelling solution contained 110 mM sodium TPP and 0.75 M NaOH. The beads were subsequently covalently crosslinked with 300 mM glyoxal. The beads were subsequently washed in Millipore water and dried in an oven at a constant temperature of 37 ± 1°C for 7 days. The weight of the swollen beads was measured after surface solution was removed by filter paper.

4.2.3 DCD Release Properties

4.2.3.1 DCD Release Profiles

Chitosan xerogel beads were crosslinked in 110 mM, 300 mM and 520 mM glyoxal solutions, washed in 60 mM DCD Millipore water solution, and then dried in an oven at 37 ± 1 °C for 24 h. The DCD release profiles of the beads are compared in Figure 4.5.
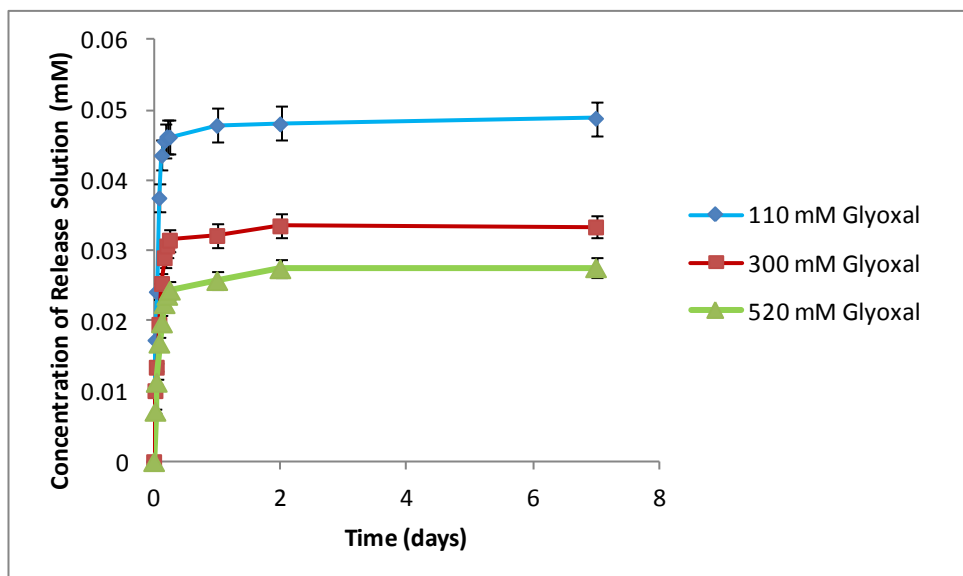
Figure 4.5 DCD release profiles from xerogel beads covalently crosslinked in 110 mM, 300 mM or 520 mM aqueous glyoxal solution. The gelling solution contained 0.75 M NaOH, 110 mM TPP and 60 mM DCD; the beads were then covalently crosslinked and washed in 60 mM DCD Millipore water solution and incubated in an oven at 37 ±1 °C for 7 days.

The DCD release profiles in Figure 4.5 show that the greater the concentration of glyoxal in the crosslinking solution the less DCD is released from the beads at equilibrium. At a crosslinking solution concentration of 110 mM glyoxal the concentration of DCD in the release solution at equilibrium was 0.05 mM but this value was reduced to 0.03 mM at a concentration of 520 mM glyoxal. The release capacity of the beads is known to be 0.06 mM as demonstrated in Section 3.2.4.3. Therefore dehydrating the hydrogel beads to xerogel beads appeared to have restricted the amount of DCD released from the beads at equilibrium. All three release profiles exhibited controlled DCD release compared with xerogel beads that had not been covalently crosslinked. Mi *et al*. studied the influence of the degree of glutaraldehyde crosslinking on the amount of immunosuppressive drug Mercaptopurine released from their chitosan beads[6]. They concluded that the higher the degree of crosslinking by the dialdehyde the slower relaxation rate of the polymer chain which resulted in a slower drug release rate. However, the influence of covalent crosslinking of chitosan on the total amount of drug released was not discussed. The rate constants for the release of DCD from the glyoxal crosslinked xerogel beads were investigated in Section 4.2.3.2 to determine if increasing the concentration of the covalent

crosslinking solution above 110 mM resulted in a reduction in the DCD release rate constant.

4.2.3.2 DCD Release Kinetics

The release data from chitosan xerogels crosslinked in glyoxal solution were fitted to the zero-order (Equation 2.6) and first-order (Equation 2.8) models (Figure 4.6) to investigate the rate constant and the mechanism of DCD release. The results are shown in Table 4.1.

(a)　　　　　　　　　　　　　　　　(b)
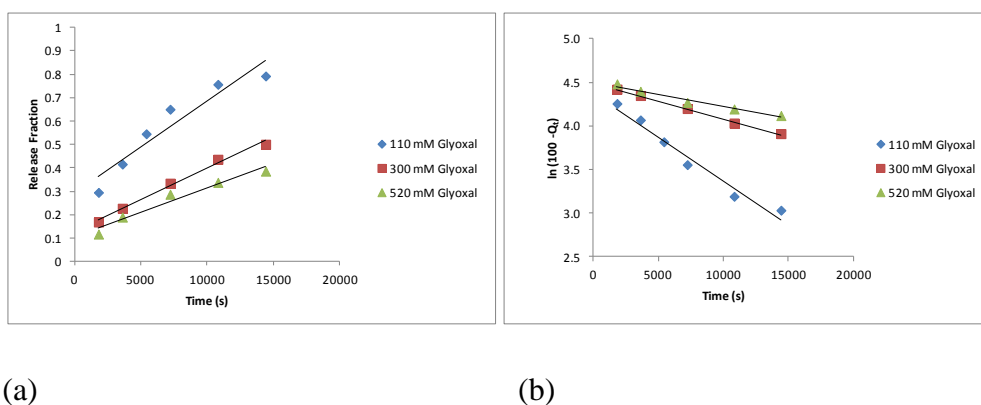
Figure 4.6 Release data from covalently crosslinked chitosan xerogel beads fitted to the (a) zero-order, (b) first-order. The gelling solution contained 0.75 M NaOH, 110 mM TPP and 60 mM DCD; the beads were then covalently crosslinked in the stated concentration of glyoxal aqueous solution then washed in 60 mM DCD Millipore water solution and incubated in an oven at 37 ± 1 °C for 7 days.

Table 4.1 Results from the fitting of release data to the zero-order and first-order models. The xerogel beads were covalently crosslinked in 110 mM, 300 mM or 520 mM aqueous glyoxal solution. The gelling solution contained 0.75 M NaOH, 110 mM TPP and 60 mM DCD; the beads were then covalently crosslinked and washed in 60 mM DCD Millipore water solution and incubated in an oven at 37 ±1 °C for 7 days.

Concentration of glyoxal crosslinking solution (mM)	Zero-Order Model		First-Order Model	
	k_0 (s^{-1})	R^2	k_1 (s^{-1})	R^2
110	4.03×10^{-5}	0.9150	1.01×10^{-4}	0.9680
300	2.68×10^{-5}	0.9904	4.12×10^{-5}	0.9978
520	2.07×10^{-5}	0.9542	2.82×10^{-5}	0.9722

According to the results presented in Table 4.1, the first-order release model had the best regression line fit for xerogel beads crosslinked in 110 mM, 300 mM and 520 mM glyoxal solutions. In addition, as the concentration of glyoxal in the crosslinking solution increased the first-order rate constant decreased from 1.01×10^{-4} s^{-1} at 110 mM glyoxal to 2.82×10^{-5} s^{-1} at 520 mM glyoxal. This meant that as the concentration of glyoxal in the covalent crosslinking solution increased the rate constant for the release of DCD from the xerogel beads decreased. The release data were analysed using the Higuchi (Equation 2.10) and Korsemeyer-Peppas (Equation 2.12) models (Figure 4.7) to investigate the release mechanism and the results are presented in Table 4.2.
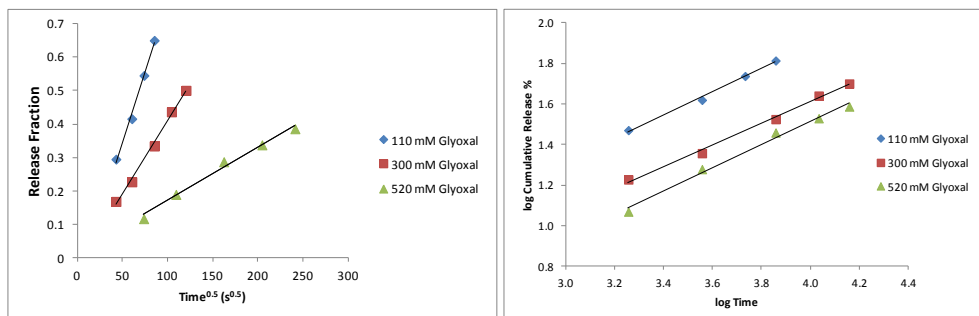
(a)   (b)

Figure 4.7 Release data from covalently crosslinked chitosan xerogel beads fitted to the (a) Higuchi and (b) Korsemeyer-Peppas models. The gelling solution contained 0.75 M NaOH, 110 mM TPP and 60 mM DCD; the beads were then covalently crosslinked in the stated concentration of glyoxal aqueous solution then washed in 60 mM DCD Millipore water solution and incubated in an oven at 37 ± 1 °C for 7 days.

Table 4.2 Results from the fitting of release data to Higuchi and Korsmeyer-Peppas models. The xerogel beads were covalently crosslinked in 110 mM, 300 mM or 520 mM aqueous glyoxal solution. The gelling solution contained 0.75 M NaOH, 110 mM TPP and 60 mM DCD; the beads were then covalently crosslinked and washed in 60 mM DCD Millipore water solution and incubated in an oven at 37 ±1 °C for 7 days.

Concentration of glyoxal crosslinking solution (mM)	Higuchi Model		Korsemeyer-Peppas Model	
	k_H (s$^{-0.5}$)	R_2	n	R_2
110	8.44×10^{-3}	0.9931	0.57	0.9943
300	4.39×10^{-3}	0.9953	0.53	0.9952
520	1.59×10^{-3}	0.9887	0.57	0.9904

The DCD release data from xerogel beads covalently crosslinked in solutions of 110 mM, 300 mM and 520 mM glyoxal were fitted to the Higuchi and Korsemeyer-Peppas models and analysed. The results showed that as the covalent crosslinker solution concentration increased the Higuchi kinetic constant, k_H, decreased. This

suggested that there was a decrease in the rate of Fickian diffusion release due to an increase in the concentration of the xerogel bead covalent crosslinking solution. The Higuchi model exhibits good regression line fits which was a strong indicator that diffusion was a part of the release mechanism. The values of exponent n obtained at each glyoxal concentration suggested the release mechanism was a combination of Fickian diffusion and polymer chain relaxation. However, Fickian diffusion was the dominant mechanism as the exponent n values obtained was closer to the pure Fickian diffusion value (0.43) than pure Case-II transport caused by polymer chain relaxation (0.86). As the concentration of the cross linking solution increased the value of exponent n stayed relatively similar with a good regression line fit which indicated that the release mechanism from the xerogels was similar for all three glyoxal solution concentrations. To the best of our knowledge this appears to be the first research undertaken on the release mechanism from glyoxal crosslinked xerogel beads, however Wu *et al*. studied the release mechanism from di-sulfide crosslinked xerogel beads and obtained exponent n values ranging from 0.1604 to 0.337 and considered the mechanism of release to be diffusion controlled due to the exponent n value being closer to pure Fickian diffusion than polymer chain relaxation[7]. Likewise Stulzer *et al*. investigated the release mechanism of chitosan beads crosslinked with TPP and calculated exponent n values of between 0.21 and 0.32 which they also attributed to diffusion release [8]. The release data obtained in this study were fitted to the Peppas-Sahlin model (Equation 2.13) to determine the respective contributions of Fickian diffusion and polymer chain relaxation to release (Figure 4.8). The results are exhibited in Table 4.3.
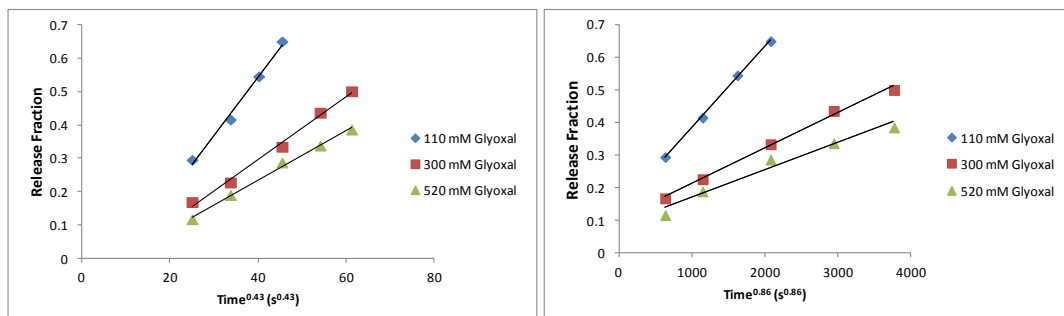
(a)   (b)

Figure 4.8 Release data from covalently crosslinked chitosan xerogel beads fitted to the (a) Fickian release contribution and (b) Polymer chain relaxation contribution models. The gelling solution contained 0.75 M NaOH, 110 mM TPP and 60 mM DCD; the beads were then covalently crosslinked in the stated concentration of glyoxal aqueous solution then washed in 60 mM DCD Millipore water solution and incubated in an oven at 37 ± 1 °C for 7 days.

Table 4.3 Results from the fitting of release data to Peppas-Sahlin release models. The xerogel beads were covalently crosslinked in 110 mM, 300 mM or 520 mM aqueous glyoxal solution. The gelling solution contained 0.75 M NaOH, 110 mM TPP and 60 mM DCD; the beads were then covalently crosslinked and washed in 60 mM DCD Millipore water solution and incubated in an oven at 37 ±1 °C for 7 days.

Concentration of Glyoxal solution used to crosslinked chitosan xerogel beads (mM)	Fickian Diffusion Contribution		Relaxation Contribution		Relaxation/ Fickian Ratio
	k_1 (s$^{-0.43}$)	R^2	k_2 (s$^{-0.86}$)	R^2	R/F
110	1.75×10^{-3}	0.9906	2.48×10^{-4}	0.9997	0.01
300	9.39×10^{-3}	0.9932	1.08×10^{-4}	0.9953	0.01
520	7.41×10^{-3}	0.9951	8.41×10^{-5}	0.9676	0.01

The results in Table 4.3 showed that Fickian diffusion clearly dominated the DCD release mechanism from the xerogel beads as the R/F ratio values obtained were very

low. As the glyoxal crosslinking solution concentration increased, both the Fickian diffusion and relaxation contribution constants decreased, but there was no change in the overall ratio of Fickian diffusion to polymer chain relaxation. This indicated that the crosslinking of the chitosan did not have a significant influence on the release mechanism. Ferrero *et al.* performed a similar study on their methyl methacrylate copolymer matrix tablets using anhydrous theophylline as model drug, and like this study observed very low relaxation/Fickian ratios. This led them to conclude release was by diffusion and described such low a relaxation contribution value as 'insignificant' in relation to the role of polymer chain relaxation in the release mechanism [9].

4.2.3.3 Influence of Release Medium pH

The results shown in Figure 4.4 demonstrated that xerogel beads covalently crosslinked with glyoxal are pH swelling sensitive. The acidic aqueous solution caused an increase in the swelling ratio of the covalently crosslinked xerogels due to the protonation of the glucosamine units leading to chain repulsion. However, for the first 7 hours of the study the values calculated were relatively similar as the swelling ratios (%) of the xerogels in pH 6.8 and pH 9.0 solution were 41% and 48%, respectively, and those xerogels in pH 5.0 solution had a swelling ratio (%) of 66%. As DCD release equilibrium was achieved after 6 hours it was likely that an acidic release medium value of pH 5.0 would not have substantive impact on DCD release from the xerogel beads. A study was performed to examine the influence of acidic and basic aqueous release solutions on DCD release from glyoxal solution crosslinked xerogel beads, the results of which are displayed in Table 4.4. The results indicated that equilibrium release time was reached at 5.5 h in the acidic release medium rather than 6 h in the basic or neutral and there was a slightly greater concentration of DCD released at equilibrium in the acidic release medium. This increase was attributed to the chain relaxation that takes place in an acidic aqueous solution that allowed the

DCD to diffuse out that otherwise would remain trapped in the polymer network under neutral conditions. This corresponds with research published by Risbud *et al.* who concluded that by decreasing the pH value of the release medium their chitosan hydrogels released more of the model drug amoxicillin at a faster rate when compared with release into a basic aqueous solution[5].

Table 4.4: Influence of release medium pH on the release of DCD from xerogel beads. The gelling solution contained 110 mM TPP, 60 mM DCD and 0.75 M NaOH. The beads were subsequently crosslinked in 60 mM DCD 300 mM glyoxal solution, washed in a 60 mM DCD Millipore water solution and dried in an oven at a temperature of $37 \pm 1^{\circ}C$ for 24 h.

pH of release medium	Time to reach release equilibrium (h)	Concentration of release solution at equilibrium (mM)
5.0	5.5	0.04
6.8	6.0	0.03
9.0	6.0	0.03

The release data from the pH medium experiment was fitted to the zero-order and first-order models (Figure 4.9) to investigate how the pH of the release medium influenced the rate constants and the mechanism of release. The results are exhibited in Table 4.5.
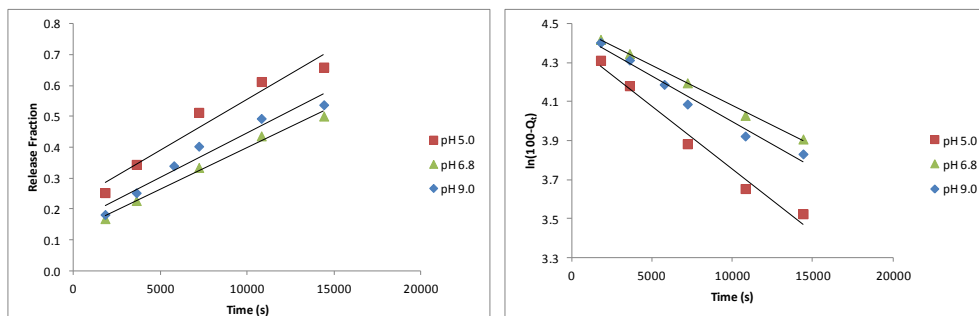
(a)   (b)

Figure 4.9 DCD release data from covalently crosslinked xerogel fitted to the (a) Zero-order and (b) first-order models. The gelling solution contained 110 mM TPP, 60 mM DCD and 0.75 M NaOH. The beads were subsequently crosslinked with 300 mM glyoxal, washed in a 60 mM DCD Millipore water solution and dried in an oven at a temperature of 37 ±1°C for 7 days.

Table 4.5 Results from the fitting of release data to the zero-order and first-order models from 10 xerogel beads in 500 mL Millipore water at a temperature of 20 ±1 °C at different pH release media. The gelling solution contained 110 mM TPP, 60 mM DCD and 0.75 M NaOH. The beads were subsequently crosslinked with 300 mM glyoxal, washed thoroughly with 60 mM Millipore water solution and dried in an oven at a temperature of 37 ± 1°C for 7 days.

pH of Release Medium	Zero-Order Model		First-Order Model	
	k_0 (s^{-1})	R^2	k_1 (s^{-1})	R^2
5.0	4.38×10^{-5}	0.9778	6.69×10^{-5}	0.9821
6.8	2.68×10^{-5}	0.9904	4.12×10^{-5}	0.9978
9.0	2.87×10^{-5}	0.9432	4.65×10^{-5}	0.9573

The results in Table 4.5 indicate that the first-order model had the best regression line fit regardless of the pH of the release medium. However, the zero-order model also exhibited a good regression line fit, especially at pH 6.8, zero-order kinetics may influence release as well. The pH 5.0 release medium has slightly smaller first-order rate constant than pH 6.8 or pH 9.0 likely due to the chain repulsion between the

polymers caused by the protonation of the glucosamine units of chitosan. However the changes in the rate constant values were not substantial and coupled with results from the swelling study in Figure 4.4 it was concluded that there was not a substantive difference in the properties or mechanism of DCD release from glyoxal crosslinked chitosan xerogel beads in pH 5.0 and pH 9.0 release solutions.

4.2.3.4 Influence of Bead Size

The results of a study performed on the influence of bead size on release behaviour of DCD-loaded xerogels covalently crosslinked in 300 mM aqueous glyoxal solution are presented in Table 4.6. The largest bead size studied (1.64 mm) had the longest equilibrium release time and released the most DCD into solution at equilibrium. This was due to water taking longer to permeate through the porous structure of larger beads than smaller bead and the larger polymer structure was able to encapsulate a greater amount of DCD.

Table 4.6 Influence of bead size on DCD release from 10 xerogel beads in 500 mL Millipore water at 20 ±1°C covalently crosslinked in 300 mM glyoxal solution. The gelling solution contained 110 mM TPP, 60 mM DCD and 0.75 M NaOH. The beads were subsequently crosslinked with 300 mM glyoxal, washed thoroughly with 60 mM DCD Millipore water solution and dried in an oven at a constant temperature of $37 \pm 1^{o}C$ for 7 days.

Bead Size (mm)	Time to reach release equilibrium (h)	Concentration of release solution at equilibrium (mM)
1.64 ± 0.06	6.00	0.03
1.25 ± 0.03	2.75	0.02
1.01 ± 0.04	1.00	0.01

The results displayed in Table 4.6 confirm that increasing the beads size has a positive effect on controlled release from the bead. A larger bead size allowed more DCD to

be loaded which in turn increased the concentration of the release solution at equilibrium.

The SEM micrographs presented in Figure 4.10 are of xerogel beads sizes (a) 1.64 mm (b) 1.25 mm and (c) 1.01 mm. The SEM micrograph of the 1.25 mm size xerogel bead appears to have a slightly smoother surface morphology than the 1.64 mm bead. However, both beads exhibit indentations to the surface and overall the surface morphologies were largely similar. The SEM micrograph of the 1.25 mm size xerogel 1.01 mm has an obvious imperfection in its spherical shape which (a) and (b) do not have. This was likely due to the fact that an important part of the gelling process which gives the bead their spherical shape is the initial couple of seconds spent submerged after the chitosan droplet hits the gelling solution. The larger the drop size, the longer this initial submersion lasts before the newly formed bead floats to the surface. Smaller beads like (c) however, hit the surface of the gelling solution and do not stay submerged for enough time for a spherical shape to set before returning to the surface of the solution. As a result they are gelled with a non-spherical shape.

(a)   (b)

(c)
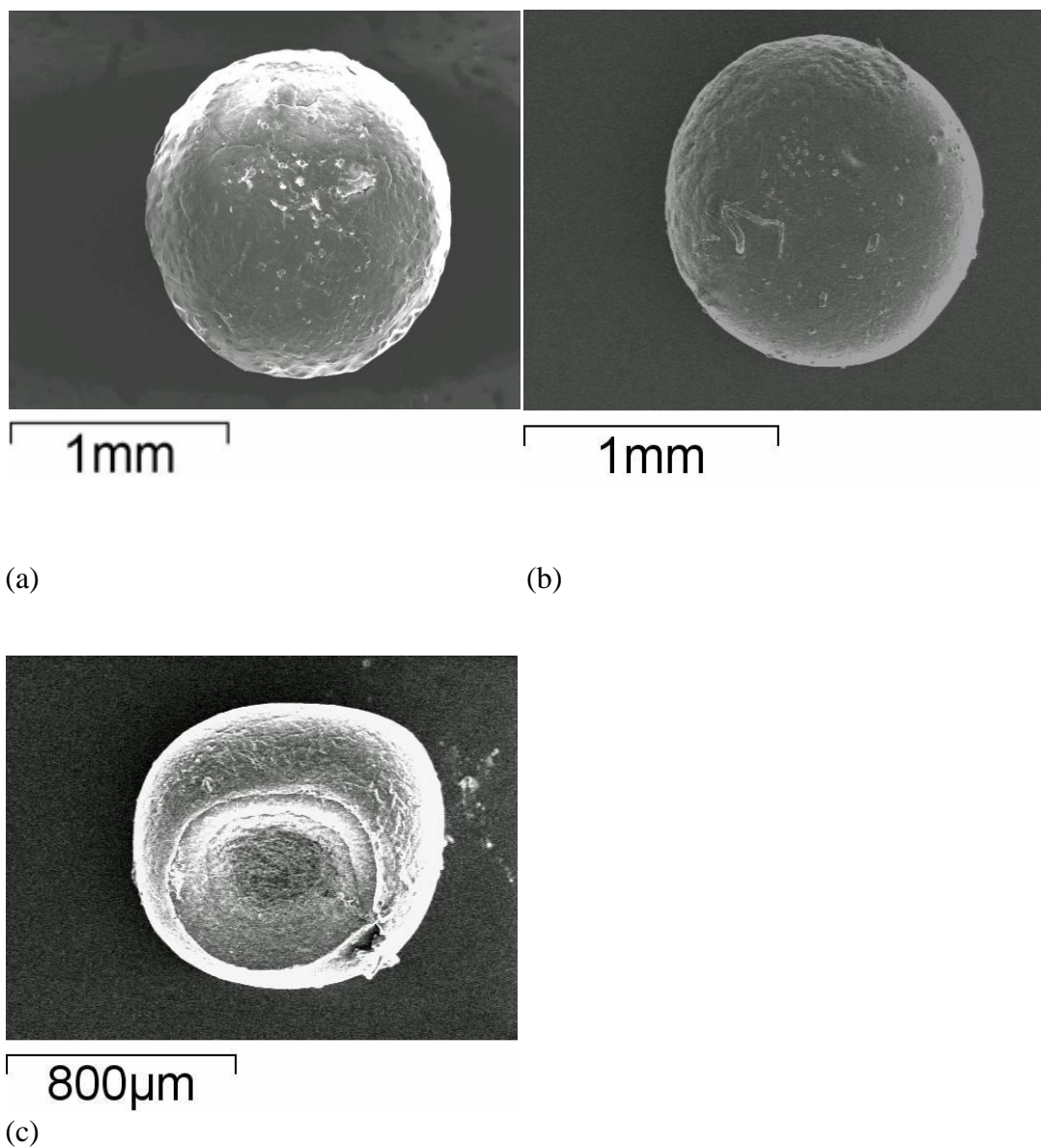
Figure 4.10 SEM micrographs of different size xerogel beads (a) 1.64 mm (b) 1.25 mm (c) 1.01 mm covalently crosslinked in 300 mM glyoxal solution. The gelling solution contained 110 mM TPP, 60 mM DCD and 0.75 M NaOH. The beads were subsequently crosslinked with 300 mM glyoxal, washed thoroughly with 60 mM DCD Millipore water solution and dried in an oven at a constant temperature of $37 \pm 1^{o}C$ for 7 days.

4.2.3.5 Influence of Ionic Crosslinker

Studies in this research have shown that the concentration and the type of covalent crosslinker used in the covalent crosslinking solution plays a large role in determining the equilibrium release time and concentration of DCD released from the xerogel beads (Table 3.8). Ionic crosslinking of the chitosan xerogel beads with TPP failed to increase DCD equilibrium release time (Section 3.2.1.2). However, studies have shown combining different crosslinkers can have a positive effect on the release properties of xerogel beads[41, 42]. Therefore a study was performed to examine the effect of different concentrations of the ionic crosslinker TPP used in the gelling solution on the release properties of xerogel beads that were subsequently crosslinked in a 300 mM aqueous solution of glyoxal. The resultant release profile is displayed in Figure 4.13 and the data were fitted to the zero-order and first-order models in Figure 4.14. The results are displayed in Table 4.7.
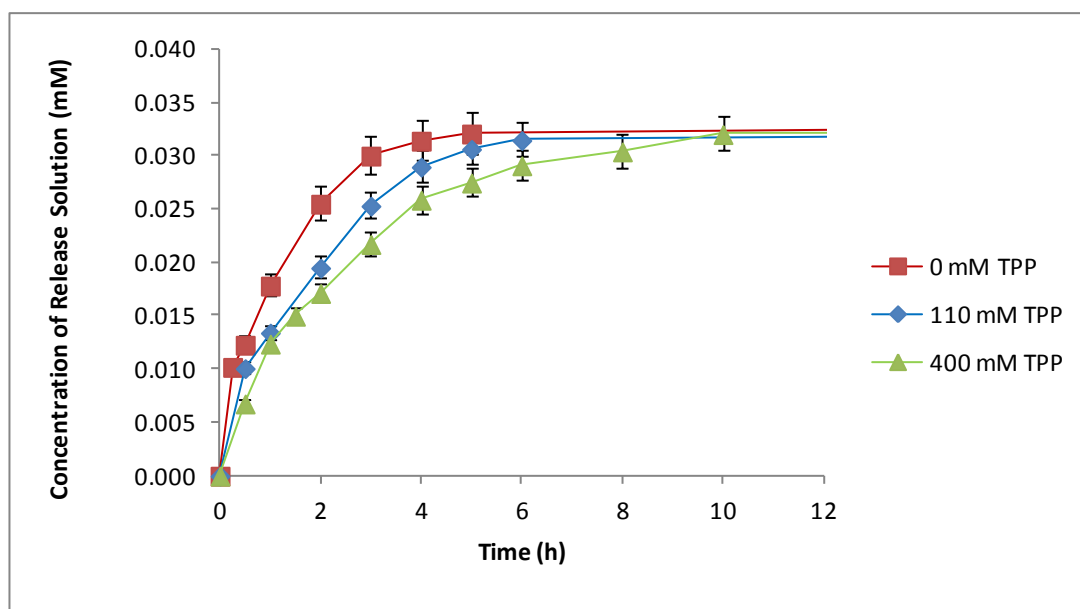
Figure 4.13 Influence of ionic crosslinker concentration in the gelling solution on DCD release from chitosan xerogels beads covalently crosslinked in 300 mM glyoxal solution. The gelling solution contained a stated amount of TPP, 60 mM DCD and 0.75 M NaOH. The beads were subsequently crosslinked in 300 mM glyoxal solution, washed thoroughly with 60 mM DCD Millipore water solution and dried in an oven at a constant temperature of $37 \pm 1^{o}C$ for 7 days.
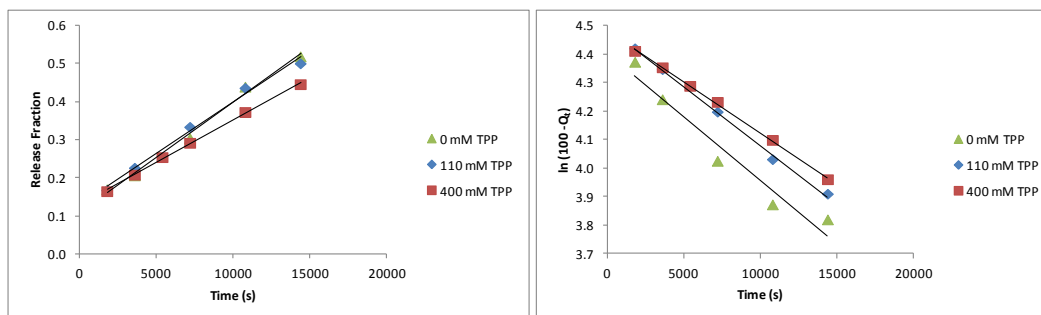
(a)   (b)

Figure 4.14 Release data from covalently crosslinked chitosan xerogel beads fitted to the (a) zero-order and (b) first-order models The gelling solution contained 0.75 M NaOH, 60 mM DCD and a stated amount of ionic crosslinker; the beads were then covalently crosslinked in 300 mM glyoxal aqueous solution then washed in 60 mM DCD Millipore water solution and incubated in an oven at 37 ± 1 °C for 7 days.

Table 4.7 Results from the fitting of release data to the (a) zero-order and (b) first-order models. The gelling solution contained 0.75 M NaOH, 60 mM DCD and a stated amount of ionic crosslinker; the beads were then covalently crosslinked in 300 mM glyoxal aqueous solution then washed in 60 mM DCD Millipore water solution and incubated in an oven at 37 ± 1 °C for 7 days.

Concentration of TPP in Gelling Solution (mM)	Zero-Order Model		First-Order Model	
	k_0 (s^{-1})	R^2	k_1 (s^{-1})	R^2
0	2.67×10^{-5}	0.9201	4.40×10^{-5}	0.9484
110	2.68×10^{-5}	0.9904	4.12×10^{-5}	0.9978
400	2.30×10^{-5}	0.9648	3.69×10^{-5}	0.9978

The release profiles in Figure 4.13 and rate constants displayed in Table 4.7 show that having sodium TPP in the gelling mixture did have a small affect the release

properties of beads subsequently crosslinked in 300 mM aqueous glyoxal solution. The glyoxal crosslinked beads gelled without any ionic crosslinker had the shortest equilibrium release time and largest first-order rate constant (4.40×10^{-5} s^{-1}). The chitosan beads ionically crosslinked with 110 mM TPP had an increased equilibrium release time and smaller rate constant (4.12×10^{-5} s^{-1}). The difference between the two rate constants, however, is minimal and the concentration of DCD released at equilibrium release time was not influenced by ionic crosslinker. It was concluded that covalent crosslinking has the primary influence on the release properties but additional crosslinking with an ionic crosslinker can cause a slight increase equilibrium release time.

4.2.3.6 Influence of Time Spent Immersed in Covalent Crosslinking Solution

This research has established that covalent crosslinking has a substantial influence on the xerogel beads release characteristics. Therefore, a study was carried out to examine if the time the bead spent immersed in the covalent crosslinking solution could be used to control the release rate. If the Schiff base crosslinking reaction does not happen instantaneously, but rather over a period of time, the duration the beads spend in the crosslinking solution could be varied to control the release parameters. Muzzarelli and co workers stated that the amount of time chitosan xerogels spend in a covalent cross-linking solution can be used to control its release properties[10]. However, studies on the effect of time spent in covalent crosslinking solution are few. One such study performed by Monteiro and co workers, reported that an hour was long enough to complete the reaction between chitosan and glutaraldehyde[11]. A study was performed on the effect of the immersion time in glyoxal solution on the DCD release properties of the xerogel beads. The investigated immersion times were 5 min, 4 h and 24 h and the resulting time to reach release equilibrium and the concentration of the release solution at equilibrium were recorded. The results are displayed in Table 4.8.

Table 4.8 Influence of time spent in glyoxal crosslinking solution on release from 10 xerogel beads in 500 mL Millipore water at 20 ± 1 °C. The gelling solution contained 0.75 M NaOH 60 mM DCD and 110 mM TPP; the beads were then covalently crosslinked in 300 mM glyoxal aqueous solution for the stated time then washed in 60 mM DCD Millipore water solution and incubated in an oven at 37 ± 1 °C for 7 days.

Time spent immersed in 300 mM Glyoxal crosslinking solution	Time to reach release equilibrium (h)	Concentration of release solution at equilibrium (mM)
5 min	5.5	0.04
4 h	6.0	0.03
24 h	6.0	0.03

The results in Table 4.8 show that after spending 5 min in the crosslinking solution the xerogel beads had a release equilibrium time of 5.5 h and the concentration of the release solution at equilibrium was 0.04 mM. The DCD release data obtained for chitosan xerogel beads that spent 4 h and 24h in the crosslinking solution were almost identical. The time to reach release equilibrium was 6.0 h and the concentration of the release solution at equilibrium was 0.03 mM for both sets of beads. It was concluded that the majority of the crosslinking reaction takes place within 5 min which meant it was easier to control the DCD release from the xerogel beads by varying the concentration of glyoxal in the crosslinking solution, rather than the amount time the beads are immersed in the crosslinking solution.

4.2.3.7 Isothermal Kinetic Release Studies

The use of temperature to control the response of a release system has been extensively studied in the biomedical field in studies seeking to mimic the release conditions of the human body[12]. Authors have found that as the temperature of the release medium increases so too does the swelling ratio. This influences the release

rate of drugs from the delivery system[13]. Release studies in this research so far had all taken place at 20 ± 1°C; therefore a study was carried out to investigate what effect, if any, increasing the release medium temperature would have on the controlled release of DCD from covalently crosslinked chitosan xerogels. The release of the DCD was investigated at 20 °C, 30 °C and 40 °C. The release profiles are shown in Figure 4.15.
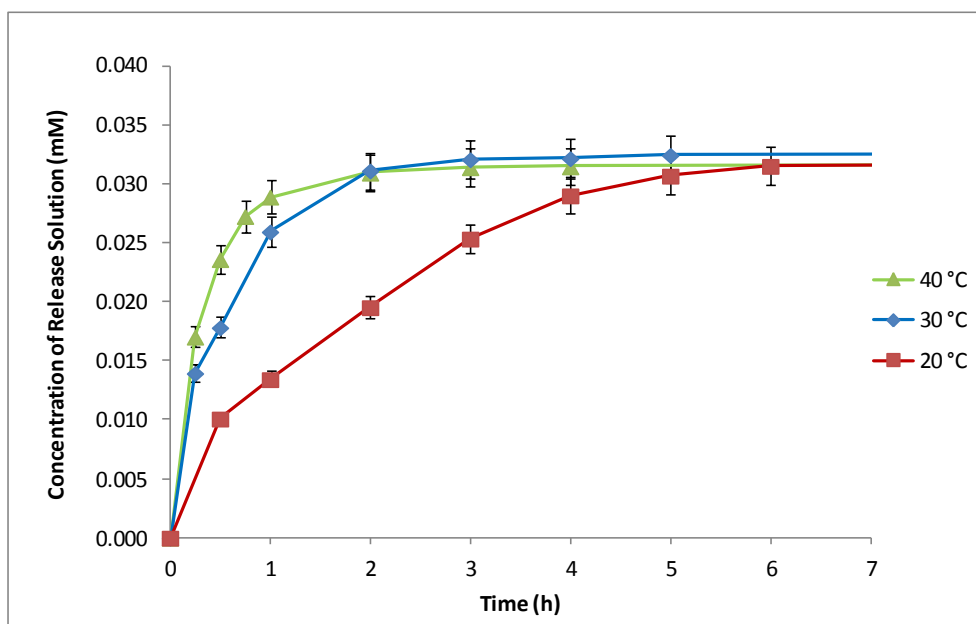
Figure 4.15 Isothermal kinetics curves of DCD release from chitosan-glyoxal xerogels at 20 °C, 30 °C and 40 °C. The temperature experimental error was ± 0.1 °C The gelling solution contained 0.75 M NaOH, 60 mM DCD and 110 mM TPP; the beads were then covalently crosslinked in 300 mM glyoxal aqueous solution then washed in 60 mM DCD Millipore water solution and incubated in an oven at 37 ± 1 °C for 7 days.

The results reveal that the release medium temperature had an effect on the time DCD release takes to reach release equilibrium. Increasing the release medium temperature resulted in faster DCD release from the xerogel beads. The DCD equilibrium release time for chitosan xerogel beads placed in a 40 °C release medium was 2 h, a third of the time reported at a release medium temperature of 20 °C. To obtain the rate constant at each release medium temperature investigated the data were fitted to the zero-order and first-order models in Figure 4.16 and the results are displayed in Table 4.9.
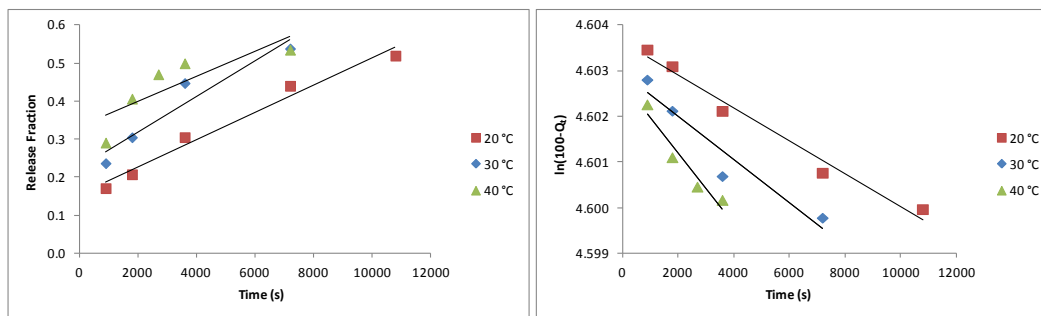
(a)   (b)

Figure 4.16 Results of the fitting of release data to the (a) zero-order and (b) first-order models comparing release medium temperatures. The gelling solution contained 0.75 M NaOH, 60 mM DCD and 110 mM TPP; the beads were then covalently crosslinked in 300 mM glyoxal aqueous solution then washed in 60 mM DCD Millipore water solution and incubated in an oven at 37 ± 1 °C for 7 days.

Table 4.9 Results from the fitting of release data to the (a) Zero-order and (b) first-order models. Release took place in release medium temperatures. The gelling solution contained 0.75 M NaOH, 60 mM DCD and 110 mM TPP; the beads were then covalently crosslinked in 300 mM glyoxal aqueous solution then washed in 60 mM DCD Millipore water solution and incubated in an oven at 37 ± 1 °C for 7 days.

Release Medium Temperature (°C)	Zero-Order Model		First-Order Model	
	k_0 (s^{-1})	R^2	k_1 (s^{-1})	R^2
20	2.68×10^{-5}	0.9904	4.12×10^{-5}	0.9978
30	4.69×10^{-5}	0.9209	7.93×10^{-5}	0.9490
40	7.66×10^{-5}	0.9265	1.28×10^{-4}	0.9478

The results indicate that at each release medium temperature investigated the first-order model had the best fit. In addition, increasing the release medium temperature leads to an increase in the first-order rate constant. For example, at a release medium

temperature of 20 °C the first order rate constant was 4.12×10^{-5} s^{-1} while at 40 °C it increased to 1.28×10^{-4} s^{-1}. This represented an increase in the rate constant of a factor of 3.1. This coincides with results presented by Adnadjevic *et al.* who reported an increase in the release rate of their model drug from poly(acrylic acid) hydrogels due to an increase in the release medium temperature[14]. However, the increase in the rate constant was not as significant as reported here. This was because the rate constant for (*E*)-4-(4-metoxyphenyl)-4-oxo-2-butenoic acid release from the poly(acrylic acid) hydrogels only increased by a factor of 1.2 between 22°C and 42 °C[14]. It was concluded that DCD release from chitosan xerogel beads covalently crosslinked in 300 mM glyoxal solution are sensitive to the temperature of the release medium.

4.2.4 Influence of Enzymatic Degradation

4.2.4.1 Swelling Properties

Lysozyme is a ubiquitous enzyme which occurs in a wide range of biological fluids and tissues within the animal and plant kingdoms, such as human serum, tears and milk. Lysozyme uses polysaccharides, such as partially deacetylated chitosan, as natural substrates[15]. A study was performed to determine what effect, if any, dissolving 0.1 mg/mL lysozyme in the release solution would have on the swelling properties and DCD release from a glyoxal crosslinked xerogel bead. This concentration of lysozyme was chosen as Genta *et al.* had demonstrated that it was capable of degrading chitosan glutamate microcapsules that had been crosslinked using calcium chloride[16]. Genta *et al.* reported that after 1.5 h in a solution of 0.1 mg/mL lysozyme the chitosan microcapsules fragmented[16]. The swelling study is exhibited in Figure 4.11 and the DCD release profile is displayed in Figure 4.12.
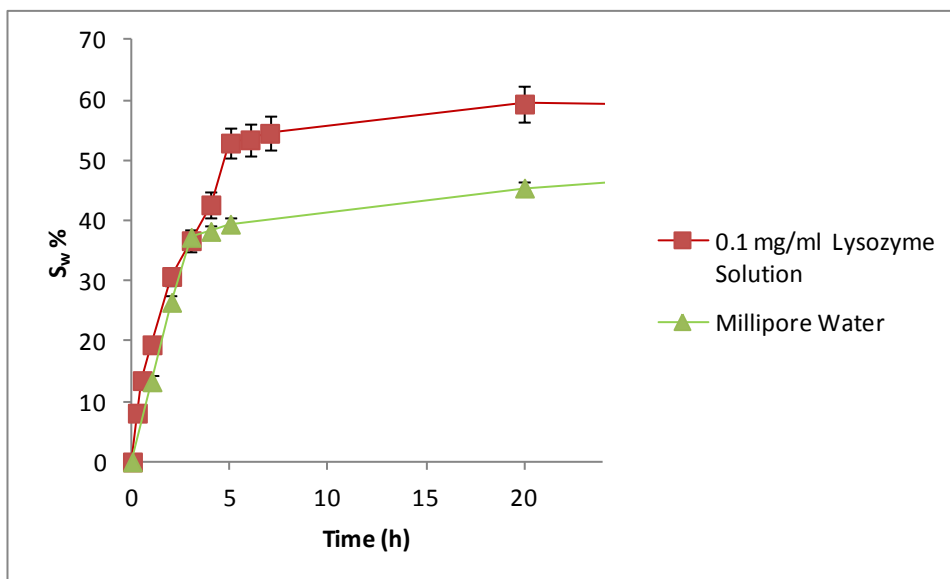
Figure 4.11 Comparison of the swelling ratio percentage of glyoxal crosslinked xerogel beads in 0.1 mg/mL lysozyme solution and Millipore water solution held at 20 ± 1. The gelling solution contained 110 mM TPP, 60 mM DCD and 0.75 M NaOH. The beads were subsequently crosslinked with 300 mM glyoxal, washed thoroughly with 60 mM DCD Millipore water solution and dried in an oven at a constant temperature of 37 ± 1°C for 7 days.

The results of the swelling study show that the swelling ratio of glyoxal crosslinked chitosan beads in lysozyme solution had a slightly higher value than those in Millipore water. After 5 h the beads in 0.1g/100 mL lysozyme solution began to exhibit a significantly higher swelling ratio than the equivalent beads in Millipore water. After one hour in the 0.1g/100 mL lysozyme and Millipore water solutions the swelling ratios were 20% and 13% respectively but after 5 h a clearer separation in swelling ratios (%) could be seen as the swelling ratios (%) were 53% and 39% , respectively. It was concluded that the lysozyme was causing an increase in the swelling ratio of the glyoxal crosslinked chitosan xerogel beads due to its ability to degrade chitosan.

4.2.4.2 DCD Release Properties

The equilibrium release time of DCD from chitosan xerogel beads crosslinked in 300 mM glyoxal was 6 h (Table 3.8). In Figure 4.11 it is evident that during the first 5 h

the lysozyme has little effect on the swelling ratio (%) of the chitosan beads. However, as release lasts for 6 h an experiment was conducted to investigate whether the DCD release profile of chitosan xerogels would be influenced by the release solution containing 0.1 mg/mL lysozyme.
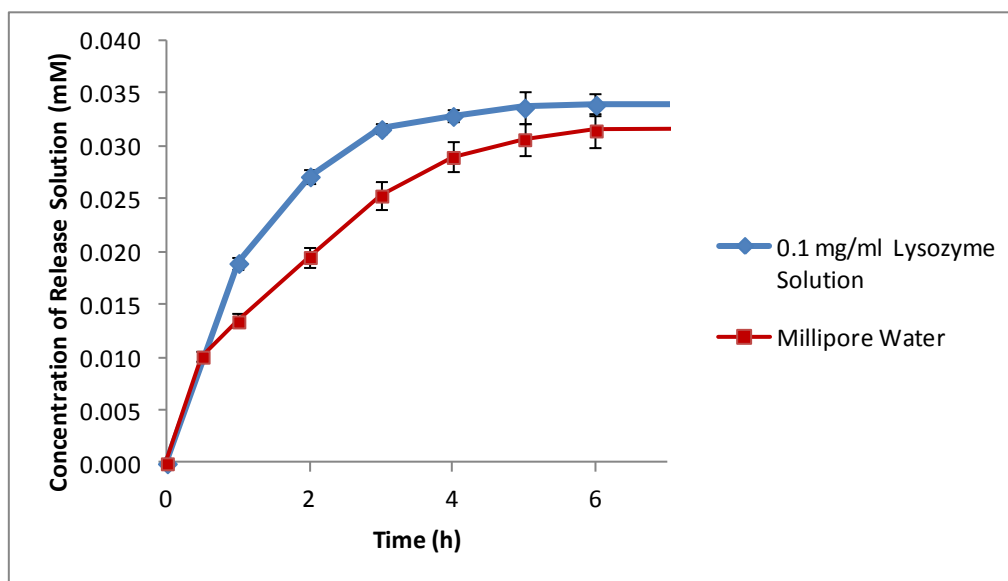
Figure 4.12 Comparison of DCD release profiles from glyoxal crosslinked xerogel beads in 0.1 mg/mL lysozyme solution and Millipore water solution held at 20 ± 1. The gelling solution contained 110 mM TPP, 60 mM DCD and 0.75 M NaOH. The beads were subsequently crosslinked with 300 mM glyoxal, washed thoroughly with 60 mM DCD Millipore water solution and dried in an oven at a constant temperature of 37 ± 1°C for 7 days.

The release profile in Figure 4.12 shows that the DCD release from glyoxal crosslinked chitosan xerogel beads is influenced by the 0.1 mg/mL lysozyme release medium. The chitosan xerogel beads in lysozyme solution has an equilibrium release time of 4 h compared with 6 h for beads in Millipore water solution and released slightly more DCD. However, any enzymatic degradation that has taken place has been limited as the release of DCD from the beads can still be considered controlled. The glyoxal crosslinked chitosan xerogel beads in this study do not appear to have degraded as fast as the calcium crosslinked chitosan beads in the study performed by Genta *et al*[16]. This may have been due to the increased polymer network density of the chitosan xerogel beads as they were subjected to covalent crosslinking. The effects

of enzymatic degradation on chitosan xerogel beads crosslinked with a covalent crosslinker appear to be even more limited. Jameela and Jayakrishnan reported that after 7 days they could not see any sign of enzymatic degradation of chitosan by lysozyme and that the mechanism of release from their glutaraldehyde crosslinked chitosan beads was unaffected[17]. However, there may be other factors as Lin *et al.* studied the effects of lysozyme degradation on non-covalently crosslinked chitosan microcapsules and discovered that the process occurred over a prolonged period of 70 hours[18]. In conclusion, although lysozyme has been shown to cause degradation of chitosan it appears to have had a limited effect on DCD release from covalently crosslinked chitosan xerogel beads.

4.2.5 Unwashed Glyoxal Crosslinked Xerogel Beads

According to the standard preparation of xerogel beads covalently crosslinked with glyoxal it was necessary to wash the xerogel beads thoroughly with Millipore water once the covalent crosslinking reaction had been completed to remove any unreacted glyoxal from the hydrogel beads. Glyoxal, the smallest dialdehyde, polymerises easily and is known to be extremely reactive[19]. In addition, glyoxal forms hydrates in water which condense to give a series of oligomers[20] which, if not removed by washing can become trapped in the chitosan xerogel bead. Studies were therefore performed to investigate the effect of the removal of the wash step after covalent crosslinking to examine whether or not this would impact on the physical characteristics or release properties of the chitosan xerogel beads.

4.2.5.1 Surface Morphology

The surface and shape of the unwashed xerogels was determined by scanning electron microscopy (SEM) and compared with a washed glyoxal crosslinked xerogel in Figure 4.17

(a)   (b)

(c)   (d)
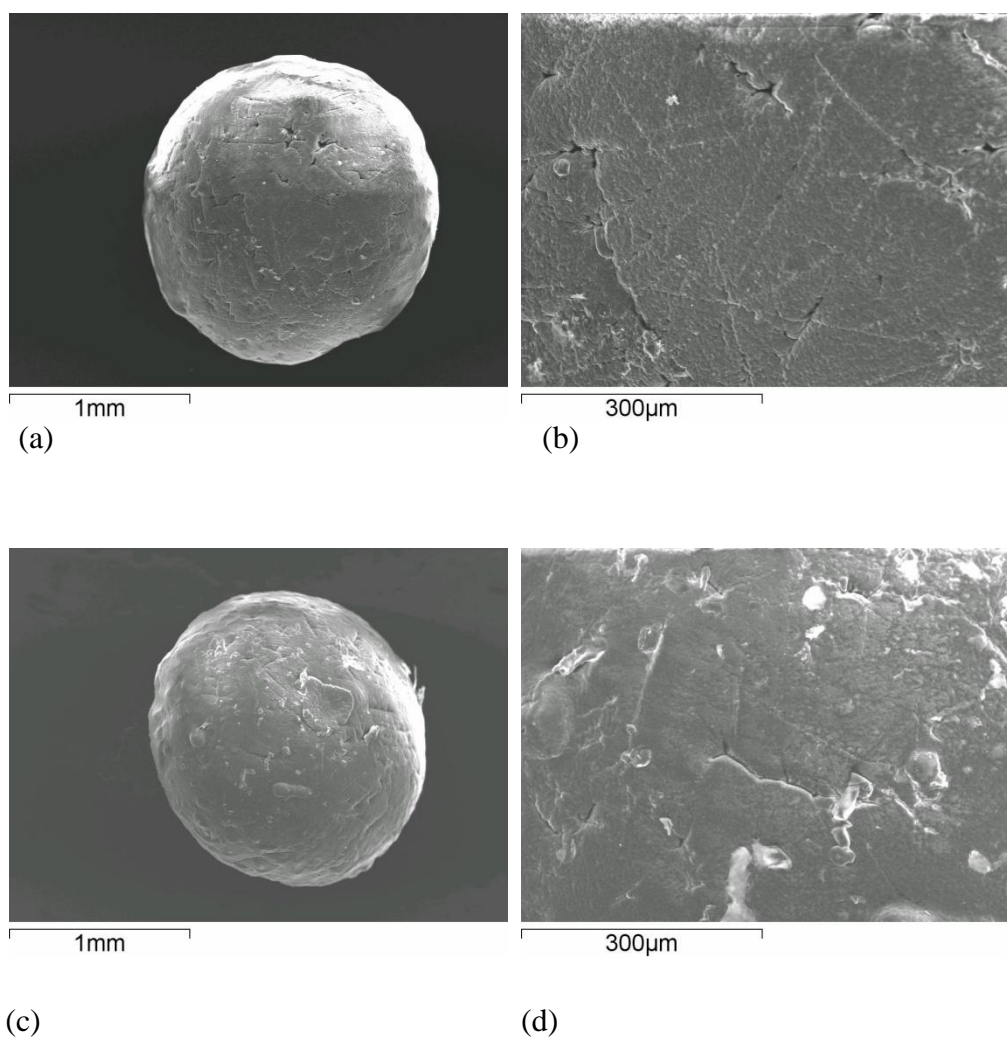
Figure 4.17 SEM micrographs of chitosan xerogels crosslinked with glyoxal. The gelling solution of all the xerogels examined contained 110 mM TPP, 60 mM DCD and 0.75 M NaOH. All the Xerogels presented were crosslinked in 300 mM glyoxal solution. However the beads in (a) and (b) were for 24 h in 60 mM DCD Millipore water solution while the beads in (c) and (d) were dried without washing.

The micrographs presented in Figure 4.17 reveal that the surface morphology of beads that were washed and unwashed after the glyoxal crosslinking reaction is similar. Figure 4.17 (c) and (d) exhibited the same rough uneven surface that the washed xerogels (Figure 4.17 (a) and (b)) displayed. The main difference however was an increase in size as the mean diameter of the beads rose from 1.64 ± 0.03 mm for the washed beads to 1.73 mm ± 0.04 mm for the unwashed. The increase in bead size was attributed to the amount of the unreacted glyoxal residue inside the unwashed beads which lead to the bead being larger when it was dehydrated.

4.2.5.2. Swelling Properties

A swelling study was conducted to examine whether the unreacted glyoxal encapsulated in the xerogel beads would have an effect on the swelling ratio percentage. A decrease in the swelling ratio (%) of the unwashed xerogel compared to the washed beads would suggest that water was finding it harder to diffuse through the pores of the unwashed beads. The swelling ratio percentage of unwashed glyoxal xerogels was compared with xerogels that had been washed in Millipore water for 24 h. The swelling ratios percentages are exhibited in Figure 4.18.
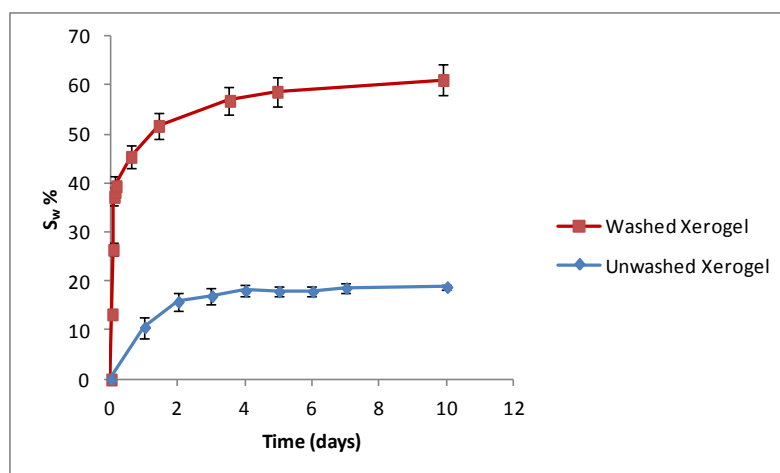
Figure 4.18 Comparison of the swelling ratio (%) of chitosan beads that were washed and not washed in Millipore water after being covalently crosslinked in 300 mM glyoxal solution. The gelling solution of both beads contained 60 mM DCD, 110 mM TPP and 0.75 M NaOH. The swelling studies were conducted at $20 \pm 1°$C and repeated in triplicate.

The swelling ratio (%) of unwashed xerogel beads over time is shown in Figure 4.18, after 10 days the swelling ratio percentage of unwashed xerogel beads was just 18%. This is a substantial decrease compared with the swelling ratio of washed xerogel beads which exhibited a swelling ratio of 61% after the same amount of time. This suggested that water has a more difficult time diffusing through xerogel beads that are not been washed after covalent crosslinking due to encapsulated unreacted glyoxal blocking the pores. DCD release from the unwashed beads was examined to investigate if the reduction in swelling ratio percentage coincided with an increase in DCD release time.

4.2.5.3 DCD Release Profile

Since glyoxal absorbs light in the same ultraviolet-visible spectral region as DCD the UV/vis spectrum obtained from a solution into which both DCD and glyoxal were released was influenced by both materials. The influence of unreacted glyoxal leaching from the beads on the UV spectra of DCD is exhibited in Figure 4.19. The UV spectra exhibited in Figure 4.19 (a) are from a release solution containing chitosan xerogel beads crosslinked in 300 mM glyoxal and 60 mM DCD aqueous solution and washed in 60 mM DCD Millipore water solution for 24 h and then incubated in an oven. A release spectrum corresponding to exactly that of DCD can be seen with no evidence of excess glyoxal leaching. In comparison, the UV spectra exhibited in Figure 4.19 (b) exhibits spectra from a release solution containing chitosan xerogel beads crosslinked in 300 mM glyoxal and 60 mM DCD aqueous solution, and then incubated in an oven without washing in Millipore water solution. The spectra observed as a result of release from these beads was a result of the absorption of light from both DCD and glyoxal being present in the release solution.
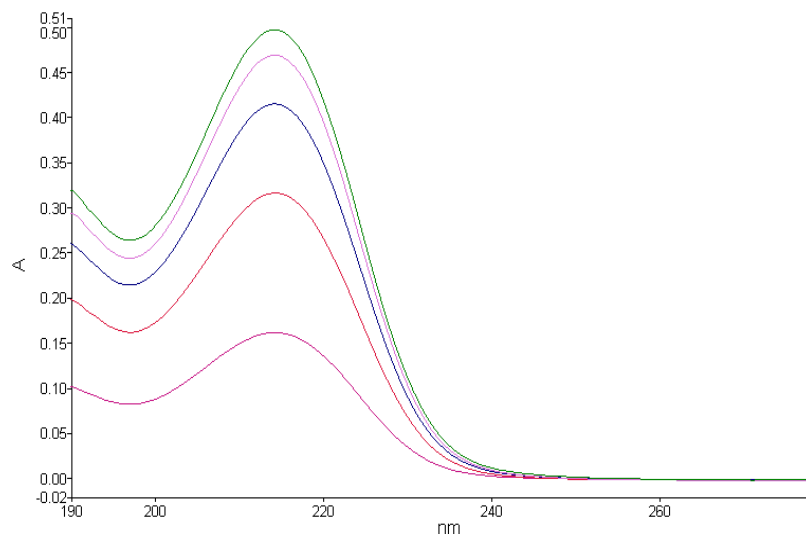
Figure 4.19 (a) UV/vis spectra obtained from samples taken from a release solution which contained chitosan xerogel beads crosslinked in 300 mM glyoxal, loaded in 60 mM aqueous DCD solution, washed in Millipore water for 7 days and then incubated in an oven at 37 ± 1 °C for 7 days. Spectra recorded after   (————) 0.5 hours   (————) 2 hours   (————) 3 hours (————) 4 hours   (————) 5 hours of DCD release.
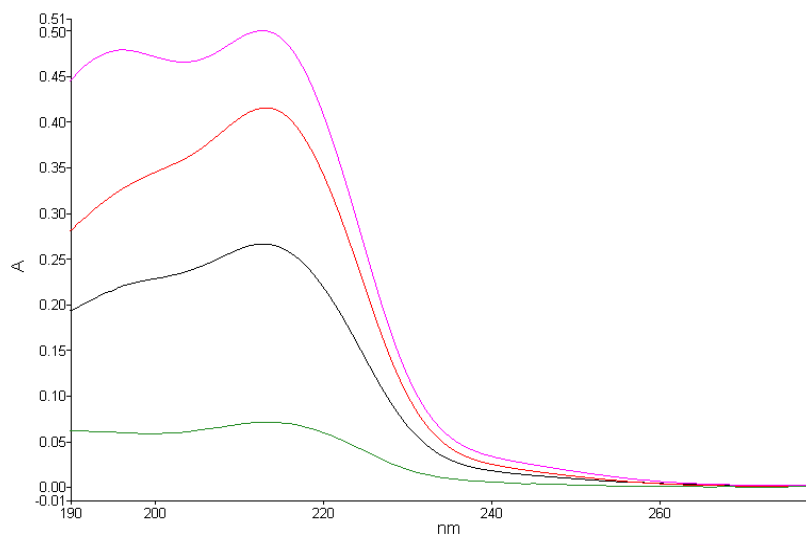
Figure 4.19 (b) UV/vis spectra obtained from samples taken from a release solution which contained chitosan xerogel beads crosslinked in 300 mM glyoxal 60 mM DCD aqueous solution and then incubated in an oven at 37 ±1 °C for 7 days. Spectra recorded after (————) 72 hours (————) 120 hours   (————) 144 hours   (————) 168 hours of DCD release.

It was apparent that although the spectra obtained of the release solution had been influenced by the release of unreacted glyoxal from the chitosan beads, the λ max of DCD remained consistent at each release time investigated. An experiment was performed to obtain a DCD release profile from glyoxal crosslinked chitosan beads that were not washed after the covalent crosslinking reaction. The result is presented in Figure 4.20.
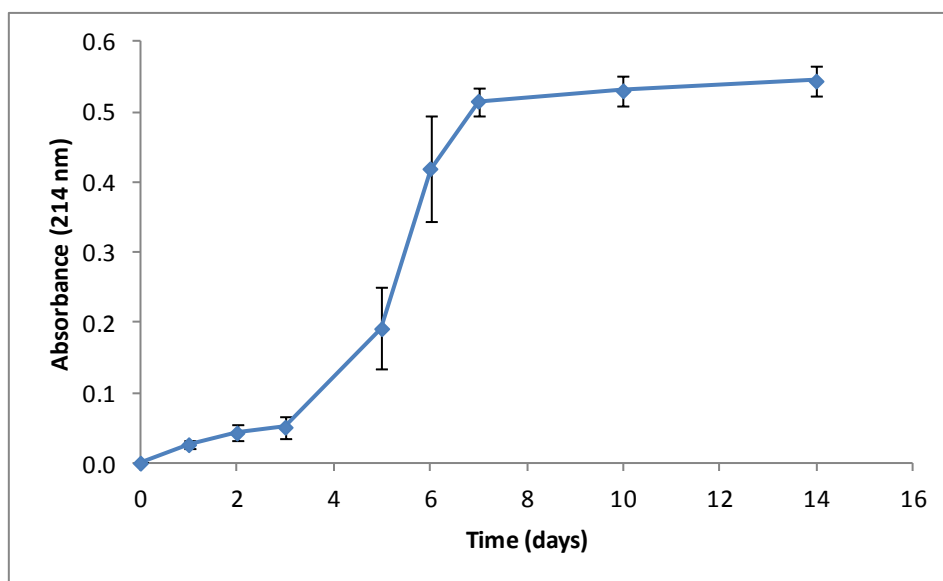
Figure 4.20 Release profile from xerogel beads that were not washed in Millipore water after being crosslinked in 300 mM glyoxal solution and loaded with 60 mM DCD. The gelling solution contained 60 mM DCD, 110 mM TPP and 0.75 M NaOH. The xerogel beads were dried in a 37 ± 1°C oven for 7 days. The release studies were conducted at 20 ± 1°C.

The DCD release profile in Figure 4.20 shows the release profile of DCD from unwashed glyoxal crosslinked xerogel beads. Significantly the absorbance values recorded at λ = 214 nm after 3 days was only 0.06 absorbance units. When you compare this to the time it takes beads washed in 60 mM Millipore water solution to reach 0.06 absorbance units (0.5 h) it is apparent that the release time has been substantially increased. Release from the unwashed xerogels has a lag time of 3 days, at which point the absorbance increases until day 7 at which time the absorbance reached equilibrium. Given that release equilibrium from xerogel beads covalently crosslinked in 300 mM glyoxal and washed for 7 days in Millipore water was reached

after 6 hours (Table 3.8), the a lag time of 72 h for the washed beads represented a significant delay in the release of DCD from the xerogel beads.

4.2.5.4 Unwashed Glyoxal Beads as a Controlled Release System

Chitosan xerogel beads crosslinked in 300 mM glyoxal solution and incubated in an oven for 7 days could delay DCD release for up to 72 h. However they also release an unquantified amount of unreacted glyoxal, which may include glyoxal hydrates and oligomers. The maximum swelling ratio (%) of the unwashed glyoxal beads was lower than that of its washed counterpart, suggesting the pores are less permeable due to the unreacted glyoxal trapped in the bead. Delaying DCD release by trapping unreacted glyoxal inside the xerogel beads resulted in a considerable lag time and controlled release lasting up to 7 days. Further research could be carried out on the ability of unreacted glyoxal encapsulated within chitosan xerogel beads to create a controlled delivery system by loading the xerogels with a model coloured compound whose UV/vis spectrum would be separated from that of glyoxal thus allowing for a quantitative calculation of the release profile.

4.3 Conclusions

In summary the results depicted in this chapter described the properties and release mechanism of DCD from xerogel chitosan beads crosslinked with glyoxal.

Glyoxal crosslinked chitosan beads delivered DCD in a controlled manner and the release time was shown to be influenced by the concentration of glyoxal in the crosslinking solution and the concentration of ionic crosslinker in the gelling solution.

Glyoxal crosslinked xerogel beads were found to exhibit considerably less swelling ability than ionically crosslinked xerogel beads which suggested that covalent crosslinking had increased the polymer mesh density thereby reducing the swelling ratio (%). The glyoxal crosslinked xerogels were found to be pH sensitive because

when placed an acidic aqueous solution they were found to swell to a greater ratio and released DCD at a slightly faster rate. However, DCD is a small and highly water soluble chemical therefore a change in the pH of the release medium was not likely to have a big effect.

The mechanism of release from the beads was investigated and it was concluded that DCD release was by a combination of diffusion and polymeric chain relaxation however diffusion was determined to be the dominant mechanism and that by increasing the covalent crosslinker in the crosslinking solution the relaxation/Fickian contribution ratio would decrease implying that using glyoxal as a crosslinker promotes diffusion as the release mechanism.

Washing the hydrogel beads after crosslinking to remove unreacted glyoxal was a standard step in the formation of covalently crosslinked chitosan xerogels however removing this step caused the incorporation of a lag time of 3 days into release profile from the xerogel beads. Instead of reaching release equilibrium after a number of hours, non-washing of the beads was found to extend the release time to 7 days. Furthermore, the maximum swelling ratio (%) obtained fell to just 18.9%, down from the 57.9% exhibited by xerogel beads that had been washed in Millipore water for 24 h after the crosslinking reaction. This was a positive result toward developing a controlled release system for DCD however further studies would have to be conducted using a model coloured release molecule to clearly investigate the influence of unreacted glyoxal on controlled release from the beads.

4.4 References

[1]   Q. Yang, F. Dou, B. Liang and Q. Shen, *Carbohydrate Polymers* **2005**, *61*, 393–398.

[2]   K. C. Gupta and F. H. Jabrail, *Carbohydrate Research* **2006**, *341*, 744-756.

[3]   L. A. Zemskova, A. V. Voit, Y. M. Nikolenk, V. I. Sergienko, I. D. Troshkina, A. V. Plevaka, S. B. Maiboroda and A. M. Chekmarevb, *Journal of Nuclear and Radiochemical Sciences* **2005**, *6*, 221-222.

[4]   X. Z. Shu and K. J. Zhu, *International Journal of Pharmaceutics* **2002**, *233*, 217-225.

[5]   M. V. Risbud, A. A. Hardikar, S. V. Bhat and R. R. Bhondeb, *Journal of Controlled Release* **2000**, *68*, 23-30.

[6]   F. Mi, C. Kuan, S. Shyu, S. Lee and S. Chang, *Carbohydrate Polymers* **2000**, *41*, 389-396.

[7]   Z. M. Wu, X. G. Zhang, C. Zheng, C. X. Li, S. M. Zhang, R. N. Dong and D. M. Yu, *European Journal of Pharmaceutical Sciences* **2009**, *37*, 198–206.

[8]   H. K. Stulzer, M. P. Tagliari, A. L. Parize, M. A. S. Silva and M. C. M. Laranjeira, *Materials Science and Engineering* **2009**, *29*, 387–392.

[9]   C. Ferrero, I. Bravo and M. R. Jimenez-Castellanos, *Journal of Controlled Release* **2003**, *92*, 69-82.

[10]   R. A. A. Muzzarelli, *Carbohydrate Polymers* **2009**, *77*, 1-9.

[11]   O. A. C. Monteiro and C. Airoldi, *International Journal of Biological Macromolecules* **1999**, *26*, 119-128.

[12]   B. L. Guo, J. F. Yuan and Q. Y. Gao, *Colloids and Surfaces B: Biointerfaces* **2007**, *58*, 151–156.

[13]   A. S. Carreira, F. A. M. M. Gonçalves, P. V. Mendonça, M. H. Gil and J. F. J. Coelho, *Carbohydrate Polymers* **2010**, *80*, 618–630.

[14]   B. Adnajevic, J. Jovanovic and B. Drakulic, *Thermochimica Acta* **2007**, *466*, 38-48.

[15]   Y. Zhang, Z. Wanga, J. Zhanga, C. Chenb, Q. Wua, L. Zhanga and X. Zhanga, *Carbohydrate Polymers* **2011**, *85*, 554–559.

[16]   I. Genta, P. Perugini, T. Modena, F. Pavanetto, F. Castelli, R. A. A. Muzzarelli, C. Muzzarelli and B. Conti, *Carbohydrate Polymers* **2003**, *52*, 11-18.

[17]   S. R. Jameela and A. Jayakrishnan, *Biomaterials* **1995**, *16*, 769-775.

[18]   W. Lin, D. Yu and M. Yang, *Colloids and Surfaces B: Biointerfaces* **2005**, *44*, 143–151.

[19]   K. Nakajima, K. Ohta, T. A. Mostefaoui, W. Chai, T. Utsukihara, C. A. Horiuchi and M. Murakami, *Journal of Chromatography A* **2007**, *1161*, 338-341.

[20]   E. E. Whipple, *Journal of the American Chemical Society* **1970**, *92*, 7183-7185.

Chapter 5: Synthesis and Characterisation of *N*-Acylated Chitosan Beads and their DCD Release Properties

5.1 Introduction

Chitosan is a linear, semi-rigid polysaccharide. As a natural renewable resource which is biodegradable, biocompatible and has relatively low toxicity it had been the subject of much research in the past decade[1]. However, the applications of chitosan are still limited. Many efforts have been made to modify the structure of chitosan to increase the applications of the biopolymer. Since chitosan has two hydroxyl and one amino group per glucosamine unit, several new chitosan derivatives have been produced with modifications to these groups, and the resulting polymers have been shown to possess unique properties[2]. The dissociation and reorganization of hydrogen bonds by chemical modification allows the production of novel molecular conformations[3]. Acylation of chitosan with acidic anhydrides or fatty acid chlorides has proved to be an effective method of preparing hydrophobic chitosan derivatives at low temperatures and under controlled conditions[4, 5]. The synthesis of *N*-acylated chitosan fibre was pioneered by Shigehiro Hirano and his research group[6]. Hirano and co-workers demonstrated that chitosan can form a thermally nonreversible gel network depending on the structure of the chitosan fibre and the concentration of the carboxylic anhydride in the reaction vessel[6]. Studies have shown that due to the different reactivity of the amino and hydroxyl sites on the chitosan, the functional group at which substitution occurs can be controlled[1].

The structure of chitosan polymer was important to this research because changing the chemical structure of chitosan hydrogels and their physico-chemical properties by introducing aliphatic carbon side chains at the amino site[2] may favourably alter the release properties of DCD from chitosan xerogel beads. Authors have shown that the structure of chitosan assumes one of three forms; hydrated, dehydrated and non-crystalline[7]. The hydrated and dehydrated forms take up a similar conformation which is an extended two fold helix stabilised by intramolecular hydrogen bonds but despite this similarity the molecular packing and water content are quite different. The

hydrated chitosan forms anti-parallel chains which are stabilised by intramolecular and intermolecular hydrogen bonding and hydrogen bridging involving water molecules. In the crystalline structure of the dehydrated form, parallel chains are organised in sheet structures via intermolecular hydrogen bonds[4].

The formation of *N*-acyl chitosan fibres has been achieved by treating a solution of chitosan in aqueous acetic acid with a carboxylic anhydride. This has been shown to result in the formation of a rigid and transparent gel within 30 min at room temperature. Examination of the gel concluded that *O*-acylation and *N*-acylation of chitosan fibre had been achieved with the ratio depending on the degree of substitution[8]. The general mechanism of the *N*-acylation reaction of chitosan with a carboxylic anhydride is shown in Scheme 5.1. The reaction is a nucleophilic addition-elimination to an acyl derivative.
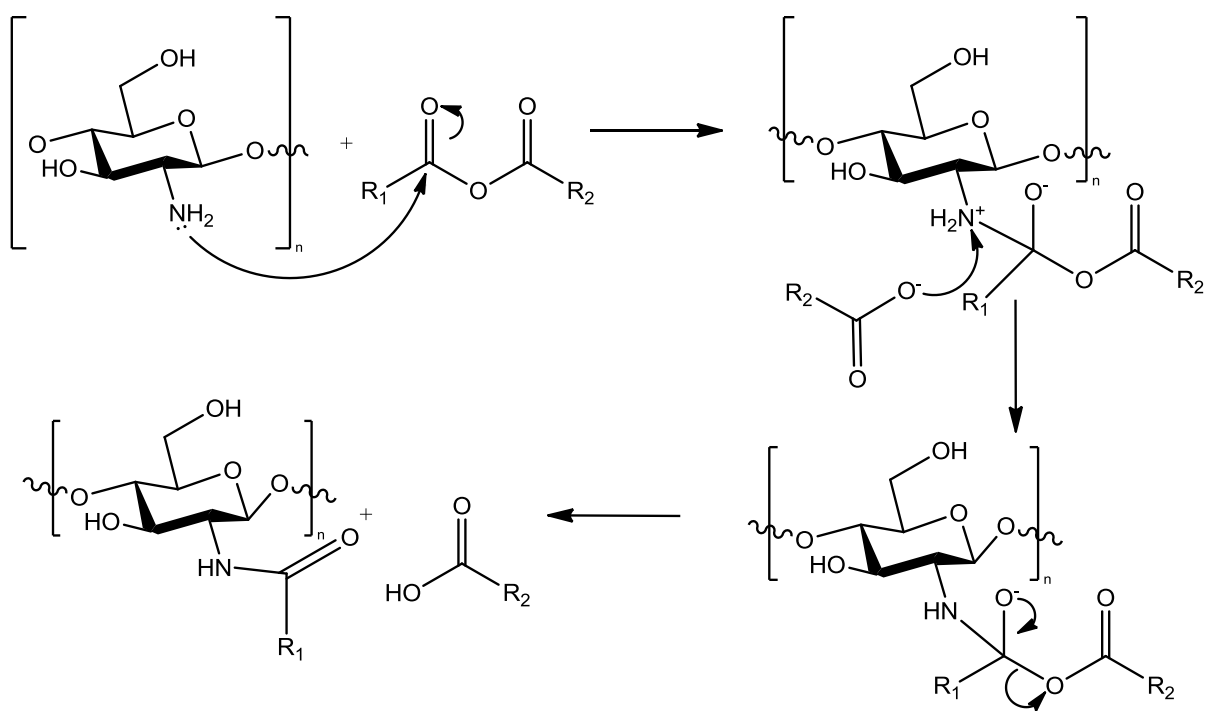
Scheme 5.1 Reaction mechanism for the *N*-acylation of chitosan with an acidic anhydride

147

Choi *et al*. investigated the effect of the *N*-acylation of chitosan on the structure and properties of chitosan fibres[2]. They confirmed by x-ray diffraction that the chemical structure of chitosan fibres was altered by the introduction of *N*-acyl groups. They deduced that the introduction of an aliphatic carbon atom chain at the glucosamine unit of chitosan caused the breakage of existing hydrogen bonds and dehydration to occur immediately. As a result the entire crystalline structure of chitosan was destabilised and the polymer main chain moved towards its most stable form. This resulted in new intermolecular interactions and the substituted aliphatic carbon atom chain participating in the formation of new hydrogen bonds. In addition, research performed by Wu *et al*. concluded that the structure formed by *N*-acylated chitosan was a crystalline sheet-type structure, in which all the flexible side chains organised themselves in a parallel direction normal to the polymer backbone and partially interdigitated with each other, as exhibited in Figure 5.1[1]. Strong hydrogen bond interactions, together with interactions between closely packed hydrophobic side chains gave the *N*-acylated chitosan striking stability and caused the chitosan to be very difficult to dissolve in any solvent[1].
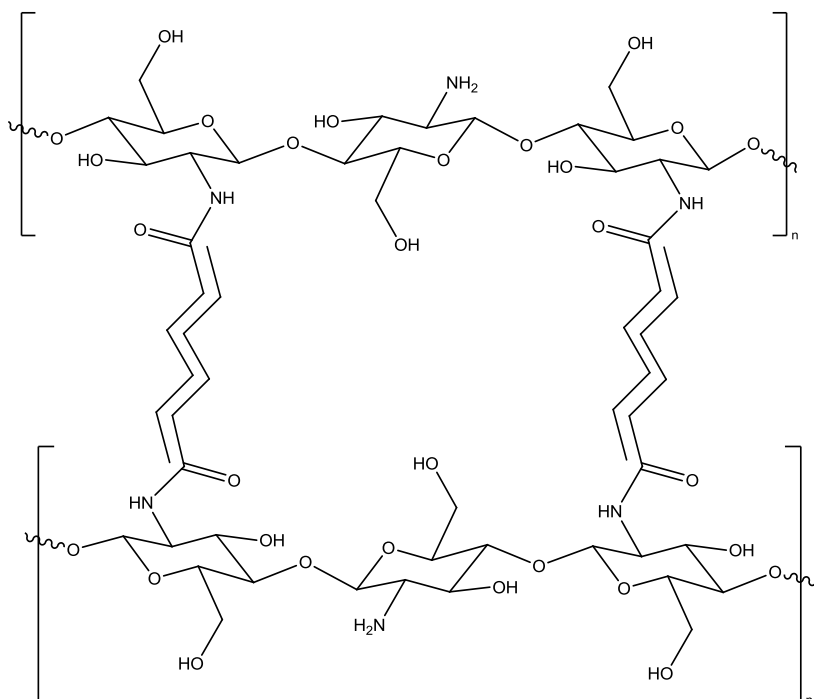
Figure 5.1 Chitosan organised into parallel chains due to *N*-acylation

N-acylation of chitosan by a carboxylic anhydride has been shown to take place at the amine group[2], this is the same site where protonation and crosslinking take place and

thus *N*-acylation had the potential to hinder the hydrogel formation process. Considerable research has taken place into developing chitosan matrices which bear hydrophobic groups but the degree of substitution achieved has been relatively low[9]. This was due to the low solubility of the acylated chitosan which limits the amount of chitosan crosslinking that can take place. For example, Lee *et al*. obtained chitosan micelles through chitosan grafted deoxycholic acid in dilute acidic solution in the presence of 1-ethyl-3-(3-dimethylaminopropyl)-carbodiiamide (EDC). However the degree of substitution of these derivatives was between 2.8%-5.1% and the micelles formed were unstable against dilution[10]. Preliminary studies carried out in this research attempted *N*-acylation of the chitosan fibre prior to the formation of the chitosan hydrogel beads. However due to the hydrophobicity of the *N*-acylated chitosan fibre it was not possible to dissolve the chitosan in an acidic aqueous solution which meant a stable chitosan hydrogel bead could not be formed. Therefore, an investigation was carried out to examine the possibility of forming the chitosan hydrogel bead first then carrying out a post-functionalization *N*-acylation reaction on the beads.   In 1990 Hirano *et al*. *N*-acetylated a chitosan hydrogel in its solid state by treating the bead with acetic anhydride under the same conditions they treated chitosan fibre. They concluded that chitosan could be *N*-modified in its hydrogel state as well as in its fibre state[6]. Despite this conclusion to be best of our knowledge no further research had been conducted to synthesise *N*-acylated chitosan hydrogels in their gel state but rather researchers continue to modify the chitosan fibre and then produce the hydrogel bead which had only proved successful with chitosan fibre that exhibited low degrees of substitution[11]. In this chapter, Hirano *et al* finding that it is possible to chemically modify the chitosan after hydrogel formation are investigated further with the aim of developing an *N*-acylated chitosan hydrogel bead that can be synthesised under relatively simple conditions which can then act as a controlled delivery system for DCD.

5.2 Results and Discussion

5.2.1 Synthesis and Characterisation of the Physical Properties of *N*-Acetyl and *N*-Hexanoyl Chitosan Beads

Chitosan hydrogel beads were synthesised by precipitation with hydroxide ion as described in Section 2.2.2.1 (i). The resulting hydrogel beads underwent a substitution reaction with an acetic or hexanoic anhydride as described in Section 2.2.3.1. In summary, chitosan hydrogel beads were suspended in 100 ml of methanol in a round bottom flask, then a pre-determined volume of the required acidic anhydride was added. The reaction mixture was refluxed for 24 h. Afterwards the treated chitosan hydrogel beads were washed several times with methanol, acetone and finally Millipore water. Characterisation of the resulting hydrogel beads was carried out and the results presented here.

5.2.1.1 FT-IR Analysis

A standard analytical technique used by authors to characterise the chemical functional groups of chitosan and *N*-acyl chitosan fibres is FT-IR spectroscopy[4, 12]. Chitosan used as the starting material in this research (85% deacetylated) exhibits a band at ~1640 cm^{-1} related to a combination of the N–H bending vibration of nonacylated 2-aminoglucose primary amines and carbonyl stretching of secondary amides[4]. However, authors have shown that *N*-acylation of chitosan causes the emergence of two separate and distinct bands which arise from stretching vibrations; one at approximately 1665 cm^{-1} ν(C=O) and another at 1555 cm^{-1} ν(*N*-acyl) [11, 13]. If these bands are visible on the FT-IR spectrum of the product of the reaction between the chitosan hydrogel and the acidic anhydride then *N*-acylation is considered to have been accomplished. Absorption bands in the range of 1710-1760 cm^{-1} are considered

indicative of the existence of *O*-acyl ester groups. However *N*-acylation has been shown to be favoured due to the higher reactivity of the amine group[11, 14].

5.2.1.1 (i) FT-IR Analysis of *N*-Acetylation of Chitosan Hydrogels

Hirano *et al*. preformed a successful *N*-acetylation reaction on chitosan hydrogels[6]. In the study presented here a similar acetylation reaction was performed to confirm that the reaction would be successful on 85% deacetylated chitosan hydrogel beads synthesised by precipitation with a hydroxide ion. After preparing the *N*-acetylated chitosan hydrogel beads using acidic anhydride and methanol as the reaction solvent the structure of the chitosan was investigated by FT-IR analysis. Figure 5.2 shows the FT-IR spectra of both 85% deacetylated chitosan xerogel bead which acts as the starting material and the *N*-substituted chitosan xerogels synthesised in the reaction. The chitosan hydrogel beads were washed in methanol, acetone and finally Millipore water, dried in an oven at 37 ± 1 °C for 24 h, then well ground before being investigated using FT-IR. The spectrum of the 85% deacetylated starting material chitosan xerogel beads exhibits the characteristic vibrational bands of chitosan at 2920 cm^{-1} $\nu(CH_3, CH_2)$ and at 1640 cm^{-1} which was assigned to a combination of the N–H bending vibration of nonacylated 2-aminoglucose primary amines and carbonyl stretching of secondary amides[4].
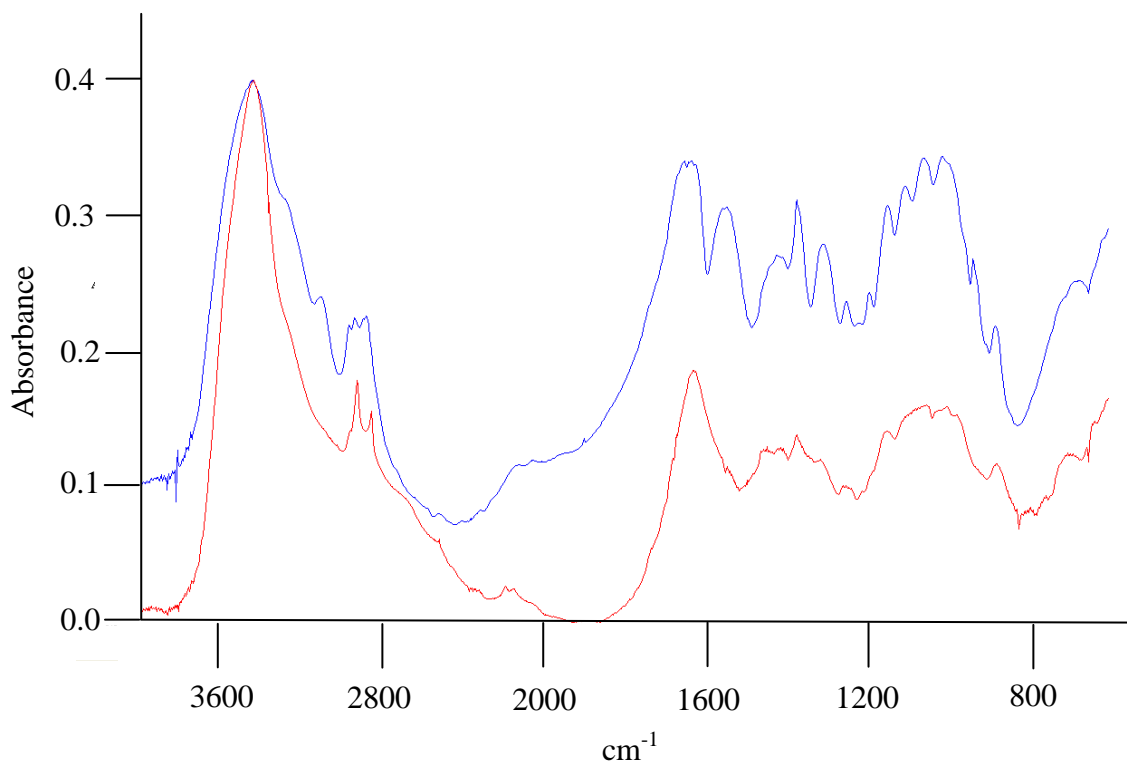
Figure 5.2 FT-IR spectra in absorbance mode of a (━━━) 85% deacetylated chitosan xerogel bead gelled in NaOH solution and a (━━━) *N*-acetylated chitosan xerogel bead gelled in NaOH solution. The beads were washed, dried and ground before analysis. FT-IR was performed using KBr discs.

In the blue spectrum the characteristic peak splitting, as described by Huan *et al* that defines *N*-substituted chitosan with aliphatic carbons chains can be seen[15]. The band at 1640 cm^{-1} is not visible due to an increase in the bands attributed to the stretching of secondary amides. The band attributed to a ν(C=O) is visible at 1655 cm^{-1} and the ν(*N*-acetyl) band is also visible at 1555 cm^{-1}. It was therefore concluded that the FT-IR spectrum observed for the reaction product is characteristic of *N*-acetylated chitosan. In addition, the spectrum has a strong resemblance to the FT-IR recorded of chitin which has bands at 1657 cm^{-1} and 1553 cm^{-1} corresponding to ν(C=O) and ν(*N*-acetyl) respectively, according to Hirano *et al.*[16]. The next stage was to investigate if the chitosan hydrogels could be successfully substituted with an acidic anhydride with a long aliphatic carbon atom chain thereby increasing the hydrophobicity of the chitosan polymer.

5.2.1.1 (ii) FT-IR Analysis of *N*-Hexanoyl Chitosan Hydrogel Beads

After successfully carrying out the *N*-acetylation of chitosan hydrogel beads using small acetyl groups the next study investigated the substitution of 85% deacetylated chitosan hydrogels in their hydrogel state with a 6 carbon long aliphatic chain by reacting the 85% deacetylated chitosan hydrogel beads with hexanoic anhydride. Successful substitution of 85% deacetylated chitosan hydrogel to form *N*-hexanoyl chitosan hydrogel beads (Scheme 5.2) would increase the hydrophobicity of the beads and potentially re-arrange the structure of the chitosan polymer[2, 17]. If the reaction was successful the FT-IR spectrum recorded of the chitosan was expected to exhibit the same band splitting displayed by *N*-acetylated chitosan xerogel shown in Figure 5.2. In addition, due to the increase in -CH$_2$ and –CH$_3$ groups attached to the chitosan unit an increase in the ν (C-H) band intensity may also be observed at around 2920 cm^{-1}. To compare the influence of the concentration of hexanoic anhydride solution used in the substitution reaction Figure 5.3 exhibits the FT-IR spectra of 85% deacetylated chitosan hydrogel beads reacted with a concentrations of 0.1 M, 0.4 M and 0.8 M hexanoic anhydride solution. The reaction mixture was refluxed for 24 h in methanol and the resulting chitosan hydrogel beads were washed several times with methanol, acetone and finally Millipore water before being dried in an oven at 37 ± 1°C, ground up and an FT-IR spectrum taken using KBr discs.
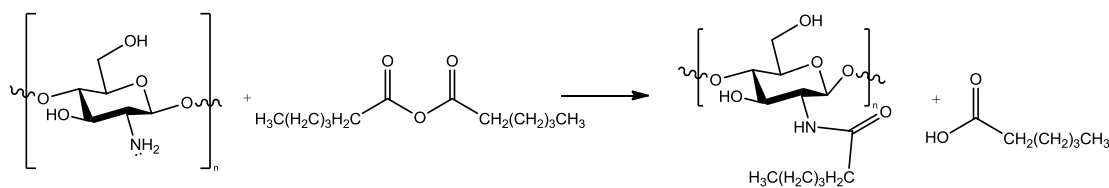
Scheme 5.2 *N*-acylation of Chitosan by Hexanoic Anhydride
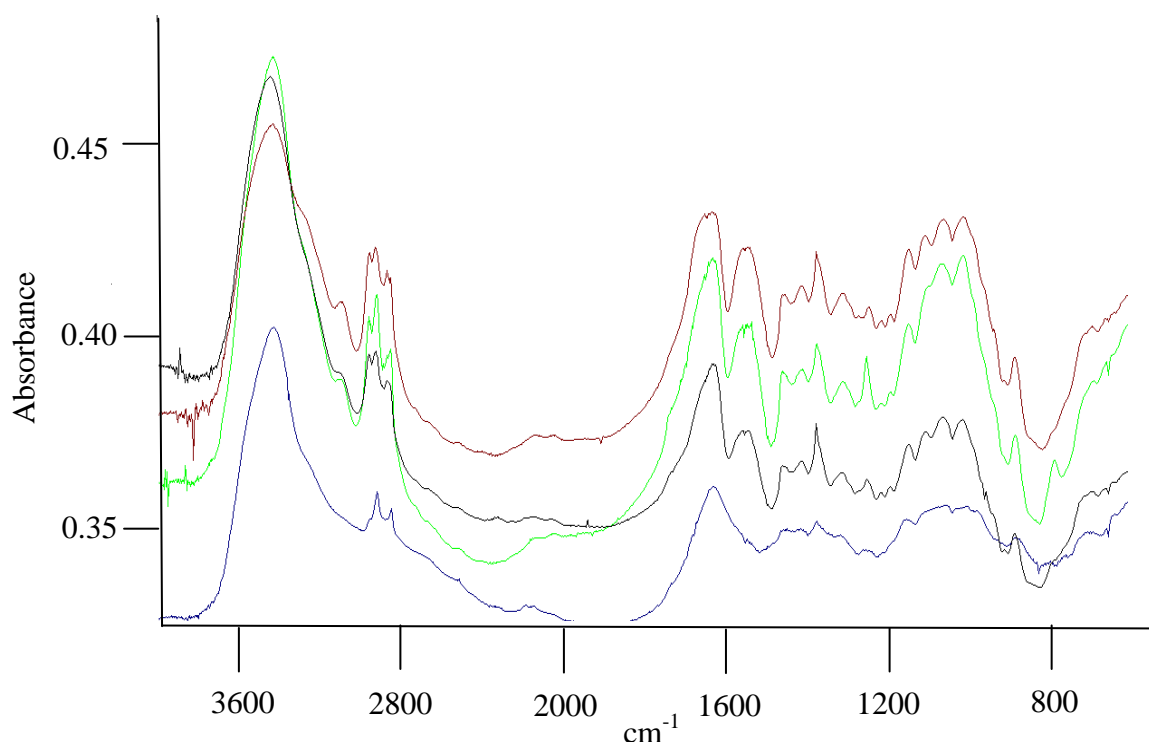
Figure 5.3 FT-IR spectra in absorbance mode of *N*-hexanoyl chitosan beads. The concentration of the hexanoic anhydride solution used to substitute the beads was (━━━) 0.8 M hexanoic anhydride (━━━) 0.4 M hexanoic anhydride (━━━) 0.1 M hexanoic anhydride (━━━) 0.0 M hexanoic anhydride. The beads were washed, dried and ground before FT-IR was performed using KBr discs.

It was apparent from the spectra exhibited in Figure 5.3 that the chitosan hydrogels reacted with hexanoic anhydride exhibited the characteristic vibrational bands for *N*-acylated chitosan fibre. The band at 1640 cm^{-1} has disappeared and two new bands are visible at 1655 cm^{-1} and 1555 cm^{-1} (ν(C=O) and ν(*N*-acyl), respectively). It is also

154

clear from the lack of vibrational bands in 1710-1760 cm^{-1} that no *O*-acyl substitution has been detected. Due to the FT-IR spectra exhibiting the expected vibrational bands for *N*-acylated chitosan it was concluded that the substitution of 85% deacetylated chitosan hydrogel beads with a 6 carbon long aliphatic chains to form *N*-hexanoyl chitosan was accomplished.

5.2.1.2 Differential Scanning Calorimetry

Differential scanning calorimetry (DSC) is a thermoanalytical technique that can be utilised to monitor characteristic physical and chemical changes in biopolymers. DSC curves have been used by authors as a method to determine the degree of *N*-acetylation in chitosan and chitin samples, based on peak area and height of the decomposition signals[18]. The exothermic degradation peak changes in temperature, area and intensity depending on the degree of *N*-acetylation. In general, the thermal properties of chitin and chitosan are similar to those of cellulose. They do not melt but degrade at elevated temperatures[13]. Each bead that was examined by DSC was washed thoroughly in acetone, methanol and Millipore water, dried in an oven at 37 ±1 °C for 24 h and then ground up. The first study carried out was on 85% deacetylated chitosan hydrogel beads that had not undergone aliphatic carbon atom chain substitution and the thermogram is shown in Section 5.2.1.2 (i).

5.2.1.2 (i) DSC Thermogram of 85% deacetylated Chitosan Xerogel Beads

Figure 5.4 exhibits a DSC thermogram obtained from an 85% deacetylated chitosan xerogel bead.
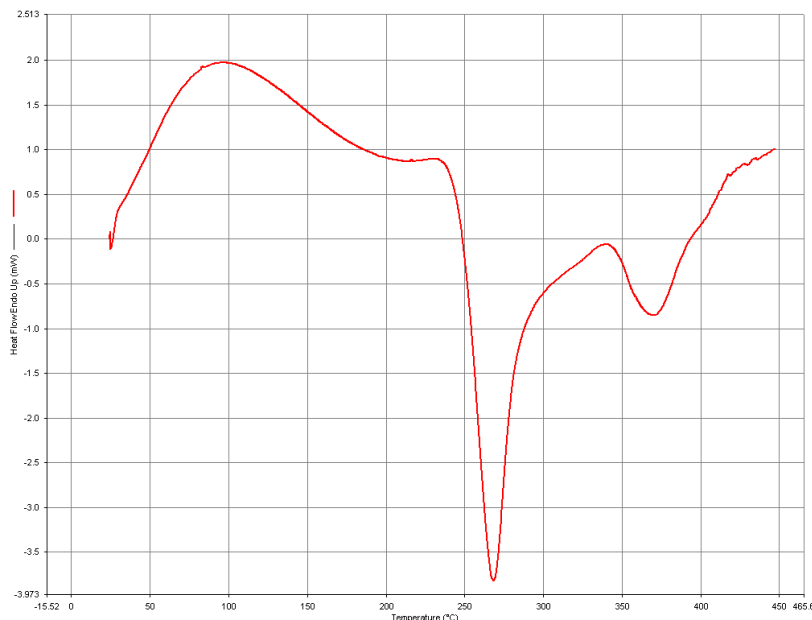
Figure 5.4 DSC Thermogram of an 85% deacetylated chitosan xerogel bead

It can be seen from Figure 5.4 that the thermal degradation of the chitosan polymer consisted of three stages. The first stage starts below 100 °C and can be attributed to the loss of water which could not be removed completely on drying. Polysaccharides have a strong affinity for water and their hydration properties depend on their primary and supramolecular structure. Water in polysaccharides forms attachments to specific functional groups, in the case of chitosan the hydroxyl and amine sites[19]. Depending on the different interactions of water with the polymer chain, water will be released from the polysaccharide at different temperatures. There are three different kinds of interactions between water and polymer that have been identified in polysaccharide hydrogels. The first one is unbound water that was released in the region 40-60 °C, the second is water linked through hydrogen bonds that is discharged up to 120 °C and finally water that is more tightly linked through polar interactions with amide/amine groups which can be observed up to 160 °C[20]. In the case of the chitosan investigated in Figure 5.4 the chitosan polymer exhibited an endothermic water peak

associated with the loss of water beginning at 30.0 °C and peaking at 96.1°C and finishing at 220.0 ℃. The majority of water discharged is therefore attributed to water that was tightly bound to the chitosan functional groups through hydrogen bonds that had not been removed during the drying procedure which was carried out on all the beads used in this study.

The second thermal event was attributed to the decomposition of the glucosamine units of the chitosan polymer with a correspondent exothermic peak at 268.5 °C. The third thermal event was an exothermic peak at 369.6 °C due to the decomposition of the *N*-acetyl-glucosamine units of the chitosan polymer. Thus, the glucosamine residues were shown to be less thermally stable than the *N*-acetyl-glucosamine residues. These two thermal events are characteristic for a chitosan sample[21]. The areas under the peaks at 268.5 ℃ and 369.6 ℃ had ratios of 821:155 respectively. This corresponds well with the manufacturers' data which states that this chitosan was 85% deacetylated. Thus it was deduced that the chitosan sample was approximately 84% deacetylated and helped confirm that measuring the relative size of the two decomposition peaks is a reasonable method to calculate the degree of acetylation[21].

5.2.1.2 (ii) DSC Thermogram of *N*-Acetylated Chitosan Hydrogel

A DSC thermogram of 85% deacetylated chitosan hydrogel beads reacted with acetic anhydride (0.1 M) according to the reaction conditions stipulated in Section 2.2.3.1 was exhibited in Figure 5.5. Chitin has been shown to have more thermal stability than chitosan due to it consisting of *N*-acetylated-glucosamine units[21]. Considering that chitin cannot form hydrogel beads due its lack of solubility, post-modification of chitosan hydrogels to add *N*-acetyl functional groups to its glucosamine unit could potentially be a means of conferring the thermal stability of chitin on chitosan xerogel beads.
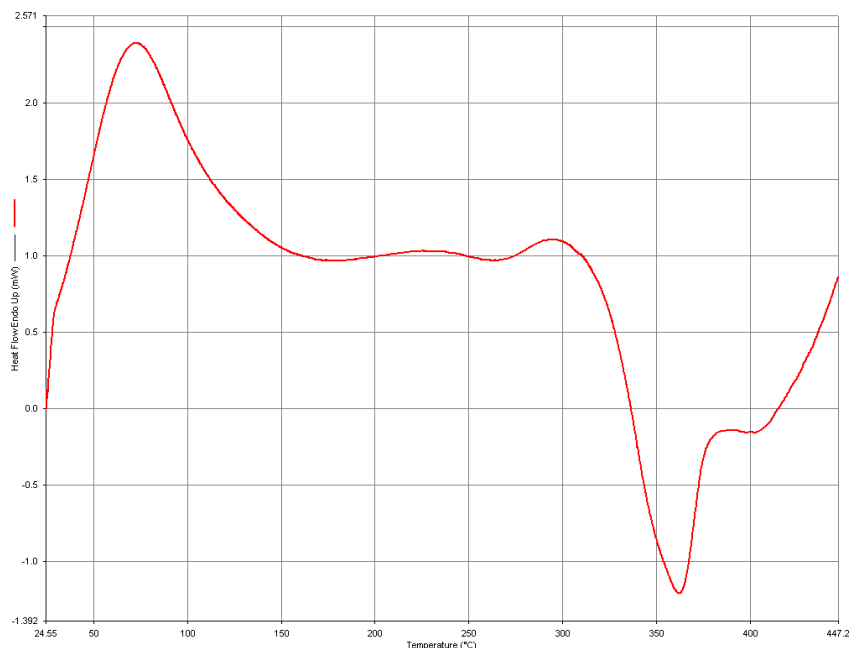
Figure 5.5 DSC Thermogram of an *N*-acetyl chitosan xerogel bead

The DSC thermogram obtained from the product of the substitution reaction between an 85% deacetylated chitosan hydrogel and a 0.1 M acetic anhydride solution is exhibited in Figure 5.5. The most noticeable feature was the substantial reduction in the area attributed to thermal degradation of the deacylated glucosamine units. The degradation peak corresponding to the deacylated glucosamine units of the chitosan polymer was barely observed whilst the degradation peak for the *N*-acetylated polymer unit was visible at 362.5 °C and had grown in area. In addition, a peak at 460.3 °C appeared as a shoulder to the 362.5 °C peak. Along with the FT-IR spectrum in Figure 5.3, the DSC thermogram in Figure 5.5 was more evidence that substitution had occurred and the thermostability of chitosan xerogels had increased as thermo degradation took place at a higher temperature. In addition the area under the peak assigned to the loss of water was reduced from 552.2 J g^{-1} in beads composed of 85% deacetylated chitosan to 462.1 J g^{-1} in the DSC thermogram (Figure 5.5). One possible reason for that is there was less water content in the *N*-acetylated chitosan beads than the 85% deacetylated chitosan hydrogel beads after drying. This was likely due to the added hydrophobicity caused by the addition of *N*-acetyl groups to the polymer.

158

5.2.1.2 (iii) DSC of *N*-Hexanoyl Chitosan Beads

Figure 5.6 exhibits the DSC thermogram of a chitosan hydrogel bead which was *N*-acylated in a substitution reaction with 0.1 M hexanoic anhydride solution. When the DSC thermogram of the hydrogel beads resulting from this reaction was compared to the thermogram of the 85% deacetylated chitosan hydrogel beads (Figure 5.4) it was apparent that the decomposition peak area attributed to the glucosamine units of chitosan had been reduced and the peak temperature had increased from 268.5°C to 297.2 °C. In addition, the peak area attributed to the thermal degradation of the *N*-acetyl-glucosamine units of chitosan known to occur at 369.6 °C (attributed in the 85% deacetylated chitosan xerogel thermogram exhibited in Figure 5.4) was obstructed by a degradation peak at 348.0 °C in the DSC of *N*-hexanoyl chitosan beads in Figure 5.6. This new degradation peak was attributed to the *N*-hexanoyl-glucosamine units of chitosan which was an indication that the substitution reaction had successfully *N*-acylated the chitosan hydrogels.
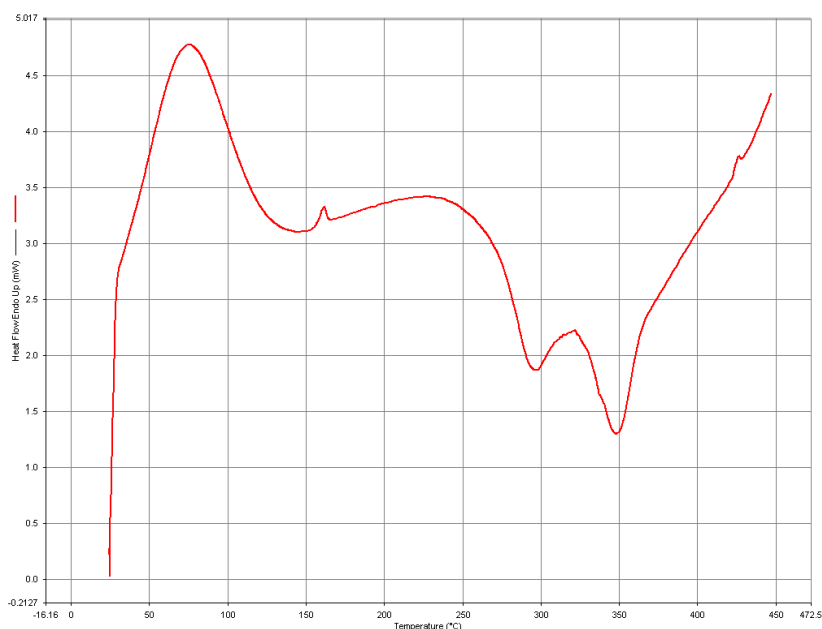
Figure 5.6 DSC Thermogram of an *N*-hexanoyl chitosan xerogel bead

In addition, when compared to the DSC thermogram of the 85% deacetylated chitosan hydrogel beads the area under the peak associated with the loss of water was reduced

159

from 552.2 J g^{-1} to 505.1 J g^{-1} and the upper temperature limit at which water loss was observed had also been reduced from 241.3 °C to 162.6 °C and the peak attributed to water linked to chitosan through polar interactions with amide/amine groups was now clearly distinguishable at 161.5 °C. DSC thermograms were obtained for 85% deacetylated chitosan hydrogel beads that were substituted in 0.1 M, 0.4 M or 0.8 M hexanoic anhydride solution in order to form *N*-hexanoyl chitosan hydrogel beads. Afterwards the treated chitosan hydrogel beads were washed several times with methanol, acetone and finally Millipore water. They were then placed in an oven at 37 ± 1 °C and dehydrated, ground and DSC thermograms were obtained and the resulting data are presented in Table 5.1.

Table 5.1 The thermo-degradation temperatures of *N*-acylated chitosan xerogel beads obtained by DSC analysis.

Concentration of Hexanoic Anhydride in the reaction solution	Peak Temperature of Water Loss Area (°C)	Area Under Water Endo Peak (J g^{-1})	Glucosamine Unit decomposition Peak Temp (°C)	*N*-acetyl- Glucosamine Unit decomposition Peak Temp (°C)	*N*-hexanoyl - Glucosamine Unit degradation Peak Temp (°C)
0.0 M	96.1	552.2	268.5	369.6	-
0.1 M	75.3	505.1	297.2	-	348.0
0.4 M	72.8	74.1	-	-	354.4
0.8 M	65.2	18.2	-	-	360.4
0.1 M (Acetic Anhydride)	72.6	462.1	265.0	362.5	-

The data in Table 5.1 showed that as the concentration of the carboxylic anhydride in the reaction solution increased the endothermic peak corresponding to water loss decreased in peak temperature and the area under the peak was also reduced. This

suggested that due to the *N*-acylation of the glucosamine unit of chitosan with an aliphatic carbon atom chain water molecules had a reduced number of amino functional group sites with which to form hydrogen bonds, thus lowering the amount of energy needed to remove water molecules.

When the 85% deacetylated chitosan hydrogel beads were reacted with hexanoic anhydride (0.4 M solution) and DSC was performed on the resulting beads the thermogram obtained indicated that the glucosamine unit degradation peak had disappeared all together and a new degradation peak appeared which was attributed to a *N*-hexanoyl-glucosamine unit which had formed as a result of the substitution reaction. The degradation of the *N*-hexanoyl-glucosamine units was the only exothermic thermal event on the thermogram. The peak temperature attributed to water loss and the area under the peak had again been reduced, this time to 72.8 °C and the peak attributed to the loss of water linked to chitosan thorough polar interactions with amide/amine groups was no longer present. The 85% deacetylated chitosan hydrogel beads were reacted with hexanoic anhydride (0.8 M solution) and a DSC was recorded on the resulting *N*-hexanoyl chitosan hydrogel beads. When the thermogram obtained was compared to the thermogram obtained from 85% deacetylated chitosan hydrogel beads the area under the water peak had been reduced from 552.2 J g^{-1} to 18.2 J g^{-1}, which represented a substantial reduction in the water content, and there was now only one exothermic peak instead of two. This peak which occurred at 360.4 °C which was attributed to the thermal degradation of the *N*-hexanoyl-glucosamine units which had formed as a result of the substitution reaction.

The DSC measurements showed that as the concentration of hexanoic anhydride was increased in the substitution reaction the peak associated with water decreased in sized and moved to a lower temperature. It was likely that this was due to the beads having a lower water content due to their *N*-acylation. The glucosamine unit degradation peaks were reduced in size and then completely disappeared due to the formation *N*-hexanoyl-glucosamine units. The *N*-acetyl-glucosamine degradation peak was also distorted by the formation of *N*-hexanoyl-glucosamine units as their thermo degradation occurred in close proximity to each other which made accurate peak areas difficult to evaluate which resulted in it not being possible to calculate the degree of *N*-acylation substitution using DSC.

However, it appeared that the reaction resulted in the *N*-acylation of the chitosan polymer throughout the hydrogel bead and not just at the surface due to the extensive change of the sample properties.

5.2.1.3 Surface Morphology

The effect of *N*-acylation on the morphology of chitosan xerogel beads was examined using SEM and shown in Figure 5.7. Each *N*-acylated bead that was examined using SEM had been washed thoroughly in acetone, methanol and finally Millipore water, loaded in 60 mM DCD Millipore water solution and dried in an oven at 37 ±1 °C for 24 h with the exception of Figure 5.7 (e) and (f) which were loaded in 60 mM DCD methanol solution.
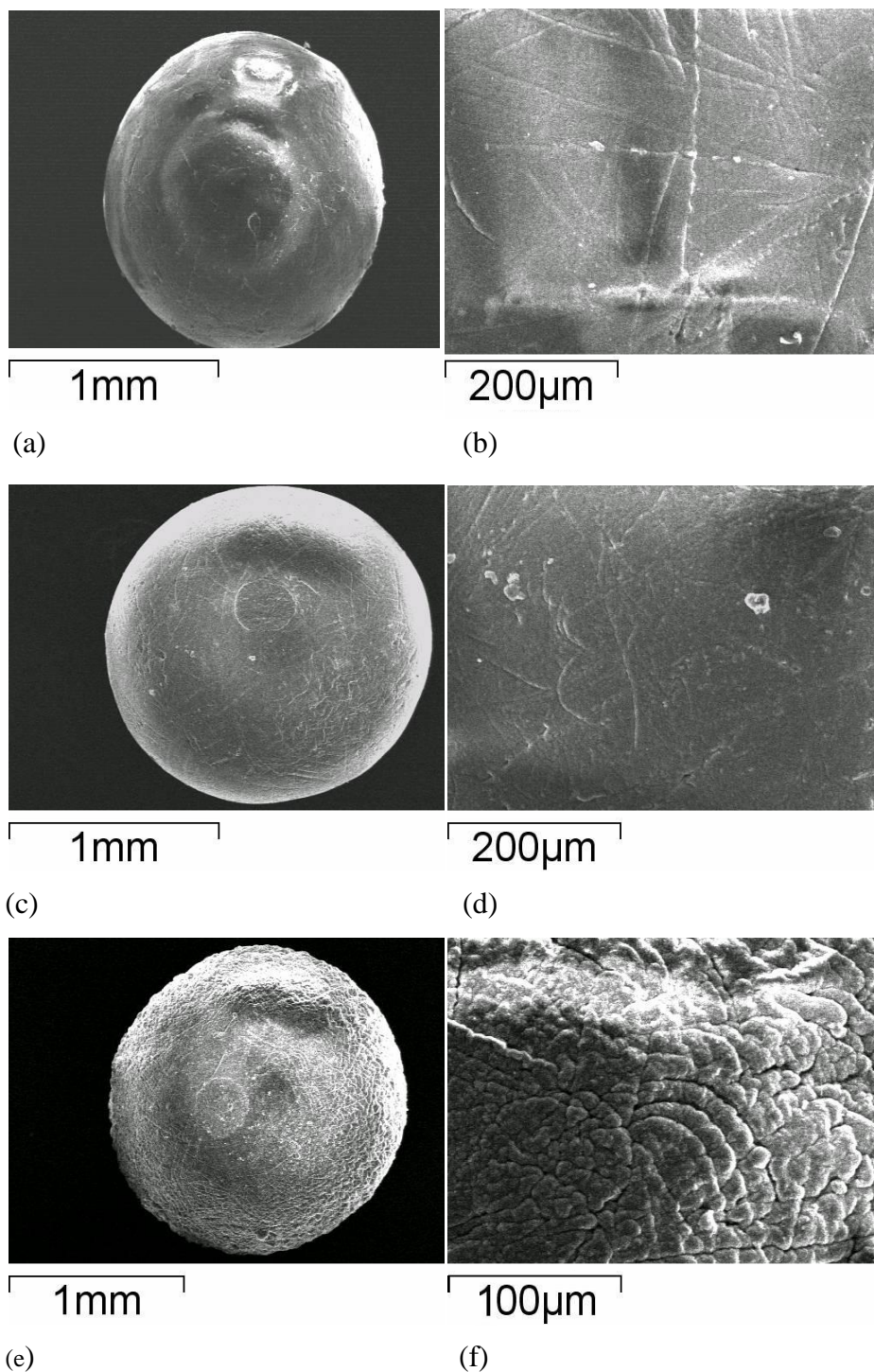
Figure 5.7 The SEM micrographs of [(a) and (b) *N*-hexanoyl Chitosan Xerogel bead; (c) and (d) *N*-acetyl Chitosan Xerogel bead; (e) and (f) *N*-hexanoyl Chitosan Xerogel bead that was loaded in methanol solution.

The surface morphology of *N*-hexanoyl chitosan hydrogel beads was shown in Figure. 5.7 (a) and (b). The *N*-hexanoyl chitosan xerogels possessed a spherical shape with a smooth surface morphology. This corresponds with research by Hirano and Moriyasu who treated chitosan with a series of anhydrides and also reported that the surface of the substituted chitosan appeared to be smooth[22]. The surface morphology of *N*-acetyl chitosan hydrogel beads was shown in Figure 5.7 (c) and (d). These beads were more flat than spherical in shape but also exhibited a relatively smooth surface. The *N*-hexanoyl chitosan hydrogel beads displayed in Figure 5.7 (e) and (f) were synthesised in the same reaction as the bead in Figure 5.7 (a) but loaded with DCD in methanol instead of Millipore water. It had a rough surface characterised by a mosaic like pattern. However, the indentations on its surface appeared to be shallow. Choi *et al*. noted that their *N*-acylated chitosan fibre prepared in methanol exhibited a rough and stretched pattern which they considered to be due to dehydration[2]. Water molecules are known to be involved in hydrogen bonding in the polymer structure which meant the final wash of the bead in methanol rather than Millipore water could have had an impact on the intramolecular hydrogen bonding between monomers which resulted in a change of the surface morphology. It was concluded that *N*-hexanoyl chitosan beads loaded in water had a smooth surface but changing the solvent inside the hydrogel had a significant impact on the surface morphology.

5.2.1.4 Swelling Properties of *N*-Hexanoyl Chitosan Xerogel Beads

The swelling properties of *N*-hexanoyl chitosan xerogel beads were investigated in the following sections. Swelling studies were performed at 20 ± 1 °C and in triplicate. Millipore water was used as the swelling solution unless otherwise stated.

5.2.1.4 (i) Influence of the Hexanoic Anhydride Concentration

The swelling properties of chitosan xerogel beads are considered important as they are closely related to the structural integrity and release characteristics of the bead[23]. A

swelling study was therefore conducted to examine the swelling capacity of *N*-hexanoyl chitosan xerogel beads to investigate whether the concentration of hexanoic anhydride in the reaction solution influences the swelling properties of the beads. The swelling ratio % obtained was displayed in Figure 5.8 and all swelling studies in this research were conducted in Millipore water at a temperature of 20 ± 1 °C in triplicate. The swelling ratio (%) was calculated using Equation 2.2.
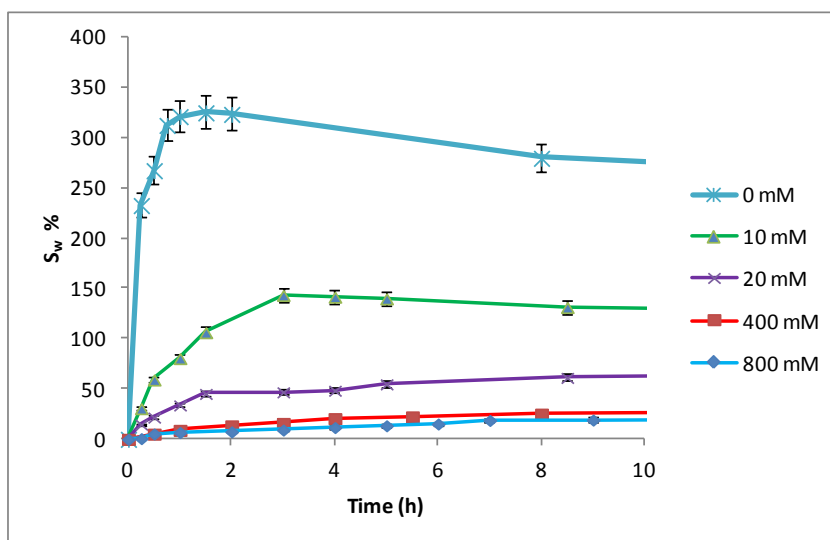
Figure 5.8 Comparison of the swelling ratio (%) of *N*-hexanoyl chitosan xerogels beads synthesised by refluxing 85% deacetylated chitosan hydrogel beads in a stated concentration of hexanoic anhydride. The newly formed *N*-hexanoyl hydrogel beads were washed in methanol, acetone and finally Millipore water and dried in an oven at 37 ± 1 °C.

The results displayed in Figure 5.8 demonstrated that as the concentration of hexanoic anhydride in the reaction solution increased the swelling ratio of chitosan xerogel beads decreased which was concluded as being due to their increasing hydrophobicity. After 5 h xerogel beads that were reacted with a 10 mM hexanoic anhydride solution exhibited a swelling ratio percentage of 140% whilst xerogel beads reacted in a 800 mM hexanoic anhydride solution exhibited a swelling ratio of just 13.4 %. Thus, it was concluded that an increase in the concentration of hexanoic anhydride in the reaction solution increased the degree of *N*-hexanoyl substitution which hindered the Millipore water from penetrating the pores of the xerogel bead. From examination of the results in Section 4.2.2 it appeared that the *N*-hexanoyl

chitosan xerogel beads could exhibit smaller swelling ratio percentage values than those prepared by glyoxal crosslinking. For example, after 5 h the swelling ratio percentage obtained for chitosan xerogel beads crosslinked in 520 mM glyoxal solution was 39 % (Section 4.2.2.1), while the swelling ratio percentage calculated for *N*-hexanoyl chitosan xerogel beads substituted in 400 mM hexanoic anhydride solution was 22%. In addition, there was no rapid increase in the swelling ratio of the *N*-hexanoyl xerogel beads whose swelling ratio rose gradually to 9% in the first hour and continued to increase to a steady rate unlike the chitosan xerogel beads crosslinked in glyoxal solution whose swelling ratio percentage rose rapidly in the first hour to 35%. This indicated that water found it more difficult to permeate through the outer pores of the hydrophobic *N*-hexanoyl xerogel beads than the beads crosslinked in glyoxal solution. This could be due to the structure of *N*-acylated chitosan which organises itself in parallel sheet structures[2]. This could result in a more a effective barrier against water compared to the random arrangement of glyoxal crosslinked chitosan and is probably more hydrophobic.

 It was difficult to compare these results directly with literature values for related systems, however if we compare the swelling ratio obtained in this study with authors who have modified chitosan hydrogel beads in other ways we can get an appreciation of the size of the reduction of the swelling ratio achieved in this study. Kim *et al*. synthesised chitosan hydrogel beads crosslinked with poly(vinyl alcohol) to investigate their potential use as a drug release system, at a medium temperature of 25°C in pH 7 buffer their hydrogels achieved swelling ratios of between approximately 200% and 280% after one hour[24]. Gupta and Jabrail compared the swelling ratios of chitosan xerogels crosslinked with 12% glyoxal and 12% glutaraldehyde. The swelling ratio percentage the authors recorded at equilibrium was 150% and 145%, respectively, in a buffered solution of pH 7, the authors concluded that this was 'a low degree of swelling'[25]. Yuan *et al*. developed chitosan xerogel beads with the aim of using them as a controlled release system for protein. They reported that chitosan xerogel beads that had been crosslinked in 2 mM genipin solution for 4 h had a swelling ratio of just over 115% at swelling equilibrium[26]. Comparing the swelling ratio achieved in this research with the aforementioned

studies it appeared that the reduction in swelling ratio percentage achieved in this study was substantial.

5.2.1.4 (ii) Influence of Swelling Medium pH

A study was performed to examine the influence of an acidic and basic release medium on the swelling ratio percentage of *N*-hexanoyl chitosan xerogel beads that had been formed by the reaction of 85% deacetylated chitosan hydrogel beads with hexanoic anhydride (0.4 M solution). The resulting swelling ratios (%) are exhibited in Figure 5.9. In an acidic medium below the pK_a value of chitosan ($pK_a = 6.3$) the amine functional groups of chitosan are protonated thus inducing electrostatic repulsions between the polymer segments. The ionization of the amine functions may therefore lead to the dissociation of hydrogen bonds between chitosans glucosamine units and the relaxation of the polymer chains causing the swelling of the beads to increase. In basic mediums however the swelling should be less than an acidic medium due to the absence of amine groups ionization[27]. However, in this research we have *N*-acylated the chitosan xerogels at the amine site where the chitosan would usually be protonated in an acidic medium. Therefore, a reduction in the swelling ratio (%) obtained could be expected in the acidic medium due to the decrease in electrostatic repulsions between the polymer segments.
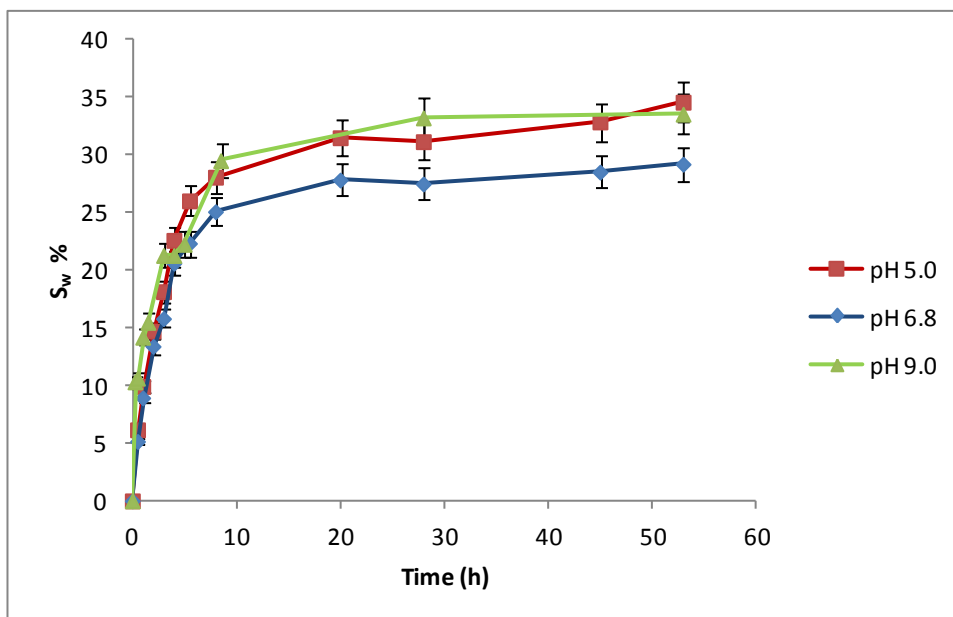
Figure 5.9 The swelling ratio (%) values of *N*-hexanoyl chitosan xerogels in different pH mediums. The beads were washed in methanol, acetone and finally Millipore water and dried in an oven at 37 ± 1 °C.

The results of the study can be seen in Figure 5.9. It was apparent that the *N*-hexanoyl chitosan beads were not pH swelling sensitive between pH 5.0 and pH 9.0 as the swelling ratio (%) did not change to any considerable degree. This was likely due to the *N*-acylation of the chitosan polymer removing the amine site and preventing the acid from protonating the polymer which would eliminate the electrostatic repulsions between the polymer segments in an acidic medium. This was a positive outcome as it was desirable that *N*-acylated xerogel beads exhibited good structural integrity in acidic as well as basic media. This was in contrast to chitosan beads crosslinked in 300 mM glyoxal solution that were examined in Section 4.2.2.2. These beads were shown to be pH swelling sensitive as they exhibited higher swelling ratio in a solution that was set to pH 5.0 when compared to those obtained in solutions that had pH values above the pK_a of chitosan ($pK_a = 6.3$). This result is encouraging and we would aim to carry out a more extensive pH study to investigate the swelling of the beads at more acidic pH values for the application of drug release into the stomach.

5.2.2 DCD Release Properties of *N*-Hexanoyl Chitosan Xerogel Beads

5.2.2.1 Influence of Hexanoic Anhydride Concentration

The swelling studies conducted in Section 5.2.1.4 (i) showed that by increasing the concentration of hexanoic anhydride used in the substitution reaction the swelling ratio (%) of the resulting *N*-hexanoyl chitosan beads decreased. It was therefore logical to assume that increasing the concentration of hexanoic anhydride in the substitution reaction would also influence the release of DCD from the resulting *N*-hexanoyl chitosan xerogel beads as the hydrophobicity of the chitosan appears to increase depending on the concentration of hexanoic anhydride used in the substitution reaction. The release profiles of DCD from *N*-hexanoyl chitosan xerogel beads formed by substitution of 85% deacetylated chitosan in 0.80 M, 0.10 M and 0.01 M hexanoic anhydride solutions are shown in Figure 5.10.
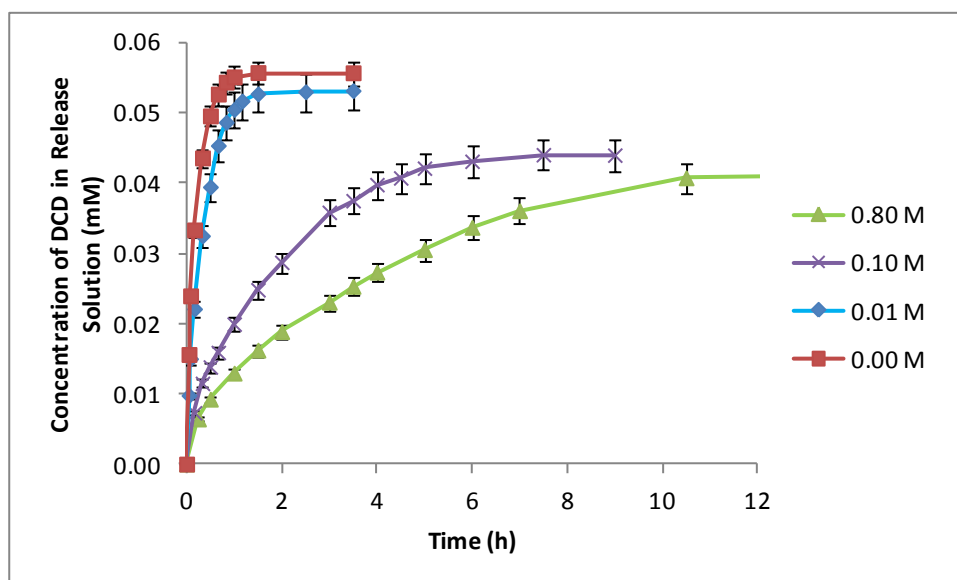
Figure 5.10 Release profiles of DCD from chitosan xerogel beads substituted in 0.80 M, 0.10 M, 0.01 M and 0.00 M hexanoic anhydride solution with methanol as the reaction solvent. The hydrogels were subsequently washed in acetone, methanol and Millipore water. All the beads were loaded in 60 mM DCD Millipore water solution and dried in an oven at 37 ± 1°C for 24 hours.

The release profiles of DCD from *N*-hexanoyl chitosan xerogel beads displayed in Figure 5.10 revealed that as the concentration of hexanoic anhydride increased, the time to reach release equilibrium also increased. Conversely however, the concentration of DCD released at release equilibrium decreased from 0.05 mM when the beads were reacted with hexanoic anhydride (0.01 M solution) to 0.04 mM when the beads were substituted in hexanoic anhydride (0.80 M solution). In addition to increasing the equilibrium release time of the beads, the addition of the aliphatic carbon chains also increased the polymer network density inside the bead. This may have reduced the amount of DCD that could be loaded into the beads, thus accounting for the reduction in the concentration of the release solution at equilibrium. It was concluded that *N*-hexanoyl chitosan xerogel beads are capable of exhibiting controlled DCD release. In addition, the time required to reach DCD release equilibrium and the amount of DCD released is influenced by the concentration of hexanoic anhydride in the reaction vessel.

5.2.2.2 Influence of the DCD Loading Solution Concentration

A study of the influence of different loading concentrations on the DCD release profile from *N*-hexanoyl chitosan xerogel beads is presented in Figure 5.11. When *N*-hexanoyl chitosan xerogel beads were loaded in a 120 mM DCD solution the concentration of the release solution at release equilibrium was 0.08 mM with an equilibrium release time of 6 hours. When *N*-hexanoyl chitosan xerogel beads were loaded in a 30 mM DCD solution the concentration of the release solution at release equilibrium was 0.02 mM but the equilibrium release time remained at 6 hours. Therefore it was concluded that the DCD loading concentration did not have an effect on the time to reach DCD release equilibrium but did influence the amount of DCD released from the beads.
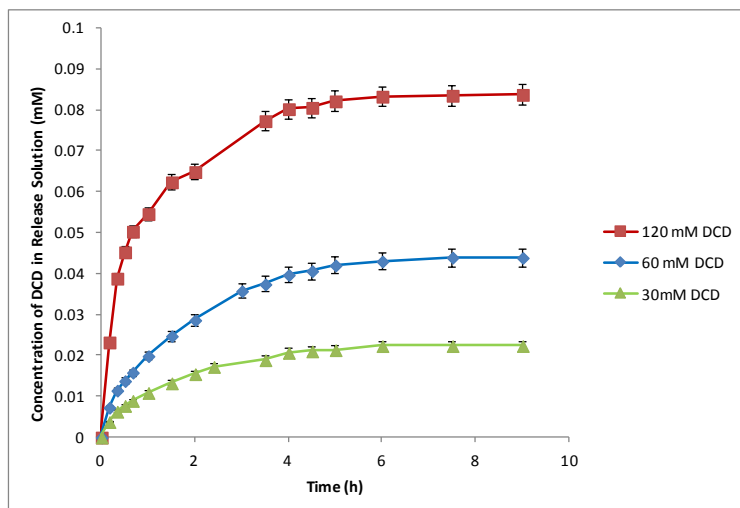
Figure 5.11 Release data of DCD from *N*-hexanoyl chitosan xerogel beads that were loaded in 30 mM , 60 mM or 120 mM DCD solutions. The beads were formed by reacting 85% deacylated chitosan hydrogel beads with hexanoic anhydride (0.1 M solution). The hydrogels were subsequently washed in acetone, methanol and Millipore water and dried in an oven at 37 ± 1°C for 24 hours.

5.2.2.3 Investigation of the Release Kinetics and Mechanism

The release kinetics of *N*-hexanoyl chitosan xerogel beads substituted in different concentration solutions of hexanoic anhydride solution were investigated to determine how the *N*-acylation of the chitosan polymer would affect the release mechanism of the beads. The release data of DCD from *N*-hexanoyl chitosan xerogel beads substituted in different concentration solutions of hexanoic anhydride solution was fitted to the zero-order and first-order models in Figure 5.12 and the data is shown in Table 5.2.
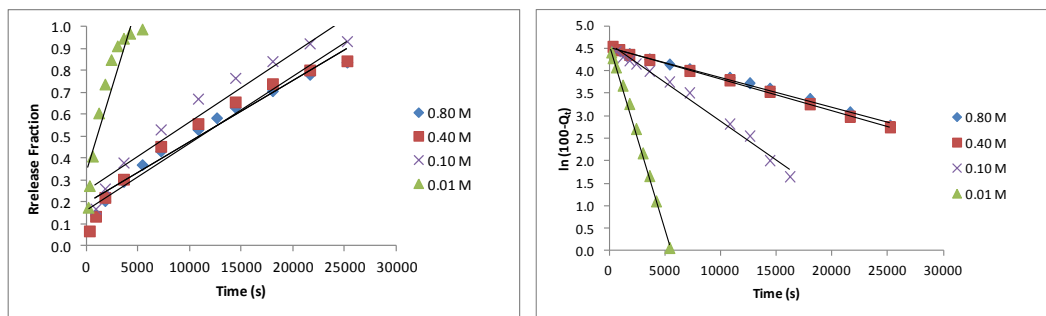
(a)   (b)

Figure 5.12 Release data of DCD from *N*-hexanoyl chitosan xerogel beads fitted to (a) zero-order and (b) first-order models. The *N*-hexanoyl chitosan xerogel beads were formed by the substitution of 85% deacylated chitosan hydrogel beads with a stated concentration of hexanoic anhydride.

Table 5.2 Results from the fitting of DCD release data from *N*-hexanoyl chitosan xerogel beads to the (a) zero-order and (b) first-order models. The *N*-hexanoyl chitosan xerogel beads were formed by the substitution of 85% deacylated chitosan hydrogel beads with a stated concentration of hexanoic anhydride.

Concentration of Hexanoic Anhydride in the Reaction Vessel	Zero-Order Model		First-Order Model	
	k_0 (s^{-1})	R^2	k_1 (s^{-1})	R^2
0.80 M	2.24×10^{-5}	0.9162	6.61×10^{-5}	0.9953
0.40 M	3.06×10^{-5}	0.9505	7.025×10^{-5}	0.9985
0.10 M	5.70×10^{-5}	0.9654	1.54×10^{-4}	0.9951
0.01 M	2.31×10^{-4}	0.9254	7.93×10^{-4}	0.9965
0.00 M	4.52×10^{-4}	0.9144	1.23×10^{-3}	0.9925

According to the data presented in Table 5.2 the first-order model exhibited the best regression line fit.   Release from beads reacted in hexanoic anhydride (0.01 M solution) had a first-order rate constant of 7.93×10^{-4} s^{-1} whereas release from beads reacted in hexanoic anhydride (0.80 M solution) had a much reduced rate constant of 6.61×10^{-5} s^{-1} which represented a decrease of a factor of 12. It was clear that as the concentration of hexanoic anhydride in reaction vessel increased the first-order rate constant decreased which indicated that increasing the concentration of the acidic anhydride used in the substitution reaction resulted in a more controlled DCD release from the xerogel. Despite the changes in the rate constant values there was no change in the fact that the best regression line fit corresponded to first-order kinetics for release from all the *N*-hexanoyl chitosan xerogel beads investigated. The mechanism of release was further investigated by fitting the release data to the Higuchi (Equation 2.10) and Korsemeyer-Peppas models (Equation 2.12) and the models and results are presented in Figure 5.13 and Table 5.3, respectively.

(a)   (b)
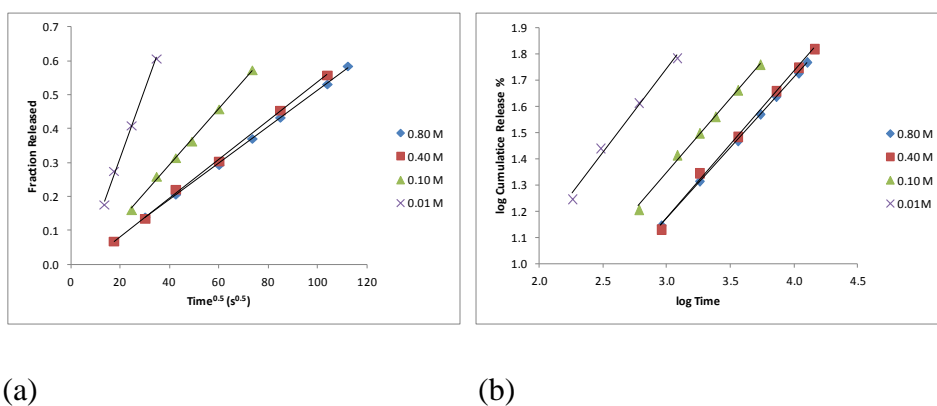
Figure 5.13 Release data from *N*-hexanoyl chitosan xerogel beads fitted to (a) Higuchi and (b) Korsemeyer-Peppas models. The *N*-hexanoyl chitosan xerogel beads were formed by the substitution of 85% deacylated chitosan hydrogel beads with a stated concentration of hexanoic anhydride.

Table 5.3 Results of fitted data for DCD release from *N*-hexanoyl chitosan xerogel beads to the Higuchi and Korsemeyer-Peppas models. The *N*-hexanoyl chitosan xerogel beads were formed by the substitution of 85% deacylated chitosan hydrogel beads with a stated concentration of hexanoic anhydride.   The release study was performed at 20 ± 1 °C in Millipore water in triplicate.

Concentration of Hexanoic Anhydride in the Reaction Vessel	Higuchi Model		Korsemeyer-Peppas Model	
	$k_H(\text{s}^{-0.5})$	R^2	n	R^2
0.80 M	5.37×10^{-3}	0.9995	0.54	0.9998
0.40 M	5.67×10^{-3}	0.9991	0.58	0.9966
0.10 M	8.29×10^{-3}	0.9986	0.56	0.9961
0.01 M	1.99×10^{-2}	0.9978	0.59	0.9916
0.00 M	2.39×10^{-2}	0.9678	0.54	0.9508

The DCD release data from the *N*-hexanoyl chitosan xerogel beads was fitted to the Higuchi and Korsemeyer-Peppas models and analysed. The Higuchi model exhibited good regression line fit for release from all the beads investigated, which was strong indicator that Fickian diffusion was a part of the release mechanism. The Higuchi model showed that as the concentration of hexanoic anhydride in the reaction vessel increased the Higuchi model kinetic constant, K_H, decreased. This showed that there was a decrease in the rate of diffusion release from the xerogel beads due to an increase in the degree of *N*-hexanoyl substitution of the beads. That Fickian diffusion was the primary mechanism of DCD release from the beads was confirmed upon fitting the data to the Korsemeyer-Peppas model. The values of exponent n obtained for DCD release from each set of *N*-hexanoyl xerogel beads investigated suggested that a combination of Fickian diffusion and polymer chain relaxation was the mechanism of release. However, Fickian diffusion was determined to be the dominant mechanism as the exponent n values were closer to the pure Fickian diffusion value

(0.43) than pure Case-II transport caused by polymer chain relaxation (0.86). The Fickian diffusion and polymer chain relaxation contribution to DCD release was examined in Figure 5.14 by fitting the data to the Sahlin-Peppas equation (Equation 2.13). The results are presented in Table 5.4.

(a)   (b)
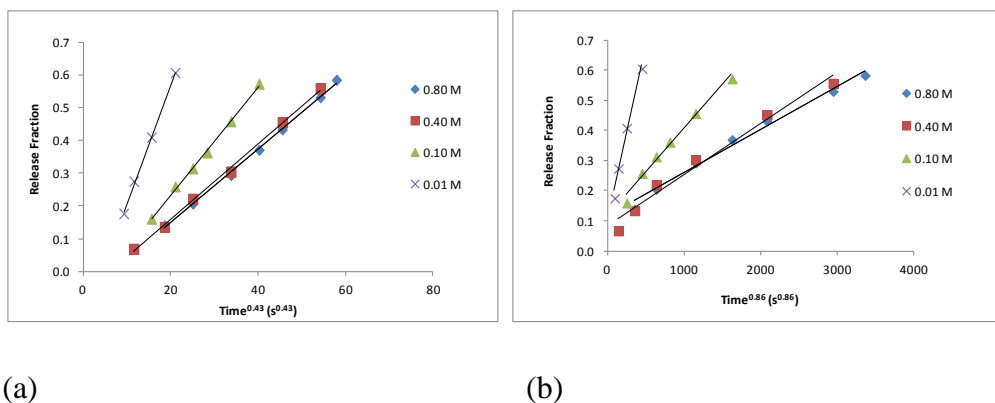
Figure 5.14 DCD release data from *N*-hexanoyl chitosan xerogel beads fitted to the Sahlin-Peppas (a) Fickian diffusion and (b) relaxation contribution model. The *N*-hexanoyl chitosan xerogel beads were formed by substitution of an 85% deacylated chitosan hydrogel with a stated concentration of hexanoic anhydride. The release study was performed at 20 ± 1 °C in Millipore water in triplicate.

Table 5.4 Results from the fitting of DCD release data from *N*-hexanoyl chitosan xerogel beads to the Sahlin-Peppas (a) Fickian diffusion and (b) relaxation contribution models. The *N*-hexanoyl chitosan xerogel beads were formed by substitution of an 85% deacylated chitosan hydrogel with a stated concentration of hexanoic anhydride. The release study was performed at 20 ± 1 °C in Millipore water.

Concentration of Hexanoic Anhydride Solution in Reaction Vessel	Fickian Diffusion Contribution		Relaxation Contribution		Relaxation/ Fickian Ratio
	k_1 (s$^{-0.43}$)	R^2	k_2 (s$^{-0.86}$)	R^2	R/F
0.80 M	1.39×10^{-2}	0.9977	1.44×10^{-4}	0.9881	0.01
0.40 M	1.16×10^{-2}	0.9982	1.69×10^{-4}	0.9986	0.02
0.10 M	1.65×10^{-2}	0.9981	2.89×10^{-4}	0.9856	0.02
0.01 M	3.61×10^{-2}	0.9982	1.16×10^{-3}	0.9842	0.03
0.00 M	3.93×10^{-2}	0.9618	2.12×10^{-3}	0.9689	0.05

The results from fitting the release data to the Peppas-Sahlin model were exhibited in Table 5.4. The regression line fits for Fickian and relaxation contributions were good for DCD release from all the *N*-hexanoyl chitosan beads investigated in this study. It was clear that *N*-acylation of the chitosan hydrogel beads did not affect the release mechanism. The relaxation/Fickian ratios calculated by fitting the release data to the Sahlin-Peppas model shows that Fickian diffusion was the dominant release mechanism for the all beads studied.

5.2.3 Synthesis and Characterisation of the Physical Properties of *N*-Palmitoyl and *N*-Octanoyl Chitosan Hydrogel Beads

A decrease in the first-order rate constant of DCD release from chitosan xerogel beads was accomplished in Section 5.2.2.3 due to the successful *N*-acylation of the 85% deacetylated chitosan hydrogels to form *N*-hexanoyl chitosan beads, however it is possible that if the length of the aliphatic carbon atom chain attached to the amino group was increased this could lead to a further reduction in the rate constant of DCD release from the beads. Hexanoic anhydride is a 6 carbon atom chain acidic anhydride which was relatively cost effective. However acidic anhydrides that have a longer aliphatic carbon atom chain were not, so an alternative starting material was found. The acyl chlorides, palmitoyl and octanoyl, were found to be a cost effective alternative, moreover palmitoyl chloride has a 16 carbon atom long aliphatic chain that had been previously shown to react with chitosan fibre to increase its hydrophobic character and make changes in its structural features[4]. A series of studies were therefore carried out to investigate if the post-functionalization of chitosan hydrogel beads could be accomplished with an acyl chloride (Scheme 5.3) and what influence substitution of chitosan with a 16 and an 8 carbon atom aliphatic chain would have on the physical and release properties of the hydrogel beads.

To *N*-acylate the chitosan hydrogel beads with an acyl chloride 85% deacylated chitosan hydrogel beads a substitution reaction was performed as described in Section 2.2.3.2. In summary, 85% deacylated chitosan hydrogel beads were suspended in 100 ml of acetone in round bottom flask which also contained 5 ml of triethylamine to remove any acid formed and then a pre-determined volume of an acyl chloride was added. The reaction mixture was refluxed for 24 h. Afterwards, the treated chitosan hydrogel beads were washed several times with methanol, acetone and finally Millipore water. Characterisation of the resulting hydrogel beads was carried out and the results are presented here.

$R_1 = CH_2(CH_2)_{13}CH_3$

$R_2 = CH_2(CH_2)_5CH_3$
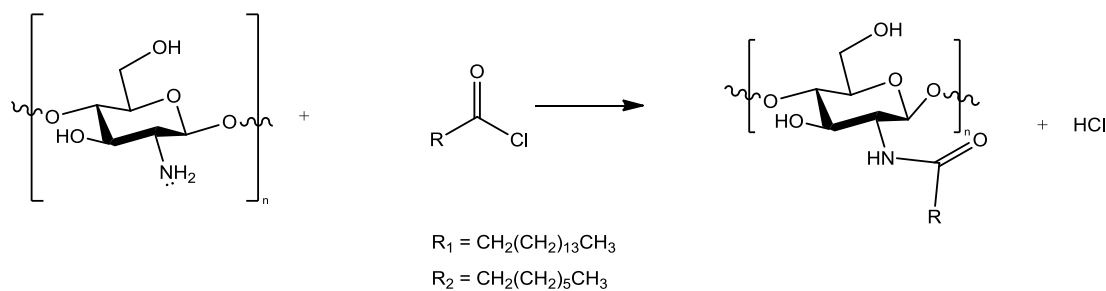
Scheme 5.3 *N*-Acylation of Chitosan with palmitoyl chloride (R$_1$) and octanoyl chloride (R$_2$)

5.2.3.1 FT-IR Analysis

5.2.3.1 (i) FT-IR Spectra of *N*-Palmitoyl Chitosan Beads

85% deacylated chitosan hydrogels beads were substituted in 0.8 M and 0.1 M palmitoyl chloride solutions and the resulting FT-IR spectra are exhibited in Figure 5.15. If the *N*-acylation reaction was successful the same characteristic FT-IR vibrational bands as shown in Figure 5.2 would be expected except that the vibrational bands at 2920 cm^{-1} and 2940 cm^{-1} ν(CH$_2$ and CH$_3$) would exhibit greater intensity as the length of the aliphatic carbon atom chain to be substituted onto the chitosan glucosamine unit had increased from 6 to 16 carbon atoms.
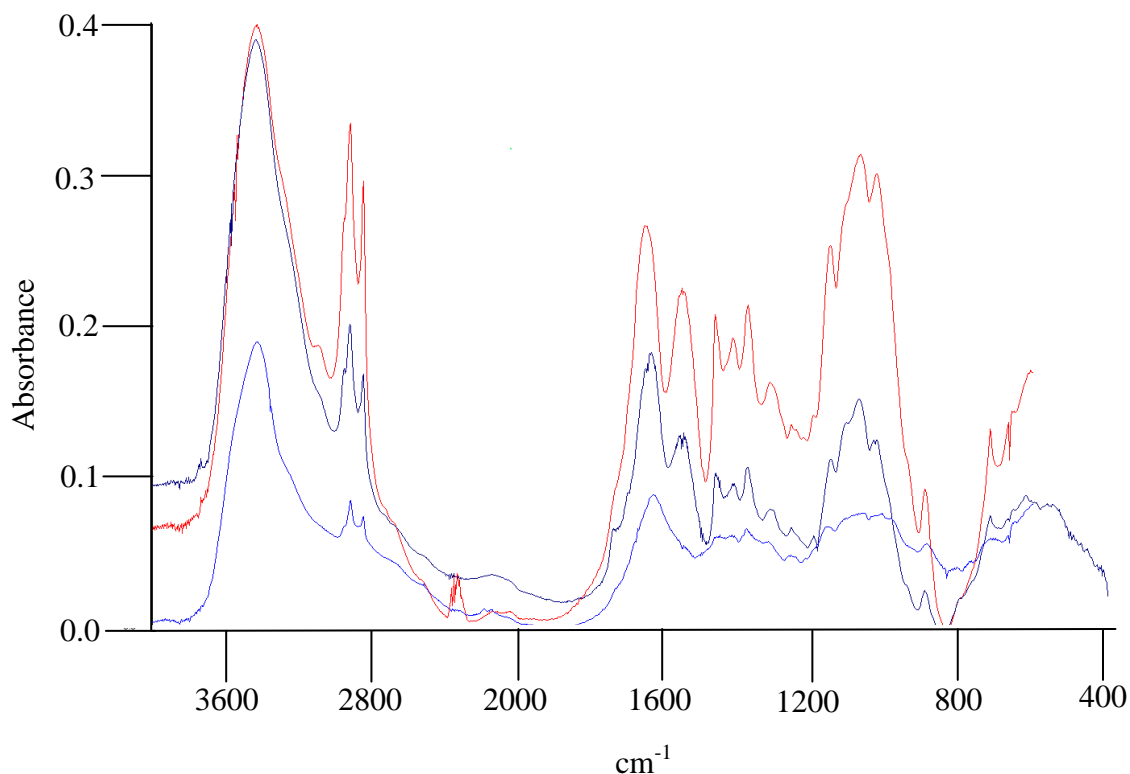
Figure 5.15 FT-IR spectra in absorbance mode of chitosan hydrogel beads reacted in 0.8 M and 0.1 M solutions of palmitoyl chloride with acetone as the reaction solvent. (▬▬) 0.8 M and (▬▬) 0.1 M. A spectrum of a 85% deacetylated chitosan xerogel bead was exhibited for comparison (▬▬). FT-IR analysis was performed on the beads after they were washed, dried and ground. FT-IR analysis was carried out using KBr discs.

The FT-IR spectra of chitosan hydrogel beads reacted with 0.8 M and 0.1 M palmitoyl chloride solutions showed the same characteristic vibrational bands as *N*-hexanoyl chitosan beads (Section 5.2.1.1). The intensity of the vibrational bands at 2920 cm^{-1} and 2940 cm^{-1} $\nu(CH_3$ and $CH_2)$ increased with palmitoyl chloride concentration, which would occur in the event of an increase in the degree of substitution. In addition, the broad band at 1640 cm^{-1} was no longer visible, instead there were two bands at 1655 cm^{-1} and 1555 cm^{-1} $\nu(C=O$ and *N*-acyl). It was also clear from the lack of vibrational bands from 1710-1760 cm^{-1} that no *O*-acyl substitution was detected and by including triethylamine in the reaction flask any acid that may have formed was removed. These FT-IR spectra indicated that *N*-acylation of chitosan with palmitoyl chloride had been achieved and suggested that increasing the concentration

of the acyl chloride in the reaction increased the degree of substitution of the chitosan polymer.

5.2.3.1 (ii) FT-IR Spectra of *N*-Octanoyl Chitosan Beads

The FT-IR spectrum of an 85% deacetylated chitosan hydrogel bead reacted with 0.8 M octanoyl chloride solution to form an *N*-octanoyl chitosan bead is displayed in Figure 5.16. The FT-IR spectra of a chitosan hydrogel bead reacted with palmitoyl chloride (0.8 M solution) and 85% deacetylated chitosan are also shown for comparison.
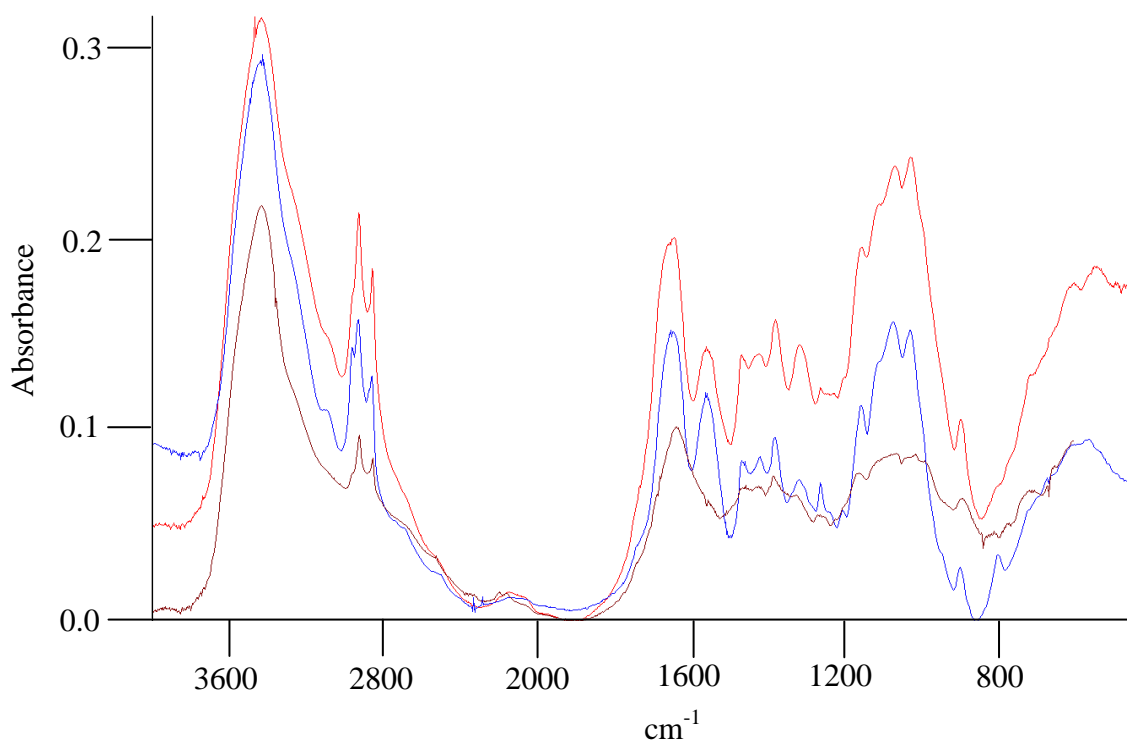
Figure 5.16 FT-IR spectra in absorbance mode of chitosan hydrogel beads reacted in 0.8 M solutions of (▬▬) palmitoyl chloride and (▬▬) octanoyl chloride with acetone as the solvent. An 85% deacetylated chitosan bead is exhibited for comparison (▬▬). The beads had been washed in acetone, methanol and Millipore water and dried in an oven at 37 ± 1 °C for 24 hours.

In Figure 5.16 three FT-IR spectrums are exhibited. Figure 5.16 (red) was chitosan modified with palmitoyl chloride and Figure 5.16 (blue) was chitosan modified with

octanoyl chloride. The spectra of chitosan hydrogel beads reacted with 0.8 M octanoyl chloride solution exhibited two peaks at 1655 cm^{-1} and 1555 cm^{-1} ν(C=O and *N*-acyl) which suggested that the chitosan hydrogels had been *N*-acylated It was concluded from the FT-IR spectroscopy study that the chitosan hydrogel beads had been successfully *N*-acylated using both palmitoyl chloride and octanoyl chloride.

5.2.3.1 (iii) Influence of the Reaction Solvent

The *N*-acylation reaction of chitosan fibre with an acyl chloride has been carried out previously by authors using either acetone (Hirano *et al.*[16]) or DMSO (Jiang *et al.*[11]) as the reaction solvent[11, 16] and it was unclear which provided the greatest degree of substitution. Furthermore Duarte *et al.* found that the solvent they used had a significant influence on the chitosan matrices they obtained when synthesising chitosan scaffolds and highlighted the lack of discussion on the role of reaction solvent in the literature[28]. Therefore a study was performed in this research to investigate the influence the reaction solvent had over the reaction between the chitosan hydrogel beads and the palmitoyl chloride. A FT-IR spectrum of 85% deacetylated chitosan hydrogel beads reacted with palmitoyl chloride (0.8 M solution) using different reaction solvents are exhibited in Figure 5.17. The reaction solvents acetone, DMSO, THF and DCM were investigated.
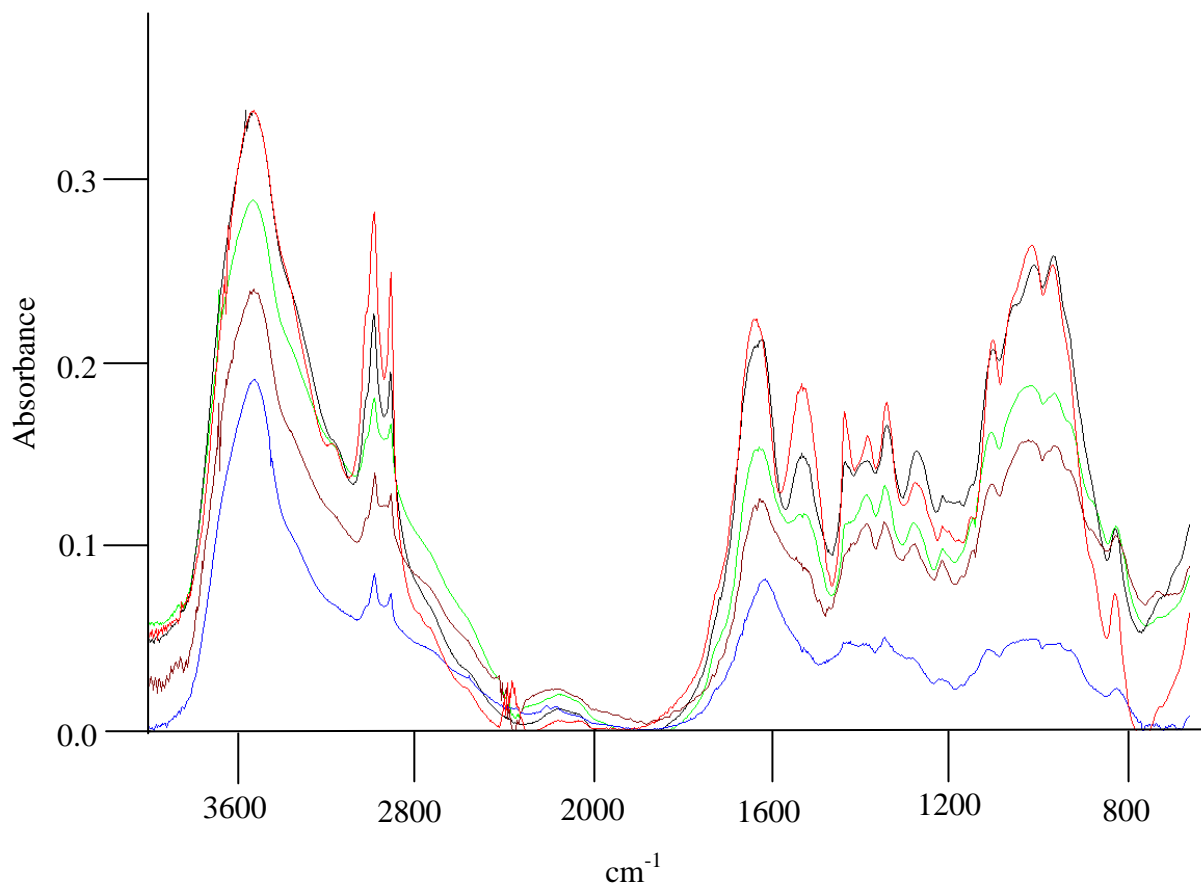
Figure 5.17 FT-IR spectra of *N*-palmitoyl chitosan hydrogel beads. To form the beads 85% deacetylated chitosan hydrogel beads were reacted with palmitoyl chloride (0.8 M solution) using different reaction solvents (　━━　) Acetone (　━━) DMSO (　━━) THF (　━━) DCM. All the resulting beads were washed in acetone, methanol and Millipore water. The beads were then dried in an oven at 37 ± 1 °C for 24 hours. A FT-IR spectrum of an 85% deacetylated chitosan hydrogel bead was included for comparison (　━━　).

The FT-IR spectra obtained for the *N*-acylation of chitosan hydrogels with palmitoyl chloride indicated that the reaction solvent influenced the degree of aliphatic chain substitution of chitosan. The FT-IR spectra corresponding to chitosan hydrogel beads reacted with palmitoyl chloride (0.8 M solution) employing either the relatively polar reaction solvents acetone or DMSO shared the same characteristic vibrational bands of those obtained from chitosan hydrogel beads *N*-acylated with hexanoic anhydride in Section 5.2.1.1. The vibrational bands at 1655 cm^{-1} and 1555 cm^{-1} representing the C=O and *N*-acyl functional groups respectively were present and the intensity of the bands at 2920 cm^{-1} and 2940 cm^{-1} ν(CH$_3$ and CH$_2$) increased, which was an

indication that *N*-acylation of the 85% deacetylated chitosan hydrogel beads had been achieved. However, the FT-IR spectra of the 85% deacetylated chitosan hydrogel beads reacted with palmitoyl chloride solution using the less polar reaction solvents THF or DCM did not exhibit significant changes in the vibrational bands, which suggested that they were not effective reaction solvents for the reaction and had a low degree of substitution.

5.2.3.2 Elemental Analysis

A study was performed to investigate the degree of substitution of the *N*-acylated chitosan hydrogel beads using elemental analysis. In order to do this Equation 5.2 is used to calculate the degree of substitution by comparing the ratio of carbon to nitrogen between our starting material chitosan and the *N*-acylated chitosan.

$$DS = \frac{(\frac{C}{N}_m - \frac{C}{N}_o)}{n} \qquad \text{(Equation 5.2)}$$

where $(C/N)_m$ is the C/N ratio of the chitosan derivative, $(C/N)_o$ was the C/N ratio of the starting material chitosan, n is the number of carbon atoms introduced after the chitosan was functionalised[29]. After the *N*-acylation reaction, all the beads investigated were washed in acetone, methanol and an extensive final wash in Millipore water to remove any organic solvent that would distort the carbon to nitrogen ratio. The first study carried out was to investigate the relationship between the concentration of palmitoyl chloride in the reaction solution and the degree of substitution. The results are displayed in Table 5.5.

Table 5.5 Elemental Analysis of *N*-palmitoyl chitosan hydrogels beads compared with the concentration of the palmitoyl chloride solution in the substitution reaction solution. The solvent used in the reaction was acetone. All the beads were washed in acetone, methanol and finally in Millipore water. The beads were then dried in an oven at 37 ± 1 °C for 24 h.

Concentration of Palmitoyl Chloride in Reaction Solution	Degree of Substitution %
0.8 M	49
0.4 M	43
0.1 M	27

The results displayed in Table 5.5 indicate that as the concentration of palmitoyl chloride in the reaction solution increased so too did the degree of substitution exhibited by the chitosan hydrogels. These data complement the FT-IR spectra exhibited in Figure 5.15 which indicated a similar relationship. The conclusion was that the degree of substitution can be controlled by the concentration of acyl chloride in the reaction mixture. A comparison study was then conducted between the degree of substitution values for chitosan beads substituted by acyl chloride and acidic anhydrides at the same concentration in the reaction solution, the results of which are exhibited in Table 5.6.

Table 5.6 Elemental analysis of *N*-acylated chitosan hydrogel beads, each hydrogel beads was *N*-acylated in a 0.8 M solution of the respective acyl chloride or acid anhydride. The reaction solvent used to form *N*-hexanoyl and *N*-aceylated chitosan beads was methanol while the reaction solvent to form *N*-palmitoyl and *N*-octanoyl chitosan beads was acetone. All the beads were washed in acetone, methanol and finally in Millipore water. The beads were then dried in an oven at 37 ± 1 °C for 24 hours.

Formulation	Degree of Substitution %	*n*
N-Aceylated Chitosan	92	2
N-Hexanoyl Chitosan	75	6
N-Octanoyl Chitosan	59	8
N-Palmitoyl Chitosan	49	16

The degree of substitution values displayed in Table 5.6 showed that as the n value increased the degree of substitution decreased when the same molar ratio of reagents were used. This meant that as the length of the aliphatic carbon atom chain to be added increased the degree of substitution decreased. This could be due to the effects of steric hindrance from longer chain molecules involved in the substitution reaction. Comparing the degree of substitutions presented in Table 5.6 to those obtained in literature similarities and differences were found. Desbrierés *et al*. substituted chitosan with C8 and C10 aldehydes and reported a substitution degree of 12.5% for both alkyl chains, substantially lower than the degree of substitution achieved by substitution with octanoyl chloride in this research (59%)[30]. Jiang *et al*. grafted hydrophobic stearoyl, palmitoyl and octanoyl chloride aliphatic chains onto molecules of chitosan in the fibre state and obtained degrees of substitution from 0.9% to 29.6% using DMSO as the reaction solvent[11]. Complementing the results displayed in Table 5.6 Jiang *et al*. found that increasing the length of the aliphatic chains lead to a decrease in the degree of substitution of chitosan[11]. Significantly, it would appear that the post-modification method of *N*-acylation of chitosan hydrogel beads as performed in this study facilitated the high degree of *N*-substitution values which were higher than any previously described in the literature for chitosan beads modified for the purpose of controlled drug release.

5.2.3.3 DSC Analysis of *N*-Palmitoyl Chitosan Beads

In Section 5.2.1.2 the DSC thermograms of chitosan hydrogels *N*-acylated with hexanoic anhydride were examined. The *N*-hexanoyl chitosan hydrogels were substituted with a 6 carbon atom long aliphatic chain which resulted in a decrease in the band corresponding to the thermal degradation of the glucosamine unit of chitosan. This was due to its *N*-acylation and the distortion of the band attributed to *N*-acetyl-glucosamine degradation due to the close proximity of the *N*-hexanoyl-glucosamine unit degradation temperature peak. In this study, a DSC thermogram of chitosan hydrogel beads reacted with palmitoyl chloride (0.8 M solution) was

examined using acetone as the reaction solvent. The DSC thermogram of *N*-palmitoyl chitosan hydrogel beads after they were washed, dried and ground was exhibited in Figure. 5.18 (a) and compared with a thermogram of a hydrogel bead synthesised using 85% deacetylated chitosan (Figure 5.18 (b)).
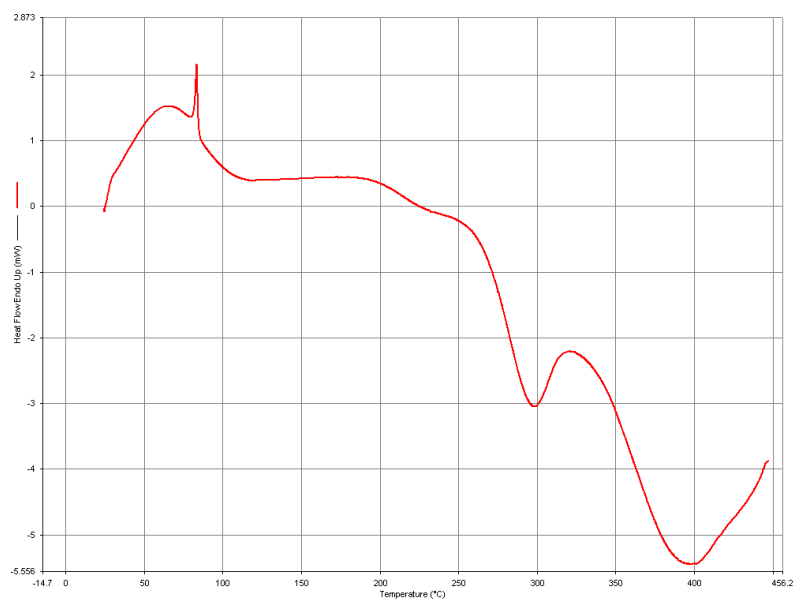
(a)
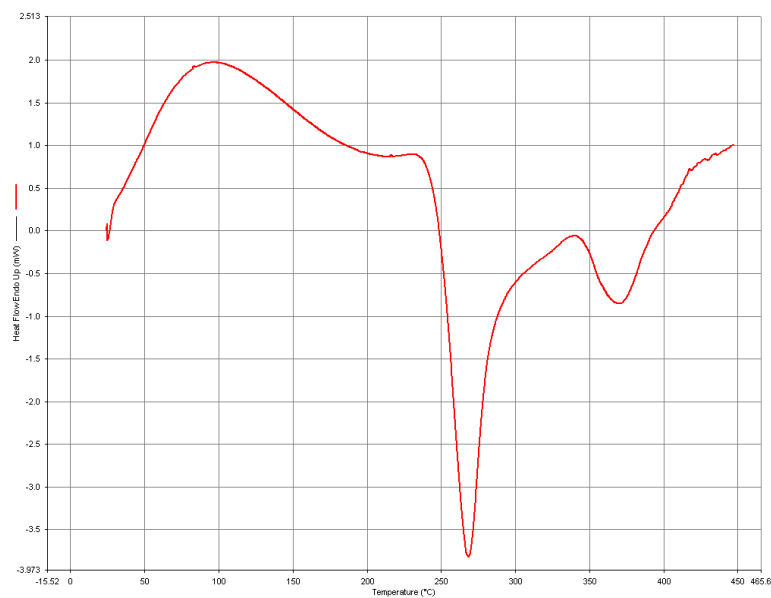
(b)

Figure 5.18 DSC Thermogram of (a) *N*-palmitoyl chitosan xerogel bead (b) 85% deacetylated chitosan xerogel bead.

The DSC thermogram of chitosan hydrogel beads reacted with palmitoyl chloride (0.8 M solution) demonstrates the change in thermo-degradation properties the modified chitosan exhibits when *N*-palmitoyl-glucosamine units are substituted onto the chitosan polymer. Comparing this thermogram to the thermogram of an 85% deacetylated chitosan bead (Figure 5.18 (b)) it is important to note that the thermal degradation of chitosan still consisted of three stages, but what had changed was the temperature at which these stages occurred. The first stage was the loss of water which had an endothermic peak at 65.0 °C. This was a substantial decrease when compared with unmodified chitosan which exhibits the same peak at 96.1 °C. The decrease in the temperature of the peak of the area attributed to water loss can be attributed to the increased hydrophobicity of the modified chitosan. In addition, the substitution of chitosan at the amino site would have resulted in a significant reduction in the number of functional groups capable of interacting with water. At 83.3 °C there was a very distinct sharp endothermic peak, this is due to the evaporation of a small amount solvent which was used to wash the *N*-acylated chitosan beads. The next exothermic peak occurs at 295.4 °C and was attributed to the thermal degradation of the *N*-acetyl-glucosamine units. This peak had actually decreased in temperature, but it was being distorted by a larger peak, which was likely to have influenced the peak temperature obtained. The degradation peak which occurred at 400.0 °C was attributed to the *N*-palmitoyl-glucosamine units which were formed as a result of the substitution reaction. This peak did not appear in the 85% deacetylated chitosan bead thermogram and occurred at a higher temperature than the degradation peak corresponding to the degradation of the *N*-hexanoyl-glucosamine units in the *N*-hexanoyl chitosan beads (Section 5.2.1.2). The DSC thermogram obtained for chitosan hydrogel beads substituted in 0.8 M palmitoyl chloride solution supported the conclusion that the chitosan hydrogel beads had been successfully substituted with *N*-palmitoyl-glucosamine unit and that this reaction had occurred throughout the bead.

5.2.3.4 Surface Morphology: Influence of the Reaction Solvent

In Section 5.2.3.1 (iii) it was shown that the reaction solvent influenced the degree of *N*-substitution of the *N*-palmitoyl chitosan hydrogel beads. SEM micrographs of chitosan beads reacted with palmitoyl chloride (0.8 M solution) are displayed in Figure 5.19. Each substitution reaction was performed under the same conditions except the reaction solvent used was changed. The investigation into the influence of reaction solvent was carried out because Duarte *et al.* found that the reaction solvent had a significant influence on the chitosan matrices they obtained when synthesising scaffolds for tissue engineering purposes[28]. It was clear from examining the SEM micrographs that the surface morphology was influenced by the solvent used in the acylation reaction. A chitosan bead *N*-acylated using DCM as the reaction solvent was displayed in Figures 5.19 (a) and (b) and exhibited a structure that was highly porous. On the other hand chitosan beads *N*-acylated using DMSO as the reaction solvent, displayed in Figure. 5.19 (c) and (d), had a rough surface with small indentations. Pores were not visible on the surface and the beads appeared to have good structural integrity. Chitosan beads *N*-acylated using THF as the reaction solvent (Figure 5.19 (e) and (f)) were characterised by an uneven, yet smooth, surface that featured a considerable number of lacerations. Depending on the depth of these lacerations it was possible that the DCD release from these beads could be affected. Chitosan beads substituted using acetone as the reaction solvent displayed a good reproducible spherical shape and a surface with random shallow dents (g) and (h).

(a)   (b)

(c)   (d)

(e)   (f)

(g)   (h)

(i)   (j)
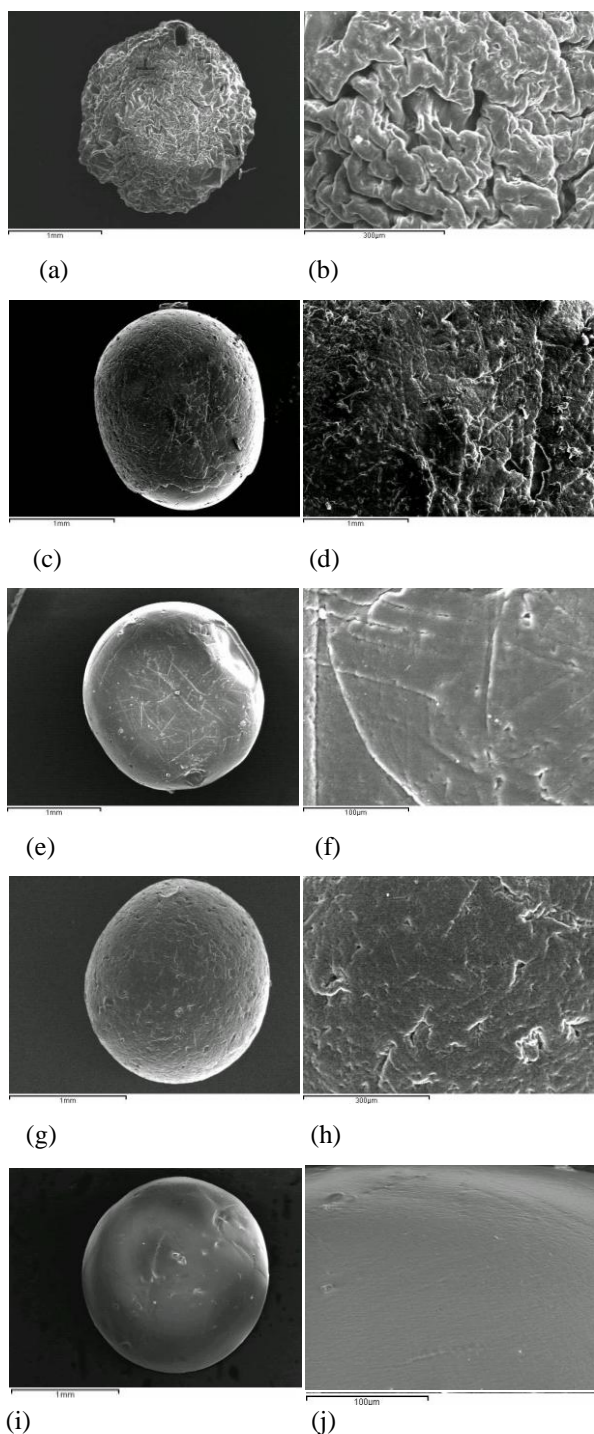
Figure 5.19 SEM micrographs of the influence of the solvent used in the substitution reaction on the surface morphology of the *N*-palmitoyl chitosan beads. The reaction solvent used to substitute the bead in each micrograph was [(a) DCM (b) DCM, (c) DMSO (d) DMSO, (e) THF (f) THF, (g) Acetone (h) Acetone] The beads exhibited in (i) and (j) are 85% deacylated chitosan beads formed by precipitation in NaOH and are displayed here for comparative purposes.

189

5.2.3.5 Swelling Properties of *N*-Palmitoyl Chitosan Beads

5.2.3.5 (i) Influence of Reaction Solvent

The swelling behaviour of chitosan beads *N*-acylated in palmitoyl chloride solution in different reaction solvents was examined in this study. The swelling ratios (%) of the beads were calculated using Equation 5.1. The *N*-palmitoyl chitosan beads have been substituted with a longer aliphatic carbon atom chain which increased the hydrophobic properties of the chitosan polymer; therefore we expect that *N*-palmitoyl chitosan xerogel beads to exhibit a lower swelling ratio than 85% deacylated chitosan beads (233% after 1 hour in Millipore water as shown in Section 3.2.2.1). The swelling study is presented in Figure 5.20.
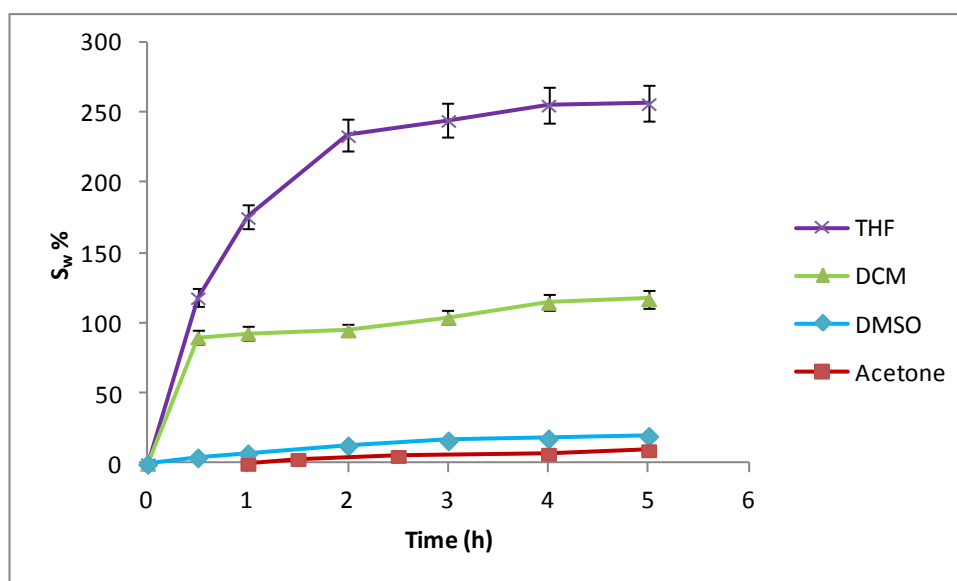
Figure 5.20 A comparison of the swelling ratio (%) of *N*-palmitoyl chitosan xerogel beads depending on the reaction solvent used in the *N*-acylation substitution reaction. After the substitution reaction all the beads were washed in acetone, methanol and Millipore water and dried in an oven at 37 ± 1 °C for 24 hours. Swelling studies were conducted at 20 ± 1 °C.

As can be seen from Figure 5.20, *N*-palmitoyl chitosan xerogel beads substituted using the reaction solvents THF and DCM exhibited high swelling ratios (%) after 5 h (256% and 117%, respectively). This was not surprising as their respective FT-IR

spectra (Section 5.2.3.1 (iii)) indicated they had a low degree of substitution and the SEM micrograph of beads which were reacted using DCM as the reaction solvent had shown that the bead had a rough and porous surface (Figure 5.19 (a)). However, using the DMSO or acetone as the reaction solvent substantially reduced the amount of swelling exhibited by the *N*-palmitoyl chitosan xerogel beads. As Table 5.7 shows, after 5 h the swelling ratio (%) of beads substituted using acetone as the reaction solvent was 12%. After the same amount of time the *N*-palmitoyl beads substituted using the reaction solvent DMSO had a swelling ratio of 20%. This showed that for these two sets of beads water was being inhibited from entering the polymer matrix of the bead. A comparison of the swelling ratio (%) of *N*-hexanoyl chitosan beads (Section 5.2.1.4) and *N*-palmitoyl chitosan beads substituted using the same concentration of hexanoic anhydride and palmitoyl chloride (0.8 M solution) after 5 hours indicated that the values were quite comparable as the swelling ratio (%) of *N*-hexanoyl chitosan beads was 13 % while the swelling ratio (%) of *N*-palmitoyl chitosan beads (using acetone as the reaction solvent) was 12%. The results in Table 5.7 indicated that the reaction favours a polar reaction solvent.

Table 5.7 A comparison of the swelling ratio percentages of *N*-palmitoyl chitosan xerogel beads in Millipore water after 5 hours swelling time depending on the reaction solvent used in the *N*-acylation substitution reaction. Swelling studies were conducted at 20 ± 1 °C.

Reaction Solvent Used in the *N*-acylation reaction	Swelling Ratio of the *N*-palmitoyl chitosan beads after 5 hours (%)
THF	256
DCM	117
DMSO	20
Acetone	12

5.2.3.5 (ii) Influence of the Palmitoyl Chloride Concentration

The swelling behaviour of chitosan xerogel beads *N*-acylated to form *N*-palmitoyl chitosan beads in different concentrations of palmitoyl chloride solution were examined in this study. As shown in Table 5.6 the higher the concentration of palmitoyl chloride in the reaction solution the greater the degree of substitution, therefore we can expect that *N*-palmitoyl chitosan xerogel beads substituted in higher concentrations of palmitoyl chloride will exhibit the smallest swelling ratios (%). The swelling study is presented in Figure 5.21.
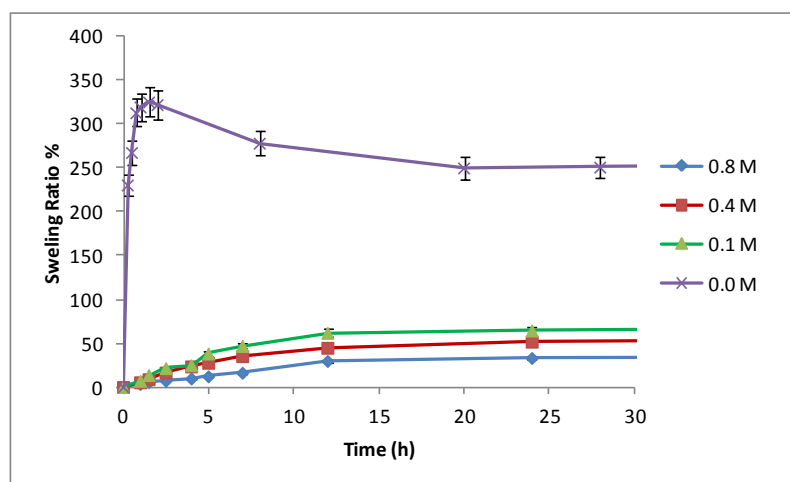
Figure 5.21 Comparison of the swelling ratio (%) of *N*-palmitoyl chitosan xerogels formed by substitution in different concentrations of palmitoyl chloride. All xerogels were subsequently washed in acetone, DMSO methanol and Millipore water and dried in an oven at 37 °C for 24 hours. Swelling studies were conducted in Millipore water at a temperature of 20 ± 1 °C.

It was clear that as the concentration of palmitoyl chloride in the reaction solution increased the swelling ratio (%) of the resulting chitosan beads decreased. At swelling equilibrium the swelling ratio percentages of *N*-palmitoyl chitosan xerogels acylated in 0.8 M, 0.4 M and 0.1 M palmitoyl chloride solution were 35%, 58% and 70% respectively. It was apparent from the swelling ratio (%) values calculated that the *N*-acylation of the chitosan xerogel beads substantially reduced their swelling capacity, as chitosan xerogel beads gelled in NaOH only without *N*-acylation has a swelling ratio (%) value of 322% after two hours. Comparing the data in Table 5.6 with the

results exhibited in Figure 5.21 it was observed that the higher degree of substitution of the chitosan xerogel beads the lower the swelling ratio (%) at any given time. It was also apparent that the swelling ratio (%) values obtained for *N*-palmitoyl chitosan xerogel beads was less than those obtained for chitosan xerogel beads crosslinked in glyoxal solution in Section 4.2.2.1. In addition like the swelling study performed on *N*-hexanoyl chitosan xerogel beads (Section 5.2.1.4) the swelling ratio (%) of *N*-acylated chitosan beads was much slower to reach their maximum value than chitosan beads that had been crosslinked in glyoxal solution. This was likely due to the hydrophobicity of the *N*-palmitoyl chitosan xerogel beads into which water appeared to take a longer time to permeate, compared to glyoxal crosslinked chitosan xerogel beads.

5.2.4 DCD Release Properties of *N*-Palmitoyl Chitosan Beads

5.2.4.1 Influence of Reaction Solvent

5.2.4.1. (i) DCD Release Profiles

A comparison of the release profiles of DCD from *N*-palmitoyl chitosan beads formulated by substituting 85% deacetylated chitosan hydrogel beads in 0.8 M palmitoyl chloride solution using different solvents is displayed in Figure 5.21. It is apparent that the *N*-palmitoyl chitosan beads that exhibited the least amount of swelling (Table 5.7) displayed the longest time to reach release equilibrium. Using THF and DCM as the reaction solvent resulted in a more rapid and uncontrolled release of DCD from the chitosan beads. Chitosan beads that had been *N*-acylated using THF as the reaction solvent reached DCD equilibrium release time after 50 min. This was approximately the same release time as chitosan hydrogel formed only by precipitation with NaOH and they released the greatest amount of DCD into the release solution in this study. Although the beads used in the present study showed the different release concentration of DCD it was shown previously in Section 5.2.2.2 that the amount of DCD loaded into the beads does not influence the time for the DCD release to reach equilibrium. Chitosan hydrogel beads *N*-acylated using DCM as the reaction solvent reached equilibrium release time after 1 h, but the concentration of

DCD in the release solution at equilibrium was just 0.01 mM compared with 0.03 mM for beads *N*-acylated using THF as the reaction solvent.

A previous study in this research, Section 5.2.3.4, indicated that using DCM as a reaction solvent resulted in beads with a rough and porous surface morphology. It would be expected that this surface morphology would have a detrimental influence on DCD release. This may be the reason the amount of DCD released from these beads was relatively low. Release from chitosan beads substituted using the reaction solvents acetone and DMSO both exhibited significantly improved equilibrium release times of over 5 h which was not surprising considering the low swelling ratio values obtained for the beads (Table 5.7). The concentration of the release solution at equilibrium of beads substituted in DMSO was 0.03 mM compared to 0.01 mM for beads synthesised in acetone. The amount of DCD loaded into the xerogel beads and therefore released was likely to be influenced by the structural arrangement of chitosan inside the bead caused by the *N*-acylation reaction. This result could be an indication that a greater deal of substitution of the chitosan polymer has taken place by using acetone as the reaction solvent as an increase in the polymer density would restrict the loading capacity.
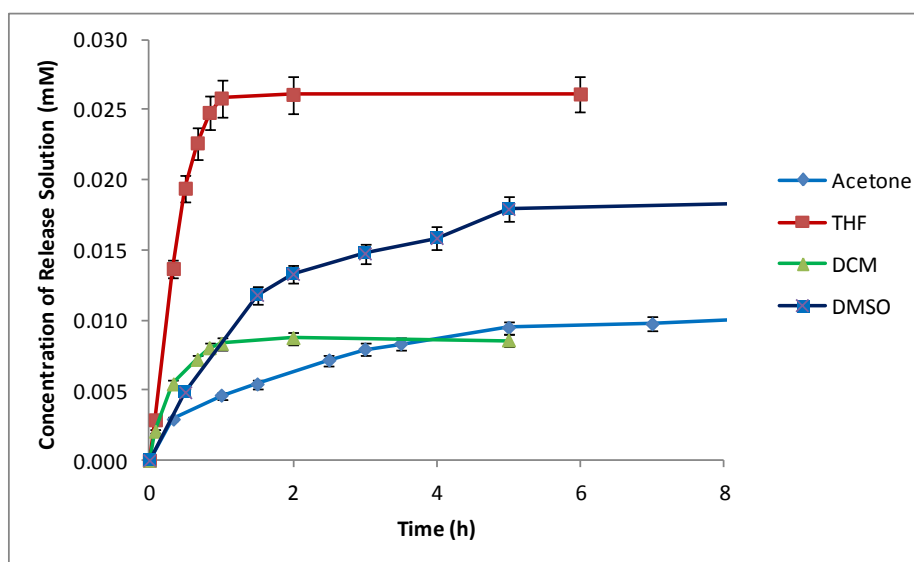
Figure 5.22 A comparison of the DCD release profiles from *N*-palmitoyl chitosan xerogels that were substituted using different reaction solvents. All xerogels were reacted with palmitoyl chloride (0.8 M solution), then washed in acetone, methanol and Millipore water, loaded in a 60 mM DCD Millipore water solution and dried in an oven at 37 ± 1°C for 24 hours.

5.2.4.1 (ii) DCD Release Kinetics and Mechanism

A comparison of the rate constants and regression fits of DCD release from *N*-palmitoyl chitosan beads was carried out to investigate which reaction solvent resulted in greatest degree of controlled DCD release from the beads. After the *N*-acylation reaction each set of beads was washed in acetone, methanol and Millipore water and loaded in 60 mM aqueous DCD solution then dried in an oven at a constant temperature of 37 ± 1 °C for 24 h. Figure 5.23 exhibits the release data of DCD from palmitoyl chitosan xerogel beads substituted in 0.8 M palmitoyl chloride solution using DMSO, THF, DCM and Acetone as the reaction solvent fitted to the zero-order and first-order model and Table 5.8 contains the rate constants and regression line fits.

(a)   (b)
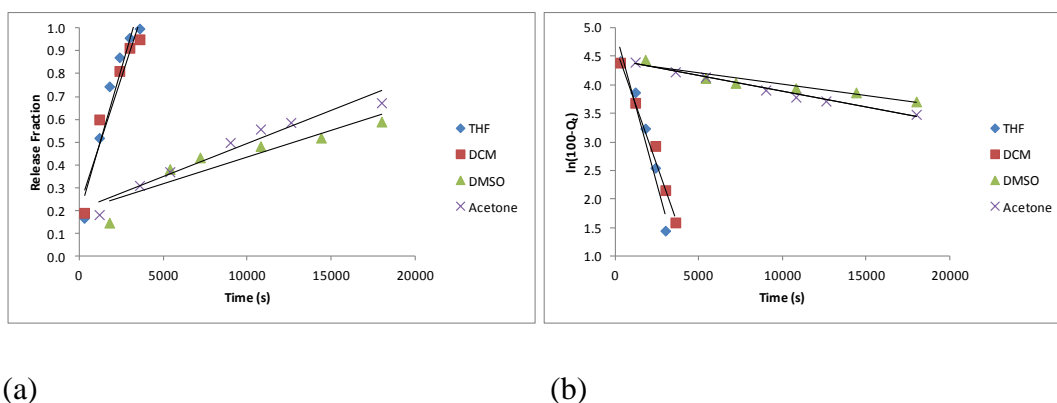
Figure 5.23 DCD release data from *N*-palmitoyl chitosan xerogel beads that were substituted using a stated reaction solvent fitted to (a) zero-order and (b) first-order models.

Table 5.8 Results from the fitting of DCD release data from *N*-palmitoyl chitosan xerogel beads substituted using different reaction solvents to the zero-order and first-order models.

Reaction Solvent	Zero-Order Model		First-Order Model	
	k_0 (s^{-1})	R^2	k_1 (s^{-1})	R^2
Acetone	2.21×10^{-5}	0.9906	3.56×10^{-5}	0.9986
THF	2.97×10^{-4}	0.9631	1.08×10^{-3}	0.9544
DCM	2.30×10^{-4}	0.9212	1.07×10^{-3}	0.9551
DMSO	2.36×10^{-5}	0.8443	3.34×10^{-5}	0.9050

It was apparent from release data of each set of beads investigated that only the beads formed using acetone had a very good first-order model fit. Analysing the first-order rate constant values obtained for each reaction solvent used, it was apparent that chitosan hydrogel beads *N*-acylated using DMSO or acetone as the reaction solvent exhibited substantially smaller rate constants than beads *N*-acylated using THF or DCM as the reaction solvents. DCD release from chitosan beads that were *N*-acylated using DMSO as the reaction solvent had the lowest first-order kinetic constant value (3.34×10^{-5} **s^{-1}**) but DCD release from *N*-palmitoyl chitosan beads that were acylated using acetone as the reaction solvent also exhibited a low first-order kinetic constant value (3.56×10^{-5} **s^{-1}**). **T**he first-order rate constant of DCD release from chitosan beads that were *N*-acylated using DCM as the reaction solvent was approximately 16 times greater than the rate constant of chitosan beads that were *N*-acylated using acetone as the reaction solvent. Therefore, subsequent studies were performed concentrating on the two best systems, chitosan beads that were substituted to form *N*-palmitoyl chitosan beads using acetone or DMSO as the reaction solvent. To further investigate the release mechanism of DCD from these beads the release data were fitted to the Higuchi and Korsmeyer–Peppas models shown in Figure 5.24 and the subsequent results are displayed in Table 5.9.

(a)   (b)
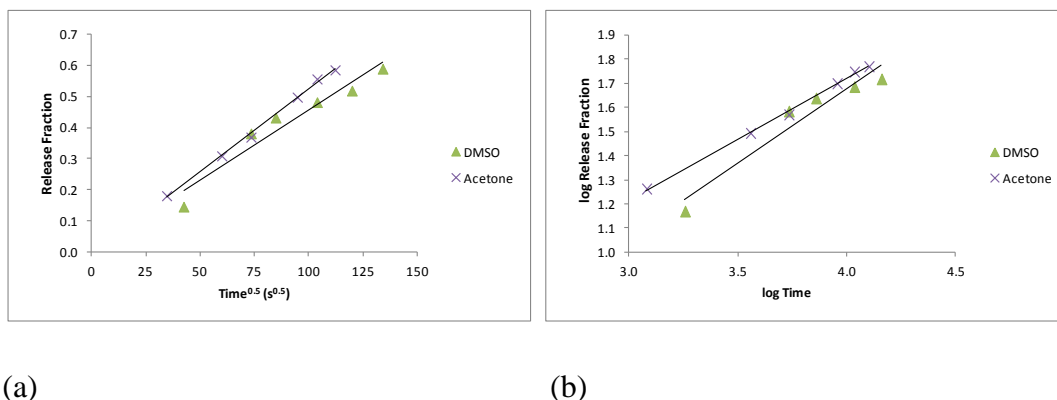
Figure 5.24 DCD release data from *N*-palmitoyl chitosan xerogel beads substituted in a 0.8 M palmitoyl chloride solution where DMSO or acetone was used as the reaction solvent fitted to (a) Higuchi and (b) Korsmeyer-Peppas models.

Table 5.9 Results from the fitting of DCD release data from from *N*-palmitoyl chitosan xerogel beads substituted using DMSO or acetone as the reaction solvent to (a) Higuchi and (b) Korsmeyer-Peppas models.

Reaction Solvent	Higuchi Model		Korsemeyer-Peppas Model	
	k_H (s$^{-0.5}$)	R^2	n	R^2
Acetone	4.02×10^{-3}	0.9893	0.46	0.9852
DMSO	4.01×10^{-3}	0.9344	0.58	0.9329

The results in Table 5.9 shows that DCD release from *N*-palmitoyl chitosan beads that were acylated using acetone or DMSO as the reaction solvent both exhibited almost identical Higuchi rate constants and both displayed good fits for the Higuhci model. Furthermore, release of DCD from chitosan beads that were *N*-acylated using acetone as the reaction solvent had an exponent n value of 0.46 which was close to the value for pure Fickian diffusion ($n = 0.43$). Release from *N*-palmitoyl chitosan beads that were acylated using DMSO as the reaction solvent had a higher exponent n value

($n = 0.58$) than *N*-palmitoyl chitosan beads that were *N*-acylated using acetone as the reaction solvent. This suggested release was more a combination of Fickian diffusion and Case-II transport caused by polymeric chain relaxation from these beads. However, the exponent n value obtained for *N*-palmitoyl chitosan beads that were acylated using DMSO as the reaction solvent can still be considered to be heavily influenced by Fickian diffusion as it remains closer to the exponent n value representing pure Fickian diffusion ($n = 0.43$) than pure polymer chain relaxation ($n = 0.86$). Comparing these results to studies undertaken by other authors it was apparent that the results given here were in contrast to those found in the literature. Release from our system appeared to be predominantly due to Fickian diffusion, whereas release from others systems tended to be due to a mixture of diffusion and polymer chain relaxation. For example, Obitte *et al.* obtained exponent n values of up to 2.33 for release of Metronidazole, a nitroimidazole antibiotic medication, from the hydrophobic polymer capsule release system which was made from methylcellulose. They attributed the release to polymeric chain relaxation and diffusion as they obtained a high regression square value for the Higuhci model[31]. Serra *et al.* obtained exponent n values ranging from 0.56 to 0.92 for release of theophylline, a methylxanthine drug structurally similar to caffeine, from poly(acrylic acid-g-ethylene glyocol) hydrogels, and they interpreted the release as being anomalous[32]. The DCD release data was fitted to the Sahlin-Peppas models to determine Fickian diffusion and relaxation contribution to DCD release. The plots are shown in Figure 5.25 and the results are exhibited in Table 5.10.

(a)   (b)
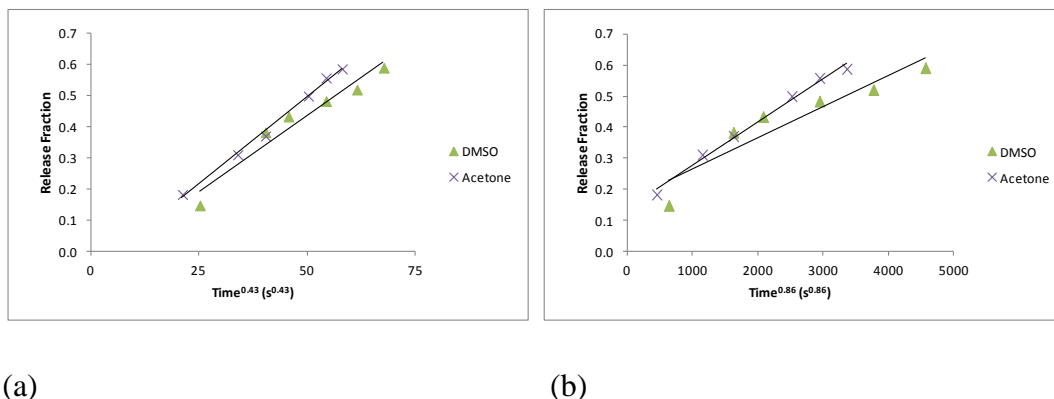
Figure 5.25 DCD release data from *N*-palmitoyl chitosan xerogel beads substituted in a 0.8 M palmitoyl chloride solution using DMSO or Acetone as the reaction solvent fitted to the Sahlin-Peppas (a) Fickian contribution and (b) Relaxation contribution models.

Table 5.10 Results from the fitting of the release data from *N*-palmitoyl chitosan xerogel beads synthesised using acetone or DMSO as the reaction solvent to the Sahlin-Peppas models.

Solvent Used in Reaction Vessel	Fickian Diffusion Contribution		Relaxation Contribution		Relaxation/ Fickian Ratio
	k_1 (s$^{-0.43}$)	R^2	k_2 (s$^{-0.86}$)	R^2	R/F
Acetone	8.59×10^{-3}	0.9910	9.25×10^{-5}	0.9511	0.01
DMSO	8.73×10^{-3}	0.9449	8.90×10^{-5}	0.8709	0.01

As expected, the values obtained for the Fickian diffusion and polymer chain relaxation release contribution ratios showed that Fickian diffusion is the dominant release mechanism for *N*-palmitoyl chitosan beads *N*-acylated using acetone or DMSO as the reaction solvent. Furthermore, by comparing the values obtained from *N*-palmitoyl chitosan beads with those from an unmodified chitosan xerogel (Table 5.22) we can see that the addition of palmitoyl aliphatic carbon chains to the glucosamine unit of chitosan had decreased the relaxation / Fickian ratio slightly from 0.05 to 0.01. This implies that increasing the hydrophobicity of the beads promoted Fickian diffusion. This result corresponds to the conclusions made for DCD release

from *N*-hexanoyl chitosan xerogel beads (Section 5.2.2.3) as they both exhibited decreased relaxation / Fickian ratios compared to release from 85% deacetylated chitosan beads. Comparing our results to the literature, it was apparent that we had achieved relatively low relaxation / Fickian ratio values for a release system. Serra *et al*. fitted the release data of theophylline, a methylxanthine drug structurally similar to caffeine, from poly(acrylic acid-g-ethylene glyocol) hydrogels to the Peppas-Sahlin model. They obtained relaxation / Fickian ratio values between 0.79 and 0.01 depending on the design of their hydrogel system and concluded that the release mechanism was near Case-II transport at a ratio value of 0.79 but otherwise anomalous[32]. Sasa *et al*. investigated the release mechanism of water-soluble pentoxifylline and vancomycin hydrochloride from cellulose ether matrices and obtained relaxation / Fickian ratio values between 0.79 and 0.13. They concluded that release was mainly governed by diffusion[33]. The fact that Fickian diffusion was favoured over Case-II transport (caused by polymer chain relaxation) in this study would be influenced by the fact that DCD is a small molecule and is highly soluble in water.

DCD release from *N*-palmitoyl chitosan beads substituted using acetone as the reaction solvent exhibited a comparatively low first-order rate constant, a good fit for the Higuchi models and the lowest swelling ratio (%) observed of any chitosan xerogels studied in this research. Therefore acetone was used as the reaction solvent for the *N*-substitution of 85% deacetylated chitosan with acyl chlorides for all future studies in this chapter.

5.2.4.2 Influence of the Palmitoyl Chloride Concentration

In order to investigate the effect of an increase in the concentration of palmitoyl chloride in the reaction solution a study was conducted and the experimental release data obtained were analysed using mathematical models. The data were fitted to the zero-order and first-order models in Figure 5.26 and the resulting rate constants and regression fits are exhibited in Table 5.11. After the *N*-acylation reaction all the beads

examined in this study were washed in acetone, methanol and Millipore water, loaded in 60 mM DCD Millipore water solution and dried in an oven at 37 °C for 24 hours.

(a)　　　　　　　　　　　　　　　　　　(b)
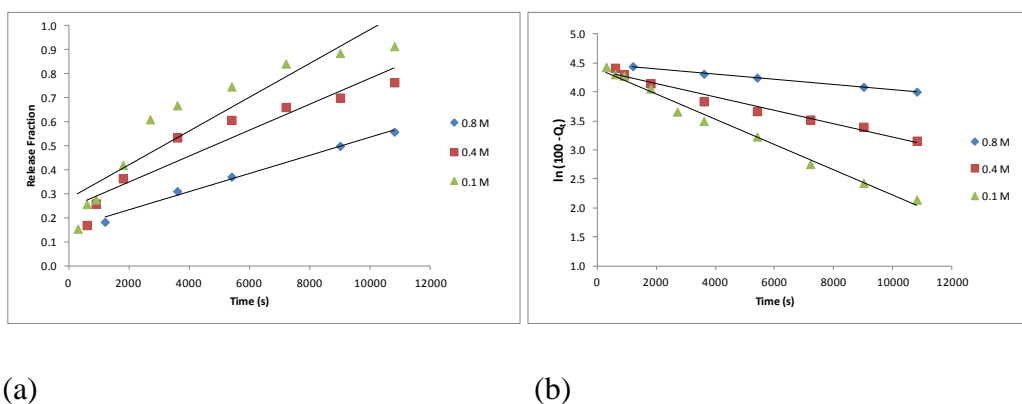
Figure 5.26 Release data of DCD from *N*-palmitoyl chitosan xerogel beads that were substituted in different concentrations of palmitoyl chloride solution fitted to (a) zero-order and (b) first-order models.

Table 5.11 Results from the fitting of DCD release data from *N*-palmitoyl chitosan xerogel beads that were substituted in different concentrations of palmitoyl chloride to the zero-order and first-order models.

Concentration of Palmitoyl Chloride solution (M)	Zero-Order Model		First-Order Model	
	k_0 (s^{-1})	R^2	k_1 (s^{-1})	R^2
0.8	2.21×10^{-5}	0.9906	3.56×10^{-5}	0.9986
0.4	5.43×10^{-5}	0.9012	1.16×10^{-4}	0.9716
0.1	1.19×10^{-4}	0.9201	2.19×10^{-4}	0.9884
0.0	4.52×10^{-4}	0.9144	1.23×10^{-3}	0.9925

The results in Table 5.11 show the rate constants obtained from fitting the DCD release data to the zero-order and first-order models. The DCD release data from the *N*-palmitoyl chitosan beads for all palmitoyl chloride concentrations fit best to the first-order model. When the data were fitted to the zero-order model there was a poor fit with the exception of *N*-palmitoyl chitosan beads that were *N*-acylated in a 0.8 M palmitoyl chloride solution. There did not appear to be a relationship between the linear regression line fit and the palmitoyl chloride concentration used in the reaction vessel. This would suggest that the release order was not altered by an increase in the hydrophobicity of the chitosan. However, the effect of the concentration of palmitoyl chloride in the reaction vessel on the rate constants was apparent, as the first-order rate constant was reduced as the palmitoyl chloride concentration increased. This meant that by increasing the degree of substitution of the *N*-palmitoyl chitosan hydrogels the rate constant was reduced. Kiortsis *et al*. came to a similar conclusion, when they increased the hydrophobicity of their drug release tablets they found that this did not affect the mechanism of drug release of their four model drugs (diclofenac sodium, ibuprofen, naproxen and indomethacin), but did affect the release rate constant[34]. In this study, at all concentrations of palmitoyl chloride used in the reaction vessel, the *N*-palmitoyl chitosan xerogels showed a marked decrease on the rate constant of DCD release compared with chitosan hydrogel formulated with 85% deacetylated chitosan. This was a favourable outcome as it suggested that DCD release from the xerogels was moving from uncontrolled to controlled. Even at the lowest concentration of palmitoyl chloride examined (0.1 M), the rate constant was 5.5 times lower than that of DCD release from hydrogels formulated from 85% deacetylated chitosan. Le Tien *et al*. developed chitosan tablets *N*-acylated with various fatty acid chlorides to increase their hydrophobic character[4]. Le Tien *et al*. found that by modifying their chitosan fibre by *N*-acylation they were able to extend the release time of their model drug, Acetaminophen, from their chitosan tablets and concluded release took place by diffusion[4]. Le Tien *et al*.'s research draws similar conclusions to the results presented in this study, as in both cases release of the model chemicals slowed due to *N*-acylation of the chitosan polymer.

The release data for DCD from *N*-palmitoyl chitosan xerogels substituted using increasing concentrations of palmitoyl chloride were applied to the Higuhci and

Korsemeyer-Peppas models to further investigate the mechanism of release. The models are shown in Figure 5.27 and the results of the analysis are presented in Table 5.12.

(a)   (b)
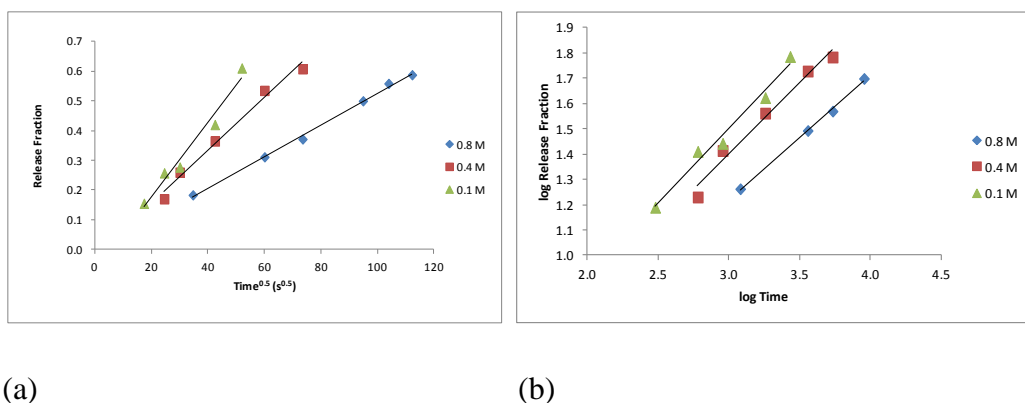
Figure 5.27 Release data of DCD from *N*-palmitoyl chitosan xerogel beads that were substituted in different stated concentrations of palmitoyl chloride solution were fitted to the (a) Higuchi and (b) Korsmeyer-Peppas models.

Table 5.12 Results from the fitting of DCD release data from *N*-palmitoyl chitosan xerogel beads that were substituted in different concentrations of palmitoyl chloride solution to the Higuchi and Korsmeyer-Peppas models.

Concentration of Palmitoyl Chloride solution (M)	Higuchi Model		Korsemeyer-Peppas Model	
	$k_H(\text{s}^{-0.5})$	R^2	n	R^2
0.8	4.02×10^{-3}	0.9893	0.46	0.9852
0.4	8.86×10^{-3}	0.9846	0.56	0.9761
0.1	1.23×10^{-2}	0.9816	0.59	0.9782
0.0	2.39×10^{-2}	0.9678	0.55	0.9508

When the release data of DCD from *N*-palmitoyl chitosan beads was fitted to the Higuchi model a good linear regression line fit was achieved. This suggested that diffusion plays a prominent role in the mechanism of release from the *N*-palmitoyl chitosan xerogel beads. The n exponent value obtained by applying the release data to the Korsemeyer-Peppas model decreased as the concentration of palmitoyl chloride in the reaction mixture increased. The n exponent value of 0.43 represents pure Fickian diffusion. Therefore, as the value of the calculated exponent n value moved towards 0.43 as the acyl chloride concentration increased this suggested that an increase in the hydrophobicity of the beads promoted release by Fickian diffusion. The release data was applied to the Sahlin – Peppas model to determine the Fickian contribution and polymer chain relaxation contribution to DCD release from the *N*-palmitoyl chitosan xerogel beads. The models are exhibited in Figure 5.28 and the results are shown in Table 5.13.
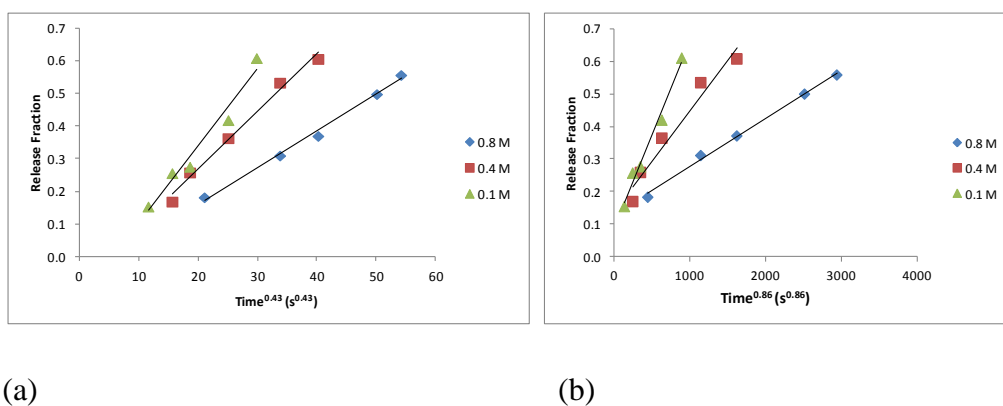
(a)   (b)

Figure 5.28 Release data of DCD from *N*-palmitoyl chitosan xerogel beads that were substituted in a stated concentration of palmitoyl chloride solution were fitted to the Sahlin – Peppas model to determined the influence of (a) Fickian contribution and (b) polymer chain relaxation.

Table 5.13 Results from the fitting of data to the Sahlin-Peppas Model for DCD release from *N*-palmitoyl chitosan xerogel beads that were substituted in a stated concentrations of palmitoyl chloride solution.

Concentration of Palmitoyl Chloride solution (M)	Fickian Diffusion Contribution		Relaxation Contribution		Relaxation/ Fickian Ratio
	k_1 (s$^{-0.43}$)	R^2	k_2 (s$^{-0.86}$)	R^2	R/F
0.8	8.59×10^{-3}	0.9910	9.25×10^{-5}	0.9511	0.01
0.4	1.77×10^{-2}	0.9833	3.14×10^{-4}	0.9958	0.01
0.1	2.36×10^{-2}	0.9637	5.67×10^{-4}	0.9841	0.02
0.0	3.93×10^{-2}	0.9618	2.12×10^{-3}	0.9689	0.05

The release data was fitted to the Sahlin-Peppas model and the results are displayed in Table 5.13. The data has a good regression line fit to the Sahlin – Peppas model and the results demonstrate the dominance of Fickian diffusion as the mechanism of release. Between a concentration of 0.1 M and 0.8 M palmitoyl chloride in the reaction vessel the Fickian diffusion rate constant of DCD release from the resulting *N*-palmitoyl chitosan beads decreased from 2.36×10^{-2} s$^{-0.43}$ to 8.59×10^{-3} s$^{-0.43}$, respectively. However, release by Case-II transport caused by polymer chain relaxation decreased by a greater degree over the same range from 5.67×10^{-4} s$^{-0.86}$ to $9.25 \, x10^{-5}$ s$^{-0.86}$ which resulted in their being almost no change in the relaxation/Fickian ratio. A comparison of the relaxation/Fickian contribution values obtained in the literature to the values obtained in the present study revealed the values obtained were comparatively low with those exhibited by other release systems. Serra *et al*. fitted their release data from release of theophylline, from their poly(acrylic acid-g-ethylene glyocol) hydrogels to the Peppas-Sahlin model and obtained relaxation / Fickian ratio values between 0.79 and 0.01[32]. Sasa *et al*. investigated the mechanisms of release of water-soluble pentoxifylline and vancomycin hydrochloride from cellulose ether matrices and obtained relaxation /

Fickian ratio values between 0.79 and 0.13 and concluded that release was mainly governed by diffusion[33].

5.2.4.3 Influence of the pH of the Release Medium

A characteristic trait of chitosan hydrogels designed for *in vitro* drug release is the fact that they can change their swelling properties in response to the pH of the release medium. This can lead to a change in drug release rate from the hydrogels[35]. This trait is considered desirable for drug release into the human body, as different organs of the human body have different pH values, therefore the hydrogels can be tailored to release at specific sites[36]. For an agricultural application however, it would be more beneficial to develop a bead that released at a controlled rate in both slightly acidic and slightly basic pH release media. Therefore we want to develop a delivery system that is equally effective in different environmental conditions. Consequently, the influence of the pH of the release medium on the rate constants and mechanism of DCD release from palmitoyl and octanoyl *N*-acylated chitosan xerogel beads was investigated. The study was conducted at pH values above and below the pK_a value of chitosan ($pK_a = 6.3$). When chitosan is in a solution below its own pK_a value, the amine group on its glucosamine unit becomes protonated. This causes electrostatic repulsions between the polymer chains which have the potential to increase the DCD release rate constant from the beads. In addition, the study was performed in an ion solution as the pH values were obtained by adjusting the pH of the Millipore water solution with either HCl or NaOH. This may also influence the size of the rate constants calculated. The DCD release data from *N*-palmitoyl and *N*-octanoyl chitosan xerogels beads were fitted to the zero-order and first-order models in Figure 5.29 and Figure 5.30 respectively, and the results are exhibited in Tables 5.14 and 5.15 respectively.
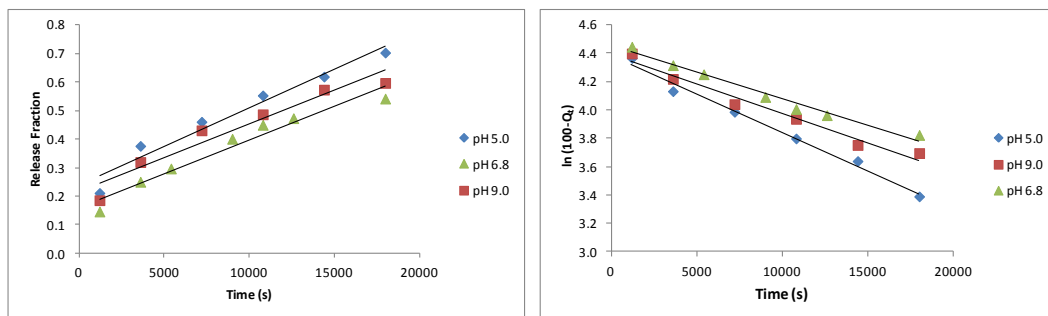
(a)   (b)

Figure 5.29 DCD release data from *N*-palmitoyl chitosan xerogel beads with a degree of substitution of 49% in pH 5.0, pH 6.8 and pH 9.0 release media fitted to the (a) zero-order and (b) first-order models.
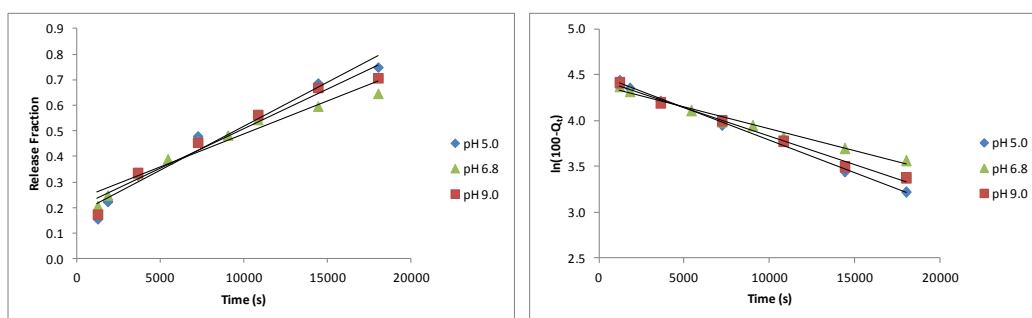
(a)   (b)

Figure 5.30 DCD release data from *N*-octanoyl chitosan xerogel beads with a degree of substitution of 59% fitted in pH 5.0, pH 6.8 and pH 9.0 release media to the (a) zero-order and (b) first-order models.

Table 5.14 Results of fitted data for DCD release from *N*-palmitoyl chitosan xerogel beads with a degree of substitution of 49% in pH 5.0, pH 6.8 and pH 9.0 release media to the zero-order and first order models.

pH of release medium	Zero-Order Model		First-Order Model	
	k_0 (s^{-1})	R^2	k_1 (s^{-1})	R^2
5.0	2.19×10^{-5}	0.9208	5.43×10^{-5}	0.9953
6.8	2.21×10^{-5}	0.9292	3.56×10^{-5}	0.9655
9.0	2.36×10^{-5}	0.9331	4.14×10^{-5}	0.9705

Table 5.15 Results of fitted data for DCD release from *N*-palmitoyl chitosan xerogel beads with a degree of substitution of 59% in pH 5.0, pH 6.8 and pH 9.0 release media to the zero-order and first order models.

pH of release medium	Zero-Order Model		First-Order Model	
	k_0 (s^{-1})	R^2	k_1 (s^{-1})	R^2
5.0	3.45×10^{-5}	0.9665	7.06×10^{-5}	0.9953
6.8	2.45×10^{-5}	0.9451	4.32×10^{-5}	0.9810
9.0	2.58×10^{-5}	0.9320	6.23×10^{-5}	0.9903

By analysing the results in Tables 5.14 and Table 5.15 it is clear that DCD release from *N*-palmitoyl and *N*-octanoyl chitosan xerogel beads is best described by the first-order model at each pH value investigated. DCD release from the beads into pH 5.0 release medium exhibited the highest first-order rate constant for both *N*-palmitoyl and *N*-octanoyl chitosan xerogels respectively (5.43×10^{-5} s^{-1} and 7.06×10^{-5} s^{-1}). DCD

release into the pH 9.0 release had the second highest first order rate constant values, 4.14×10^{-5} s^{-1} and 6.23×10^{-5} s^{-1}, respectively. The fact that release into a pH 9.0 solution had a higher rate constant than release into pH 6.8 may have been due to the ionic strength of the solution, but the effect is not substantial and would require further investigation. Release from the *N*-palmitoyl chitosan xerogel beads exhibited a smaller first-order rate constant than release from *N*-octanoyl chitosan beads at each pH value investigated. The release data was applied to the Higuhci and Korsemeyer-Peppas models to help determine the mechanism of release. The models of DCD release from *N*-palmitoyl chitosan xerogels are exhibited in Figure 5.31 and the resulting data exhibited in Table 5.16. The models of DCD release from *N*-octanoyl chitosan xerogels were exhibited Figure 5.32 and the resulting data exhibited in Table 5.17.
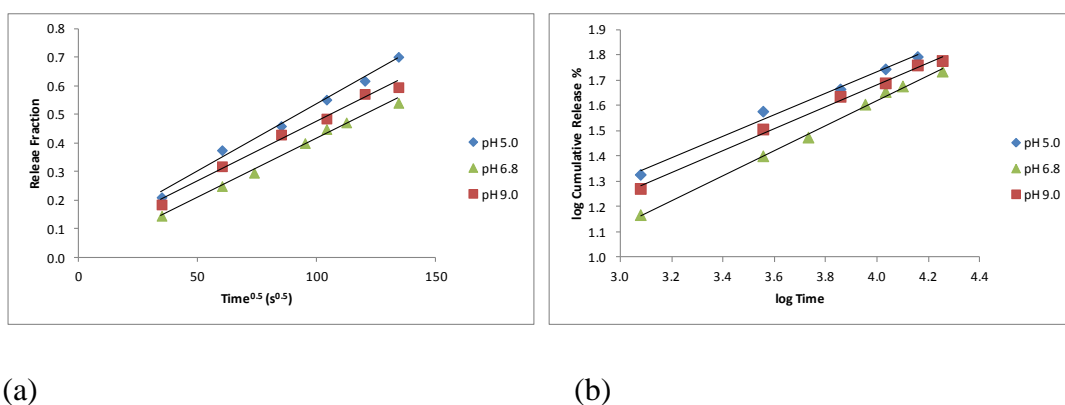
(a)   (b)

Figure 5.31 DCD release data from *N*-palmitoyl chitosan xerogel beads with a degree of substitution of 49% in pH 5.0, pH 6.8 and pH 9.0 release media fitted to the (a) Higuchi model and (b) Korsemeyer-Peppas model.
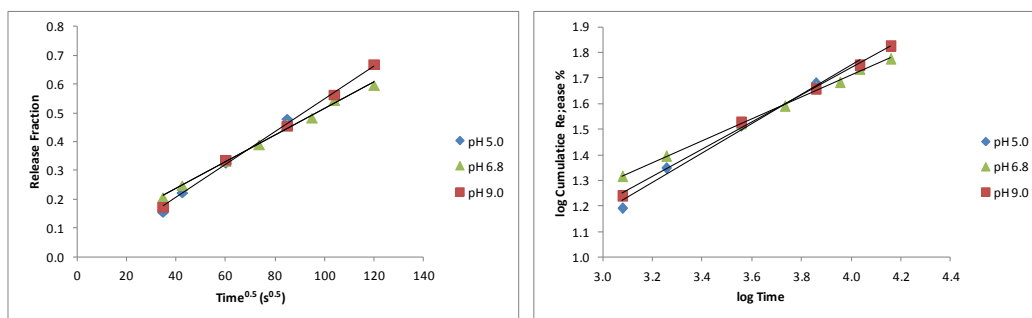
(a)   (b)

Figure 5.32 DCD release data from *N*-octanoyl chitosan xerogel beads with a degree of substitution of 59% in pH 5.0, pH 6.8 and pH 9.0 release media fitted to the (a) Higuchi model and (b) Korsemeyer-Peppas model.

Table 5.16 Results of fitted data for DCD release from *N*-palmitoyl chitosan xerogel beads with a degree of substitution of 48% in pH 5.0, pH 6.8 and pH 9.0 release media to the Higuhci and Korsemeyer-Peppas models.

pH of release medium	Higuchi Model		Korsemeyer-Peppas Model	
	$k_H(\mathrm{s}^{-0.5})$	R^2	n	R^2
5.0	4.64×10^{-3}	0.9880	0.42	0.9998
6.8	4.02×10^{-3}	0.9893	0.46	0.9852
9.0	4.39×10^{-3}	0.9930	0.44	0.9959

Table 5.17 Results from the fitting of DCD release data from *N*-octanoyl chitosan xerogel beads with a degree of substitution of 59% in pH 5.0, pH 6.8 and pH 9.0 release media to the Higuhci and Korsemeyer-Peppas models.

pH of release medium	Higuchi Model		Korsemeyer-Peppas Model	
	$k_H(\text{s}^{-0.5})$	R^2	n	R^2
5.0	5.86×10^{-3}	0.9937	0.56	0.9898
6.8	4.62×10^{-3}	0.9957	0.46	0.9957
9.0	3.90×10^{-3}	0.9648	0.53	0.9959

The results in Tables 5.16 and 5.17 show that DCD release from both *N*-palmitoyl and *N*-octanoyl xerogels fit well to both the Higuhci and Korsemeyer-Peppas models in pH 5.0, pH 6.8 and pH 9.0 release media. As the release data fit well to the Higuchi model and did not alter to any tangible degree depending on the pH we can conclude that diffusion controlled release had a strong influence at all pH release medium values investigated for both *N*-palmitoyl and *N*-octanoyl xerogels. This conclusion was corroborated for *N*-palmitoyl xerogels by the exponent n values calculated for the release data as both acidic and basic pH exponent n values were close to the value that represents pure Fickian diffusion ($n = 0.43$). The exponent n values calculated for DCD release from *N*-octanoyl xerogels however suggested that release was a combination of diffusion and polymer chain relaxation. The biggest difference between the two sets of beads can be seen at the data calculated from the pH 5.0 release medium where the exponent n value of DCD release from *N*-palmitoyl chitosan xerogel beads was 0.42 but for *N*-octanoyl chitosan xerogel beads was 0.56. This suggests the acidic medium was causing polymer chain relaxation in *N*-octanoyl chitosan xerogel beads, however release remained predominantly Fickian. A change in the pH of the release medium is known to influence the exponent n value. When Serra *et al*. fitted the release data of their poly(acrylic acid-g-ethylene glycol) hydrogels to the Korsemeyer-Peppas model they found that by decreasing the pH of the release medium from pH 7.0 to pH 4.5 the value of exponent n dropped from 0.92

to 0.56. This suggests that altering the medium of the pH had a significant effect on the release mechanism of theophylline from the hydrogel beads[32]. The authors attributed the change in mechanism to the ionization of the carboxylic groups in the acrylate structure and the consequent repulsion between polymer chains. It appears that neither the *N*-palmitoyl chitosan beads nor the *N*-octanoyl xerogels examined in this study are subject to the same degree of chain repulsion. It is likely that the *N*-acylation of the amino functional group of chitosan removes that site for protonation which leads to chain repulsion occurring in chitosan polymer in an acidic medium. Hunabutta *et al*. compared the release of theophylline from chitosan matrix tablets in pH 5.0 and pH 6.8 release media using the Higuhci model and reported that at pH 5 the k_H value increased from 0.061 s^{-1} to 0.073 s^{-1} respectively, denoting a faster diffusion release rate[37]. The regression line fit remained at 0.996 for both pH values which lead the authors to conclude that, like the results presented in Table 5.16 and Table 5.17, release was heavily influence by Fickian diffusion[37]. The DCD release data from *N*-palmitoyl and *N*-octanoyl chitosan xerogels beads were fitted using the Sahlin-Peppas model to determine the Fickian diffusion and relaxation contribution. The plots are given in Figure 5.33 and Figure 5.34, respectively, and the results of the analysis are presented in Tables 5.18 and 5.19 respectively.

(a)   (b)
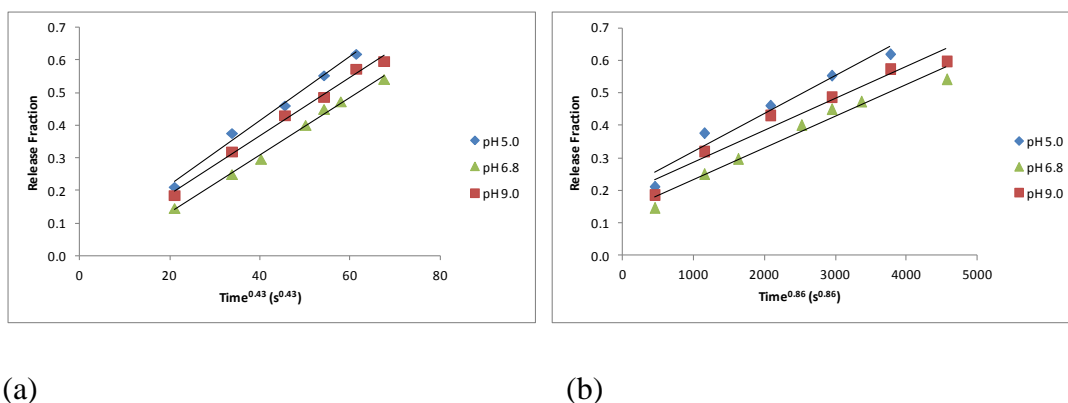
Figure 5.33 DCD Release data from *N*-palmitoyl chitosan xerogel beads with a degree of substitution of 49% in pH 5.0, pH 6.8 and pH 9.0 release media fitted to the Sahlin-Peppas models corresponding to (a) Fickian contribution and (b) polymer chain relaxation contribution.
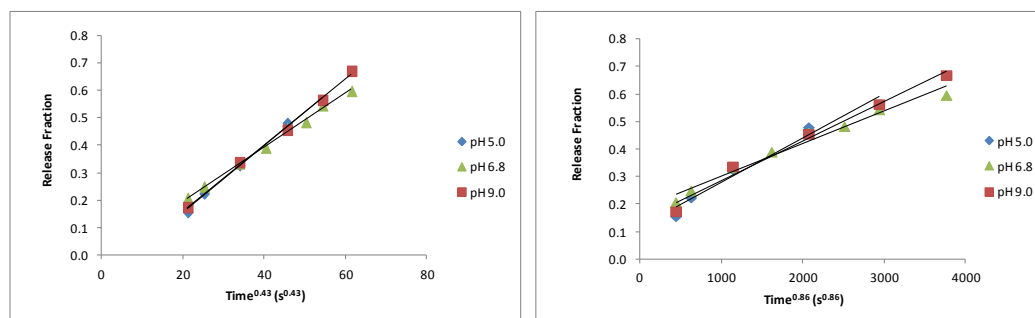
(a)   (b)

Figure 5.34 DCD release data from *N*-octanoyl chitosan xerogel beads with a degree of substitution of 59% in pH 5.0, pH 6.8 and pH 9.0 release media fitted to the Sahlin-Peppas models corresponding to (a) Fickian contribution and (b) polymer chain relaxation contribution.

Table 5.18 Results from the fitting of DCD release data from *N*- palmitoyl chitosan xerogel beads with a degree of substitution of 49% in pH 5.0, pH 6.8 and pH 9.0 release media to the Sahlin – Peppas models.

pH of release medium	Fickian Diffusion Contribution		Relaxation Contribution		Relaxation/ Fickian Ratio
	k_1 (s$^{-0.43}$)	R^2	k_2 (s$^{-0.86}$)	R^2	R/F
5.0	9.85×10^{-3}	0.9915	1.16×10^{-4}	0.9575	0.01
6.8	8.59×10^{-3}	0.9910	9.25×10^{-3}	0.9511	0.01
9.0	9.33×10^{-3}	0.9949	1.11×10^{-4}	0.9856	0.01

Table 5.19 Results from the fitting of DCD release data from *N*- octanoyl chitosan xerogel beads with a degree of substitution of 59% in pH 5.0, pH 6.8 and pH 9.0 release media to the Sahlin – Peppas model.

pH of release medium	Fickian Diffusion Contribution		Relaxation Contribution		Relaxation/ Fickian Ratio
	k_1 (s$^{-0.43}$)	R^2	k_2 (s$^{-0.86}$)	R^2	R/F
5.0	1.22×10^{-2}	0.9961	1.61×10^{-4}	0.9716	0.01
6.8	9.77×10^{-3}	0.9967	1.18×10^{-4}	0.9737	0.01
9.0	1.51×10^{-2}	0.9976	1.11×10^{-4}	0.9856	0.01

Upon fitting the release data to Sahlin-Peppas plots to determine the Fickian and polymer chain relaxation contributions to DCD release from *N*-palmitoyl chitosan xerogel beads it was clear that the pH of the release medium did not have a substantial impact on the release mechanism. At release mediums pH values of 5.0, 6.8 and 9.0 the ratio of release by Case-II transport by polymer chain diffusion to Fickian diffusion remained at 0.01. The Fickian and relaxation rate constants increased slightly between pH 5.0 and pH 6.8 but compared to the differences seen in Fickian and relaxation rate constants in other studies, e.g., the difference seen by varying the palmitoyl chloride concentration in Table 5.13 these changes are very small and would not have had a significant impact on release. The models revealed similar conclusions for DCD release from *N*-octanoyl chitosan at release media pH values of 5.0, 6.8 and 9.0. The ratio between the Fickian and relaxation rate constants are the same for DCD release from all the beads investigated which indicated that a change in the release medium pH did not alter the release mechanism. In addition, it was clear that at all pH release medium values investigated for DCD from *N*-palmitoyl and *N*-octanoyl chitosan xerogel beads that Fickian diffusion was the favoured release mechanism.

5.2.5 Isothermal Kinetic Analysis

The objective of this study was to evaluate the kinetics and mechanism of DCD release from chitosan xerogel beads at various release medium temperatures. These experiments were conducted as previous studies investigating drug release from chitosan formulations and hydrogel beads have shown that increasing the release medium temperature can result in a change in the release properties of the delivery system[38-41]. For example, Yoshizawa *et al*. synthesised films made from chitosan and polyalkyleneoxide maleic acid to be used as a delivery system, they used salicylic acid and phenol as model drugs. They reported that an increase in the release medium temperature causes an increase in the polymer chain relaxation of chitosan which promoted the release of salicylic acid by Case-II transport over Fickian diffusion[39]. Adjnadejevic *et al*. investigated the isothermal kinetics of (*E*)-4-(4-metoxyphenyl)-4-oxo-2-butenoic acid (MEPBA) release from poly(acrylic acid) hydrogels and found that increasing the release medium temperature caused a change in the release mechanism as release of MEPBA became more Fickian in nature[42].

In this research, a study was conducted on *N*-acylated chitosan xerogel beads to determine the isothermal DCD release kinetics and release mechanism of the beads at various release medium temperatures. An identical study was also performed on chitosan xerogels beads synthesised using simple gelation in sodium hydroxide solution for comparison.

5.2.5.1 Study Conditions

 Each experiment was performed in triplicate by placing 10 beads in 500 ml Millipore water at a stated release medium temperature. The 85% deacetylated beads were synthesised using the method outlined in Section 2.2.2.1 *(i)* while the *N*-hexanoyl chitosan beads were synthesized using the method in Section 2.2.3.1 using methanol as the reaction solvent and the *N*-palmitoyl and *N*-octanoyl beads synthesised outlined using the method outlined in Section 2.2.3.2 using acetone as the reaction solvent. It should be noted that the degree of substitution of each set of beads investigated was different and the experimental error of the temperature release medium was ± 0.1 °C.

5.2.5.2 Influence of the Release Medium Temperature on the Kinetics and Mechanism of DCD Release from 85% deacetylated Chitosan Xerogel Beads

The first isothermal kinetic studies were performed on 85% deacetylated chitosan xerogel beads loaded in 60 mM DCD Millipore water solution. The results from these experiments would serve as a reference and comparison tool for the isothermal kinetic data obtained for DCD release from chitosan beads that had undergone an *N*-acylation reaction. The release data were fitted to the zero-order and first-order models (Figure 5.35) and the results are shown in Table 5.20.

(a)   (b)
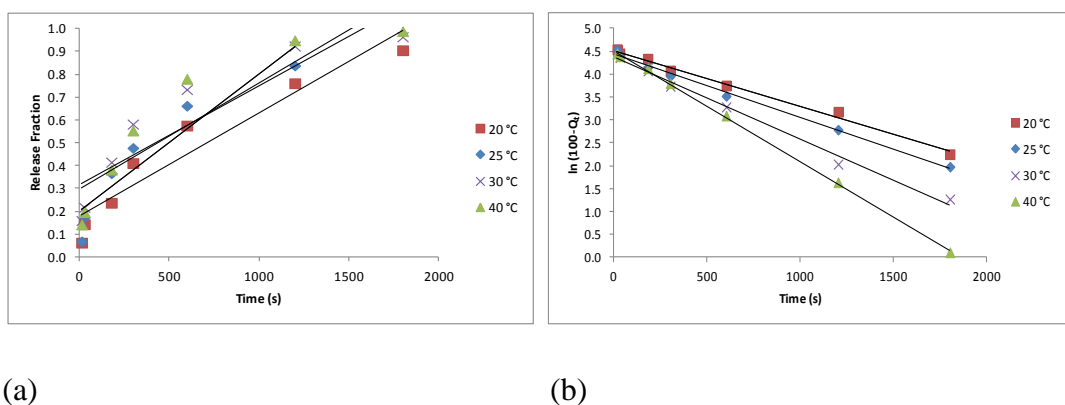
Figure 5.35 DCD release data from 85% deacetylated chitosan xerogel beads fitted to (a) zero-order and first-order models at different release medium temperatures.

Table 5.20 Results from the fitting of DCD release data from 85% deacetylated chitosan xerogel beads at different release medium temperatures to (a) zero-order and (b) first-order models.

Temperature of Release Medium	Zero-Order Model		First-Order Model	
	k_0 (s^{-1})	R^2	k_1 (s^{-1})	R^2
20 °C	4.52×10^{-4}	0.9144	1.23×10^{-3}	0.9925
25 °C	6.20×10^{-4}	0.8777	1.39×10^{-3}	0.9946
30 °C	4.35×10^{-4}	0.8275	1.80×10^{-3}	0.9968
40 °C	4.67×10^{-4}	0.8274	2.43×10^{-3}	0.9991

It is evident from the results of the fitting of release data to the zero-order and first–order model exhibited in Table 5.20 that the best regression line fit for DCD from the beads was for the first-order model at all the release medium temperatures investigated. This compared well with the release medium temperature experiment performed on glyoxal crosslinked chitosan xerogel beads (as outlined in Section 4.2.3.7) as both studies indicated that first-order kinetics was the best fitting model at each release medium temperature studied. As the release medium temperature increased so too did the first-order rate constant, at a release temperature of 20 °C the first-order rate constant is 1.23×10^{-3} s^{-1}, whilst at the highest release temperature investigated, 40 °C, the rate constant had increased to 2.43×10^{-3} s^{-1}. The temperature of the release medium was clearly influencing the rate constant of DCD release. The release data were then fitted to the Higuchi and Korsemeyer-Peppas models to further investigate the mechanism of release (Figure. 5.36) and the results are exhibited in Table 5.21.
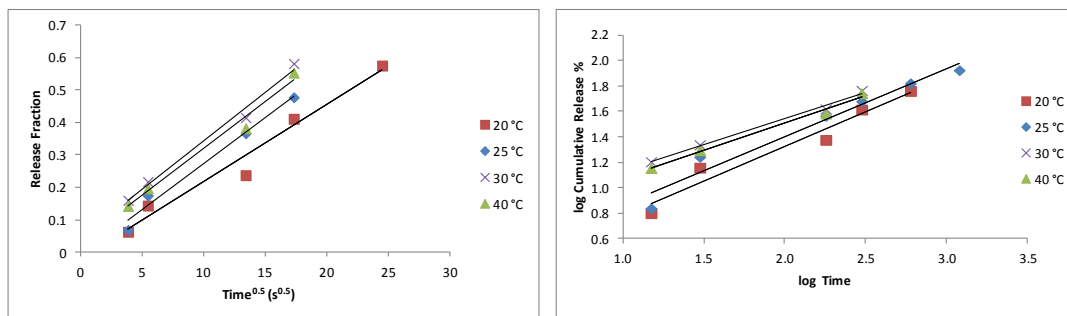
(a)   (b)

Figure 5.36 DCD release data from 85% deacetylated chitosan xerogel beads fitted to the (a) Higuchi (b) Korsmeyer – Peppas models. The studies were carried out at the stated release medium temperature.

Table 5.21 Results from the fitting of DCD release data from 85% deacetylated chitosan xerogel beads to the Higuchi and Korsemeyer-Peppas models.

Temperature of Release Medium	Higuchi Model		Korsemeyer-Peppas Model	
	k_H (s$^{-0.5}$)	R^2	n	R^2
20 °C	2.39×10^{-2}	0.9678	0.55	0.9508
25 °C	2.85×10^{-2}	0.9821	0.53	0.9371
30 °C	2.89×10^{-2}	0.9824	0.43	0.9895
40 °C	2.99×10^{-2}	0.9876	0.41	0.9948

The results from the fitting of the release data to the Higuchi and Korsemeyer-Peppas models in Table 5.21 show that the data has a good fit for the Higuchi model at each release medium temperature investigated. This suggested release occurred by a diffusion controlled release process. As the temperature of the release medium increases so too does the kinetic Higuchi constant, k_H, which indicates that there was an increase in the rate of the diffusion controlled release. At release medium temperatures of 20 °C and 25 °C the value of exponent n obtained indicates Fickian diffusion was the predominant mechanism of an overall anomalous transport

mechanism. However, when the release medium temperature was set at 30 °C the drug transport mechanism moved from anomalous diffusion closer towards the pure Fickian diffusion value ($n = 0.43$) and then at 40 °C entered n values incapable of being described by the Korsemeyer-Peppas model. Obtaining values for exponent n below those capable of being described by the Korsemeyer-Peppas model does not mean there has been a change in the release mechanism; on the contrary, literature suggests that obtaining values below $n = 0.43$ indicates that the release exhibited Fickian diffusional characteristics. Ahuja *et al*. obtained exponent n values between 0.22 and 0.84 for release of the model drug, Rofecoxib, from a wide range of water soluble carriers. They concluded that release with an exponent n value below the value corresponding to pure Fickian diffusion, exhibited Fickian diffusion characteristics[43].   In addition, Wu *et al*. synthesised disulfide-crosslinked chitosan hydrogels for controlled protein release and they observed values for exponent n below 0.43 and concluded that the release mechanism was diffusion controlled[44]. The size distribution and general shape of the bead have been suggested as factors which influence the exponent n value[45]. The work presented by Adnadjevic *et al*. investigated the release of (E)-4-(4-metoxyphenyl)-4-oxo-2-butenoic acid from poly(acrylic acid) hydrogels and they observed decreasing exponent n values as the temperature of the release medium increased[42].

The release data were then fitted to the Peppas-Sahlin Fickian diffusion and polymer chain relaxation models to determine their respective contributions to DCD release (Figure 5.37) and the results are exhibited in Table 5.22.

(a)   (b)
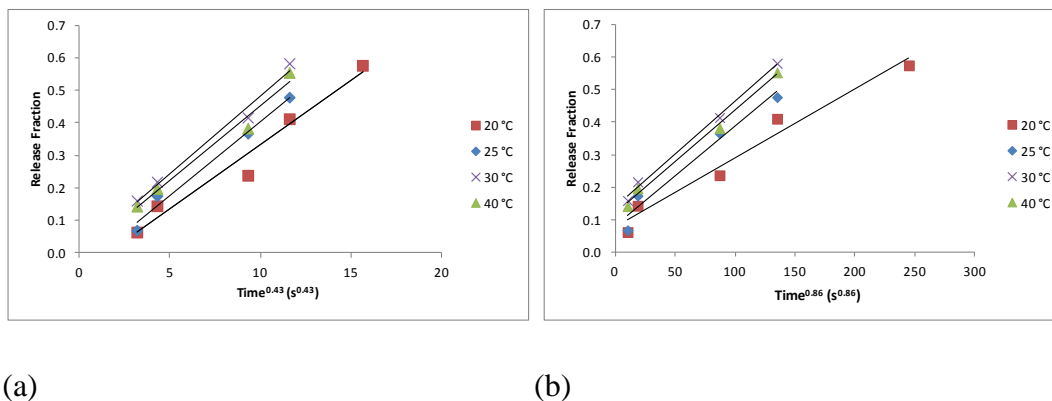
Figure 5.37 DCD release data from 85% deacetylated chitosan xerogel beads at different release medium temperatures fitted to the Sahlin-Peppas (a) Fickian contribution (b) polymer chain relaxation contribution models.

Table 5.22 Results from the fitting of DCD release data from 85% deacetylated chitosan xerogel beads at different release medium temperatures to the Peppas-Sahlin models.

Temperature of Release Medium	Fickian Diffusion Contribution		Relaxation Contribution		Relaxation/ Fickian Ratio
	k_1 (s$^{-0.43}$)	R^2	k_2 (s$^{-0.86}$)	R^2	R/F
20 °C	0.039	0.9618	2.12×10^{-3}	0.9689	0.05
25 °C	0.046	0.9846	3.05×10^{-3}	0.9619	0.07
30 °C	0.046	0.9783	3.15×10^{-3}	0.9941	0.07
40 °C	0.047	0.9842	3.25×10^{-3}	0.9952	0.07

It is evident from the results displayed in Table 5.22 that as the release medium temperature increased the rate constant for both the Fickian diffusion contribution and relaxation contribution increased. In addition, over the release medium temperature range studied the Relaxation/Fickian Ratio increased slightly. However this increase was not considered significant as the value remained low at all temperatures investigated indicating that diffusion was the primary mechanism of release.

5.2.5.3 Influence of the Release Medium Temperature on the Kinetics and Mechanism of DCD Release from *N*-Hexanoyl Chitosan Xerogel Beads

Isothermal kinetic studies were performed on DCD release from *N*-hexanoyl chitosan xerogels that had undergone *N*-substitution in 1.0 M hexanoic anhydride solution. The release data were fitted to the zero-order and first-order models to investigate the release kinetics (Figure. 5.38) and the results are exhibited in Table 5.23.

(a)   (b)
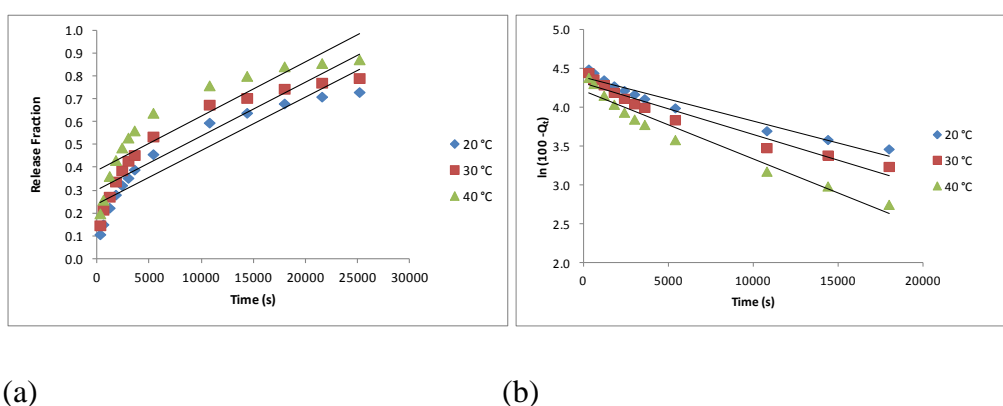
Figure 5.38 DCD release data from *N*-hexanoyl chitosan xerogel beads at different release medium temperatures fitted to (a) zero-order and (b) first-order models.

Table 5.23 Results from the fitting of DCD release data from *N*-hexanoyl chitosan xerogel beads to the zero-order and first-order models at different release medium temperatures.

Temperature of Release Medium	Zero-Order Model		First-Order Model	
	k_0 (s^{-1})	R^2	k_1 (s^{-1})	R^2
20 °C	2.34×10^{-5}	0.8704	4.75×10^{-5}	0.9500
30 °C	2.37×10^{-5}	0.8478	5.55×10^{-5}	0.9453
40°C	2.40×10^{-5}	0.8052	7.29×10^{-5}	0.9468

The results in Table 5.23 show the best regression line fit for the release of DCD from *N*-hexanoyl chitosan xerogel beads at each release temperature is for the first-order model. However, the first-order fits are not as good as for the other beads examined in this chapter. The plot in Figure 5.38 (b) appears to have a burst release phase and a slow release phase. This is an indication that DCD release from the *N*-hexanoyl chitosan xerogel beads was a two-step process. It was also apparent by comparing these results to DCD release from 85% deacetylated chitosan that the first-order rate constants had been substantially reduced at all the release medium temperatures investigated. This was attributed to the *N*-acylation of the chitosan xerogel beads which was shown in Section 5.2.2.1 to slow the release of DCD from the beads. As expected, an increase in the release medium temperature caused the first-order rate constant to increase from 4.75×10^{-5} s^{-1} at 20 °C to 7.29×10^{-5} s^{-1} at 40 °C. The release data were fitted to the Higuchi and Korsemeyer-Peppas models to further investigate the DCD release mechanism (Figure. 5.39) and the results are exhibited in Table 5.24.

(a)   (b)
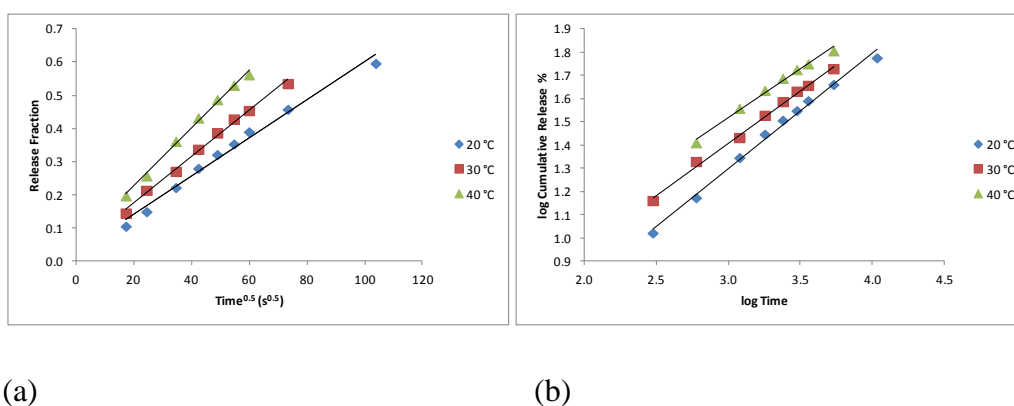
Figure 5.39 DCD release data from *N*-hexanoyl chitosan xerogel beads at different release medium temperatures fitted to the (a) Higuchi and (b) Korsmeyer –Peppas models.

Table 5.24 Results from the fitting of DCD release data from *N*-hexanoyl chitosan xerogel beads at different release medium temperature to the Higuchi and Korsemeyer-Peppas release models.

Temperature of Release Medium	Higuchi Model		Korsemeyer-Peppas Model	
	$k_H(\text{s}^{-0.5})$	R^2	n	R^2
20 °C	5.75×10^{-3}	0.9874	0.50	0.993
30 °C	6.97×10^{-3}	0.9947	0.45	0.9961
40 °C	8.76×10^{-3}	0.9960	0.43	0.9982

The results presented in Table 5.24 indicate that the release data fits well to the Higuchi model which meant that Fickian diffusion was the primary release mechanism of DCD from the *N*-hexanoyl chitosan xerogel beads. The data shows that as the temperature of the release medium increased so too did the kinetic constant, K_H, value which indicates there was an increase in the rate of DCD release by Fickian diffusion due to an increase in release medium temperature. All the exponent n values obtained were within the range applicable to the Korsemeyer-Peppas model. The value of exponent n obtained for all medium release temperatures suggested DCD release was strongly influenced by Fickian diffusion. The exponent n values decreased slightly towards the value representing pure Fickian release ($n = 0.43$) as the release medium temperature increased. This indicated that the release medium temperature had a small influence on the mechanism of release. A similar decrease in the exponent n values as the temperature of the release medium increased was also seen in Section 5.2.5.2 for DCD release from 85% deacetylated chitosan xerogel beads. The release data were fitted to the Sahlin-Peppas model and the plots exhibited in Figure 5.40. The results are shown in Table 5.25
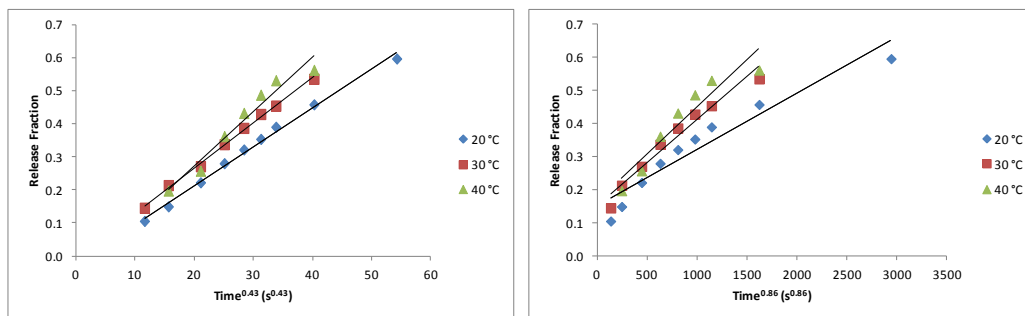
(a)   (b)

Figure 5.40 DCD release data from *N*-hexanoyl chitosan xerogel beads at different release medium temperature fitted to the Sahlin-Peppas (a) Fickian contribution (b) Polymer chain relaxation contribution models.

Table 5.25 Results from the fitting of DCD release data from *N*-hexanoyl chitosan xerogel beads at different release medium temperatures to the Peppas-Sahlin release models.

Temperature of Release Medium	Fickian Diffusion Contribution		Relaxation Contribution		Relaxation /Fickian Ratio
	k_1 (s$^{-0.43}$)	R^2	k_2 (s$^{-0.86}$)	R^2	R/F
20 °C	1.17×10^{-2}	0.9942	1.70×10^{-4}	0.9178	0.01
30 °C	1.36×10^{-2}	0.9969	2.59×10^{-4}	0.9597	0.02
40°C	1.68×10^{-2}	0.9977	3.64×10^{-4}	0.9720	0.02

From the data displayed in Table 5.25 it is apparent that as the release medium temperature increased the relaxation/Fickian ratio essentially remained the same. At each temperature investigated the Fickian diffusion contribution clearly remained the dominant release mechanism. The regression line fit for the Fickian diffusion contribution was satisfactory at each temperature; however the regression line fits for the relaxation contribution were not as good. For example, the R^2 value, was 0.9178 at a release medium temperature of 20 °C. Comparing the data obtained for the DCD release from *N*-hexanoyl chitosan xerogel beads in Table 5.23 with DCD release from

85% deacetylated chitosan in Table 5.22 at a release medium temperature of 40 °C the relaxation/Fickian ratio of DCD release from *N*-hexanoyl chitosan beads was 0.02, however the equivalent value for 85% deacetylated chitosan xerogels was 0.07. This suggested that the *N*-substitution of the glucosamine unit of the chitosan polymer promoted DCD release by Fickian diffusion over case-II transport caused by polymer chain relaxation. This was likely to be influenced by the rearrangement of the chitosan sheets from an anti-parallel structure to a parallel one which is known to occur in *N*-acylated chitosan, this would have hindered polymer chain relaxation[2]. Despite the 85% deacetylated chitosan xerogels possessing a marginally higher relaxation/Fickian ratio, DCD release from all the beads investigated at each release medium temperature was dominated by Fickian diffusion.

5.2.5.4 Influence of the Release Medium Temperature on the Kinetics and Mechanism of DCD Release from *N*-Palmitoyl Chitosan Xerogel Beads

The next isothermal kinetic studies were performed on *N*-palmitoyl chitosan xerogel beads which were reacted with 0.8 M palmitoyl chloride and loaded in a 60 mM DCD Millipore water solution. The degree of substitution was determined to be 49% in Section 5.2.3.2. The release data were fitted to the zero-order and first-order models to further investigate the release model (Figure 5.31) and the results are exhibited in Table 5.26.

(a)   (b)
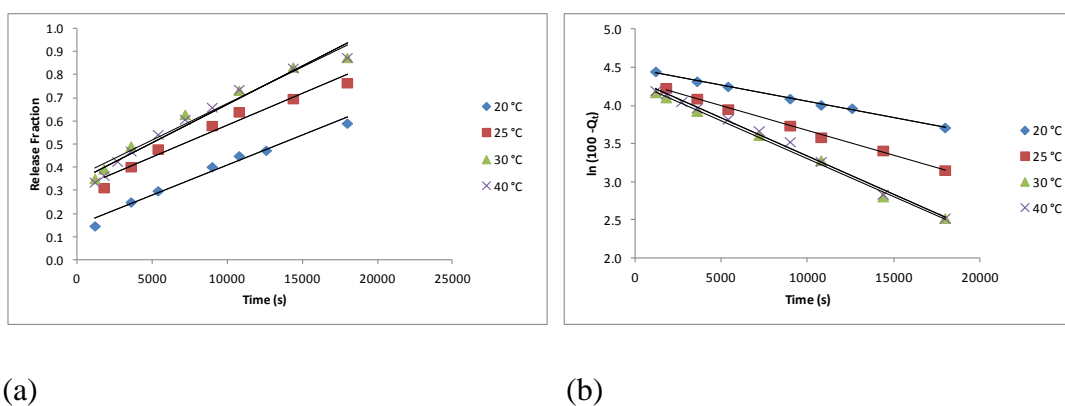
Figure 5.41 DCD release data from *N*-palmitoyl chitosan xerogel beads at different release medium temperatures fitted to (a) zero-order and (b) first-order models.

Table 5.26 Results from the fitting of DCD release data from *N*-palmitoyl chitosan xerogel beads at different release medium temperatures to the (a) zero-order and (b) first-order models.

Temperature of Release Medium	Zero-Order Model		First-Order Model	
	k_0 (s^{-1})	R^2	k_1 (s^{-1})	R^2
20 °C	2.25×10^{-5}	0.9292	3.56×10^{-5}	0.9655
25 °C	2.73×10^{-5}	0.9637	6.53×10^{-5}	0.9967
30 °C	3.17×10^{-5}	0.9657	9.89×10^{-5}	0.9966
40 °C	3.31×10^{-5}	0.9672	1.01×10^{-4}	0.9947

It is evident from the results that the best regression line fit for DCD release from *N*-palmitoyl chitosan xerogel beads at 20 °C is for the first-order model. This indicates that release took place by a similar mechanism to 85% deacetylated chitosan xerogels and *N*-hexanoyl chitosan xerogel beads, which was by a membrane controlled diffusion system where the gradient is reduced due to decreasing concentration on the donor side in combination with sink conditions in the release medium. Similar to this study, Kiortis *et al*. found that making their cellulose tablet release system more hydrophobic influenced the rate constant but not the release mechanism [34]. However, it is worth noting that the regression line fit for the zero-order model is better for DCD release from *N*-palmitoyl chitosan xerogel beads than from 85% deacetylated chitosan beads especially at release medium temperatures above 20 °C. At a release medium temperature of 40 °C for example, the R^2 value for release by zero-order process for *N*-palmitoyl chitosan xerogel beads is 0.9672 compared with 0.8274 at the same temperature for DCD release from 85% deacetylated chitosan xerogel beads. As the release medium temperature increases, so too does the first-order rate constant. It should be noted however, that there was only a small increase in the first-order rate constant between release in a 30 °C and 40 °C medium. At a release temperature of 20

°C the first-order rate constant is 3.56×10^{-5} s^{-1}, whilst at the highest release temperature recorded, 40 °C, the rate constant is 1.01×10^{-4} s^{-1}, which represents an increase by a factor of 2.8. This is a larger increase in the rate constant than what was observed for DCD release from 85% deacetylated chitosan xerogels (rate constant increased by a factor of 2.0) or from the *N*-hexanoyl chitosan xerogel beads (rate constant increased by factor of 1.5). This suggested that DCD release from the *N*-palmitoyl chitosan xerogel beads was more sensitive to changes in release medium temperatures than DCD release from 85% deacetylated or *N*-hexanoyl chitosan xerogel beads. The release data were fitted to the Higuchi and Korsemeyer-Peppas models to further investigate the mechanism of release (Figure. 5.42). The results are exhibited in Table 5.27.

(a)   (b)
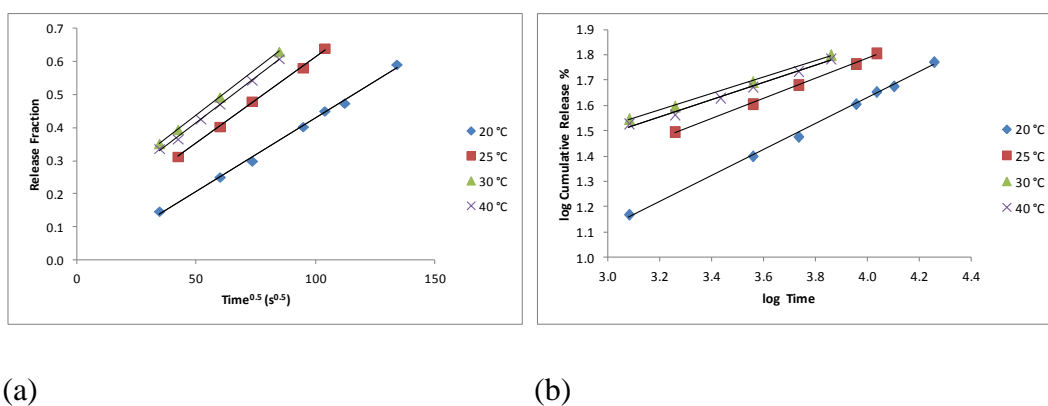
Figure 5.42 DCD Release data from *N*-palmitoyl chitosan xerogel beads at different release medium temperatures fitted to the (a) Higuchi (b) Korsmeyer –Peppas models.

Table 5.27 Results from the fitting of DCD release data from *N*-palmitoyl chitosan xerogel beads at different release medium temperatures to the Higuchi and Korsemeyer-Peppas release models

Temperature of Release Medium	Higuchi Model		Korsemeyer-Peppas Model	
	$k_H(\text{s}^{-0.5})$	R^2	n	R^2
20 °C	3.52×10^{-3}	0.9623	0.46	0.9852
25 °C	5.26×10^{-3}	0.9985	0.40	0.9979
30 °C	5.54×10^{-3}	0.9999	0.33	0.9977
40 °C	5.45×10^{-3}	0.9957	0.33	0.9898

The results in Table 5.27 show that as the release medium temperature increased so did the kinetic constant, k_H, value which shows that an increase in the release medium temperature caused an increase in the Higuchi rate constant. The Higuchi model exhibits good regression line fits, which indicates that Fickian diffusion was a part of the release mechanism. Only at 20 °C does the value of exponent n obtained fit the Korsemeyer-Peppas model. At all other release medium temperatures the exponent n obtained cannot be explained by the Korsemeyer-Peppas model as they are below the value attributed to pure Fickian diffusion ($n = 0.43$). However, as stated previously, authors describe release systems with exponent n values below $n = 0.43$ as having Fickian diffusion characteristics[43]. Torre *et al*. concluded that their chitosan and poly(acrylic acid) release complexes exhibited exponent n values below 0.43 due to a high initial burst release[46], however as the *N*-palmitoyl chitosan xerogels do not have a high initial bust release this can be discounted as a reason for the low exponent n values. As the exponent n values are known to be influenced by the shape of the release system[45] it was theorized that the increase in the release medium temperature may have had an effect on the spherical shape of the beads. The release data were then fitted to the Sahlin-Peppas Fickian diffusion and polymer chain relaxation models to determine their respective contributions to DCD release (Figure 5.43) and the results are exhibited in Table 5.28.

(a)   (b)
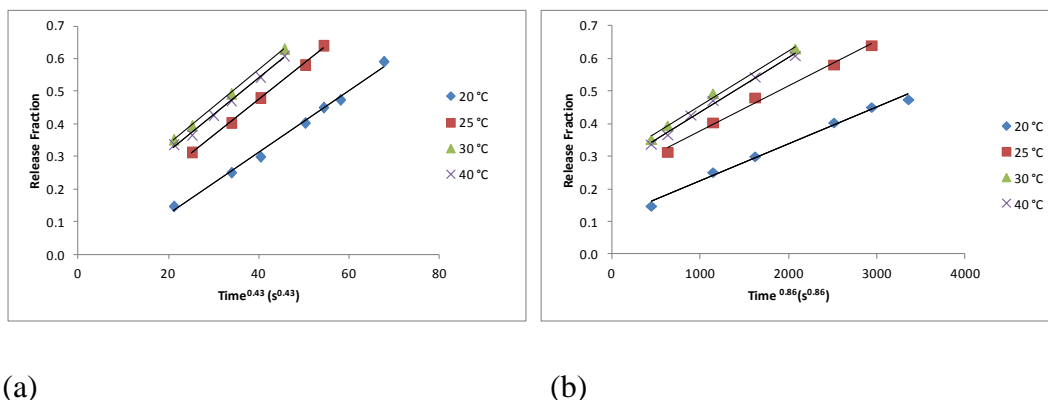
Figure 5.43 DCD release data from *N*-palmitoyl chitosan xerogel beads at different release medium temperatures fitted to the Sahlin-Peppas (a) Fickian contribution (b) polymer chain relaxation contribution models.

Table 5.28 Results from the fitting of DCD release data from *N*-palmitoyl chitosan xerogel beads at different release medium temperatures to the Sahlin-Peppas (a) Fickian contribution (b) Polymer chain relaxation contribution models.

Temperature of Release Medium	Fickian Diffusion Contribution		Relaxation Contribution		Relaxation/ Fickian Ratio
	k_1 (s$^{-0.43}$)	R^2	k_2 (s$^{-0.86}$)	R^2	R/F
20 °C	8.59×10^{-3}	0.9910	1.06×10^{-4}	0.9912	0.01
25 °C	1.11×10^{-2}	0.9981	1.38×10^{-4}	0.9919	0.01
30 °C	1.14×10^{-2}	0.9995	1.68×10^{-4}	0.9939	0.02
40 °C	1.12×10^{-2}	0.9970	1.67×10^{-4}	0.9921	0.02

As it may be seen from the results displayed in Table 5.28 as the release medium temperature increased, the relaxation/Fickian ratio stayed essentially the same. This indicated that an increase in the release medium temperature did not alter the

mechanism of DCD release from the beads. Comparing the relaxation/Fickian ratio for palmitoyl chitosan with those obtained for 85% deacetylated chitosan xerogels exhibited it was clear that Fickian diffusion was the predominant DCD release mechanism for both sets of beads. However, DCD release from *N*-palmitoyl chitosan xerogel beads possessed a slightly higher Fickian diffusion contribution at all release medium temperatures investigated. When the release medium temperature was 40 °C, the calculated relaxation/Fickian ratio value for palmitoyl chitosan was 0.02, whilst for 85% deacetylated chitosan xerogels it was 0.07, representing a small decrease in favour of Fickian diffusion for DCD release from *N*-palmitoyl chitosan xerogels. Combined with the results from Table 5.27 these results are another indication that the DCD transport mechanism was controlled by Fickian diffusion in all investigated cases.

5.2.5.5 Influence of the Release Medium Temperature on the Kinetics and Mechanism of DCD Release from *N*-Octanoyl Chitosan Xerogel Beads

The next isothermal kinetic studies were performed on DCD release from *N*-octanoyl chitosan xerogel beads that had undergone *N*-substitution in 0.8 M octanoyl chloride solution. The degree of substitution was determined to be 59% in Section 5.2.3.2. The release data were fitted to the zero-order and first-order models to investigate the release mechanism (Figure. 6.13) and the results are exhibited in Table 5.29.
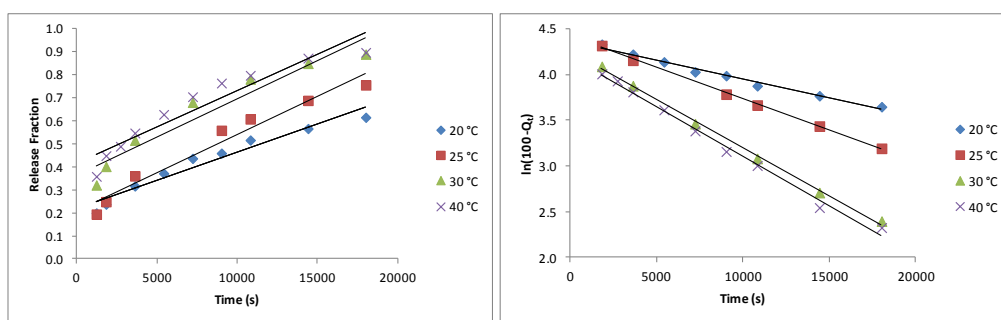
(a)   (b)

Figure 5.44 DCD Release data from *N*-octanoyl chitosan xerogel beads at different release medium temperatures fitted to (a) zero-order and (b) first-order models.

Table 5.29 Results of fitted data for DCD release from *N*-octanoyl chitosan xerogel beads at different release medium temperatures to (a) zero-order and (b) first-order models.

Temperature of Release Medium	Zero-Order Model		First-Order Model	
	k_0 (s^{-1})	R^2	k_1 (s^{-1})	R^2
20 °C	2.45×10^{-5}	0.9470	4.34×10^{-5}	0.9829
25 °C	3.33×10^{-5}	0.9616	7.00×10^{-5}	0.9976
30 °C	3.39×10^{-5}	0.9236	1.08×10^{-4}	0.9963
40 °C	3.77×10^{-5}	0.9612	1.19×10^{-4}	0.9976

The results in Table 5.29 indicate that the best regression line fit for *N*-octanoyl chitosan xerogel beads at all release medium temperatures investigated was for the first-order model. Similar to DCD release from the *N*-palmitoyl chitosan xerogel beads the linear regression line fits for the zero-order model were better than previous results for 85% deacetylated chitosan xerogel beads (Table 5.20). As the release medium temperature increased so too did the first-order rate constant. Like the first order rate constants calculated for DCD release from *N*-palmitoyl chitosan xerogel beads, the smallest increase in the rate-constant is seen between 30 °C and 40 °C. At a release temperature of 20 °C the first-order rate constant is 4.34×10^{-5} s^{-1} whilst at the highest release temperature recorded, 40°C, the rate constant is 1.19×10^{-4} s^{-1}, which represented an increase in rate constant of a factor of 2.7. This value is comparative to the increase in the rate constant of DCD release from *N*-palmitoyl chitosan xerogel beads which increased over the same temperature range by a factor of 2.8. It is apparent that there was very little difference between the first-order rate constants obtained for DCD release from *N*-palmitoyl and from *N*-octanoyl chitosan xerogel beads. For example at a release medium temperature of 20 °C DCD release from *N*-octanoyl chitosan had a first-order rate constant of 4.34×10^{-5} s^{-1} and at the same

temperature *N*-palmitoyl chitosan had a rate constant of 3.56×10^{-5} s^{-1}. At 40 °C, DCD release from *N*-palmitoyl chitosan xerogel beads exhibited an almost identical rate constant to that of DCD release from the *N*-octanoyl chitosan (1.01×10^{-4} s^{-1} compared to 1.19×10^{-4} s^{-1}). The release data were then fitted to the Higuchi and Korsemeyer-Peppas models to further investigate the mechanism of release (Figure. 5.45) and the results are exhibited in Table 5.30.
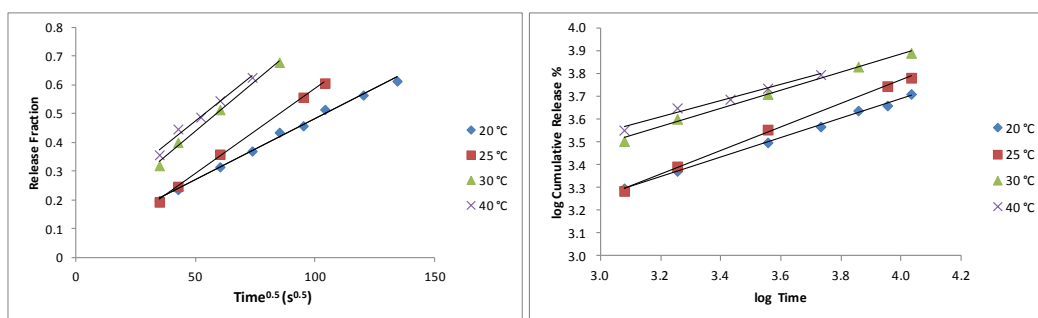
(a)   (b)

Figure 5.45 DCD Release data from *N*-octanoyl chitosan xerogel beads at different release medium temperatures fitted to the (a) Higuchi (b) Korsmeyer–Peppas models.

Table 5.30 Results from the fitting of DCD release data from *N*-octanoyl chitosan xerogel beads at different release medium temperatures to the (a) Higuchi (b) Korsmeyer –Peppas models.

Temperature of Release Medium	Higuchi Model		Korsemeyer-Peppas Model	
	k_H(s$^{-0.5}$)	R^2	n	R^2
20 °C	4.37×10^{-3}	0.9957	0.42	0.9981
25 °C	5.66×10^{-3}	0.9988	0.51	0.9980
30 °C	5.76×10^{-3}	0.9951	0.41	0.9947
40 °C	5.96×10^{-3}	0.9818	0.36	0.9818

The results in Table 5.30 show that the Higuchi model exhibited a good regression line fit for the release data which indicates that Fickian diffusion was a substantial part of the release mechanism. It is also evident that as the release medium temperature increased so did the kinetic constant value which indicated there was an increase in the rate of release by diffusion as release medium temperature increased. In general, the exponent n values obtained were quite similar to those determined using their *N*-palmitoyl chitosan counterparts (Table 5.27). For example, at a release temperature of 40 °C the exponent n for DCD release from *N*-octanoyl chitosan xerogels was 0.36 whilst for palmitoyl chitosan xerogels it was 0.33. Similar to DCD release from *N*-palmitoyl chitosan xerogel beads, as the release medium temperature increased the drug transport mechanism moved away from anomalous release towards exponent n values incapable of being described by the Korsemeyer-Peppas model with the exception of 25 °C, where the exponent n indicated Fickian diffusion dominated release. The release data were fitted to the Sahlin-Peppas Fickian diffusion and polymer chain relaxation models to determine their respective contributions to DCD release (Figure 5.46). The results are exhibited in Table 5.31.

(a)   (b)
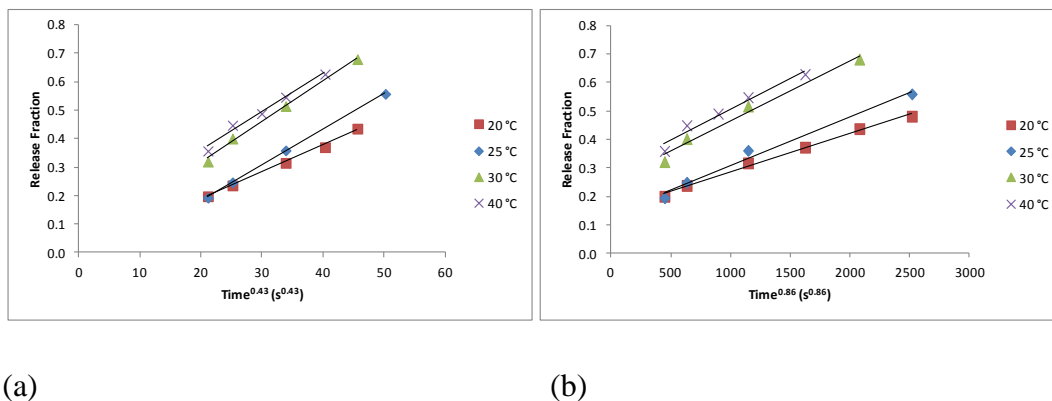
Figure 5.46 DCD Release data from *N*-octanoyl chitosan xerogel beads at different release medium temperatures fitted to the Sahlin-Peppas (a) Fickian contribution (b) Polymer chain relaxation contribution models.

Table 5.31 Results from the fitting of DCD Release data from *N*-octanoyl chitosan xerogel beads at different release medium temperatures to the Sahlin-Peppas (a) Fickian contribution (b) Polymer chain relaxation contribution models.

Temperature of Release Medium	Fickian Diffusion Contribution		Relaxation Contribution		Relaxation/Fickian Ratio
	k_1 (s$^{-0.43}$)	R^2	k_2 (s$^{-0.86}$)	R^2	R/F
20 °C	9.08×10^{-3}	0.9967	1.01×10^{-4}	0.9641	0.01
25 °C	1.24×10^{-2}	0.9997	1.61×10^{-4}	0.9874	0.01
30 °C	1.04×10^{-2}	0.9965	2.11×10^{-4}	0.9803	0.02
40 °C	1.35×10^{-2}	0.9841	2.17×10^{-4}	0.9636	0.02

It is apparent from the results displayed in Table 5.31 that as the release medium temperature increased there was essentially no change in the relaxation/Fickian ratio. This indicates that the increase in the release medium temperature had no effect on the DCD release mechanism and Fickian diffusion dominated the release mechanism. Comparing the relaxation/Fickian ratio for DCD from *N*-octanoyl chitosan xerogel

beads with those obtained for *N*-palmitoyl chitosan in Table 5.28 it was clear that both possessed very similar relaxation/Fickian ratios. For example, when the release medium temperature is 20 °C, the relaxation/Fickian ratio values for *N*-palmitoyl chitosan xerogels and *N*-octanoyl chitosan xerogels are both calculated to be 0.01.

5.3 Conclusions

In this chapter chitosan hydrogel beads were successfully substituted in their solid state to form *N*-acylated chitosan xerogel beads. The successful acylation of chitosan at the amino function group was confirmed by FT-IR analysis. The spectra obtained showed increased intensity of the vibrational bands at 2920 cm^{-1} and 2940 cm^{-1} ν(CH$_3$ and CH$_2$) and the broad vibrational band at 1640 cm^{-1} disappeared and two separate bands appeared at 1655 cm^{-1} and 1555 cm^{-1} ν(C=O and *N*-acyl).

The solid state substitution of chitosan hydrogel beads with acyl chlorides or acidic anhydrides resulted in regioselective acylation of the chitosan at the amino site. The FT-IR spectrum obtained for the *N*-acylation reaction of chitosan with acyl chlorides was also shown to be influenced by the solvent used in the reaction.

DSC thermograms of the *N*-acylated chitosan confirmed that the substituted chitosan polymer degraded at a higher temperature compared with the chitosan polymer starting material as was expected from literature investigations. The temperature at which water loss occurred also decreased as the concentration of hexanoic anhydride in the reaction solution increased which may have been dues to the increased hydrophobicity of the *N*-acylated chitosan beads.

Studies on the surface morphology of *N*-acylated chitosan xerogel beads formed by substitution of chitosan hydrogels with hexanoic anhydride showed that the loading solvent influenced the surface morphology of the bead. While studies on the *N*-acylation of chitosan with palmitoyl chloride showed that the reaction solvent could also affect the beads surface morphology. The beads *N*-acylated using DCM as the reaction solvent had a highly porous surface but when THF, acetone or DMSO was used as the reaction solvent a smoother surface morphology was obtained. It was concluded the *N*-acylation reaction favoured a polar solvent.

Determining the degree of substitution using elemental analysis confirmed that the higher the concentration of acyl chloride in the reaction mixture, the higher the degree of substitution of the chitosan polymer. Experimental analysis also indicated that the length of the aliphatic chain to be substituted onto the chitosan polymer influenced the

degree of substitution, as the longer the chain the less substitution was achieved. It was also concluded that compared to similar research conducted by other authors, the degree of substitution achieved by this research was relatively high due to the post-functionalisation of the hydrogel beads.

Swelling studies indicated that *N*-acylation of the chitosan polymer had reduced the swelling ratio (%) of all the beads examined, compared with chitosan xerogels synthesised using the starting material chitosan only. It was confirmed that the greater the concentration of acidic anhydride or acyl chloride in the reaction mixture, the lower the swelling ratio of the resulting chitosan xerogels.

Release profiles indicated that *N*-palmitoyl, *N*-octanoyl and *N*-hexanoyl chitosan xerogel beads all exhibited increased DCD release times, when compared with chitosan xerogels made from 85% deacetylated chitosan precipitated in NaOH as the equilibrium release time was extended from minutes to hours. The DCD equilibrium release time of *N*-acylated chitosan xerogel beads compared well with release from glyoxal crosslinked hydrogel beads (Section 3.2.4.3). For example, the equilibrium release time of DCD from *N*-hexanoyl chitosan xerogel beads was 6 h, the same time as chitosan xerogel beads crosslinked in 300 mM glyoxal solution. In addition, the release mechanism of DCD from the *N*-acylated beads was attributed to Fickian diffusion.

A study of the isothermal kinetics of DCD release from *N*-acylated chitosan xerogel beads revealed that the first-order model had the best regression line fit in all the release studies performed. The data also indicated that DCD release from all the *N*-acylated chitosan xerogel beads and 85% deacetylated chitosan beads had good regression line fits for the Higuchi model at each release medium temperature investigated. This indicated that diffusion was the dominant release mechanism of DCD release from all the chitosan xerogel bead formulations investigated. Fitting the release data to the Korsemeyer-Peppas model revealed a general trend; that as the release medium temperature increased, the exponent n value decreased. The exponent n values calculated at different release medium temperatures for DCD release from 85% deacetylated chitosan xerogel beads and for *N*-hexanoyl xerogel beads showed that release was predominantly due to Fickian diffusion at all the release medium

temperatures investigated. However, when the release medium temperature was set above 25 °C the exponent n value of *N*-octanoyl chitosan xerogel beads calculated were below the values applicable to the Korsemeyer-Peppas model, likewise for release medium temperatures above 20 °C for *N*-palmitoyl chitosan xerogel beads.

When the release data from all the studies was applied to the Sahlin-Peppas model it was apparent that Fickian diffusion dominated the release mechanism. It was concluded that increasing the temperature of the release medium increased the rate constant of DCD release from the beads but did not change the release mechanism.

5.4 References

[1]   Y. Wu, T. Seo, T. Sasaki, S. Irie and K. Sakurai, *Carbohydrate Polymers* **2006**, *63*, 492-499.

[2]   C. Y. Choi, S. B. Kim, P. K. Pak, D. I. Yoo and Y. S. Chung, *Carbohydrate Polymers* **2007**, *68*, 122-127.

[3]   S. Tokuraa, S. Babaa, S. Urakia, Y. Miuraa, N. Nishia and O. Hasegawaa, *Carbohydrate Polymers* **1990**, *13*, 273-281.

[4]   C. L. Tien, M. Lacroix, P. Ispas-Szabo and M.-A. Mateescu, *Journal of Controlled Release* **2003**, *93*, 1-13.

[5]   K. Y. Lee, W. S. Ha and W. H. Park, *Biomaterials* **1995**, *16*, 1211-1216.

[6]   S. Hirano, R. Yamaguchi, N. Fukui and M. Iwata, *Carbohydrate Research* **1990**, *201*, 145–149.

[7]   K. Ogawa, T. Yui and K. Okuyama, *International Journal of Biological Macromolecules* **2004**, *34*, 1-8.

[8]   L. Félix, J. Hernández, W. M. Argüelles-Monal and F. M. Goycoolea, *Biomacromolecules* **2005**, *6*, 2408–2415.

[9]   C. Zhang, Q. Ping, H. Zhang and J. Shen, *Carbohydrate Polymers* **2003**, *54*, 137–141.

[10]   K. Y. Lee and W. H. Jo, *Langmuir* **1998**, *14*, 2329–2332.

[11]   G. Jiang, D. Quan, K. Liao and H. Wang, *Carbohydrate Polymers* **2006**, *66*, 514 - 520.

[12]   Y. Chiu, S. Chen, C. Su, C. Hsiao, Y. Chen, H. Chen and H. Sung, *Biomaterials* **2009**, *30*, 4877-4888.

[13]   C. Y. Choi, S. B. Kim, P. K. Pak, D. I. Yoo and Y. S. Chung, *Carbohydrate Polymers* **2007**, *68*, 122-127.

[14]   Y. Tong, S. Wang, J. Xu, B. Chua and C. He, *Carbohydrate Polymers* **2005**, *60*, 229-233.

[15]   R. Y. M. Huan, G. Y. Moon and R. Pal, *Journal of Membrane Science* **2000**, *176*, 223–231.

[16]   S. Hirano, M. Zhang, B. Chung and S. Kim, *Carbohydrate Polymers* **2000**, *41*, 175-179.

[17]   T. Liu and Y. Lin, *Acta Biomaterialia,* **2010**, *6*, 1423-1429.

[18]   L. S. Guinesi and É. T. G. Cavalheiro, *Thermochimica Acta* **2006**, *444*, 128-133.

[19]   S. Despond, E. Espuche, N. Cartier and A. Domard, *Journal of Polymer Science* **2005**, *43*, 48-58.

[20]   M. Avella, E. D. Pace, B. Immirzi, G. Impallomeni, M. Malinconico and G. Santagata, *Carbohydrate Polymers* **2007**, *69*, 503-511.

[21]   Y. S. Nam, W. H. Park, D. Ihm and S. M. Hudson, *Carbohydrate Polymers* **2010**, *80*, 291-295

[22]   S. Hirano and T. Moriyasu, *Carbohydrate Polymers* **2004**, *55*, 245–248.

[23]   K. L. B. Chang and J. Lin, *Carbohydrate Polymers* **2000**, *43*, 163-169.

[24]   S. J. Kim, S. J. Park and S. I. Kim, *Reactive & Functional Polymers* **2003**, *55*, 53–59.

[25]   K. C. Gupta and F. H. Jabrail, *Carbohydrate Research* **2006**, *341*, 744–756.

[26]   Y. Yuan, B. M. Chesnutt, G. Utturkar, W. O. Haggard, Y. Yang, J. L. Ong and J. D. Bumgardner, *Carbohydrate Polymers* **2007**, *68*, 561–567.

[27]   M. N. Khalida, F. Agnelya, N. Yagoubib, J. L. Grossiorda and G. Couarrazea, *European Journal of Pharmaceutical Sciences* **2002**, *15*, 425–432.

[28]   A. Duarte, J. Manoa and R. Reis, *Journal of Supercritical Fluids* **2011**, *10.1016/j.supflu.2010.12.004*.

[29]   G. Ma, B. Qian, J. Yang, C. Hu and J. Ni, *International Journal of Biological Macromolecules* **2010**, *46*, 558–561.

[30]   J. Desbrieres, C. Martinez and M. Rinaudo, *International Journal of Biological Macromolecules* **1996**, *19*, 21-28.

[31]   N. Obitte, A. Chukwu and Onyishi, *International Journal of Applied Research in Natural Products* **2010**, *3*, 1-17.

[32]   L. Serra, J. Domenechc and N. A. Peppas, *Biomaterials* **2006**, *27*, 5440–5451.

[33]   B. Sasa, P. Odon, S. Stane and K. Julijana, *European Journal of Pharmaceutical Sciences* **2006**, *27*, 375-383

[34]   S. Kiortsis, K. Kachrimanis, T. Broussali and S. Malamataris, *European Journal of Pharmaceutics and Biopharmaceutics* **2005**, *59*, 73–83.

[35]   Y. Liu, X. Fan, B. Wei, Q. Si, W. Chen and L. Sun, *International Journal of Pharmaceutics* **2006**, *308*, 205–209.

[36]   L. Ma, M. Liu, H. Liu, J. Chen and D. Cui, *International Journal of Pharmaceutics* **2010**, *385*, 86-91.

[37]   K. Huanbutta, P. Sriamornsak, S. Limmatvapirat, M. Luangtananan, Y. Yoshihashi, E. Yonemochi, K. Terada and J. Nunthanid, *European Journal of Pharmaceutics and Biopharmaceutics* **2011**, *77*, 320-326.

[38]   B.-L. Guo and Q.-Y. Gao, *Carbohydrate Research* **2007**, *342*, 2416-2422.

[39]   T. Yoshizawa, Y. Shin-ya, K.-J. Hong and T. Kajiuchi, *European Journal of Pharmaceutics and Biopharmaceutics* **2005**, *59*, 347-354.

[40]   L. Wei, C. Cai, J. Lin and T. Chen, *Biomaterials* **2009**, *20*, 2606-2613.

[41]   J. Chen, M. Liu, H. Liu and L. Ma, *Materials Science and Engineering: C* **2009**, *29*, 2116-2123.

[42]   B. Adnadjevic, J. Jovanovic and I. Krkljus, *Journal of Applied Polymer Science* **2007**, *107*, 2768-2755.

[43]   N. Ahuja, O. P. Katare and B. Singh, *European Journal of Pharmaceutics and Biopharmaceutics* **2007**, *65*, 26-38

[44]   Z. Wu, X. G. Zhang, C. Zheng, C. X. Li, S. M. Zhang, R. N. Dong and D. M. Yu, *European Journal of Pharmaceutical Sciences* **2009**, *37*, 198–206.

[45]   N. A. Peppas and J. J. Sahlin, *International Journal of Pharmaceutics* **1989**, *57*, 169-172.

[46]   P. M. d. l. Torre, S. Torrado and S. Torrado, *Biomaterials* **2003**, *24*, 1459–1468.

Chapter 6: Adsorption of Paraquat by Chitosan Hydrogel Beads

6.1 Introduction

Paraquat (1-1'-dimethyl-4-4'-bipyridyl) (Figure 6.1), a bi-quaternary ammonium compound, is a non-selective contact herbicide which is normally synthesised as the dichloride salt. Paraquat is extensively used in direct sowing management systems as well as for weed control in uncultivated areas, pasture renewal and pre-harvest drying[1]. According to the United States Environmental protection agency, the acceptable limit for paraquat in drinking water is 0.03 mg L^{-1} and the toxicity limit with respect to aquatic organisms is 15 mg L^{-1}. Its Environmental Danger Protocol classification is II (very dangerous), and its toxicological classification is type II (highly toxic)[2]. This hazardous compound is found in agricultural wastewater and in the blood of poisoned human bodies[3]. Therefore, its removal from water supplies is very important.
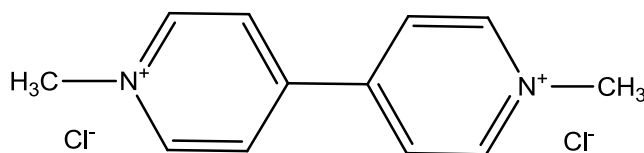
Figure 6.1 Paraquat

Recently, chitosan beads have shown to be effective biosorbents for the removal of dyes[4] and heavy metals[5]. To improve the adsorption capacity, chemical modifications can be made to the chitosan such as crosslinking or insertion of new functional groups[6]. Chitosan beads modified by cross-linking with epichlorohydrin (ECH) have been shown to have an increased adsorption capacity for nitrate, one of the most common groundwater contaminants in rural areas, thus facilitating its effective removal from water[6]. Therefore it was theorised that removal of paraquat from

aqueous solution may be accomplished by crosslinking chitosan beads with a complex capable of binding with paraquat. Previous work carried out by Guo *et al.* and Wang *et al* demonstrated that a strong binding complex is formed between *p*-sulfonatocalix[4]arene and paraquat[7, 8]. Yanagi *et al.* have shown that chitosan hydrogel beads can be formed by crosslinking with *p*-sulfonatocalix[*n*]arenes (C4S) (Figure 6.2) due to polyion complex formation with the cationized glucosamine units of chitosan[9]. They used these beads to investigate the adsorption of di-*n*-butyl phthalate, a suspected endocrine disrupter, from a phosphate buffer solution. They determined that the amount of di-*n*-butyl phthalate adsorbed by chitosan beads modified with *p*-sulfonatocalix[*n*]arenes was approximately five times the amount adsorbed by unmodified chitosan beads[9]. The aim of this chapter was to carry out a preliminary study to investigate the potential removal of paraquat from an aqueous solution by chitosan beads crosslinked with C4S.
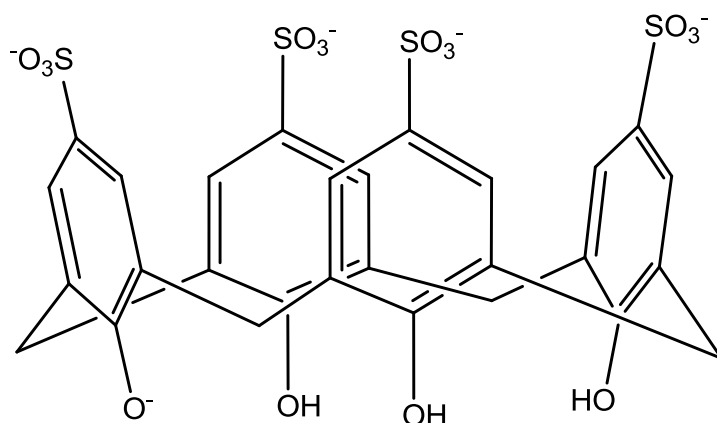
Figure 6.2 *p*-Sulfonatocalix[4]arene anion

6.2. Results and Discussion

6.2.1 Formulation and Characterization of C4S-Chitosan Hydrogel Beads

The beads were synthesised as detailed in Section 2.2.4.2. In brief, an 85% deacetylated chitosan solution was dropped via syringe needle into a solution of *p*-sulfonatocalix[4]arene sodium salt in order to form crosslinked chitosan hydrogel beads (C4S-Chitosan Hydrogel Beads). The newly formed beads were left to crosslink overnight and then washed thoroughly with Millipore water. The concentrations of *p*-sulfonatocalix[4]arene sodium salt used to crosslink the beads were quite low as it was difficult to synthesise in large quantities.

6.2.2 Surface Morphology

The influence of *p*-sulfonatocalix[4]arene anion crosslinking on the surface morphology of chitosan beads was examined using SEM and the resulting micrographs are shown in Figure 6.3. For comparison, the morphology of a xerogel synthesised by precipitation in a NaOH solution is exhibited in Figure 6.3 (a) and (b).

1mm   100µm

   (a)   (b)

1mm   100µm

   (c)   (d)
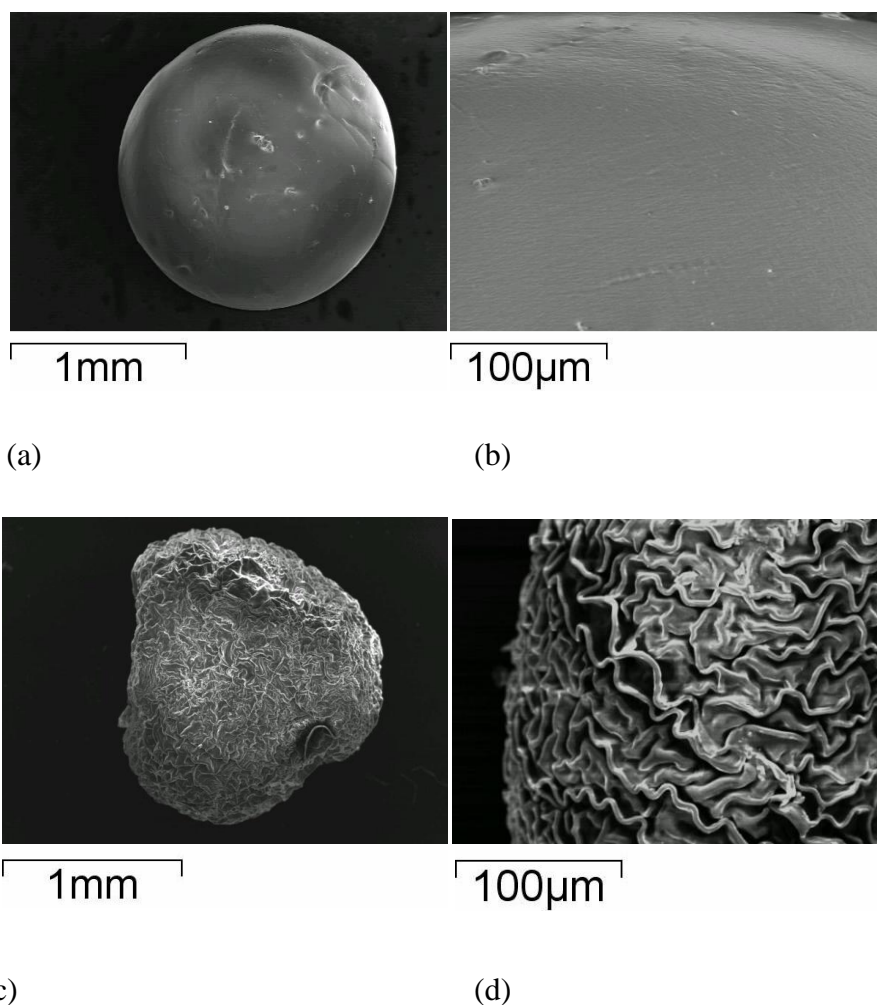
Figure 6.3 Influence of *p*-sulfonatocalix[4]arene sodium salt crosslinking on the shape and surface morphology of chitosan hydrogel beads. Chitosan beads in micrographs (a) and (b) were chitosan hydrogel beads gelled in 0.75 M NaOH only. Chitosan hydrogel beads in micrographs (c) and (d) were formed by crosslinking chitosan hydrogel beads in 12 mM *p*-sulfonatocalix[4]arene sodium salt solution.

It is apparent that crosslinking the chitosan beads with the sulfonated calixarene has a significant impact on the surface morphology of the beads. The surface morphology

of chitosan beads gelled in 0.75 M NaOH solution is that of a smooth surface that was spherical in shape. Whereas the chitosan beads crosslinked in *p*-sulfonatocalix[4]arene sodium salt are irregular in shape rather than spherical and the surface is characterised by an uneven surface of folds.

6.2.3 Energy-Dispersive X-Ray Analysis

Energy-Dispersive X-ray analysis (EDX) is an analytical technique used for elemental characterization of a sample. EDX was performed on a C4S-chitosan hydrogel bead and the resulting spectrum is shown in Figure 6.4.
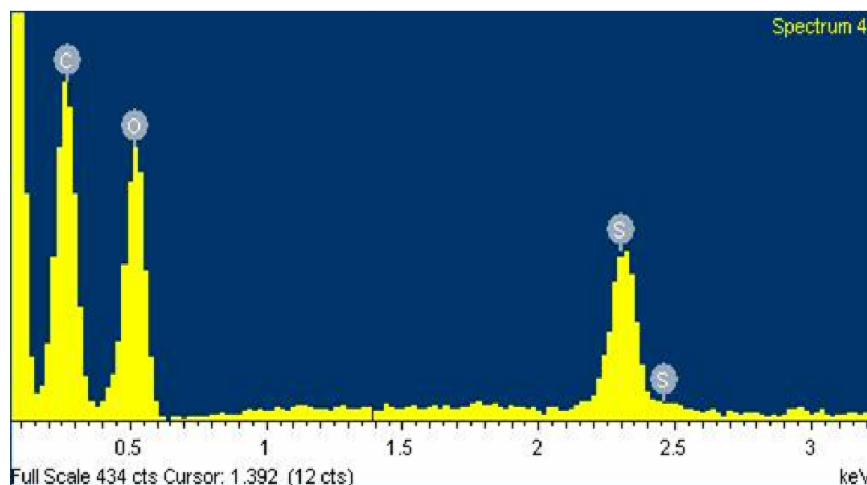
Figure 6.4 An EDX spectrum of a C4S-chitosan hydrogel bead that was crosslinked in 12 mM *p*-sulfonatocalix[4]arene sodium salt solution.

Examination of the EDX spectrum revealed that carbon, oxygen and sulfur were detected in the sample. This was a positive result as extensive washing of the beads meant that the sulfur band was most likely detected due to the *p*-sulfonatocalix[4]arene anion having crosslinked the chitosan hydrogel bead.

6.2.4 Adsorption Studies

The procedure used to carry out the adsorption study is stated in Section 2.5. In summary, 0.3 g of *p*-sulfonatocalix[4]arene anion crosslinked chitosan hydrogel beads were placed in solution of paraquat of known concentration held at 25 ± 1°C. At predetermined time intervals, samples were removed from the solution and the concentration of paraquat in the sample determined using UV/vis spectroscopy. The sample was then returned to the solution.   The amount of paraquat that was adsorbed by the hydrogels at a given time was calculated using Equation 2.15. The effect of contact time on paraquat adsorption by the chitosan hydrogels at different initial paraquat concentrations was investigated and the results are shown in Figure 6.5.
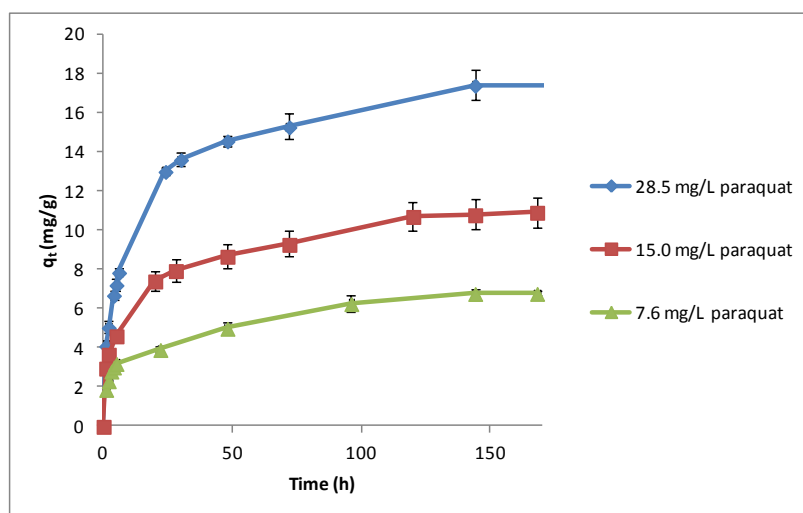
Figure 6.5 Influence of contact time on paraquat adsorption by chitosan hydrogels crosslinked in 12 mM *p*-sulfonatocalix[4]arene sodium salt solution. The initial concentration of the paraquat solution is stated for each adsorbance profile.

The results shown in Figure 6.5 indicate that as the concentration of paraquat in the solution increased so too did the amount of paraquat adsorbed by the chitosan hydrogel beads crosslinked with *p*-sulfonatocalix[4]arene sodium salt. This was evident as at adsorption equilibrium the hydrogel beads in 28.5 mg/ L paraquat solution had adsorbed 17.4 mg g^{-1} of paraquat whereas hydrogel beads in 15.0 mg/L

paraquat solution had adsorbed 10.9 mg g^{-1} of paraquat. It appeared that the kinetics of paraquat adsorption consisted of two phases, an initial paraquat uptake phase when the process was fast and a second slower phase as it reached equilibrium. The initial high rate of paraquat uptake was probably due to the large availability of binding sites near the surface of the hydrogel beads. The adsorption capacity of the hydrogel beads increased with an increase in the paraquat concentration, but the time to reach adsorption equilibrium was independent of the initial paraquat concentration. Chatterjee and Woo reached similar conclusions in their study of the removal of nitrate from aqueous solutions by chitosan hydrogel beads[6]. Their research indicated that adsorption also consisted of two phases and that the initial concentration of nitrate in solution influenced the adsorption capacity of their chitosan hydrogel beads. Similarly, Hu *et al*. investigated the sorption of acid dye onto chitosan nanoparticles and found that the higher the original concentration of dye in solution the greater amount adsorbed by the chitosan nanoparticles[10]. A study was preformed to investigate whether increasing the concentration of *p*-sulfonatocalix[4]arene sodium salt in the crosslinking solution would lead to an increase in the adsorption capacity[11]. The results are displayed in Table 6.1.

Table 6.1 Influence of *p*-sulfonatocalix[4]arene sodium salt concentration in the chitosan hydrogel crosslinking solution on the equilibrium adsorption values in a solution of 28.5 mg L^{-1} paraquat.

Concentration of *p*-sulfonatocalix[4]arene sodium salt solution in hydrogel beads crosslinking solution (mM)	q_e (mg g^{-1})
18	29.2
12	17.4
6	3.2
0*	0

*beads formed by precipitation in NaOH solution.

The results in Table 6.1 indicate that as the *p*-sulfonatocalix[4]arene sodium salt concentration in the chitosan hydrogel crosslinking solution increased so too did the adsorption capacity of the hydrogel beads. This was expected, as the chitosan *p*-sulfonatocalix[4]arene crosslinking density increased, the number of adsorption sites available for the adsorbent-adsorbate interaction also increased. It was also noteworthy that unmodified chitosan hydrogel beads that were not crosslinked in *p*-sulfonatocalix[4]arene sodium salt solution had a negligible uptake of paraquat from solution. This result confirmed that it was the *p*-sulfonatocalix[4]arene binding with parquat, and facilitating its removal from aqueous solution rather than the amino or hydroxyl groups on chitosan acting as binding sites. The highest q_e value achieved was 29.2 mg g^{-1} by chitosan hydrogels crosslinked in 18 mM *p*-sulfonatocalix[4]arene sodium salt solution. In Table 6.2 this value was compared to the maximum adsorption capacities obtained using other adsorbents.

Table 6.2 Maximum adsorption capacities of paraquat obtained by adsorbents.

Adsorbent	q_e (mg g^{-1})
Regenerated clay mineral from bleaching earth waste[12]	24.80
Activated carbon derived from used tires[13]	33.70
Commercial activated carbon[13]	75.80
Methacrylic acid-modified rice husk[3]	317.70
Activated Clay[14]	58.48
Ayous Sawdust[15]	9.47

By comparing the maximum adsorption capacity achieved in this research with those obtained by other adsorbents it can be observed that there are some which are more effective and some that are less effective at adsorbing paraquat. The q_e values obtained in this research were higher than those obtained by regenerated clay mineral from bleaching earth waste and Ayous sawdust. Methacrylic acid-modified rice husk is clearly the best adsorbent as its adsorption capacity was significantly higher than any other adsorbent exhibited in Table 6.2. However, as 18 mM was a very low concentration of *p*-sulfonatocalix[4]arene sodium salt the maximum adsorption capacities of the C4S- chitosan hydrogel beads could potentially be significantly improved on by increasing the C4S concentration in the gelling solution.

6.2.5 Kinetic Modelling of Paraquat Adsorption

In order to investigate the mechanism of adsorption the experimental data were fitted to the *pseudo*-first order (Equation 2.20), *pseudo*-second order (Equation 2.21) and the intraparticle diffusion models (Equation 2.22). The procedure used to carry out the adsorption study is stated in Section 2.5. The temperature of the adoption solution was held at 25 ± 1 °C. The plots are exhibited in Figure 6.6 and the results are displayed in Table 6.3.

(a)   (b)

(c)
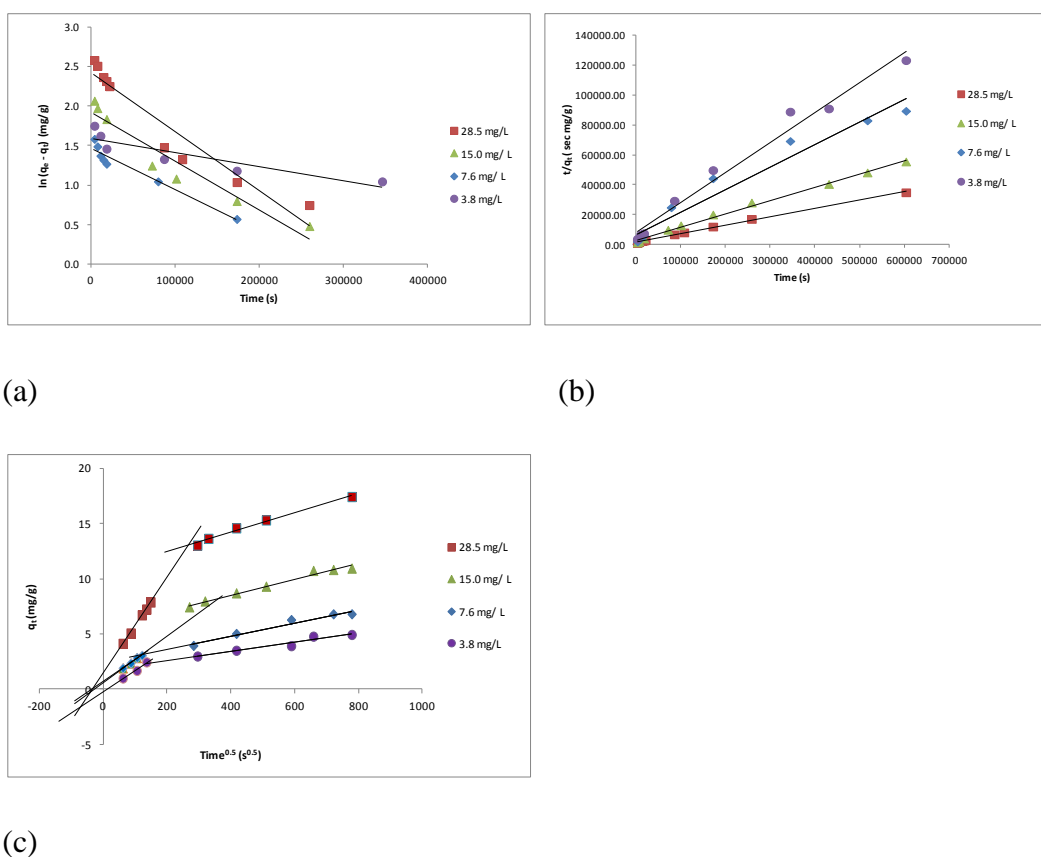
Figure 6.6 Adsorption data fitted to the (a) *pseudo*-first order (b) *pseudo*-second order and the (c) intraparticle diffusion model. The initial concentration of the paraquat solution is stated for each plot. The concentration of *p*-sulfonatocalix[4]arene sodium salt in the chitosan crosslinking solution was 12 mM.

Table 6.3 The *pseudo*-first order and *pseudo*-second order rate constants and correlation coefficient data for the adsorption of paraquat from C4S-chitosan hydrogel beads. The concentration of *p*-sulfonatocalix[4]arene sodium salt in the chitosan crosslinking solution was 12 mM.

Concentration of Paraquat (mg/L) in solution	*Pseudo*-first Order Model		*Pseudo*-second Order Model	
	k_1 (s^{-1})	R^2	k_2 (g mg^{-1} s^{-1})	R^2
28.5	7.49×10^{-6}	0.9209	3.23×10^{-6}	0.9980
15.0	6.18×10^{-6}	0.9268	3.48×10^{-6}	0.9899
7.6	5.26×10^{-6}	0.9425	3.59×10^{-6}	0.9616
3.8	1.79×10^{-6}	0.8133	5.12×10^{-7}	0.9796

Analysing the data in Table 6.3 it is apparent that the adsorption of paraquat ions onto the C4S-chitosan hydrogel beads follows the *pseudo*-second order model as the regression line fits for the *pseudo*-second order were better than for the *pseudo*-first order model. The *pseudo*-second order model assumes that chemisorption is the rate controlling mechanism[16]. A trend can be seen as the rate constant of the *pseudo*-second order model increases as the concentration of paraquat (mg/L) in the solution increases. This indicates that the rate of the adsorption process was influenced by the concentration of paraquat (mg/L) in the solution. In order to evaluate the contribution of diffusion within the hydrogel in the adsorption process the intra-particle diffusion model was applied to the experimental data and the results are presented in Table 6.4.

Table 6.4 Intra-particle diffusion model rate constant and correlation coefficient data for the adsorption of paraquat onto C4S-chitosan hydrogel beads. The concentration of *p*-sulfonatocalix[4]arene sodium salt in the chitosan crosslinking solution was 12 mM.

Concentration of Paraquat (mg/L) in solution	$k_{int,1}$ (mg g^{-1} s$^{-0.5}$)	R^2	$k_{int,2}$ (mg g^{-1} s$^{-0.5}$)	R^2
28.5	0.043	0.9985	0.0088	0.9822
15.0	0.021	0.9882	0.0071	0.9809
7.6	0.019	0.9891	0.0059	0.9629
3.8	0.019	0.9810	0.0042	0.9396

If the intraparticle diffusion model gives a straight line, then the adsorption is controlled solely by the intraparticle diffusion mechanism i.e. the size of the pores[17]. However, if the adsorption data exhibit multi-linear plots (as has been obtained in this study), its shows that there are two or more steps influencing the adsorption process. If the lines pass through the origin, it indicates that intraparticle diffusion is the rate determining step. In the present study, the slope of the initial adsorption process was used to derive the values for $k_{int,1}$ and the slope of the second to obtain the $k_{int,2}$ value. A trend can be seen based on the data presented in Table 6.4 that $k_{int,1} > k_{int,2}$. A similar trend was found by Ngah *et al.* who also found that adsorption of Cu (II) ions in aqueous solution by chitosan beads followed a two step process where $k_{int,1}$ >$k_{int,2}$ [11]. After applying their experimental data to the intraparticle diffusion model Nanseu-Njiki *et al.* found that the biosoption of paraquat onto Ayous sawdust was a three step process with the third step having a negative slope which implied that some of the paraquat was diffusing back into solution[15]. It is concluded that $k_{int,1}$ >$k_{int,2}$ in our study because the initial paraquat uptake phase (which is associated with $k_{int,1}$) took place when there was greater availability of binding sites near the surface of the hydrogel beads. However, as the lines did not pass through the origin it shows that intraparticle absorption is not the rate-determining step.

6.2.6 Sorption Isotherms of Paraquat Adsorption onto C4S-Chitosan Hydrogel Beads

The equilibrium isotherm is an important tool for describing the interactive behaviour between the solute and adsorbent. It is also essential in the design of an adsorption system[11]. Thus, the correlation of equilibrium data using either a theoretical or empirical equation is important for adsorption data interpretation and prediction. Several mathematical models can be used to describe experimental data of adsorption isotherms. The two most famous isotherm equations, the Langmuir and Freundlich, were employed for further interpretation of the adsorption data obtained in this study (exhibited in Table 6.5). The experiments were conducted as reported in Section 2.5.

Table 6.5 Adsorption of paraquat onto C4S-chitosan hydrogel beads at different concentrations of paraquat in the aqueous solution. The concentration of *p*-sulfonatocalix[4]arene sodium salt in the chitosan crosslinking solution was 12 mM.

Initial concentration of paraquat (mg/L)	Paraquat concentration at equilibrium (mg/L)	Equilibrium adsorption mg/g - adsorbent (q_m)
2.7	1.7	3.4
3.8	2.5	4.9
6.3	4.8	5.8
7.6	5.8	6.7
15.0	12.1	10.9
28.5	24.4	17.3

The Freundlich isotherm describes a heterogeneous system and is not restricted to the monolayer formation[6, 18]. It usually applies to a small range of concentrations and, in particular, to dilute solutions. The Freundlich model assumes that there are many adsorption sites acting simultaneously, each with a different free energy of sorption, and that there is a large amount of available sites[19]. If the magnitude of the exponent

$1/n$ lies between 0 and 1, and the value of n is greater than 1 this indicates favourable conditions for adsorption[20]. The experimental data were plotted to the Freundlich isotherm (Equation 2.19) in Figure 6.7. The results are presented in Table 6.6.

For the Langmuir isotherm model it is assumed that intermolecular forces decrease rapidly with distance and thus lead to the coverage of adsorbent by a monolayer of adsorbate. Furthermore, it is assumed that once an adsorbate species occupies the available site, no further adsorption takes place at that site[18]. Theoretically, an adsorbent has a finite number of sites and after occupation of sites by adsorbent, no further adsorption is possible. The values of Langmuir constants and the regression line coefficient were derived from the linear form of the isotherm (Equation 2.17). The isotherm plot is exhibited in Figure 6.8 and the results are reported in Table 6.7.
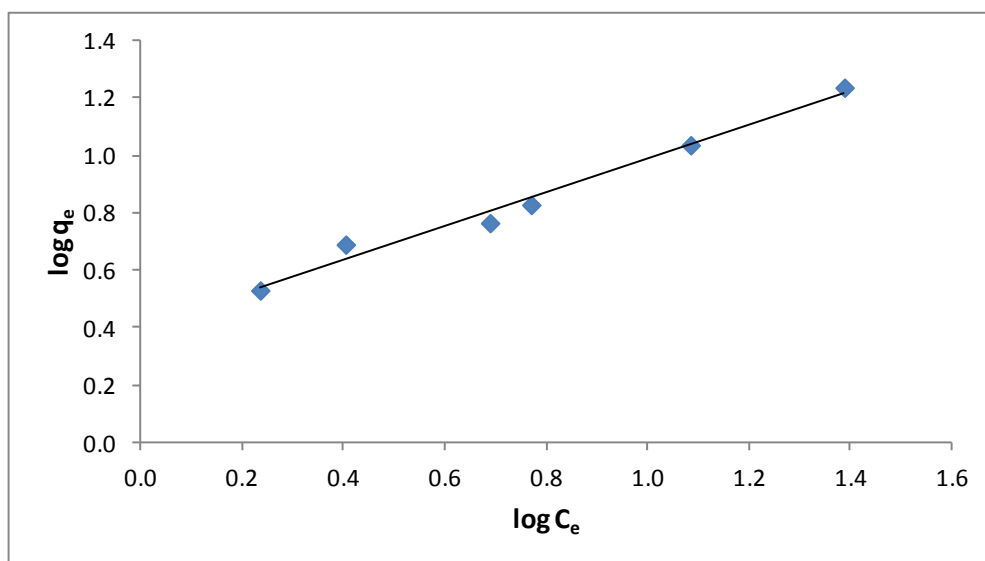
Figure 6.7 Linear Freundlich isotherm for the adsorption of paraquat into C4S-chitosan hydrogel beads. The concentration of *p*-sulfonatocalix[4]arene sodium salt in the chitosan crosslinking solution was 12 mM. The temperature of the adsorption medium was 25 ±1 °C.

Table 6.6 Freundlich isotherm constants and correlation coefficient for the adsorption of paraquat into C4S-chitosan hydrogel beads at different concentrations of paraquat in the aqueous solution. The concentration of *p*-sulfonatocalix[4]arene sodium salt in the chitosan crosslinking solution was 12 mM. The temperature of the adsorption medium was 25 ±1 °C.

Freundlich Constants			
K_F (mg g^{-1}) (L mg^{-1})$^{1/n}$	$\dfrac{1}{n}$	n	R^2
2.52	0.588	1.7	0.9830
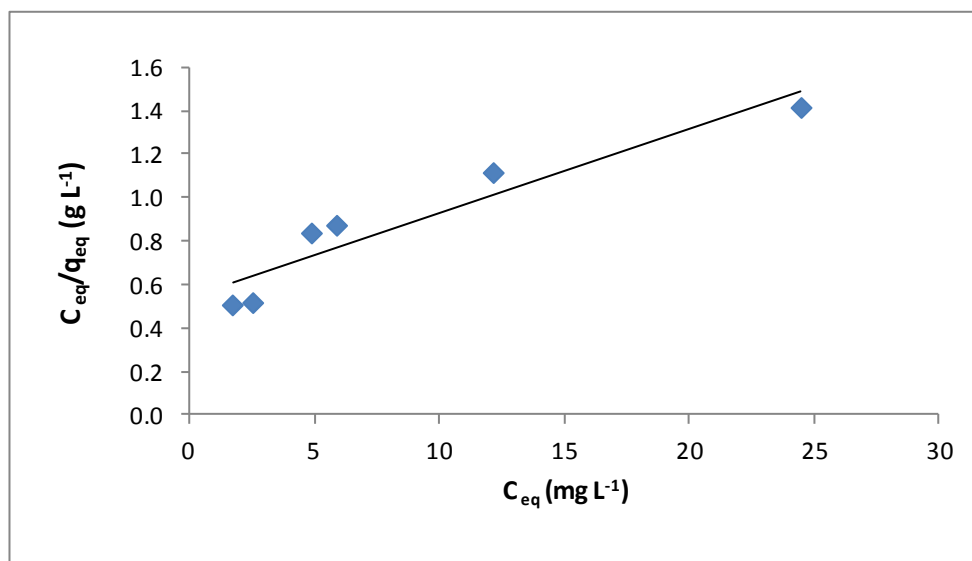
Figure 6.8 Linear Langmuir isotherm for the adsorption of paraquat into C4S-chitosan- hydrogel beads. The concentration of *p*-sulfonatocalix[4]arene sodium salt in the chitosan crosslinking solution was 12 mM. The temperature of the adsorption medium was 25 ±1 °C.

Table 6.7 Langmuir isotherm constants and correlation coefficient for the adsorption of paraquat onto C4S-chitosan hydrogel beads. The concentration of *p*-sulfonatocalix[4]arene sodium salt in the chitosan crosslinking solution was 12 mM. The temperature of the adsorption medium was 25 ±1 °C.

Langmuir Constants			
K_L (L g^{-1})	a_L (L mg^{-1})	Q_0 (mg g^{-1})	R^2
1.84	0.071	25.92	0.8966

Based on the correlation coefficients exhibited in Table 6.6 and Table 6.7, the experimental data show a good fit to the Freundlich model ($R^2 = 0.9830$) but a poor fit to the Langmuir model ($R^2 = 0.8966$). It was therefore concluded that the adsorbance properties of the C4S-chitosan hydrogel beads are best described by the Freundlich model. This suggested that there were a large number of available adsorption sites each with a different free energy of sorption[19]. This result is appropriate for our system, as the binding sites towards the centre of the hydrogel bead would require more energy to reach compared to binding sites on the surface. Inigo *et al.* studied the adsorption of phenol onto sucrose polymers crosslinked with Epichlorohydrin, which followed the Freundlich model, and concluded that the Freundlich equation yields better results for polymers whose networks consist of a heterogeneous distribution of chemical groups[19].

6.3 Conclusions

Initially, the rate of adsorption of paraquat onto the C4S-chitosan hydrogel beads was fast due to the high number of binding sites available. This was followed by a slower rate of adsorption which gradually approached a plateau. The adsorption kinetics can be well described by the *pseudo*-second order model equation. This meant that chemisorption was the rate controlling mechanism which in this study would refer to the complexation that took place between the paraquat and the *p*-sulfonatocalix[4]arene. The influence of the initial concentration of the paraquat solution and the concentration of *p*-sulfonatocalix[4]arene sodium salt used to crosslinked the hydrogel beads was found to be of considerable significance on the rate of adsorption and the equilibrium adsorption value. The experimental data fitted well to the Freundlich isotherm which suggested that the paraquat concentration bound to the C4S-chitosan hydrogel beads will increase so long as there is an increase in the paraquat concentration in the aqueous solution. Compared to the adsorption capacities of other systems designed to remove paraquat from aqueous solution the highest q_e value obtained in this study (29.2 mg g^{-1}) appeared to be a standard value, however it was substantially lower than the value obtained for methacylic acid-modified rice husk, which had a maximum paraquat adsorption capacity of 317.70 mg g^{-1}. In future studies, an increase in the concentration of *p*-sulfocalix[4]arene in the hydrogel bead crosslinking solution is likely to increase the maximum adsorption capacity of the C4S-chitosan hydrogel beads. In addition, future studies should also be conducted to examine the adsorption of paraquat by C4S-chitosan hydrogel beads in acidic media as they could be used as a medical aid in cases of paraquat poisoning. It would also be necessary to look at the regenerative properties of the adsorption system.

6.4 References

[1]　M. d. S. Silva, D. S. Cocenza, R. Grillo, N. F. S. d. Melo, P. S. Tonello, L. C. d. Oliveira, D. L. Cassimiro, A. H. Rosa and L. F. Fraceto, *Journal of Hazardous materials* **2011**, *190*, 366-374.

[2]　USEPA, *United States Environmental Protection Agency* accessed in September 2011, *http://www.epa.gov/.*

[3]　S. T. Hsu and T. C. Pan, *Bioresource Technology* **2007**, *98*, 3617-3621.

[4]　M. S. Chiou, P. Y. Ho and H. Y. Li, *Dyes and Pigments* **2004**, *60*, 69-84

[5]　B. Kannamba, K. L. Reddy and B. V. AppaRao, *Journal of Hazardous Materials* **2010**, *175*, 939-948.

[6]　S. Chatterjee, D. S. Lee, M. W. Lee and S. H. Woo, *Journal of Hazardous Materials* **2009**, *166*, 508-513.

[7]　D. Guo, L. Wang and Y. Liu, *Journal of Organic Chemistry* **2007**, *72*, 7775-7778.

[8]　G. Wang, X. Ren, M. Zhao, X. Qiu and A. Qi, *Journal of Agriculture and Food* **2011**, *59*, 4294–4299.

[9]　A. Yanagi, H. Otsuka and A. Takahara, *Polymer Journal* **2005**, 939-945.

[10]　Z. G. Hu, J. Zhang, W. L. Chan and Y. S. Szeto, *Polymer* **2006**, *47*, 5838-5842.

[11]　W. Ngah and S. Fatinathan, *Chemical Engineering Journal* **2008**, *143*, 62-72.

[12]　W. Tsai and C. Lai, *Journal of Hazardous Materials* **2006**, *134*, 144-148

[13]　N. K. Hamadi, S. Swaminathan and X. D. Chen, *Journal of Hazardous Materials* **2004**, *112*, 133-141.

[14]　W. T. Tsai, C. W. Lai and K. J. Hsien, *Journal of Colloid and Interface Science* **2003**, *263*, 29-34.

[15]   C. P. Nanseu-Njiki, G. K. Dedzo and E. Ngameni, *Journal of Hazardous Materials* **2010**, *179*, 63-71.

[16]   A. L. Ahmad, S. Sumathi and B. H. Hameed, *Water Research* **2005**, *39*, 2483–2494.

[17]   W. H. Cheung, Y. S. Szeto and G. McKay, *Bioresource Technology* **2007**, *98*, 2897–2904.

[18]   J. C. Y. Ng, W. H. Cheung and G. McKay, *Chemosphere* **2003**, *52*, 1021–1030.

[19]   X. Iñigo, García-Zubir, G. González-Gaitano and J. R. Isasi, *Journal of Colloid and Interface Science* **2009**, *337*, 11-18.

[20]   N. Viswanathan, C. S. Sundaram and S. Meenakshi, *Colloids and Surfaces B: Biointerfaces* **2009**, *68*, 48–54.

[21]   W. Tsai, K. Hsien, Y. Chang and C. C. Lo, *Bioresource Technology* **2005**, *96*, 657–663.

Chapter 7: Conclusions

7.1 Conclusions

In this work, chitosan hydrogel beads and their dehydrated counterparts, chitosan xerogel beads, were developed as a delivery system for the nitrification inhibitor DCD. The beads were characterised and their DCD release properties studied.

SEM micrographs were recorded for chitosan xerogel beads that had been synthesised by ionic crosslinking and NaOH precipitation. The micrographs of these beads indicated that the ionic crosslinker in the gelling solution influenced the surface morphology of the xerogel bead. The chitosan xerogels gelled in TPP and NaOH exhibited a relatively smooth surface morphology and were spherical in shape, in contrast, chitosan xerogels gelled in trisodium citrate and NaOH solution were rough and irregular in shape. The smoothest and most uniform surface morphology observed was of chitosan xerogel beads gelled in NaOH solution only. The swelling ratios (%) of chitosan xerogel beads synthesised gelled in TPP and NaOH solution were investigated. The lowest equilibrium swelling ratio(%) observed was for chitosan xerogel beads ionically crosslinked in 400 mM TPP and NaOH solution, which exhibited a swelling ratio (%) of 183% after 20 h. This is in agreement with literature reports that chitosan beads have high swelling ratios (%)[1, 2]. An examination of the DCD release profiles of chitosan xerogels crosslinked with 110 mM TPP, trisodium citrate, sodium molybdate and sodium alginate revealed that release equilibrium occurred within 45 min. In addition, the crosslinking of chitosan xerogels with an ionic crosslinker did not increase the release time of DCD from the beads when compared with a xerogel gelled in aqueous hydroxide ion solution only.

An investigation was carried out to determine whether using a covalent crosslinker in addition to TPP would result in controlled DCD release from the beads. The chitosan hydrogel beads were crosslinked with glyoxal, glutaraldehyde or genipin. All three covalent crosslinkers extended the release time of DCD from the chitosan xerogel beads from minutes to hours. Glyoxal proved to be the most effective covalent crosslinker, as it could extend the release time of DCD from the beads to 8 h. The

swelling ratio (%) of chitosan xerogel beads crosslinked in 300 mM glyoxal solution was 59% after 120 h, which indicated that covalent crosslinking had reduced the swelling ratio (%) of the beads. The swelling ratio (%) of the beads was shown to be pH sensitive, as in pH 5.0 solution the swelling ratio (%) of the beads was 200% after 120 h in contrast to 59% in pH 9.0 solution.

The release kinetics of DCD from the glyoxal crosslinked hydrogel beads were investigated and it was determined that DCD release followed the first-order model. This is characteristic of a membrane-controlled diffusion system where the gradient is reduced due to decreasing concentration on the donor side in combination with sink conditions in the dissolution medium[3]. The DCD release mechanism from glyoxal crosslinked hydrogel beads was also investigated. The release data fitted the Higuhci model well which suggested the DCD release process was based on Fickian diffusion[4]. This result was confirmed by fitting the data to the Sahlin-Peppas model and calculating the relaxation/Fickian ratio which implied that Fickian diffusion was the primary mechanism of DCD from chitosan xerogel beads crosslinked in 110 mM, 300 mM and 520 mM glyoxal solution.

Washing the hydrogel beads in Millipore water after covalent crosslinking to remove excess glyoxal from the beads was a standard step in the formation of covalently crosslinked chitosan xerogels. However, removing this step caused the incorporation of a lag time of 3 days into the release profile. Instead of reaching release equilibrium after a number of hours, the release time was extended to 7 days. Furthermore, the maximum swelling ratio (%) obtained fell to just 19%, compared to 59% exhibited by chitosan xerogel beads that had been washed in Millipore water after the crosslinking reaction. Precise release studies were hindered by glyoxal and DCD both absorbing light in the same ultraviolet-visible spectral region. In order to further investigate the influence of unreacted glyoxal on controlled release from the unwashed beads future studies could be conducted using a model coloured molecule.

Chitosan hydrogel beads were successfully substituted in their solid state to form *N*-acylated chitosan xerogel beads. The successful acylation of chitosan at the amino functional group was confirmed by FT-IR analysis. The spectra obtained showed increased intensity of the vibrational bands at 2940 cm^{-1} and 2920 cm^{-1} ν(CH$_3$ and

CH$_2$), and the broad vibrational band at 1640 cm^{-1} disappeared and two separate bands appeared at 1655 cm^{-1} and 1555 cm^{-1} v(C=O and *N*-acyl). The appearance of bands at 1655 cm^{-1} and 1555 cm^{-1} v(C=O and *N*-acyl) in an FT-IR spectrum of chitosan are characteristic of *N*-acylation[5].

SEM micrographs of the surface of *N*-hexanoyl chitosan xerogel beads showed that the loading solvent influenced the morphology of the bead. While studies on the *N*-palmitoyl chitosan xerogel beads showed that the reaction solvent also affected the surface morphology of the beads.

DSC thermograms of the *N*-acylated chitosan indicated that the substituted chitosan polymer degraded at a higher temperature compared with the chitosan polymer starting material and that the reaction had occurred throughout the bead.

The degree of substitution of the *N*-acylated chitosan was determined using elemental analysis. The study confirmed that the higher the concentration of palmitoyl chloride in the reaction solution, the higher the degree of substitution of the chitosan polymer. Experimental analysis also indicated that the length of the aliphatic chain to be substituted onto the chitosan polymer influenced the degree of substitution, with less substitution observed for increasing chain lengths.

Swelling studies indicated that *N*-acylation of the chitosan beads reduced their swelling capacity compared with 85% deacetylated chitosan xerogel beads. It was confirmed that the higher the concentration of acid anhydride or acyl chloride in the reaction mixture, the lower the swelling ratio (%) of the resulting chitosan xerogel beads. In addition the *N*-acylated chitosan xerogel beads exhibited a slower swelling process than that of chitosan xerogel beads crosslinked with glyoxal. The swelling ratio (%) of chitosan xerogel beads crosslinked in glyoxal solution increased substantially over the first hour and then reached a plateau. The swelling ratio of *N*-acylated chitosan xerogel beads, however, increased at a much slower rate and reached a swelling ratio (%) plateau over a period of 10 h.

Release profiles indicated that *N*-palmitoyl, *N*-octanoyl and *N*-hexanoyl chitosan xerogel beads all exhibited increased DCD equilibrium release times compared with chitosan xerogels made from 85% deacetylated chitosan precipitated in NaOH. The

N-acylation of the chitosan hydrogel beads resulted in the equilibrium release time being extended from minutes to hours. The DCD equilibrium release time of *N*-acylated chitosan xerogel beads and glyoxal crosslinked hydrogel beads were similar. For example, the equilibrium release time of DCD from both *N*-hexanoyl chitosan xerogel beads and glyoxal crosslinked chitosan xerogel beads was 6 h.

DCD release from all the *N*-acylated chitosan xerogel beads followed first-order kinetics. An investigation into the mechanism of DCD release from the *N*-acylated beads concluded that release was primarily due to Fickian diffusion, with release by Case-II transport having little or no influence. As the temperature of the release medium increased from 20 °C to 40 °C the influence of Case-II transport increased, but only very slightly.

The degree of *N*-acylation of the chitosan hydrogel beads achieved in this research appears to be considerably greater than that achieved in previous literature studies. Chitosan hydrogel beads with a high degree of *N*-acylation may be of interest to researchers studying acylated chitosans ability to influence cholesterol adsorption[6], controlled drug delivery[7] and blood clotting[8].

The highest amount of DCD released from chitosan xerogel beads was by beads ionically crosslinked with 110 mM TPP and loaded in 1.2 M DCD solution. Each of these beads released on average 4 mg of DCD. For a DCD application of 7.5 kg ha^{-1} an estimated 1.8 million beads would be required. However, as the size of the beads can be increased by changing the size of the tube nozzle used in the preparation step, this number could be reduced for field trials. Controlled release had been achieved by unwashed glyoxal crosslinked xerogel beads and *N*-palmitoyl chitosan xerogel beads exhibited a release time of up to 10 h. These two formulations had the most potential to maintain an effective amount of DCD in a release medium over time.

Chitosan hydrogel beads were ionically crosslinked with *p*-sulfonatocalix[4]arene sodium salt for the purpose of paraquat adsorption from aqueous solution. The beads were characterised by scanning election microscopy and energy dispersive X-ray analysis. The SEM micrographs exhibited a dense folding pattern all over the bead

while the energy dispersive X-ray analysis confirmed the presence of sulphur. The adsorption data fitted the pseudo-second order model equation which meant that chemisorption was the rate controlling mechanism[9]. The experimental data also fitted well to the Freundlich isotherm which suggested that adsorption occurred on a multilayer surface with heterogeneous distribution of active sites[10].

A comparison of the adsorption capacities of other systems designed to remove paraquat from aqueous solution revealed that the highest q_e value obtained in this study (29.2 mg g^{-1}) appeared to be a relatively standard value[11]. However, it was not as high as the value obtained for methacrylic acid-modified rice husk, which had a maximum paraquat adsorption capacity of 317.7 mg g^{-1} [12]. A future study could be conducted to improve the adsorption capacity of chitosan hydrogel beads by increasing the concentration of *p*-sulfonatocalix[4]arene sodium salt in the crosslinking solution.

7.2 References

[1]   X. Liu, W. Xu, Q. Liu, W. Yu, Y. Fu, X. Xiong, X. Ma and Q. Yuan, *Carbohydrate Polymers* **2004**, *56*, 459-464.

[2]   Z. M. Wu, X. G. Zhang, C. Zheng, C. X. Li, S. M. Zhang, R. N. Dong and D. M. Yu, *European Journal of Pharmaceutical Sciences* **2009**, *37*, 198–206.

[3]   K. Jørgensen and F. N. Christensenb, *International Journal of Pharmaceutics* **1996**, *143*, 223-232

[4]   D. R. Paul, *International Journal of Pharmaceutics* **2011**, *418*, 13-17.

[5]   C. Y. Choi, S. B. Kim, P. K. Pak, D. I. Yoo and Y. S. Chung, *Carbohydrate Polymers* **2007**, *68*, 122-127.

[6]   Y. Tong, S. Wang, J. Xu, B. Chua and C. He, *Carbohydrate Polymers* **2005**, *60*, 229-233.

[7]   C. L. Tien, M. Lacroix, P. Ispas-Szabo and M.A. Mateescu, *Journal of Controlled Release* **2003**, *93*, 1-13.

[8]   K. Y. Lee, W. S. Ha and W. H. Park, *Biomaterials* **1995**, *16*, 1211-1216.

[9]   A. L. Ahmad, S. Sumathi and B. H. Hameed, *Water Research* **2005**, *39*, 2483–2494.

[10]   S. Chatterjee, D. S. Lee, M. W. Lee and S. H. Woo, *Journal of Hazardous Materials* **2009**, *166*, 508-513.

[11]   C. P. Nanseu-Njiki, G. K. Dedzo and E. Ngameni, *Journal of Hazardous Materials* **2010**, *179*, 63-71.

[12]   S. T. Hsu and T. C. Pan, *Bioresource Technology* **2007**, *98*, 3617-3621.